Regulation of the renin-angiotensin-aldosterone system in adipose tissue by AMP-activated protein kinase

Anna Dorothy White

BSc(Hons), MBChB(Hons), MRCP (UK)

Submitted in fulfillment of the requirements for the

Degree of Doctor of Philosophy

June 2018

School of Medical, Veterinary and Life Sciences

Institute of Cardiovascular and Medical Sciences

University of Glasgow

Abstract

Obesity and type 2 diabetes are a growing concern worldwide and changes within adipose tissue are implicated in their development. Adipocytes contain a complete renin angiotensin aldosterone system (RAAS) implicated in obesity-related complications. The energy regulating kinase AMP-activated protein kinase (AMPK) has anti-inflammatory properties in adipose tissue and systemic insulin sensitising effects.

Initial studies compared the human adipocyte model SW872 with the well-described murine 3T3-L1 adipocyte model. AMPK signalling in SW872 adipocytes was evident with similar responses to two structurally-unrelated AMPK activators, AICAR and A769662 compared with 3T3-L1 adipocytes. Key components of the RAAS were present in SW872 adipocytes and induced upon adipocyte differentiation. AICAR and A769662 were found to negatively regulate classical RAAS components including the mineralocorticoid receptor and angiotensinogen whilst upregulating the ratio of expression of angiotensin converting enzyme-2 to angiotensin converting enzyme-1. However, AMPK activation increased aldosterone secretion and the downstream target SGK1. Interestingly, angiotensin II, likely via the type 2 angiotensin II receptor, and angiotensin 1-7, likely via the Mas receptor, both increased AMPK activity. Despite this AMPK activation there was no effect of angiotensin 1-7 seen on inflammatory processes or insulin signalling in adipocytes so the functional effects of this AMPK activation remain unknown. Wild type and AMPKα1-/- mice were subjected to 12 weeks of high fat diet (HFD) with no significant metabolic differences. Interestingly, the adipose tissue from AMPKα1-/- mice fed chow diet showed increased basal inflammatory signalling which decreased following HFD suggesting a possible pro-inflammatory effect of AMPK upon HFD exposure. However, the systemic RAAS appeared to be upregulated in the AMPKα1-/- HFD group.

The cross-talk between AMPK and RAAS in adipose tissue likely has an important part to play in the development of obesity-related disorders and this work identifies several potential therapeutic avenues.

Acknowledgements

I must first thank my primary supervisor Dr. Ian Salt for his encouragement from the beginning of this process, his enthusiastic teaching and love of science made settling into the lab a pleasure. I would also like to express sincere thanks to Prof. Rhian Touyz, whose expertise and advice was crucial for the progression of this work. This PhD would not have been possible without the Sir George Alberti Research Training Fellowship funded by Diabetes UK for which I am truly grateful.

I would like to thank all members of the Salt and Touyz lab groups for their support, advice and technical help particularly during the time I was pregnant. Drs. Sarah Mancini and Aurelie Dinh Cat Nguyen provided a great deal of scientific advice and support as well as friendship over the years. Working in Lab 241 would not have been the same without Dr. Helen Heathcote and Dr. Jess Sadler who became great friends and were inspirational PhD students to follow.

Most of all I would like to thank my husband Richard and my parents who have supported my research interest from the beginning and provided a great deal of love and support. To my son Harris who may one day read this, thanks for learning how to sleep eventually and filling every day with joy.

Table of Contents

List of Figures and Tables

Declaration

I declare that the work presented in this thesis has been completed by myself, unless stated otherwise. It is entirely of my own composition and has not, in whole or in part, been submitted for any other degree.

Anna White

June 2018

List of Publications

Original articles

Almabrouk, T.A.M., White, A.D., Ugusman, A.B., Skiba, D.S., Katwan, O.J., Alganga, H., Guzik, T.J., Touyz, R.M., Salt, I.P., Kennedy, S. 2018. High Fat Diet Attenuates the Anticontractile Activity of Aortic PVAT via a Mechanism Involving AMPK and Reduced Adiponectin Secretion. Front Physiol, 9, 51.

Mancini, S.J., White, A.D., Bijland, S., Rutherford, C., Graham, D., Richter, E.A., Viollet, B., Touyz, R.M., Palmer, T.M., Salt, I.P. 2017. Activation of AMP-activated protein kinase rapidly suppresses multiple pro-inflammatory pathways in adipocytes including IL-1 receptor-associated kinase-4 phosphorylation. Mol Cell Endocrinol, 440, 44-56.

Review article

Dinh Cat, A.N., Friederich-Persson, M., White, A., Touyz, R.M. 2016. Adipocytes, aldosterone and obesity-related hypertension. J Mol Endocrinol, 57(1), F7-F21.

Abstracts

White, A.D., Dinh Cat, A.N., Montezano, A.C., Salt, I.P., Touyz, R.M. 2016. AMPK as a target for metabolic disorders: interactions with the renin-angiotensin-aldosterone system in adipocytes. The Lancet, 387, S105. Poster presentation.

White, A.D., Mancini, S.J., Dinh Cat, A.N., Montezano, A.C., Salt, I.P., Touyz, R.M. 2015. AMPK activators modulate pro-inflammatory responses in human adipocytes. Endocrine Abstracts, 38, P200. Poster presentation.

White, A.D., Dinh Cat, A.N., Montezano, A.C., Salt, I.P., Touyz, R.M. 2015. Activators of AMP-activated protein kinase regulate adipocyte aldosterone

secretion and mineralocorticoid receptor signalling. Endocrine Abstracts, 37, OC5.3. Oral presentation.

White, A.D., Dinh Cat, A.N., Montezano, A.C., Salt, I.P., Touyz, R.M. 2015. Regulation of adipocyte mineralocorticoid receptor expression and aldosterone secretion by activators of AMP-activated protein kinase. Diabetic Medicine 32, suppl 1, 30. Poster presentation.

Other presentations

European AMPK Workshop, Maastricht, Netherlands, 2015.
White, A.D., Mancini, S.J., Dinh Cat, A.N., Montezano, A.C., Salt, I.P., Touyz, R.M. Modulation of adipocyte inflammation by activators of AMP-activated protein kinase. Oral and poster presentation.

ADMIRE COST Meeting, Padua, Italy, 2014.
White, A.D., Dinh Cat, A.N., Mancini, S.J., Bijland, S., Montezano, A.C., Salt, I.P., Touyz, R.M. Regulation of mineralocorticoid receptor expression and aldosterone production by AMP-activated protein kinase in adipocytes. Poster presentation.

Council for High Blood Pressure Research, San Francisco, U.S.A, 2014.
White, A.D., Dinh Cat, A.N., Jenkins, C., Mancini, S.J., Montezano, A.C., Salt, I.P., Touyz, R.M. AMP-activated protein kinase activator AICAR attenuates TNFα-induced inflammation in murine adipocytes. Poster presentation.

List of Abbreviations

ACC	Acetyl-CoA carboxylase
ACE	Angiotensin converting enzyme
AICAR	5-Aminoimidazole-4-carboxamide ribonucleoside
AGT	Angiotensinogen
AMP	Adenosine monophosphate
AMPK	AMP-activated protein kinase
ang 1-7	Angiotensin 1-7
ang 1-9	Angiotensin 1-9
AP-1	Activator protein 1
ARB	Angiotensin receptor blocker
AS-160	Akt substrate of 160 kDa
AT1R	Angiotensin II type 1 receptor
AT2R	Angiotensin II type 2 receptor
ATP	Adenosine triphosphate
BAT	Brown adipose tissue
BMI	Body mass index
CaMKK	Calcium/calmodulin-dependent protein kinase kinase
cAMP	Cyclic-AMP
CCR2	C-C motif chemokine receptor type 2
CXCL-10	C-X-C motif chemokine 10; interferon-γ inducible protein 10
DGAT	Diacylglycerol acyltransferase
DHAP	Dihydroxyacetone phosphate
DMEM	Dulbecco's modified eagle medium
ELISA	Enzyme-linked immunosorbant assay
ERK	Extracellular signal-regulated kinase
EVAT	Epididymal visceral adipose tissue
FA	Fatty acid
FAS	Fatty acid synthase

FCS	Fetal calf serum
G3P	Glyceraldehyde 3-phosphate
GAPDH	Glyceraldehyde 3-phosphate dehydrogenase
GR	Glucocorticoid receptor
HDL	High density lipoprotein
HFD	High fat diet
HSL	Hormone sensitive lipase
IL	Interleukin
IRS	Insulin receptor substrate
JAK-STAT	Janus kinase/signal transducers and activators of transcription
JNK	c-Jun N-terminal kinase
LKB1	Liver kinase B1
LPL	Lipoprotein lipase
MAPK	Mitogen activated protein kinase
MCP-1	Monocyte chemoattractant protein 1
MEF	Mouse embryonic fibroblast
MR	Mineralocorticoid receptor
NCS	Newborn calf serum
NEFA	Non-esterified fatty acid
NF-κB	Nuclear factor kappa-light-chain-enhancer of activate B cells
NGAL	Neutrophil gelatinase-associated lipocalin
NOX	Nicotinamide adenine dinucleotide phosphate oxidase
PGC1α	PPAR γ coactivator 1-alpha
PI3-K	Phosphatidylinositol 3 kinase
PKA	Protein kinase A
PP2C	Protein phosphatase 2C
PPAR	Peroxisome proliferator activated receptor
RAS	Renin angiotensin system
RAAS	Renin angiotensin aldosterone system
ROS	Reactive oxygen species
SCUT	Subcutaneous adipose tissue

SGK-1	Serum and glucocorticoid-regulated protein kinase 1
SOCS3	Suppressor of cytokine signalling 3
STAT3	Signal transducer and activator of transcription 3
TAG	Triacylglycerol
TLR	Toll like receptor
TORC2	Transducer of regulated CREB protein 2
UCP	Uncoupling protein
VLDL	Very low density lipoprotein
VSMC	Vascular smooth muscle cell
WAT	White adipose tissue

1 Chapter 1 - Introduction

1.1 The impact of obesity

Obesity and diabetes are now two of the most important public health problems worldwide. In the UK, obesity and overweight associated problems cost the NHS £5 billion each year and diabetes treatment alone accounts for 10% of the NHS budget in England and Wales (£14 billion). Diabetes affects an estimated 347 million people worldwide (Danaei et al. 2011), with type 2 diabetes accounting for 90% of cases. Despite increased understanding of type 2 diabetes and newer medications becoming available the associated mortality is predicted to continue to rise, predominantly in developing countries (Mathers and Loncar, 2006). This is an area in huge need of improved understanding of aetiology and development of cure. Chronic inflammation in adipose tissue is hypothesised to contribute to insulin resistance and therefore further understanding adipose tissue biology may be the key to a future without type 2 diabetes. This chapter describes the relevant literature which had been reported prior to the outset of this study.

1.1.1 Metabolic impact of chronic obesity

Obesity is defined by a body mass index (BMI) greater than 30 kg/m^2 and describes a heterogeneous group of individuals at risk of major metabolic disturbance. However, a proportion of obese and severely obese (BMI > 40 kg/m^2) individuals do not develop significant metabolic upset or health complications. For the 75% of obese individuals who develop metabolic problems there are several mechanisms which lead to these changes. Insulin resistance is the primary metabolic change resulting in type 2 diabetes, hyperlipidaemia, non-alcoholic fatty liver disease and cardiovascular disease and understanding its development is therefore crucial. Several mechanisms are associated with insulin resistance with varying significance and therapeutic potential, in reality the importance of each likely varies between individuals. Such mechanisms, which will be discussed further, include inflammation (systemic and tissue specific), mitochondrial dysfunction, altered adipokine secretion and sensitivity, and reactive oxygen species (ROS) (Reviewed in Xu et al. 2013).

1.2 Adipose Tissue

Adipose tissue is a dynamic structure with a key role in energy homeostasis. Traditionally known as an energy storage tissue, its other properties such as the synthesis and secretion of hormones and cytokines have been well-described (Guilherme et al. 2008; Kershaw and Flier, 2004). Adipocytes are the predominant cell type in adipose tissue which also consists of the stromal vascular fraction made up of fibroblasts, immune cells and connective tissue (Bijland et al. 2013).

Adipose tissue is anatomically defined as visceral or subcutaneous, with visceral adiposity particularly associated with cardiovascular risk (Smith et al. 2012). Histologically, it is recognized as white adipose tissue (WAT) or brown adipose tissue (BAT) due to differences in the adipocytes – a unilocular lipid droplet is seen in WAT and multilocular lipid droplets in BAT (Bijland et al. 2013). Brown adipose tissue plays a major role in non-shivering thermogenesis and is reliant on uncoupling protein 1 (UCP-1) for this process (Bijland et al. 2013). Beige adipocytes have more recently been defined as multilocular adipocytes present in WAT which are UCP-1 positive and may be amenable to manipulation in future treatments of obesity (Wu et al. 2013).

1.2.1 Adipose tissue physiology

Maintenance of energy homeostasis requires harmonious communication between several organs including adipose tissue, liver, pancreas, skeletal muscle and areas of the central nervous system concerned with appetite regulation and energy expenditure. The primary function of adipose tissue is to store energy for future use; lipid stores also provide support for visceral structures. Dietary glucose and lipids not immediately required are stored in WAT as triacylglycerol via the process of lipogenesis.

1.2.1.1 Lipogenesis

The majority of lipid stores originate from circulating lipids – chylomicrons and very low density lipoproteins (VLDL) release fatty acids in the presence of

lipoprotein lipase (LPL) at the surface of adipocytes (Sadur and Eckel, 1982). Fatty acids enter the adipocytes where they undergo esterification with Coenzyme A by fatty acyl-CoA synthetase (Watkins, 1997). Glyceryl phosphate acyltransferase catalyses the addition of two fatty acids to glycerol-3-phosphate (G3P) forming phosphatidate. Phosphatidate is hydrolysed to diacylglycerol which is further acylated by diacylglycerol acyltransferase (DGAT) yielding triacylglcerol (TAG) (Coleman and Lee, 2004).

Glucose is the other energy source stored as TAG in adipocytes. On entering the cytoplasm glucose undergoes glycolysis forming dihydroxyacetone phosphate (DHAP) which can be converted to G3P and therefore used to form phosphatidate as described above (Nye et al. 2008). Circulating glucose can also be utilized to form fatty acids for lipogenesis, whereby the 3 carbon intermediates continue through glycolysis to form pyruvate which is converted to acetyl-CoA in the mitochondria. After transfer of acetyl-CoA to the cytoplasm, acetyl-CoA carboxylase (ACC) and fatty acid synthase (FAS) catalyse the conversion of acetyl-CoA and malonyl-CoA to long chain fatty acids (Tong, 2005). Figure 1.1 summarises the main steps in lipogenesis.
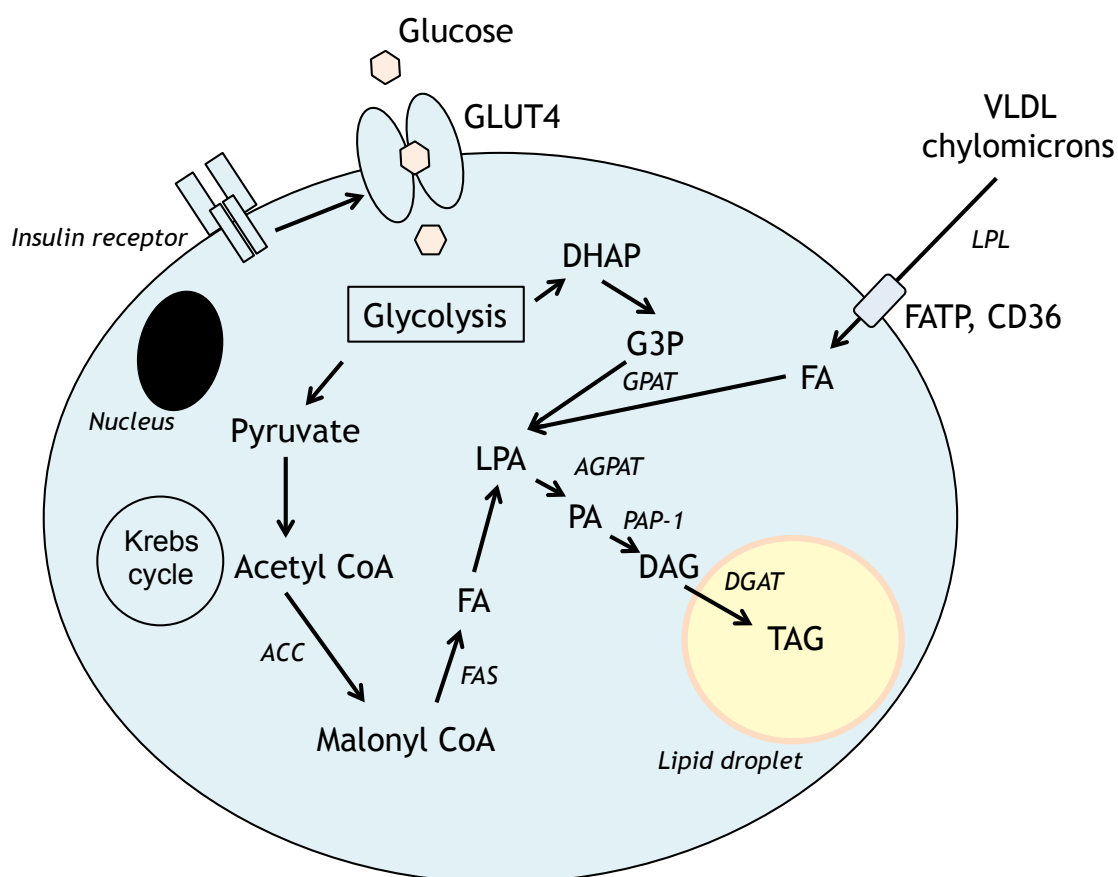
Figure 1.1 Key steps in lipogenesis

Circulating fatty acids enter the adipocyte and combine with G3P to form triglyceride in the lipid droplet. Glucose undergoes glycolysis within the adipocyte which produces either DHAP or pyruvate. Pyruvate can be converted into acetyl CoA and go on to produce fatty acids. G3P and fatty acids are processed to lysophosphatidic acid (LPA), phosphatidic acid (PA), diacylglycerol (DAG) then triglyceride (TAG). Key enzymes in this process include glycerol-3-phosphate acyltransferase (GPAT), acylCoA acylglycerol-3-phosphate acyltransferase (AGPAT), phosphatidic acid phosphatase (PAP-1) and diglyceride acyltransferase (DGAT). Figure compliments body text (Saponaro et al. 2015).

1.2.1.2 Lipolysis

In the fasted state energy can be released from stores in adipose or liver. Lipolysis, the breakdown of triglycerides to form glycerol and three free fatty acids, is a catabolic process under exquisitely tight inhibitory control by

insulin and stimulated by catecholamines (Czech et al. 2013). In adipocytes, an increase of intracellular cAMP in response to catecholamines leads to activation of protein kinase A (PKA) which subsequently phosphorylates hormone sensitive lipase (HSL) and perilipins (Collins et al. 2004). The action of HSL is blocked when perilipins are in place covering the lipid droplet. Once HSL and perilipins are phosphorylated, HSL is free to hydrolyse TAG forming diacylglycerides and monoacylglycerides. Monoglyceride lipase is required for the final step of monoacylglyceride hydrolysis into non-esterified fatty acids (NEFAs) (Fredrikson et al. 1986). These steps are summarised in Figure 1.2.
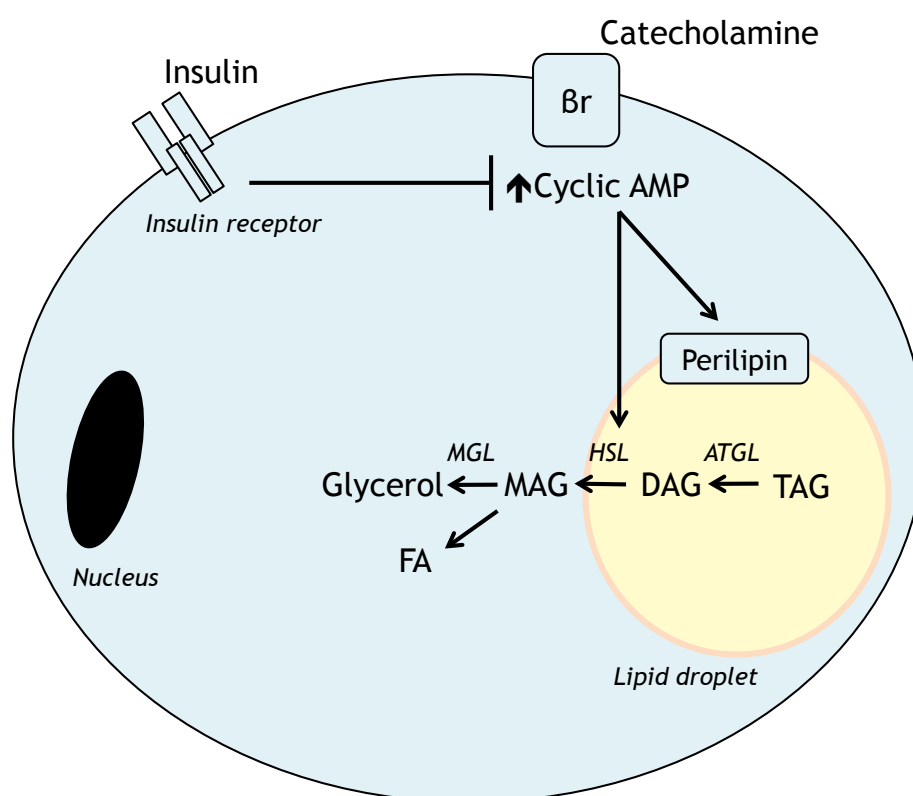
Figure 1.2 Key steps in lipolysis

Triglycerides are broken down to form glycerol and fatty acids following catcholamine stimulation and the phosphorylation of HSL and Perilipin by cAMP. Insulin inhibits this process by suppressing cAMP levels. Key enzymes include adipose triacylglycerol lipase (ATGL), hormone sensitive lipase (HSL) and monoacylglycerol lipase (MGL) (Saponaro et al. 2015).

1.2.1.3 Regulation of lipogenesis and lipolysis by insulin

Insulin is a key anabolic hormone facilitating lipogenesis and inhibiting lipolysis. Insulin signalling via phosphoinositol 3-kinase (PI3 kinase) facilitates glucose transporter GLUT4 translocation to the adipocyte plasma membrane allowing influx of glucose (Cheatham et al. 1994; Huang and Czech, 2007). Insulin also stimulates gene expression of FAS and activates ACC thus facilitating TAG synthesis. As mentioned in 1.2.1.2, catecholamines stimulate beta-adrenergic G-protein coupled receptors leading to increased intracellular cAMP and PKA phosphorylation allowing HSL and perilipin phosphorylation and mobilisation of triglycerides. Insulin acts to inhibit lipolysis by decreasing intracellular cAMP and resultant PKA phosphorylation thereby preventing the action of HSL and allowing perilipins to block HSL access to TAGs (Czech et al. 2013).

1.2.1.4 Importance of adipose tissue

The metabolic and immune functions of adipose tissue are abundant. Once calorific intake exceeds the storage capacity of adipose tissue or there is a lack of adipose tissue altogether, as in lipodystrophy, ectopic deposition of lipid has catastrophic effects. Storage of lipids in the liver, skeletal muscle and multiple other metabolic sites leads to gross dysregulation in glucose metabolism and severe impairment of insulin signalling in addition to causing liver disease including cirrhosis (Semple et al. 2011). Interestingly, leptin replacement in such indivisuals with lipodystrophy, where circulating leptin is absent or very low, improves the metabolic problems outlined above (Moon et al. 2013).

1.2.2 Insulin, insulin resistance and type 2 diabetes

Type 2 diabetes is a chronic metabolic disorder diagnosed when hyperglycaemia is detected. Glucose homeostasis is governed primarily by the peptide hormone insulin. Type 2 diabetes develops after years of insulin resistance and reactive hyperinsulinaemia when the pancreas can no longer produce enough insulin to meet the demands of peripheral tissues and

metabolic dysfunction ensues (van Greevenbroek et al. 2013). Type 1 diabetes is an autoimmune condition resulting in insulin deficiency and therefore hyperglycaemia (Vehik et al. 2013).

1.2.2.1 Insulin

Insulin is an essential peptide hormone released from ß cells in the islets of Langerhans which consist of 2-3% of the pancreas volume. Insulin synthesis begins with pre-proinsulin (11.5kDa, 86 amino acids) which is cleaved to form proinsulin (9kDa). Proinsulin is then cleaved further to form insulin (a 21 amino acid A chain bound to a 30 amino acid B chain by disulphide bonds) and c-peptide (30-35 amino acids). Insulin and c-peptide are stored together in secretory vesicles prior to release in response to secretagogues. Transcription of pre-proinsulin mRNA is stimulated by high circulating glucose concentrations. Furthermore, as the circulating glucose concentration rises it stimulates insulin secretion, with a threshold plasma glucose concentration of approximately 5mmol/l. In addition to glucose a number of other agents can stimulate or inhibit insulin secretion including amino acids, fatty acids and hormones. Insulin enters the portal circulation and binds membrane bound insulin receptors in target tissues (Reviewed in Holt et al. 2010).

1.2.2.2 Insulin receptor and signalling

The primary action of insulin is to regulate serum glucose levels. In response to high plasma glucose concentrations insulin acts to stop the production of glucose by the liver and increase glucose transit via the glucose transporter GLUT4 into cells of striated muscle and adipose tissue, thereby normalizing plasma glucose concentrations (van Greevenbroek et al. 2013).

Circulating insulin mediates it's action through the insulin receptor, a member of the receptor tyrosine kinase family formed of a heterotetramer consisting of two extracellular α subunits and two membrane spanning ß subunits (Lee and Pilch, 1994). Binding to the receptor results in tyrosine kinase activation and autophosphorylation of the cytoplasmic domains of the ß subunits. The phosphotyrosine residues act as binding motifs to allow

recruitment and subsequent phosphorylation of intracellular proteins such as the insulin receptor substrates (IRSs). IRSs are then able to recruit effector proteins such as PI3 kinase (Czech et al. 2013).

In adipocytes insulin increases glucose uptake, stimulates adipogenesis and inhibits lipolysis. Following phosphorylation of IRS1 or IRS2, downstream signalling is mediated initially via PI3 kinase which catalyses the formation of phosphatidylinositol 3,4,5-trisphosphate, which acts to recruit and activate both atypical protein kinase C and Akt at the plasma membrane (Czech et al. 2013). Akt is a serine/threonine protein kinase that phosphorylates and inactivates the Rab GTPase activating protein, AS160. As a consequence, Rab proteins remain GTP-bound and stimulate subsequent GLUT4 translocation to the cell surface. Glucose enters via GLUT4 and is then processed to form triacylglycerol as described in 1.2.1.1 (Figure 1.3).

Insulin signalling can prevent catecholamine mediated lipolysis by influencing cAMP levels. This is mediated via Akt-mediated phosphorylation and activation of phosphodiesterase 3B which lowers cAMP levels. Secondly, insulin has been reported to activate adipose specific phospholipase A2 which inhibits adenylate cyclase, similarly reducing catecholamine-stimulated cAMP levels (Czech et al. 2013).
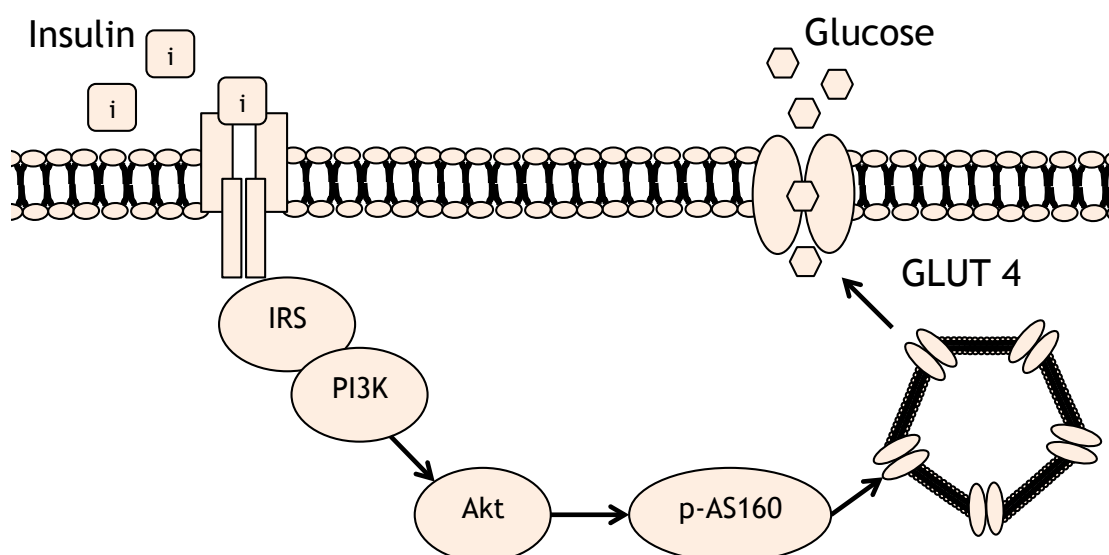
Figure 1.3 Insulin signalling

Insulin binds to its tyrosine kinase receptor instigating a signalling cascade through PI3-kinase, Akt and AS160 to ultimately translocate vesicles containing GLUT4 to the cell membrane allowing glucose influx.

1.2.2.3 Insulin resistance

Insulin resistance occurs when cells no longer respond appropriately to insulin. It is associated with obesity, metabolic syndrome and is a key component of type 2 diabetes. Within adipose tissue, insulin resistance has been reported to occur when factors interfere with insulin receptor levels or the sensitivity of the insulin signalling pathway. Hyperinsulinaemia has been associated with reduced expression of insulin receptors leading to reduced insulin signalling (Puig and Tjian, 2005). Furthermore, inhibitory phosphorylation of IRS1 on serine residues has been proposed to occur in response to proinflammatory signalling, mediated by c-Jun N-terminal kinase (JNK) and inhibitor of kappa B kinase (IKK) (Copps and White, 2012). Selective insulin resistance plays a key role in the pathogenesis of diabetes complications. This was first described in the liver when the inhibitory effect of insulin on gluconeogenesis (via FoxO1) is impaired whilst the lipogenic effect (via SREBP-1c) is unimpaired leading to hyperglycaemic and lipotoxicity commonly seen in poorly controlled type 2 diabetes (Shimomura et al. 2000,

Brown and Goldstein, 2008). Laterally this concept has also been described in endothelial cells. Endothelial dysfunction is a key characteristic of type 2 diabetes and contributes significantly to its cardiovascular complications. Insulin signalling in endothelial cells occurs via two pathways, on results in nitric oxide production and vasorelaxation (via PI3K) and the other results in endothelin-1 and vasoconstriction (via MAPK). Selective impairment of PI3K signalling is associated with type 2 diabetes leading to uncontrolled MAPK signalling and endothelial dysfunction (Muniyappa and Sowers, 2013).

1.2.3 Adipose tissue as an endocrine organ

In addition to the energy storage function of adipose tissue, recent decades have seen a substantial expansion in understanding of the dynamic role adipose tissue has in the regulation of metabolism. At least 600 factors are now known to be secreted by adipose tissue, termed adipokines, which may exert endocrine, paracrine and autocrine actions that influence metabolism (Blüher, 2012).

1.2.3.1 Leptin

The growing understanding of the secretory role of adipose tissue stems from the discovery of leptin in 1994 (Mantzoros et al. 2011). Leptin is a member of the type 1 helical cytokine family (Denver et al. 2011) and plays a key role in the control of satiety acting as an anorexigenic stimulus to the hypothalamus. Children with leptin deficiency due to genetic mutation of the leptin gene also exhibit hyperphagia and obesity and respond very well to treatment with leptin (Farooqi et al. 2002). It is secreted by adipocytes and positively correlates with adipose mass, although with increasing obesity, resistance to its actions develops (Banks and Farrell, 2003). Leptin deficient ob/ob and leptin receptor deficient db/db mice are obese and insulin resistant (Lutz and Woods, 2012). Leptin has been reported to have pro-inflammatory actions, activating monocytes and macrophages to secrete interleukin-6 (IL-6) and tumour necrosis factor-α (TNF-α) (Paz-Filho et al. 2012). Unfortunately, the therapeutic use of leptin in this obesity-related leptin resistance has not been

successful and is likely related to alterations in the leptin receptor and downstream signalling changes (Moon et al. 2013).

1.2.3.1.2 Central regulation of adipose tissue

The hypothalamus contains both satiety and hunger centres under the influence of leptin, and other factors, via its receptor in the arcuate nucleus. A series of neuropeptide signals are activated by leptin via PI3K signalling culminating in the paraventricular nuclei. This activity in turn stimulates the autonomic nervous system to increase sympathetic stimulation of adipose tissue resulting in increased lipolysis and thermogenesis (Breton, 2013). Beta-adrenergic stimulation of white adipose tissue also stimulates glucose uptake (Nonogaki, 2000). The parasympathetic nervous system plays a role in adipose tissue function with associated increased insulin sensitivity (Fliers et al. 2003).

1.2.3.2 Adiponectin

Another key adipokine that regulates metabolism is adiponectin, the most abundantly produced of the adipokines. Levels of adiponectin are inversely related to adipose mass and insulin resistance (Díez and Iglesias, 2003). Adiponectin activates AMP-activated protein kinase (AMPK) and has anti-inflammatory properties (Kadowaki et al. 2006). Expression of adiponectin is stimulated by peroxisome proliferator-activated receptor-γ (PPARγ) agonists and inhibited by pro-inflammatory mediators such as TNF-α, IL-6 and reactive oxygen species (ROS) (Kwon and Pessin, 2013). The use of adiponectin as a biomarker and as a therapeutic agent remains a topic of interest however one that has not been translated to the clinic (Padmalayam and Suto, 2013).

1.2.4 Adipose tissue inflammation

In addition to the adipokines described in 1.2.3, adipose tissue has also been shown to secrete several members of the cytokine family. In both animal and human studies adipose tissue inflammation has been closely correlated with obesity and insulin resistance (Glass and Olefsky, 2012; Guilherme et al.

2008). More recently it has been suggested that it is insulin resistance which underlies adipose tissue inflammation rather than inflammation leading to insulin resistance (Shimobayashi et al. 2018).

1.2.4.1 Cytokines

Cytokines are proteins with immunomodulatory properties which can have local or systemic actions. They may be pro- or anti-inflammatory and can be released from resident macrophages and/or adipocytes or other cell types in adipose tissue. Obesity is associated with an increased number of pro-inflammatory cytokines including TNF-α, IL-6, interleukin-1ß (IL-1ß) and the chemokine monocyte chemotactic protein-1 (MCP-1) (Tateya et al. 2013).

1.2.4.1.1 Tumour necrosis factor-α

TNF-α is a pro-inflammatory cytokine secreted primarily by macrophages but can be released by multiple other cells (Qi and Pekala, 2000). Two TNF-α receptors have been identified – TNF receptors 1 and 2, with most known actions mediated via TNFR1 (Wajant et al. 2003). TNF-α is important in the acute phase immune response and governs cell survival, production of other cytokines and regulates inflammation at a local and systemic level (Haider and Knöfler, 2009). In adipose tissue, TNF-α mediates it's actions via two complimentary pro-inflammatory signalling pathways which will be discussed in more detail later: the mitogen-activated protein kinases (MAPKs) and nuclear factor kappa-light-chain-enhancer of activated B cells (NFκB) activation (Wajant et al. 2003). TNF-α levels are positively correlated with obesity and insulin resistance and rodent studies show insulin sensitising effects of TNF neutralisation (Hotamisligil et al. 1993). In humans anti-TNF therapies are used for a selection of chronic inflammatory disorders such as rheumatoid arthritis. In a group of obese individuals with type 2 diabetes, 4 weeks of anti-TNF-α therapy did not improve insulin sensitivity (Ofei et al. 1996). However, following 6 months of the TNF-α receptor fusion protein etanercept, a group of obese subjects with metabolic syndrome were found to have improved fasting glucose and increased adiponectin levels (Stanley et al.

2011). This suggests prolonged treatment is required to see a metabolic benefit.

1.2.4.1.2 Interleukin-1ß

IL-1ß is initially released as a proprotein by macrophages and is cleaved to its active form by caspase 1 (Denes et al. 2012). Early studies reported that IL-1ß reduced both insulin-induced glucose transport and lipogenesis in murine and human adipocytes (Lagathu et al. 2006). Subsequently prolonged exposure of the 3T3-L1 adipocyte cell line to IL-1ß was reported to lead to down-regulation of IRS1 and reduced downstream activity of Akt and phosphorylation of AS-160, an effect not seen with short term exposure. Inhibition of ERK 1/2 signalling prevented the reduction in IRS-1 expression, suggesting a key role of ERK 1/2 in this process (Jager et al. 2007). In addition, Handa et al. reported that application of an anti-IL1ß monoclonal antibody to 3T3-L1 cells treated with IL-1ß prevented insulin resistance (Handa et al. 2013).

1.2.4.1.3 Interleukin-6

Interleukin-6 is another member of the cytokine superfamily implicated in obesity related adipose dysfunction and insulin resistance. IL-6 can be secreted by adipocytes and the stromal vascular fraction of adipose tissue (Kwon and Pessin, 2013). Visceral adipose tissue has been reported to secrete 2-3 times more IL-6 than subcutaneous adipose (Fried, 1998). Circulating levels of IL-6 are positively correlated with obesity and insulin resistance and around one third of the circulating IL-6 originates from adipose tissue (Kershaw and Flier, 2004). There are a number of mechanisms proposed by which IL-6 promotes insulin resistance. IL-6 lowers adiponectin levels and induces SOCS3 which can attenuate insulin signalling (Kwon and Pessin 2013; Senn et al. 2003). Conversely, in the central nervous system IL-6 appears to stimulate exercise and lead to weight loss suggesting different roles centrally compared to the periphery (Wallenius et al. 2003). IL-6 signalling is mediated via the Janus Kinase and Signal Transducer and Activator of Transcription (JAK-STAT) pathway which is described in 1.2.4.2.4.

1.2.4.1.4 Monocyte chemoattractant protein-1

Circulating levels of the chemokine MCP-1 are also positively correlated with obesity and insulin resistance (Panee, 2012). MCP-1 is one of the key stimuli for monocyte recruitment into adipose tissue and both adipocytes and macrophages may release MCP-1 (Gustafson, 2010). Overexpression of MCP-1 in adipose tissue was associated with insulin resistance and adipose macrophage infiltration in a transgenic mouse model (Kamei et al. 2006). It signals to monocytes via the C-C motif receptor 2 (CCR2). Studies have suggested a key role for CCR2 in adipose tissue inflammation as knock-down in macrophages resulted in reduced inflammation in adipose tissue (Weisberg et al. 2006).

1.2.4.2 Inflammatory signalling pathways

As mentioned previously, there are different signalling pathways of interest in the development of adipose tissue inflammation, the MAPKs, NFκB and the JAK-STAT pathways. The MAPK and NFκB pathways culminate in the transcription of pro-inflammatory genes as summarised in Figure 1.4.
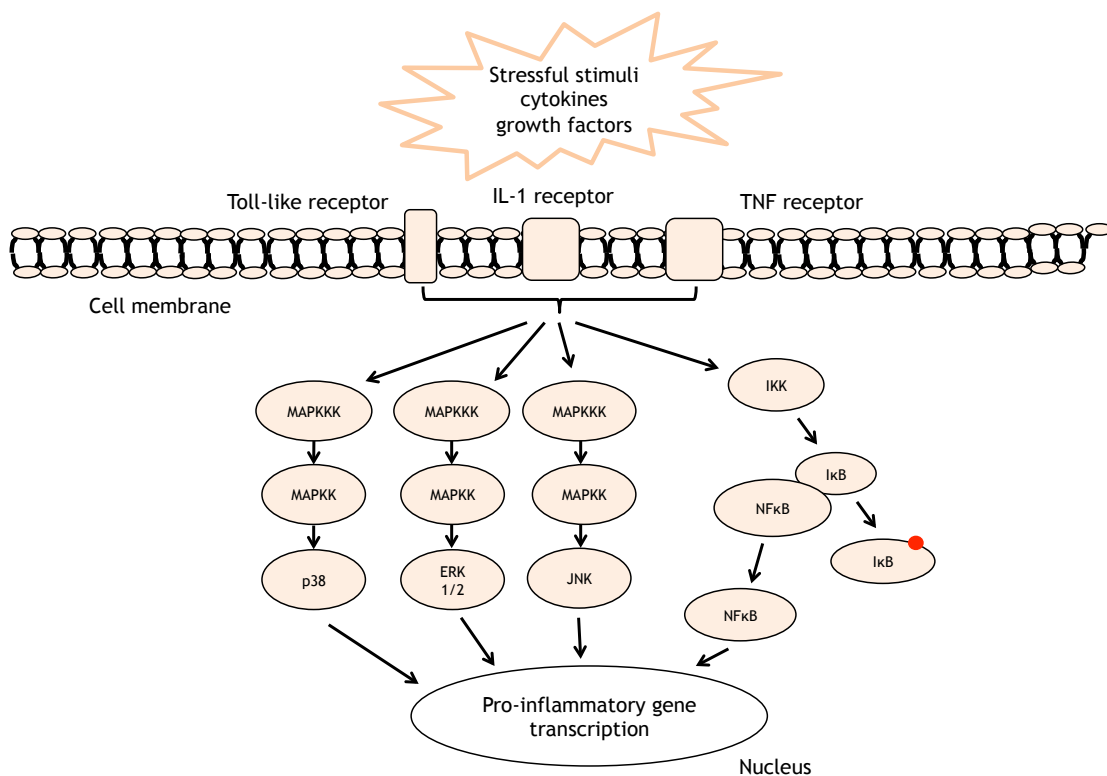
Figure 1.4 MAPK and NFκB signalling pathways

Pro-inflammatory signalling stimulated by cytokines and other factors occurs following receptor binding. The NFκB and MAPK pathways ultimately change gene transcription to increase production of pro-inflammatory proteins which may then enter the local and systemic environment.

1.2.4.2.1 Mitogen-activated protein kinases

MAPK signalling can be stimulated by a wide range of stimuli acting through cytokine or toll like receptors (TLRs) in order to regulate a multitude of functions such as proliferation, cell survival and gene expression (Thalhamer et al. 2008). The classic MAPKs require at least two phosphorylation events prior to activation, catalyzed by MAPK kinases (MAPKKs). MAPKs are present throughout eukaryotes and the principal types that regulate inflammatory pathways in humans are extracellular signal-regulated kinase 1/2 (ERK 1/2), JNK and p38. JNK activation is the MAPK most closely linked to insulin resistance (Tarantino and Caputi, 2011). JNK phosphorylates activator protein-1 (AP-1) resulting in the transcription of pro-inflammatory genes, it has also been proposed to directly phosphorylate IRS-1 on inhibitory Ser

residues, resulting in degradation and diminished insulin signalling (Aguirre et al. 2000).

1.2.4.2.2 NFκB

NFκB is recognized as a key pro-inflammatory transcription factor and mediator of TNF-α and IL-1ß action (Salt and Palmer, 2012). It is regulated by inhibitor of NFκB (IκB) and IκB kinase (IKK). Under basal conditions, IκB binds to NFκB dimers, such that they are maintained in the cytoplasm and upon phosphorylation of IκB, NFκB dimers (such as p50-p65) are released and able to translocate to the nucleus resulting in transcription of pro-inflammatory genes. Within the nucleus NFκB can work in conjunction with AP-1 leading to transcription of κB regulated genes such as IL-6, TNF-α and IL-1ß. IKK activation is also associated with insulin resistance due to its potential phosphorylation of IRS-1 on inhibitory Ser residues (similar to JNK) (Gao et al. 2002).

1.2.4.2.3 JAK-STAT signaling

IL-6 mediates its pro-inflammatory effects via JAK-STAT signalling involving increased phosphorylation of STAT3. JAK-STAT signaling is not always pro-inflammatory and is a signalling mechanism also employed by the anti-inflammatory cytokine IL-10 (Niemand et al. 2003). Binding of IL-6 to a trans-membrane IL-6 receptor (a class 1 cytokine receptor) or a soluble IL-6 receptor leads to homodimerisation of the signal transducing receptor gp130 subunits, leading to activation of JAKs which phosphorylate tyrosine residues on the cytoplasmic domains of gp130 (Murakami et al. 1993). These phospho-tyrosine motifs act as the docking site for STATs, (STAT3 in the case of IL-6) which undergo JAK-mediated phosphorylation resulting in STAT3 dimers which translocate to the nucleus and facilitate transcription of target genes including MCP-1. STAT3 activation also induces suppressor of cytokine signalling 3 (SOCS3), which acts as a negative feedback loop to interrupt JAK-STAT signalling (Schmitz et al. 2000).

1.2.4.3 Reactive oxygen species

Increased levels of ROS including superoxide, hydrogen peroxide and hydroxyl radicals are described in a rapidly expanding group of biological processes including diabetes (Sedeek et al. 2012). Production of ROS can be stimulated by a number of extra- and intracellular stimuli including the pro-inflammatory cytokines described above and ROS can stimulate pro-inflammatory signalling pathways which in turn increase production of these cytokines (Bashan et al. 2009). ROS have been implicated in the pro-inflammatory state associated with obesity and the development of type 2 diabetes. In particular, NADPH oxidase (NOX), a key source of ROS, is a multiprotein complex which is upregulated in diet induced obesity in rats (Jiang et al. 2011). NOX4 is present in adipocytes and increases ROS in response to high glucose and palmitate (Han et al. 2008). The mitochondria are an additional source of ROS and particularly relevant in the context of mitochondrial dysfunction which is associated with insulin resistance (Fisher-Wellman & Neufer, 2012). ROS is reported to increase adipose insulin resistance and contribute to obesity (Rudich et al. 1998, Pires et al. 2013).

1.2.4.4 Adipose tissue macrophages

Macrophages are phagocytes which result from differentiation of monocytes when they are resident in tissues. The primary stimulus for recruitment into adipose is MCP-1 however other stimuli have been identified including activated T cells, endoplasmic reticulum stress and α4 integrin (Patel et al. 2013). In lean adipose tissue, macrophages make up around 10% of the stromal vascular fraction and function in an alternatively activated capacity resulting in anti-inflammatory cytokine production, these have also been known as M2 macrophages. In obesity, it has been demonstrated that macrophage number increases to around 40% of adipose tissue cells and there is a phenotypic switch to M1, classically activated pro-inflammatory macrophages (Cildir et al. 2013). The key pro-inflammatory role of macrophages in WAT was first proposed by Xu et al who carried out profiling of multiple murine obesity and diabetes models (Xu et al. 2003). Interestingly, histological analysis of obese adipose tissue has identified discrete entities

named crown like structures where macrophages exist in clusters surrounding necrotic adipocytes (Cinti et al. 2005).

1.3 AMP- activated protein kinase

AMPK was discovered following a series of experiments in the 1970s and 1980s by separate groups in which ATP was found to inactivate both ACC and HMG-CoA reductase, subsequently the protein kinase AMPK was found to be responsible for both of these actions (Hardie, 2003). AMPK is a heterotrimeric serine/threonine protein kinase which acts as a key regulator of whole body energy status. It consists of 3 subunits: the catalytic alpha subunit of which there are two isoforms (α_1 and α_2) and the regulatory beta (β_1, β_2) and gamma (γ_1, γ_2, γ_3) subunits. Therefore, 12 possible hetero trimer isoforms of this kinase exist which may determine behaviour. Indeed, distribution of the α_1 subunit is primarily found in adipose tissue, with α_2 being found in striated muscle (cardiac and skeletal) (Bijland et al. 2013, Quentin et al. 2011). The γ subunit contains the AMP binding site for allosteric AMPK activation. Two AMP binding sites, known as Bateman domains, are present beyond a variable N-terminal region on each γ subunit (Bateman, 1997). These sites have a high affinity for AMP and lower affinity for ATP therefore high concentrations of ATP may inactivate AMPK (Towler and Hardie, 2007). The structure of AMPK is depicted in Figure 1.5.
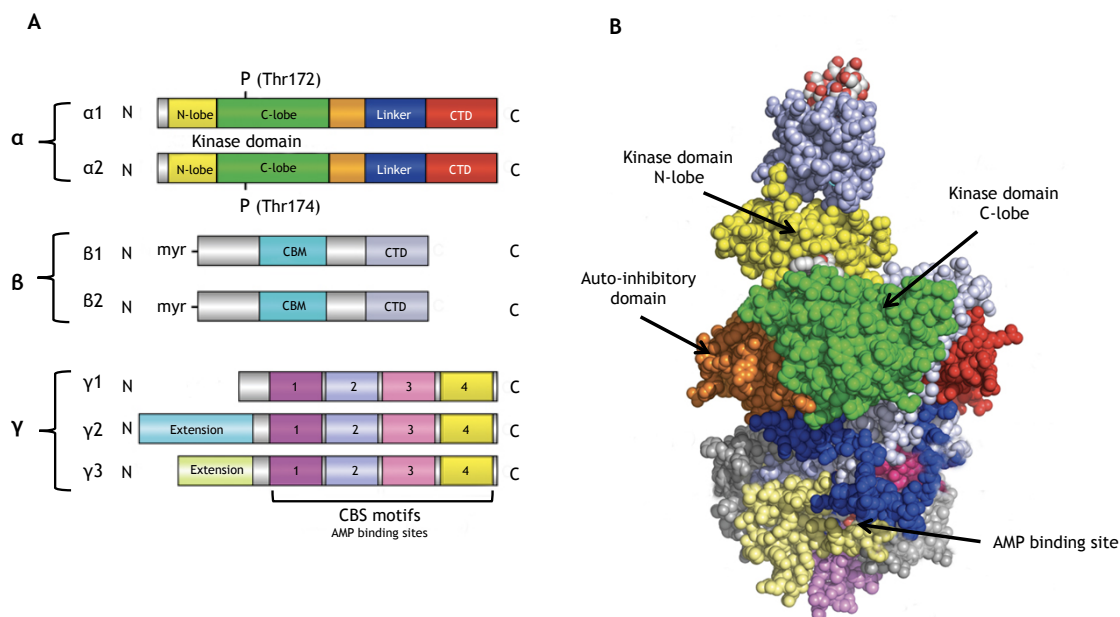
Figure 1.5 Structure of AMPK

A. AMPK subunit isoforms and B. structure of human AMPK (α1ß2γ1 complex). The two figures are colour-linked detailing common component structures. Mutations have been identified in the PRKAG2 gene encoding AMPK-γ2 leading to cardiac conditions such as pre-excitation, excess glycogen storage and cardiac hypertrophy. CBM = carbohydrate binding molecule, CTD = C-terminal domain, CBS = cystathionine ß-synthetase. Figure adapted from Salt and Hardie, 2017.

1.3.1 AMPK activation

AMPK is activated by phosphorylation of the preserved Thr172 residue in the N terminus of the α subunit in addition to allosteric activation by 5'-AMP binding to the γ subunit. There are two upstream kinases known to phosphorylate Thr172: liver kinase B1 (LKB1) and calmodulin-dependent kinase kinase ß (CaMKKß) (Salt and Palmer, 2012). LKB1 is constitutively active and not affected by AMP levels (Sakamoto et al. 2004), Thr172 phosphorylation may be decreased, however, by phosphatases such as protein phosphatase 2C (PP2C). AMP binding to the γ subunit aids activation by enhancing Thr172 phosphorylation and inhibiting PP2C. This property is antagonised by ATP which has a weaker affinity for the AMP binding site. The intracellular AMP:ATP ratio is therefore crucial for the activation status of AMPK. As

activation of AMPK is possible in the absence of LKB1, CaMKKß was subsequently identified as an alternative upstream kinase, stimulated by increased intracellular Ca^{2+} concentrations (Hawley et al. 2005).

1.3.2 Regulators of AMPK

As described above, the ratio of AMP:ATP within cells is a crucial regulator of AMPK activation. Therefore, any process resulting in decreased ATP levels or increased AMP levels will lead to activation of AMPK. Stresses such as hypoxia, ischaemia and hypoglycaemia inhibit the production of ATP and thereby stimulate AMPK activation (Hardie, 2008). Consequently, exercise has also been shown to activate AMPK in skeletal muscle due to the increased consumption of ATP. This may mediate some of the beneficial metabolic effects of exercise including increased glucose uptake and fatty acid oxidation (Sakamoto et al. 2004). In addition to the energy status within cells, several circulating factors can regulate AMPK activation, which are described below. Figure 1.6 summarises the range of mechanisms regulating AMPK.

1.3.2.1 Adipokines

Adiponectin has been shown to activate both α_1 and α_2 containing AMPK heterotrimers in the liver and skeletal muscle mediating beneficial metabolic effects of this adipokine (Yamauchi et al. 2002). In the liver, AMPK activation by adiponectin inhibits gluconeogenesis and in skeletal muscle it facilitates glucose uptake. The experimental use of dominant negative mutants of AMPK confirmed this as the mechanism by which these effects were achieved (Andreelli et al. 2006).

Leptin has also been demonstrated to activate AMPK within skeletal muscle (Steinberg et al. 2003), but this action is diminished in obese skeletal muscle (Steinberg et al. 2002). As described previously, obesity is associated with resistance to leptin. Leptin has the opposite effect on AMPK in the hypothalamus where it decreases appetite via AMPK inhibition (Lim et al. 2010).

The pro-inflammatory cytokine TNF-α has been reported to decrease AMPK activation in skeletal muscle *in vitro* and *in vivo*, whereby the mechanism is proposed to be by increased transcription of the phosphatase PP2C leading to AMPK dephosphorylation and inactivation (Steinberg et al. 2006).

1.3.2.2 Pharmacological activators

AMPK activation has been demonstrated in response to several prescribable agents for type 2 diabetes, including metformin and thiazolidinediones. Interestingly these are the two agents with insulin sensitising properties. The anti-inflammatory agent salicylate, which is known to have metabolic benefits, has also been shown to activate AMPK (Steinberg et al. 2013).

Metformin, a biguanide, is the first line oral medication for type 2 diabetes, it decreases hepatic gluconeogenesis however the exact mechanism of action has been somewhat elusive. It activates AMPK by interruption of the mitochondrial respiratory chain resulting in reduced ATP production and raised AMP:ATP ratio (Boyle et al. 2010). Metformin has been shown to activate AMPK in human adipose tissue from subjects with diabetes (Boyle et al. 2011). Despite this, data from mice lacking AMPK in the liver show that the metformin related reduction in hepatic gluconeogenesis is AMPK-independent and has been attributed to other mechanisms including reduced glucagon signalling (Rena et al. 2013).

Thiazoladinediones (TZDs) are PPARγ agonists and potent insulin sensitisers used to treat type 2 diabetes and other insulin resistant conditions. Their clinical use has now reduced due to associated adverse effects including fluid retention which can precipitate heart failure and reduced bone mineral density. They have been shown to increase adiponectin production (Astapova and Leff, 2012) which has beneficial metabolic effects mediated through AMPK as previously described. Additionally, the TZD rosiglitazone shown to stimulate AMPK, via LKB1, in endothelial cells and increase nitric oxide synthesis in an AMPK-dependent manner (Boyle et al. 2008). Studies in cultured cells expressing an AMP-insensitive AMPKγ2 isoform have indicated

that troglitazone also activates AMPK by increasing AMP:ATP (Hawley et al. 2010)

Salicylate was shown to activate AMPK by Hawley et al. *in vitro* and *in vivo*, mediated primarily by prevention of Thr172 dephosphorylation. They found increased fatty acid utilisation *in vivo* with salicylate in wild type mice but not AMPK β_1 knock-out mice, whereas improvements in carbohydrate metabolism were seen in both wild type and AMPK β_1 knock-out mice, suggesting both AMPK-dependent and -independent effects of salicylate (Hawley et al. 2012).

Experimentally two small molecule activators have been widely-used to manipulate AMPK activity. 5'-aminoimidazole-4-carboxamide riboside (AICAR) is a nucleoside that is converted to the AMP-mimetic ZMP within cells, and has been widely used in studies of AMPK both *in vitro* and *in vivo*. However, as it mimics AMP it has been shown to have a number of AMPK-independent effects (López et al. 2003) which may reflect actions on other AMP-dependent enzymes. The more specific activator A-769662 is a thienopyridine which binds to AMPK complexes containing the β_1 subunit (Scott et al. 2008) resulting in allosteric activation and, similar to salicylate, inhibition of Thr172 dephosphorylation.
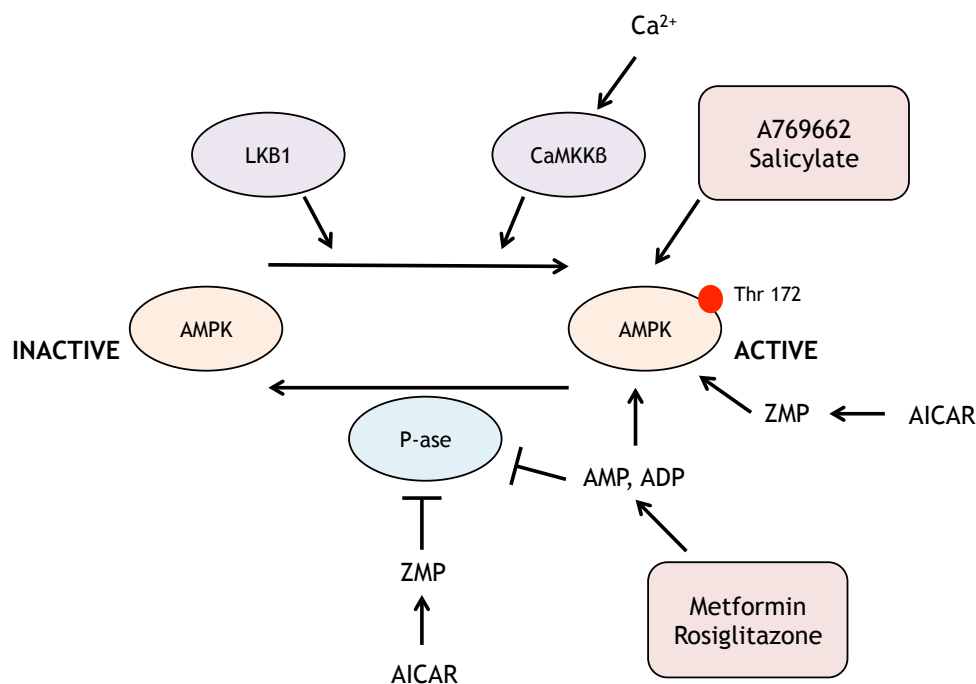
Figure 1.6 Regulation of AMPK

AMPK is activated by upstream kinases LKB1 and CaMKKß or through allosteric AMP binding to the γ subunit. Phosphatases inactivate AMPK and are inhibited by AMP. Pharmacological agents such as metformin and AICAR act to increase AMP levels or mimic AMP whereas A769662 and salicylate bind to complexes containing the ß1 subunit isoform.

1.3.3 AMPK: regulator of metabolism

The primary actions of AMPK are to conserve energy – this can be achieved by inhibiting anabolic pathways and stimulating catabolic activities (see Figure 1.7). Two of the best-characterised substrates of AMPK are ACC and HMG-CoA reductase which are key steps in lipid metabolism and cholesterol synthesis respectively. Activation of AMPK leads to phosphorylation and inactivation of ACC resulting in increased fatty acid oxidation and reduced fatty acid and triglyceride synthesis (Bijland et al. 2013).

1.3.3.1 AMPK in liver metabolism

AMPK activation can influence both lipid and glucose metabolism in the liver. Phosphorylation and inactivation of HMG-CoA reductase by AMPK reduces cholesterol and isoprenoid synthesis in the liver (Viollet et al. 2009). AMPK increases mitochondrial biogenesis and thereby increases fatty acid oxidation in hepatocytes (Towler and Hardie, 2007). Hepatic gluconeogenesis is an important contributor to hyperglycaemia in type 2 diabetes. Gluconeogenesis is inhibited by AMPK activation and this has been demonstrated in response to both AICAR and adiponectin. AMPK also regulates TORC2 which subsequently effects PGC-1α and alters the expression of gluconeogenic enzymes (Viollet and Andreelli, 2011).

1.3.3.2 AMPK in cardiac and skeletal muscle metabolism

In cardiac and skeletal muscle, AMPK activation can stimulate GLUT4 translocation and expression resulting in increased glucose uptake independently of insulin (Viollet and Andreelli, 2011; Lim et al. 2010). This can be regulated both by exercise and pharmacological AMPK activation and appears to be reduced in obesity (Musi et al. 2001). AICAR was also shown to increase both membrane FA transporter translocation (FABP$_{pm}$ and FAT/CD36) and palmitate uptake in cardiac myocytes (Chabowski et al. 2005), indicating that AMPK stimulates both glucose and fatty acid uptake in striated muscle.

1.3.3.3 AMPK in adipose tissue metabolism

The role of AMPK in adipose tissue is less well studied than the liver and skeletal muscle. Interestingly, AMPK activation decreases insulin stimulated glucose transport, which although initially seems counterintuitive may actually be in keeping with energy preservation as it will reduce lipogenesis (Salt et al. 2000). It was also reported that AICAR reduces TNF-α mediated serine phosphorylation of IRS-1 and therefore attenuates the TNF-α mediated inhibition of insulin signalling (Shibata et al. 2013). In addition, AMPK-mediated phosphorylation of HSL has been reported to impair stimulation of lipolysis, yet there is a somewhat conflicting literature regarding the role of

AMPK in lipolysis (Bijland et al. 2013; Ceddia, 2013). It has been demonstrated that AMPK activity is reduced in visceral adipose tissue of obese insulin resistant individuals with an associated increase in mRNA for angiotensinogen (Xu et al. 2013).
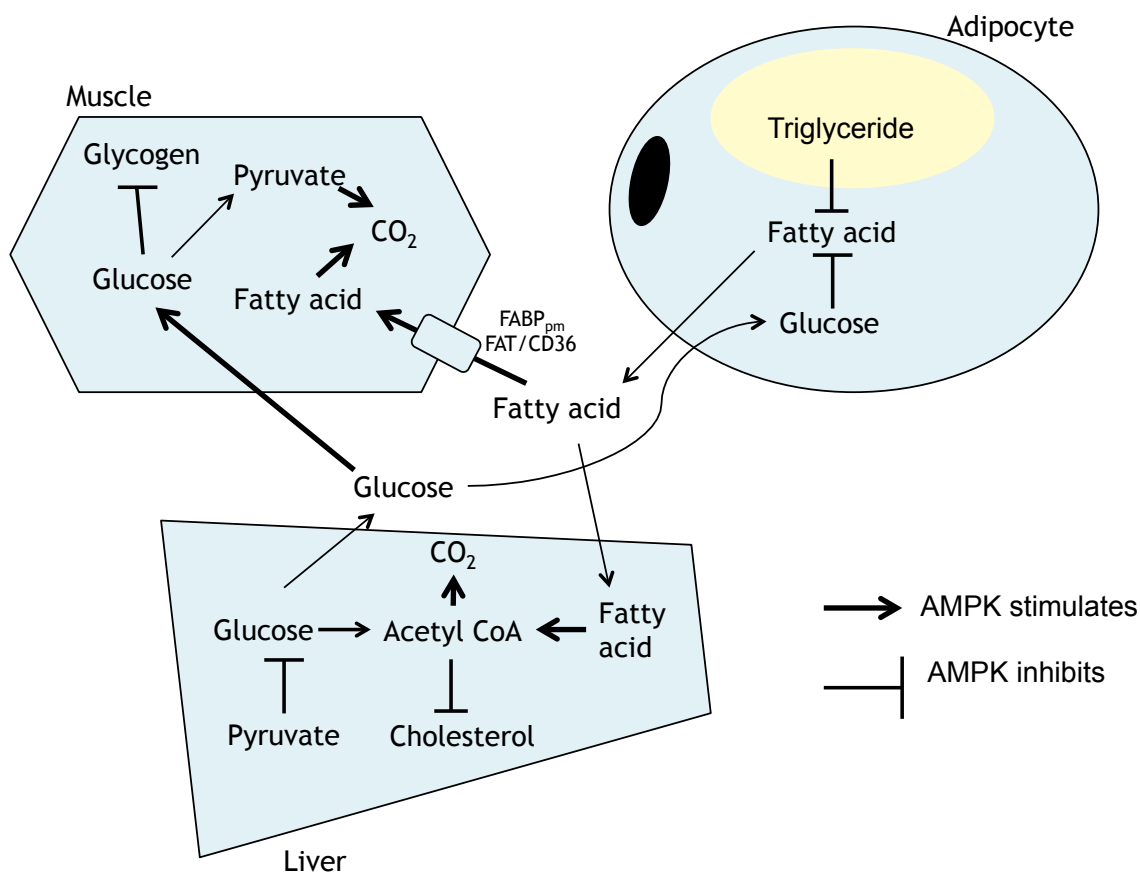
Figure 1.7 The major metabolic effects of AMPK

AMPK regulates key metabolic processes in skeletal muscle, adipocytes and the liver.

1.3.4 AMPK: anti-inflammatory properties

Metabolism and inflammation are related and there is therefore much interest in how AMPK may link the two entities. Over the past decade or so it has become clear from animal and cell culture work that AMPK may have an important anti-inflammatory role. In 2004, Nagata et al. demonstrated that AICAR treatment reduced angiotensin II induced ERK activation in rat vascular smooth muscle cells. In addition they found that angiotensin II activated AMPK

via the AT1 receptor through activation of NADPH oxidase (Nagata et al. 2004). When *ex-vivo* human subcutaneous adipose tissue was incubated with AICAR, there was decreased secretion of TNF-α and IL-6 (Lihn et al. 2004). In mice with diet-induced obesity AICAR treatment led to reduced circulating pro-inflammatory cytokines such as TNF-α, IL-6 and MCP-1, which was associated with improved insulin sensitivity (Yang et al. 2012). Studies of transgenic mice lacking either AMPKα1 or AMPKα2 have revealed many interesting roles of AMPK. AMPKα1-/- mice demonstrated increased NOX 2 expression and reactive oxygen species which was reversed by the NOX inhibitor apocynin (Schuhmacher et al. 2011).

1.3.5. Genetic mouse models

Mice lacking different AMPK subunits have increased our understanding of the role of AMPK in metabolic and other processes. As the combined lack of AMPKα1 and AMPKα2 is embryonically lethal, more selective deletion of AMPK isoforms has been performed. Initial studies utilised global knock-out models however transgenic models with tissue-specific loss of AMPK subunits have subsequently been generated and studied. The generation of AMPKα1-/- (Jorgensen et al. 2004) and AMPKα2-/- (Viollet et al. 2004) mice allowed the initial metabolic characterisation of global knock out of these catalytic subunits.

AMPKα1-/- mice, which lack a basal metabolic phenotype, have smaller adipocytes with an increased rate of lipolysis (Daval et al. 2005). In contrast, AMPKα2-/- mice exhbit an insulin resistant phenotype and demonstrate increased adipose tissue mass due to an increase in adipocyte size when exposed to high fat diet (Villena et al. 2004). As AMPKα1 is predominant in adipose tissue in terms of total cellular AMPK activity (Bijland et al. 2013), it is proposed to have a key role in the regulation of lipolysis, however lack of AMPKα2 may contribute to the development of obesity (Viollet et al. 2009).

1.4 Renin angiotensin aldosterone system

1.4.1.1 Angiotensins

The renin-angiotensin-aldosterone system (RAAS) regulates blood pressure and fluid status with precision due to a negative feedback process. Low renal perfusion pressure sensed by the juxtaglomerular apparatus in the kidneys leads to release of renin, an aspartyl protease, allowing conversion of angiotensinogen to angiotensin I (Connell et al. 2008). Angiotensin I requires activation to angiotensin II, this is mediated by angiotensin converting enzyme (ACE), and angiotensin II activates the angiotensin II type 1 receptor (AT1) leading to vasoconstriction, water retention and the release of aldosterone from the adrenal cortex (Connell et al. 2008). Angiotensin II can also activate angiotensin II type 2 receptors (AT2) leading to opposing actions including vasodilation and anti-proliferation (Munzenmaier and Greene, 1996; Carey, 2017). ACE 2 is an alternative form of ACE which acts to convert angiotensin II to angiotensin 1-7 (ang 1-7) and angiotensin I to angiotensin 1-9 (ang 1-9). Ang 1-7 is a 7 amino acid peptide which acts predominantly on the G-protein coupled Mas receptor (Santos et al. 2008). There are now several studies which suggest metabolic benefits of ACE 2 activity (Bindom et al. 2010) and ang 1-7 (Santos et al. 2008), described further in 1.4.4. Additional protective effects have been described associated with the complimentary RAAS mediated by ang 1-9 through AT2 receptors (Flores-Muñoz et al. 2011).

1.4.1.2 Aldosterone

Aldosterone is a steroid hormone synthesised in the adrenal cortex activates mineralocorticoid receptors (MR) within the kidneys leading to sodium and water retention, maintaining circulating volume and blood pressure (Connell et al. 2008). Its production and secretion are highly regulated by 3 main stimuli including angiotensin II, adrenocorticotrophic hormone (ACTH) and elevated serum potassium. These stimuli increase transcription and phosphorylation of the steroidogenic acute regulatory protein (StAR) leading to increased cholesterol transport into the mitochondria and therefore

steroidogenesis (Miller and Auchus, 2011). The components of the RAAS are detailed in Figure 1.8 and aldosterone synthesis outlined in Figure 1.9.
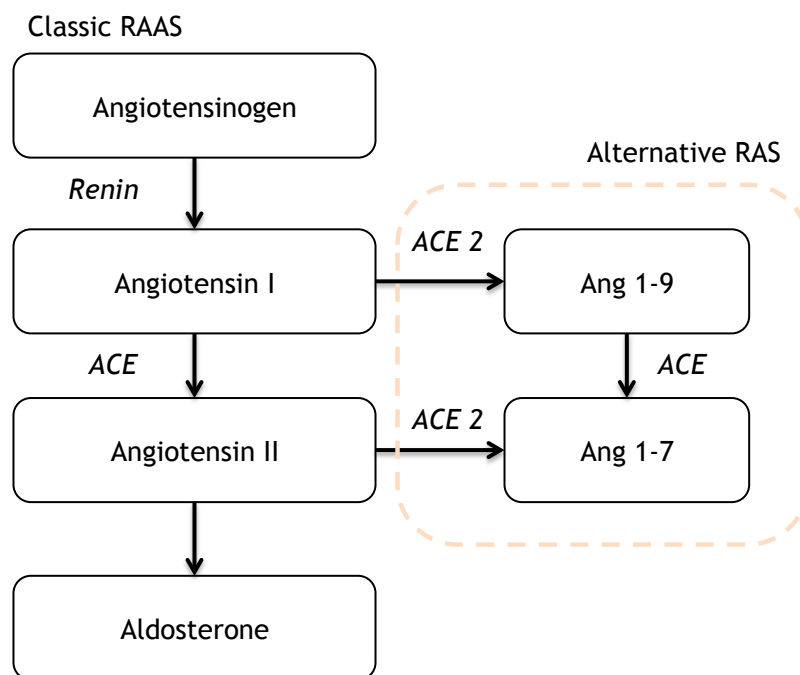
Figure 1.8 Principal components of the RAAS

The RAAS begins with angiotensinogen which is made principally by the liver. This is converted to angiotensin I by kidney-derived renin and angiotensin I is then converted to angiotensin II by ACE. Angiotensin II stimulates aldosterone production by the adrenal gland. Angiotensin I and angiotensin II can both be converted to the alternative peptides ang 1-9 and ang 1-7 respectively by ACE2.
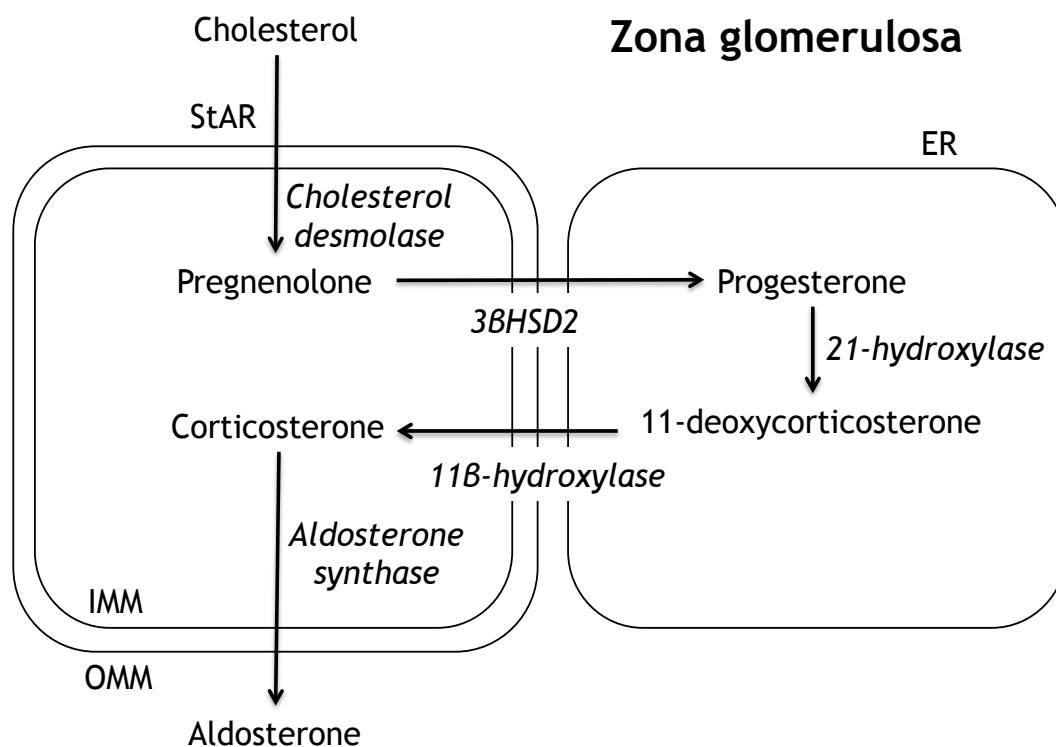
Figure 1.9 Aldosterone synthesis

Aldosterone synthesis takes place in the zona glomerulosa of the adrenal cortex. Steroid acute regulatory protein (StAR), Endoplasmic reticulum (ER), outer mitochondrial membrane (OMM), inner mitochondrial membrane (OMM). Enzymes in italics.

1.4.2.1 RAAS in cardiovascular disease

Overactivation of the RAAS is implicated in the development of hypertension and cardiac failure. Drugs which modulate this system including ACE inhibitors, angiotensin receptor blockers (ARBs) and mineralocorticoid receptor (MR) blockers have been shown to improve mortality in cardiac diseases (Ma et al. 2010). Intriguingly, complications of diabetes can be modified by drugs blocking the RAAS and people with diabetes appear to respond favourably compared to those without diabetes when mineralocorticoid receptor blockers are used post-myocardial infarction (O'Keefe et al. 2008).

1.4.2.2 RAAS and complications of diabetes

There has been much clinical interest into the use of RAAS blockers in diabetes. The well-known cardiovascular benefits of ACE inhibitors, ARBs and MR blockers are also seen in those with diabetes. Additionally, there is strong evidence supporting these medications in the treatment of diabetic nephropathy. Their use has been shown to both reduce progression of microalbuminuria to proteinuria and in some cases normalise it (ACE inhibitors in Diabetic Nephropathy Trialist Group, 2001).

1.4.3 RAAS and diabetes prevention

1.4.3.1 Clinical evidence

The large cardiovascular studies assessing ACE inhibitors and ARBs were not designed to investigate new onset diabetes. Cumulative evidence, however, has shown an association with reduced risk of the incidence of diabetes (Abuissa et al. 2005). The results from studies such as CAPPP (Niklason et al. 2004), HOPE (Yusuf et al. 2000), SOLVD (Vermes et al. 2003) and ALLHAT (Black et al. 2008) have been varied but agree that diabetes incidence is reduced. The first RCT designed specifically to answer this question, DREAM, did not show a significant reduction in new onset diabetes with ramipril (an ACE inhibitor) yet did find improved 2-hour blood glucose levels suggesting some effect on glycaemic control (Dagenais et al. 2008). In 2010 the NAVIGATOR study, another designed to look at new onset diabetes was published. In this case, valsartan (an ARB) was used in combination with lifestyle change and the findings agreed with the earlier suggestions such that a relative reduction of 14% in new diabetes was seen in those with obesity and impaired glucose tolerance (McMurray et al. 2010). It is not clear whether it is the effect of reducing angiotensin II or aldosterone or both which results in the main benefit. Certainly states of aldosterone excess such as primary aldosteronism (Conn's syndrome) and idiopathic adrenal hyperplasia are associated with metabolic syndrome (Tirosh et al. 2010; Whaley-Connell, et al. 2010). Importantly, treatment with MR antagonists or cure with adrenalectomy has been shown to reverse metabolic consequences in

aldosterone excess. It is now recognised that states of aldosterone excess are under-diagnosed and may contribute to a substantial number of cases of 'essential' hypertension.

1.4.3.2 RAAS and glycaemia *in vivo and in vitro*

Alongside the clinical trials there has been significant interest into the mechanisms underlying the benefits seen with RAAS blockade. This literature is somewhat heterogeneous but in general implicates angiotensin II and aldosterone in the development of insulin resistance and inflammation in adipose tissue and demonstrates clear benefits of antagonism of these hormones. These effects are summarised in Figure 1.10.

1.4.3.2.1 Angiotensin II

Angiotensin II has been shown to decrease insulin stimulated glucose transport in skeletal muscle in a study of *ex-vivo* rat skeletal muscle (Diamond-Stanic and Henriksen, 2010). It has also been shown to increase the production of pro-inflammatory cytokines from adipose tissue in both humans and rodents (Kalupahana and Moustaid-Moussa, 2012). In a very interesting study employing an adipose specific angiotensinogen over-expressing mouse, systemic insulin resistance was evident and this was reversed by the ACE inhibitor captopril. It was also demonstrated that the angiotensin II induced increase in MCP-1 in adipocytes was prevented by inhibitors of NOX and NFκB (Kalupahana et al. 2012). In another study, the ARB losartan improved glucose stimulated insulin release and proinsulin biosynthesis in a mouse model of obesity (db/db) (Chu et al. 2006). Other studies of ARBs have found reduced insulin resistance and inflammatory markers in humans (Pscherer et al. 2010) and decreased macrophage infiltration of adipose tissue in rats fed a high fat diet (Guo et al. 2008).

1.4.3.2.2 Aldosterone

Aldosterone excess is associated with insulin resistance and one mechanism for this has been proposed to be the degradation of IRS1 mediated by reactive

oxygen species. This was shown in 3T3-L1 adipocytes and was associated with increased phosphorylation of NFκB, associated with increased NFκB activity. When aldosterone signalling was analysed it appeared not to be mediated via the MR but the study suggested it was through the glucocorticoid receptor (Wada et al. 2009). There is much interest in aldosterone signalling in adipose and it is questioned as to whether there is an as yet undiscovered mechanism by which it mediates non-genomic effects (Nguyen Dinh Cat and Jaisser, 2012). However, one study by Hirata et al. did show the MR blocker eplerenone to reduce insulin resistance and macrophage infiltration in adipose in the obese db/db and ob/ob mouse models (Hirata et al. 2009). Another transgenic model, the aldosterone synthase knock out mouse, has been reported to be less prone to the elevated glucose, adipose tissue macrophage infiltration and hepatic steatosis associated with high fat diet (Luo et al. 2013). This clearly adds to the clinical data mentioned above and implicates aldosterone in the development of metabolic disorders.
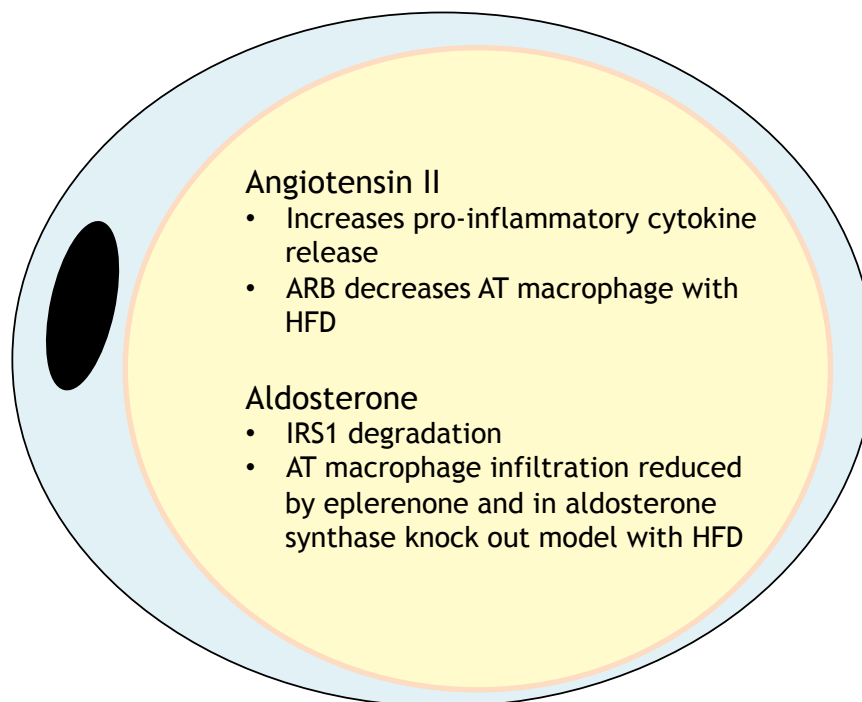
Figure 1.10 Summary of effects of angiotensin II and aldosterone on inflammation and metabolism in adipocytes

Angiotensin II and aldosterone have been shown to increase inflammation in adipocytes and contribute to insulin resistance.

1.4.4 Local production of RAAS

Over recent years it has become apparent that an autonomous/local RAAS can exist within many different tissues which could have varying degrees of clinical significance. With the increased understanding of the dynamic role adipose tissue can play in endocrine and immune functions there has been a focus on the local RAAS in at this site. Excitingly, there is now evidence that all components if the RAAS can be produced locally within adipose tissue (Jing et al. 2012, Marcus et al. 2012).

Angiotensinogen was the first RAAS component to be localised in adipose tissue, when in 1987 it was demonstrated to be expressed in rat brown adipocytes from peri-aortic and peri-atrial areas (Campbell and Habener, 1987). Subsequently, all other components including renin, angiotensin I and

angiotensin II and their receptors were reported to be expressed in adipose tissue of both rodents and humans (Marcus et al. 2012). In 2012 Briones et al. demonstrated production and secretion of aldosterone from 3T3-L1 adipocytes in addition to isolated human and murine adipocytes. Furthermore, they also described the autocrine and paracrine actions of adipocyte-derived aldosterone regulating adipogenesis and vascular tone (Briones et al. 2012). A complete RAAS can therefore exist within adipocytes and is likely to have auto- and paracrine effects and may contribute to the development of adipose inflammation.

1.4.5 The alternative RAAS

1.4.5.1 ACE 2

The alternative arm of the RAAS was described following the discovery of ACE 2 in 2000 (Donoghue et al. 2000). In 2010, it was reported that ACE 2 overexpression via adenoviral infection improved fasting glucose and reduced pancreatic β cell apoptosis in db/db mice suggesting glycaemic benefits of ACE 2 (Bindom et al. 2010). Another group found that the absence of ACE 2 led to impaired glucose tolerance in mice fed high fat, high sucrose diet compared to mice with ACE 2 present (Takeda et al. 2012). Additionally, when pioglitazone (an AMPK activating TZD) was used to treat high fat diet induced hepatic steatosis in rats, metabolic improvements were associated with increased serum and hepatic ACE 2 along with serum ang 1-7, whilst downregulating components of the classic RAAS (Zhang et al. 2013). These studies suggest a role for ACE 2 in the prevention and treatment of obesity-related diabetes.

1.4.5.2 Ang 1-7

In keeping with the above, ang 1-7 has also been shown to have some metabolic benefits including improved glucose tolerance in rats fed a high fructose diet (Giani et al. 2009). The mechanisms underlying these benefits may be related to inflammation. One study reported that ang 1-7 treatment reduced body weight, abdominal fat mass and adipose tissue IL-1β (Santos et

al. 2012) whilst another study from the same group showed down-regulation of the resistin/TLR4/NFκB pathway using an oral ang 1-7 formulation which suggests great therapeutic promise (Santos et al. 2013). In an earlier study Santos et al. reported that mice with global Mas receptor knock out had impaired insulin and glucose metabolism including reduced adipose GLUT4 and increased abdominal fat mass (Santos et al. 2008). Collectively these findings support a key role for ang 1-7/Mas signalling in maintaining metabolic health and controlling adipose tissue inflammation.

1.5 Cross-talk between AMPK and RAAS

Prior to the start of this work a small literature was available regarding the cross-talk between AMPK and RAAS. The majority of this, which is described below and summarised in Figure 1.11, relates to vascular tissues and there were no data relating to AMPK and RAAS in adipose, which is the proposed area of investigation in this project. Although angiotensin II may increase or decrease AMPK activity depending on cell type, AMPK activation consistently appears to decrease the effects of angiotensin II.

1.5.1 Vascular cells

As mentioned in 1.3.4, AICAR was reported to attenuate angiotensin II induced ERK activation in injured vascular smooth muscle cells (VSMCs). This in turn was related to a reduction in intimal hypertrophy following injury. The same study found that angiotensin II activated AMPK within VSMCs (Nagata et al. 2004). Another study assessed the effects of angiotensin II infusion in AMPKα1-/- mice and found increased endothelial dysfunction in the KO mice infused with angiotensin II, an effect which appeared related to increases in NOX2 and was partially prevented by the NOX inhibitor apocynin (Schuhmacher et al. 2011). The same study found that AMPK phosphorylation was increased in aorta samples from angiotensin II treated WT mice (Schuhmacher et al. 2011).

1.5.2 Cardiomyocytes

Two studies relate AMPK and angiotensin II in primary rat neonatal cardiomyocytes. The first of these published in 2008 found that, similar to VSMCs, activation of AMPK with AICAR decreased angiotensin II mediated expression of hypertrophy markers. Conversely, angiotensin II reduced AMPK activity, an opposite effect to that seen in VSMCs (Stuck et al. 2008). In 2009, Wang et al. demonstrated that globular adiponectin was able to reduce angiotensin II mediated cardiac hypertrophy via AMPK activation (Wang et al. 2010).

1.5.3 Renal

The only study to investigate aldosterone and AMPK was carried out in a renal model of fibrosis using HK2 tubular epithelial cells. Published in 2013, this study demonstrated that angiotensin II and aldosterone both led to renal fibrosis and that this process could be limited by both AICAR and metformin. This was shown to be mediated by AMPK with the use of AMPK inhibitor compound C and siRNA which negated the beneficial effects of metformin. The mechanism involved was proposed as increasing haemoxygenase 1 and thioredoxin leading to reduction of ROS. They also found that AMPK activity was reduced by angiotensin II (Lee et al. 2013).

1.5.4 Skeletal muscle

AMPK activity was decreased in gastrocnemius samples from mice following angiotensin II infusion, this was associated with muscle wasting and ATP depletion (Tabony et al. 2011). Interestingly, AICAR restored AMPK activity and also reversed the effects of angiotensin II (Tabony et al. 2011).
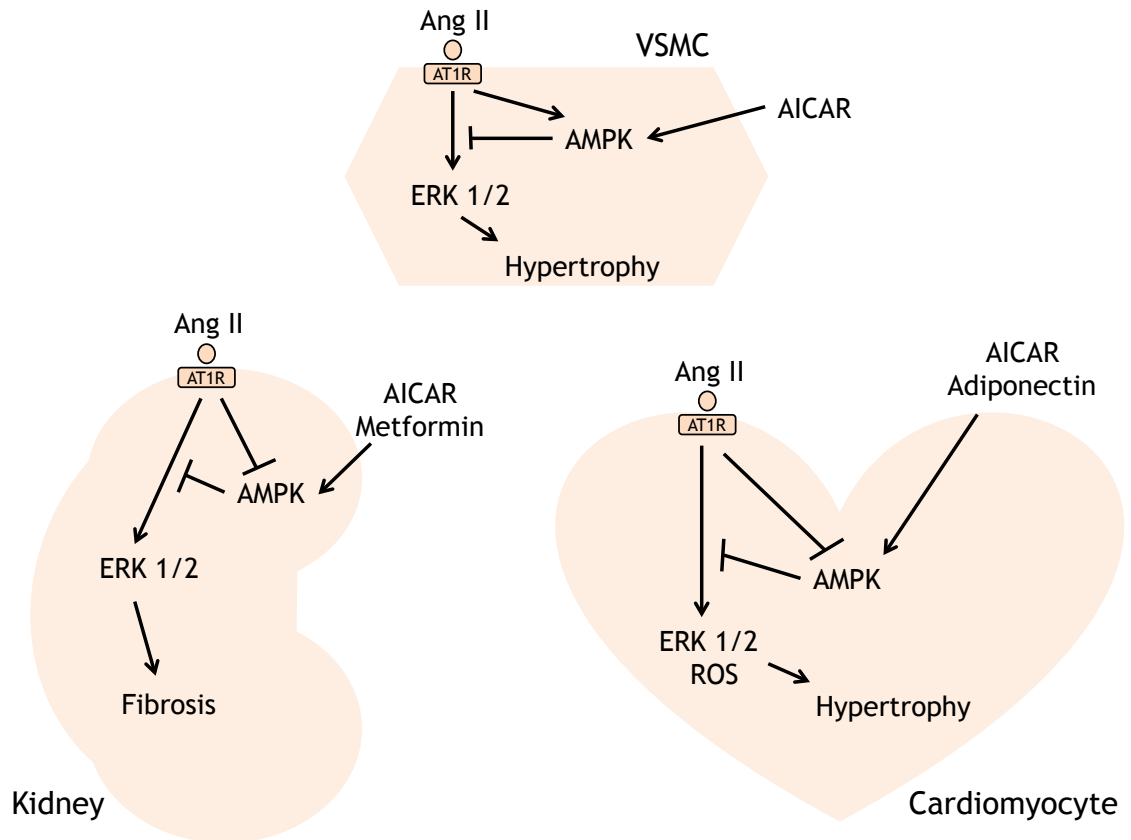
Figure 1.11 Interactions between angiotensin II and AMPK in renovascular tissues

AMPK activation reverses the effects of angiotensin II in disease models in VSMCs, cardiomyocytes and kidney cells. Angiotensin II activated AMPK in VSMCs but decreases AMPK activity in kidney and cardiac models.

1.6 Summary

Despite the known anti-lipogenic, anti-inflammatory actions of AMPK and the pro-inflammatory actions of local RAAS components in adipose tissue, there is a shortage of published work concerning whether these two important pathways are fundamentally linked in adipose tissue. As a consequence, the principal objectives of this study were:

1. To determine the effect of AMPK activation upon adipocyte and adipose tissue RAAS.
2. To characterise the effects of the RAAS on AMPK activity in adipocytes.
3. To assess how downregulation of adipose tissue AMPK influences the RAAS and metabolism *in vivo*.

2 Chapter 2 - Materials and Methods

2.1 Materials

2.1.1 List of materials and suppliers

Abcam, Cambridge, UK
A769662 (6,7-Dihydro-4-hydroxy-3-(2`-hydroxy[1,1`-biphenyl]-4-yl)-6-oxo-thieno[2,3-*b*]pyridine-5-carbonitrile)
A 779, Asp-Arg-Val-Tyr-Ile-His-D-Ala

Anachem, Luton, UK
DNAreleasy

Bachem, Bubendorf, Switzerland
Angiotensin I/II (1-7)

Bio-rad Laboratories Ltd, Hertfordshire, UK
Mini-PROTEAN® TGX^{TM} precast gels

BIOS Europe, Lancashire, UK
DPX mounting medium

Cambridge Bioscience, Cambridge, UK
Aldosterone EIA kit
CXCL-10 EIA kit

Cell Path Ltd, Powys, UK
10% acetic zinc formalin

Cell signalling Technology Inc, Danvers, MA, USA
Interleukin -1ß (IL-1ß)

Fisher Scientific UK Ltd, Loughborough, Leicestershire, UK
Ammonium persulphate (APS)
RNAse away
Tris base (tris(hydroxymethyl)aminoethane)

Invitrogen (Life Technologies Ltd), Paisley, UK

High capacity cDNA reverse transcription kit

TaqMan™ gene expression assays

TaqMan® Universal Master Mix II, no UNG

Invitrogen (GIBCO Life Technologies Ltd), Paisley, UK

Dulbecco's modified Eagles media (DMEM)

Foetal calf serum (FCS) (USA origin)

Foetal calf serum (FCS) (EU origin)

Newborn calf serum (NCS)

Penicillin/streptomycin

Trypsin

Melford Laboratories Ltd, Chelsworth, Ipswich, Suffolk, UK

Dithiothreitol (DTT)

Merck Chemical LTd, Nottingham, UK

Compound C

Insulin ELISA kit

National Diagnostics, Nottingham, UK

Histoclear

New England Biolabs, Ipswich, MA, USA

Prestained protein marker, broad range (11-190 kDa)

PALL Life Sciences, Pensacola, FL, USA

Nitrocellulose transfer membrane, 0.45 µM pore size

Perkin Elmer, Beaconsfield, Buckinghamshire, UK

ATP,[Υ-^{32}P]

2-[^{3}H]-deoxy-D-glucose

Premier International Foods, Cheshire UK

Dried skimmed milk

Promega, Southampton, UK
Go Taq amplification system

Qiagen Ltd, Crawley, West Sussex, UK
RNeasy Mini kit

Raymond A Lamb Ltd, Eastbourne, UK
Eosin
Haematoxylin

Severn Biotech Ltd, Kidderminster, Hereford, UK
Acrylamide:Bisacrylamide (37.5:1; 30% (w/v) Acrylamide)

Sigma-Aldrich Ltd, Gillingham, Dorset, UK
Aldosterone
Angiotensin II
Bovine serum albumin
Benzamidine
Cytochalasin B
Dexamethasone
D-glucose
D-mannitol
DNA primers
Ethylenediamine tetraacetic acid (EDTA)
Ethylene glycol-bis (ß-amino-ethylether)-N,N,N`,N`-tetraacetic acid (EGTA)
Isobutylmethylxanthine (IBMX)
Oil red O
Phenylmethylsulphonyl fluoride (PMSF)
Ponceau stain
Porcine Insulin
Soyabean trypsin inhibitor (SBTI)
N,N,N`,N`-Tetramethylethylenediamine (TEMED)
Triton X-100

Tumour necrosis factor-α

Tween-20

Tocris Bioscience, Bristol, UK

Angiotensin II

Troglitazone

Toronto Research Chemicals Inc, Ontario, Canada

AICAR (5-aminoimidazole-4-carboxamide-1-beta-4-ribofuranoside)

VWR International Ltd, Lutterworth, Leicestershire, UK

Falcon tissue culture 10 cm dishes and 6 / 12 well plates

HEPES (N-a-hydroxyethylpiperazine-N` 2-ethane sulphonic acid)

Worthington Biochemical Corporation, Lakewood, NJ, USA

Collagenase Type 1

2.1.2 List of specialist equipment and suppliers

Abbott Diabetes Care, Maidenhead, UK
Freestyle glucose monitor
Glucose monitor strips

Alpha Innotech Corporation, San Leandro, USA
Alpha Innotech digital imaging system

Beckman Coulter^{TM}, High Wycombe, UK
Multi-Purpose scintillation counter LS 6500

Bio-Rad Laboratories, Hemel Hempstead, UK
Protein gel casting and Western blotting equipment (Mini Protean III)

BMG Labtech, Germany
FLUOstar OPTIMA microplate reader

Fisher Scientific, Loughborough, UK
Leica Finesse 325 Microtome
Shandon Histocenter 3

Thermo Fisher, Paisley, UK
ABI-PRISM 7900HT Sequence Detection System
MJ Research PTC-225 Peltier thermal cycler

Thermo Scientific, Waltham, MA, USA
Nanodrop spectrophotometer

WPA, Cambridge, UK
S2000 spectrophotometer

2.1.3 List of cells and suppliers

American Type Culture Collection, Manassas, VI, USA

3T3-L1 preadipocytes

SW872 preadipocytes

Institut Cochin, Paris, France

AMPKα1$^{-/-}$AMPKα2$^{-/-}$ knock out and wild type mouse embryonic fibroblasts, a kind gift from Benoit Viollet (Laderoute et al. 2006)

2.1.4 List of antibodies and conditions of use

Table 2.1 Primary antibodies for immunoblotting

Epitope	Host	Dilution	Source
Adiponectin	Rabbit	1:1000	University of Glasgow (Clarke et al. 2006)
Akt	Mouse	1:1000	Cell signalling; #2920
AMPKα1	Sheep	1:1500	University of Dundee (Woods et al. 1996)
GAPDH	Mouse	1:20,000	Abcam; #AM4300
IκB	Rabbit	1:1000	Cell signalling; #4812
JNK	Rabbit	1:1000	Cell signalling; #9252
Lipocalin 2 (Ngal)	Rabbit	1:1000	Millipore; #Ab2267
Mineralocorticoid receptor	Rabbit	1:500	Santa Cruz; #H300
MCP-1	Rabbit	1:1000	Cell signalling; #2029
NF-κB p65	Mouse	1:1000	Cell signalling; #6956
p44/42 MAPK (Erk1/2)	Rabbit	1:1000	Cell Signalling; #9102
Phospho- p44/42 MAPK (Erk1/2)	Mouse	1:2000	Cell Signalling; #9106
Phospho-Acetyl-CoA Carboxylase (Ser79)	Rabbit	1:1000	Cell Signalling; #3661
Phospho-Akt (Ser473)	Rabbit	1:1000	Cell signalling; #4058
Phospho-AMPKα (Thr172)	Rabbit	1:500	Cell Signalling; #2535
Phospho-AS-160 (Thr642)	Rabbit	1:1000	Cell signalling; #8881
Phospho-IκB (Ser32)	Mouse	1:1000	Cell signalling; #9246
Phospho-JNK(Thr183, Tyr185)	Rabbit	1:1000	Cell signalling; #4668
Phospho -NF-κB p65	Rabbit	1:1000	Cell signalling; #3033
Phospho-STAT3(Ser727)	Mouse	1:1000	Cell signalling; #9136
SGK1	Rabbit	1:500	Millipore; #04-1027
STAT3	Rabbit	1:1000	Cell signalling; #4904

Table 2.2 Secondary antibodies for immunoblotting

Epitope	Host species	Conjugate	Dilution	Source
Goat IgG (H+L)	Donkey	IRDye® 800CW	1:10,000	LI-COR; #926-32214
Mouse IgG (H+L)	Donkey	IRDye® 800CW	1:10,000	LI-COR; #926-32212
Rabbit IgG (H+L)	Donkey	IRDye® 800CW	1:10,000	LI-COR; #926-32213
Rabbit IgG (H+L)	Donkey	IRDye® 680RD	1:10,000	LI-COR; #926-68023

2.1.5 List of Taqman® qPCR probes

Table 2.3 Taqman® gene expression assays

Target	Assay ID (human)	Assay ID (mouse)
Angiotensin converting enzyme I	Hs00174179_m1	Mm00802048_m1
Angiotensin converting enzyme II	Hs01085333_m1	Mm01159006_m1
Angiotensin II type 1 receptor	Hs00258938_m1	Mm01957722_s1
Angiotensin II type 2 receptor	Hs02621316_m1	Mm01341373_m1
Angiotensinogen	Hs01586213_m1	Mm00599662_m1
CXCL-10	Hs01124251_g1	Mm00445235_m1
Interleukin-1ß		Mm00434228_m1
Glucocorticoid receptor	Hs00353740_m1	Mm00433832_m1
Mas receptor	Hs00267157_s1	Mm00434823_s1
Mineralocorticoid receptor	Hs01031809_m1	Mm01241596_m1
SGK-1	Hs00985033_g1	
Steroid acute regulatory protein	Hs00986559_g1	Mm00441558_m1
TATA-box binding protein	Hs00427620_m1	Mm01277042_m1

2.1.5 Standard solutions

<u>Bradford's reagent</u>

35.0 mg/l coomassie brilliant blue

5.0% (v/v) ethanol

5.1% (v/v) orthophosphoric acid

Bradford's reagent was filtered and stored in the dark.

<u>Adipose tissue collection buffer</u>

130 mM NaCl

20 mM HEPES-NaOH, pH 7.4

4.8 mM KCl

5 mM NaH_2PO_4

3 mM glucose

1.25 mM $MgSO_4$

1.25 mM $CaCl_2$

1% (w/v) BSA

10 µM adenosine

pH 7.4 at 37°C

<u>Immunoprecipitation (IP) buffer</u>

50mM Tris-HCl, pH 7.4 at 4°C

150 mM NaCl

50 mM NaF

5 mM $Na_4P_2O_7$

1 mM EDTA

1 mM EGTA

1% (v/v) Triton-X-100

1% (v/v) glycerol

1mM DTT

0.1mM benzamidine

0.1 mM PMSF

5 µg/ml SBTI

1 mM Na_3VO_4

Krebs-Ringer HEPES (KRH) buffer

119.0 mM NaCl

20.0 mM HEPES-NaOH, pH 7.4

5.0 mM $NaHCO_3$

10.0 mM glucose

4.8 mM KCl

2.5 mM $CaCl_2$

1.2 mM $MgSO_4$

1.2 mM NaH_2PO_4

Krebs-Ringer phosphate (KRP) buffer

130 mM NaCl

4.8 mM KCl

5 mM NaH_2PO_4, pH 7.4

1.25 mM $MgSO_4$

1.25 mM $CaCl_2$

Lysis Buffer

50mM Tris-HCl, pH 7.4 at 4°C

50 mM NaF

1 mM $Na_4P_2O_7$

1 mM EDTA

1 mM EGTA

1% (v/v) Triton-X-100

1mM DTT

1 mM Na_3VO_4

0.1 mM benzamidine

0.1 mM PMSF

5 µg/ml SBTI

Phosphate-buffered saline (PBS) (pH 7.2)

85 mM NaCl

1.7 mM KCl

5 mM Na_2HPO_4

0.9 mM KH_2PO_4

Phosphate-buffered saline + Tween 20 (PBST)

85 mM NaCl

1.7 mM KCl

5 mM Na_2HPO_4

0.9 mM KH_2PO_4

0.1% (v/v) Tween 20

Ponceau S stain

0.2% (w/v) ponceau S

1% (v/v) acetic acid

SDS-polyacrylamide gel electrophoresis (SDS-PAGE) Running buffer (pH 8.3)

192 mM glycine

25 mM Tris base

0.1% (w/v) SDS

4 X SDS PAGE sample buffer

200 mM Tris-HCl, pH 6.8

8% (w/v) SDS

40% (v/v) glycerol

0.4% (w/v) bromophenol blue

200 mM DTT

Transfer buffer (pH 8.3)

192 mM glycine

25 mM Tris base

20% (v/v) ethanol

Tris-buffered saline (TBS)

20 mM Tris-HCl, pH 7.5

137 mM NaCl

Tris-buffered saline + Tween 20 (TBST)

20 mM Tris-HCl, pH 7.5

137 mM NaCl

0.1% (v/v) Tween 20

2.2 Cell Culture Methods

2.2.1 Growth of 3T3-L1 fibroblasts

3T3-L1 cells were cultured at 37°C and 10% (v/v) CO_2 in Dulbecco's modified Eagle medium (DMEM) supplemented with 10% (v/v) newborn calf serum (NCS) and antibiotics (0.1 mg/ml streptomycin and 100 U/ml penicillin (PS)). Media was refreshed every 2-3 days (Torado and Green, 1963).

2.2.1 Passage of 3T3-L1 fibroblasts

When cells reached 80% confluence in Corning T75 flasks, they were washed with sterile PBS then incubated at 37°C with 3 ml of sterile trypsin until cells detached from the flask. DMEM growth medium was added in sufficient volume to seed cells into further Corning T75 flasks and Falcon cell culture plates (6- or 12-well) or dishes as required.

2.2.2 Differentiation of 3T3-L1 adipocytes

Two days post-confluence differentiation was induced using DMEM supplemented with 10% (v/v) foetal calf serum (FCS), PS and 0.25 µM dexamethasone, 0.5 mM IBMX, porcine insulin (1 µg/ml) and 5 µM troglitazone for 3 days, culture medium was then exchanged for DMEM containing 10% (v/v) FCS, PS, porcine insulin (1 µg/ml) and 5 µM troglitazone for 3 days at which time culture medium was maintained with DMEM, 10% (v/v) FCS and PS. Differentiation was complete at day 8 and experiments conducted between day 8 and day 12.

2.2.3 Freezing of 3T3-L1 fibroblasts

Cells were detached as per 2.2.1 then 12 ml of growth medium added and the cell suspension transferred to a 15 ml centrifuge tube. Following centrifugation at 350 x g for 5 minutes the trypsin/media was aspirated leaving the cell pellet. The pellet was resuspended with 3 ml freeze medium (FCS plus 10% (v/v) DMSO) then 1 ml aliquots transferred to 1.8 ml

polypropylene cryogenic tubes. The cryogenic tubes were stored overnight in a polycarbonate container at -80°C then transferred to liquid nitrogen container for long term storage.

2.2.4 Growth of SW872 fibroblasts

SW872 cells were cultured at 37°C and 5% (v/v) CO_2 in DMEM supplemented with 10% (v/v) FCS and PS. Media was refreshed every 2-3 days (Berg et al. 1996, Guennoun et al. 2015).

2.2.5 Passage of SW872 fibroblasts

When cells reached 80% confluence in Corning T75 flasks, they were washed with sterile PBS then incubated with 3 ml of sterile trypsin until cells detached from the flask. DMEM growth medium was added in sufficient volume to seed cells into further Corning T75 flasks and Falcon cell culture plates (6- or 12-well) or dishes as required.

2.2.6 Differentiation of SW872 adipocytes

Once confluent, differentiation was induced using DMEM supplemented with 10% (v/v) FCS, PS and 0.25 µM dexamethasone, 0.5 mM IBMX and 1 µM porcine insulin for 2 days, culture medium was then exchanged for DMEM containing 10% (v/v) FCS, PS and 1µM porcine insulin for 2 days at which time culture medium was maintained with DMEM, 10% (v/v) FCS and PS.

2.2.7 Freezing of SW872 adipocytes

Freezing of SW872 adipocytes was carried out in the same manner as 3T3-L1 adipocytes described in 2.2.3.

2.2.8 Growth of mouse embryonic fibroblasts

AMPKα1$^{-/-}$AMPKα2$^{-/-}$ (Laderoute et al. 2006) and wild-type mouse embryonic fibroblasts (MEFs) were a kind gift from Dr. Benoit Viollet (Institut Cochin,

Paris, France) and cultured at 37°C and 5% (v/v) CO_2 in DMEM supplemented with 10% (v/v) FCS and PS. Media was refreshed every 2-3 days.

2.2.9 Preparation of cell lysates

Cells grown in 6 well Falcon cell culture dishes were serum deprived for at least 2 hours by replacing culture medium for serum-free medium for short incubations or 1% (v/v) NCS for incubations over 6 hours, then stimulated with test substances for different durations and maintained at 37°C. Following stimulation dishes were placed on ice and culture medium removed and stored at -20°C for ELISA. Cells were washed with ice-cold PBS then 0.1 ml of lysis buffer was added to each well. Each well was scraped and cell extracts were placed in a microcentrifuge tube, vortex mixed and placed on ice for 20 min. Lysates were subsequently centrifuged (21,910 x g at 4°C for 3 min) and supernatants stored at -20°C in new microcentrifuge tubes.

2.2.10 Oil Red O staining of 3T3-L1 and SW872 adipocytes

Preadipocyte fibroblasts or differentiated adipocytes were washed with 10% (v/v) formalin for 5 min then incubated in 10% (v/v) formalin for 1 h at room temperature. Cells were subsequently washed with 60% (v/v) isopropanol and covered with 60% (v/v) Oil Red O for 5 minutes and washed 4 times with dH_2O. Plates were allowed to dry then stored at 4°C prior to imaging.

2.3 Analysis of Cellular Proteins

2.3.1 Preparation of Bradford Reagent and protein assays

Protein content was calculated using spectrophotometric analysis as per the Bradford method (Bradford 1976). Protein standards using duplicates of 2 µg, 4 µg and 6 µg BSA were used as reference. Lysates were first diluted either 1:5 or 1:10 then 5 µl added to 95 µl dH_2O in disposable cuvettes. Bradford's reagent (1 ml) was added to all samples and standards prior to immediate analysis of absorbance at 595 nm using a WPA S2000 spectrophotometer. Mean

protein concentration per sample duplicate was calculated by comparison to the mean A_{595}/µg BSA from the linear portion of the standard reference curve.

2.3.2 SDS-Polyacrylamide gel electrophoresis

Sodium dodecyl sulphate-polyacrylamide gel electrophoresis (SDS-PAGE) was carried out with 1.5 mm thick vertical slab gels containing 8-15% acrylamide using the Bio-Rad mini-protein III system. The stacking gel comprised 5% (v/v) acrylamide/0.136% (v/v) bisacrylamide, 125 mM Tris-HCl (pH 6.8), 0.1% (w/v) SDS polymerized with 0.1% (w/v) ammonium persulphate and 0.05% (v/v) TEMED. Lysate samples were mixed with 4x sample buffer at a ratio of 3:1 then heated at 95°C for 5 minutes. Once immersed in running buffer, broad range pre-stained molecular markers were added in at least one well as standard then lysates were loaded into wells. Gels were electrophoresed at 80 V through the stacking gel then 170 V through the resolving gel until the tracking dye reached the bottom of the gel.

2.3.3 Immunoblotting

After protein separation, each gel was carefully removed from the plates and placed upon a pre-wetted equal sized piece of nitrocellulose (0.45 µm pore size) in a bath of transfer buffer then sandwiched between Whatmann 3MM filter paper and sponges within the gel holder cassette. Proteins were transferred using a Bio-Rad mini Protean III trans-blot electrophoretic transfer cell at 60 V for 2.5 h or 40 mA overnight.

2.3.4 Ponceau staining

Protein transfer was checked by washing in Ponceau stain for several seconds and immunoblots de-stained by washing the membranes 3 times in PBS.

2.3.5 Immunodetection of proteins

Nitrocellulose membranes were blocked for non-specific protein binding with 5 % (w/v) milk in PBS at room temperature for 30 min with gentle shaking.

Membranes were then washed (3 x 5 min) with PBST prior to incubation with primary antibody in PBST/50% (v/v) Odyssey® blocking buffer overnight at 4°C. Then membranes were washed (3 x 5 min) with PBST and incubated with secondary antibody for 1 h at room temperature with the appropriate fluorescent IRDye®-conjugated secondary antibody in PBST/50% (v/v) Odyssey® blocking buffer. Membranes were then washed (4 x 5 min) with PBST and once with PBS (5 min). Imaging was carried out using the *Li-cor* ODYSSEY® infrared imaging system and immunoblots were quantified using Image J software.

2.3.6 Aldosterone ELISA

Conditioned culture medium (1 ml) from 3T3-L1 and SW872 cells was concentrated using a Thermo Scientific DNA 120 SpeedVac Concentrator overnight, the concentrate was resuspended in 200 μl of culture medium and stored in 50 μl aliquots at -20°C. Aldosterone ELISA was carried out using the Aldosterone EIA kit – Monoclonal from Cayman Chemical Company as per the manufacturer's instructions. In brief, 50 μl of sample was combined with aldosterone acetylcholine esterase (AChE) tracer and monoclonal antibody for 18 hours at 4°C. Wells were emptied and washed then 200 μl of Ellman's solution and 5 μl of tracer were added and incubated shaking in the dark for 90 minutes. The plate was read using using a FLUOstar OPTIMA microplate reader (BMG Labtech, Germany). Mean absorbance at 405 nm (ref 405-420) was determined from duplicate samples and concentration calculated by comparison to the standard curve using MyAssays.

2.4 Gene Expression Analyses

2.4.1 RNA extraction from cells

Culture medium was removed from cells cultured in 6-well cell culture dishes and RNA extracted using an RNeasy kit (Qiagen) according to manufacturer's instructions including the DNase step. In summary, cells were lysed using buffer RLT, scraped from plates then homogenised by passing 5 times through a sterile 21 gauge needle. Samples were then mixed with an equal volume of

70% (v/v) ethanol and placed onto a RNeasy mini column 700 µl at a time. Columns were centrifuged (13,226 x g) for 15 seconds and waste discarded. An on-column DNase digestion was performed using the DNase kit (Qiagen) as instructed with one wash using RW1 buffer then a 15 min incubation with 80 µl of DNase I incubation mix (10 µl DNase I stock solution + 70 µl Buffer RDD) terminated with a wash with 350 µl RW1 then one further wash with 700 µl of RW1. Columns were further washed twice with 500 µl RPE buffer and 40 µl of RNase-free water added prior to centrifugation (13,226 x g, 1 min) to elute the RNA. Samples were kept on ice during whilst RNA concentration was determined using the NanoDrop (Thermo Scientific). Samples were stored at -80°C.

2.4.2 cDNA production from RNA

RNA was reverse-transcribed using a High Capacity cDNA Reverse Transcription kit (Applied Biosystems) as per the manufacturer's instructions. RNA (2 µg in 10 µl RNase-free water) was added to 10 µl of 2 x reverse transcription mastermix in RNase-free micro PCR tubes maintained at 4°C. Samples were mixed, briefly centrifuged and placed in a MJ Research PTC-225 Peltier Thermal Cycler. Reverse transcription was performed using the following parameters: 10 min at 25°C, 120 min at 37°C then 85 min at 5°C. The resultant cDNA was diluted 1:10 and stored at -20°C until PCR performed.

2.4.3 Quantitative real time polymerase chain reaction

Real-time quantitative RT-PCR was performed with an ABI-PRISM 7900HT Sequence Detection System by mixing 2 µl cDNA, 1 µl Taqman® probe, 5 µl Taqman® Universal Mastermix II (no UNG) and 2 µl RNase free water per well of a 364-well plate using the following thermal cycling pattern: 2 min 50°C, 10 min 95°C, then 40 cycles of 15 sec 95°C and 1 min 60°C. mRNA levels were normalized to TATA-box binding protein as control. All PCR experiments were carried out in duplicate. Results were analysed using the ΔΔCt method.

2.5 Radiolabelled activity assays

2.5.1 2-deoxy-D-glucose uptake assay

Differentiated adipocytes (3T3-L1 or SW872) grown in Falcon 12 well cell culture dishes were serum deprived for 2 h in serum-free DMEM then the media was removed, cells washed with PBS and placed in Krebs-Ringer Phosphate (KRP) buffer supplemented with 0.1% (w/v) BSA, at 37°C for 1 hour. Plates were transferred to a 37°C hot plate prior to stimulation with insulin for 10 min at indicated concentrations; [^{3}H]-2-deoxyglucose (final concentration 50 μM and 1 μCi/ml) was then added to cells for the times indicated and cytochalasin B (10 μM) was applied to control experiments. Transport assays were terminated by rapid washing of cells 3 times in ice cold PBS. Once air dried, 500 μl/well 1% (v/v) TX100 was added and plates incubated overnight. Solubilised cells were then added to 5 ml scintillation fluid and cell-associated radioactivity detected using a Beckman Multi-Purpose scintillation counter. Method adapted from description by Gibbs et al. 1988.

2.5.2 AMPK activity assay

Protein-G sepharose beads (10 μl 50% (v/v) slurry per immunprecipitation) were washed 3 times by the addition of 1 ml immunoprecipitation (IP) buffer then centrifuged at 17,500 x g at 4°C for 1 min. Bead density was adjust to 25% (v/v) then 1 μg each of AMPK α1 and α2 antibody (University of Dundee) per reaction added prior to rotating incubation for 1 h at 4°C. Antibody-bead complexes were then collected by centrifugation and 3 further washes in 1 ml IP buffer completed. Cell lysate (100 μg protein) was added to 5 μl of antibody-bead complex for each IP reaction then sample volumes equalised with IP buffer as required. Samples were incubated for 3 h at 4°C on a rotating platform to allow antibody-protein binding. Pellets were collected following centrifugation and 5 washes completed as follows: 2 x high salt IP buffer (1 M NaCl), 2 x IP buffer then 1 x HEPES-Brij-DTT (HBD) buffer (50 mM HEPES-NaOH (pH 7.4 at 4°C, 0.02 % (v/v) Brij-35, 1 mM DTT) and stored at -20°C. Prior to kinase assay pellets were resuspended in 20 μl HBD then

combined with 5 µl HBD, 5 µl 1 mM AMP, 5 µl 1 mM SAMS peptide and 5 µl of 0.2 µCi/µl [γ-^{32}P]-ATP (prepared in HBD containing 1 mM ATP and 25 mM MgCl$_2$). After 10 min incubating at 30°C on a vibrating platform 15 µl of sample was spotted onto a square of P-81 Whatman phosphocellulose paper then submerged in 500 ml of 0.1% (v/v) H$_3$PO$_4$. Paper squares were washed as follows: 2 x H$_2$O, 1 x H$_3$PO$_4$ (5 min), 2 x H$_2$O then added to 5 ml scintillation fluid once air dry and radioactivity detected using a Beckman Multi-Purpose scintillation counter. Samples were assayed in duplicate with an additional reaction lacking SAMS peptide. Total counts were measured in a 5 µl sample of 0.2 µCi/µl [γ-^{32}P]-ATP.

2.6 In vivo Methods

2.6.1.1 Experimental animals

Experimental animals were housed in the Central Research Facility at the University of Glasgow and experiments conducted under the United Kingdom Animals Scientific Procedures Act 1986. Wild type (WT) (SV129) mice were originally purchased from Harlan laboratories and AMPKα1 knock out (KO) mice were a kind gift from Benoit Viollet (Institut Cochin, Paris, France). KO mice were originally generated by the injection of positive embryonic stem cells into blastocysts from C57BL/6J mice (Jorgensen et al. 2004) and subsequent mating led to the present mixed C57BL6/SV129 background. Mice were maintained at an ambient temperature with 12 h light and dark cycles. They had free access to food and water. Conditions and experiments were overseen by the following project licenses 70/8572, 60/4244 and 60/4526.

2.6.1.2 Genotyping of experimental animals

DNA was extracted from ear notches using 10 µl of DNAreleasy and performing PCR the following thermal cycling pattern: 5 min at 75°C, 2 min at 96°C then 20°C indefinitely. Nuclease-free dH$_2$O (90 µl) was added prior to RT-PCR using the Go Taq amplification system. The primer sequence is described in Table 2.1. A mastermix containing Taq (Go) hot start mastermix, forward primer, reverse primer and NF-dH$_2$O was added to the DNA sample then subjected to

the following thermal cycling pattern: 5 min 95°C, 40 x (30 sec 95°C, 40 sec 58°C, 1 min 72°C), 10 min 72°C, then 4°C until electrophoresis performed. A 2% (w/v) agarose/TAE gel was used to separate DNA products then 0.1% (v/v) ethidium bromide added to allow visualization by the Alpha Innotech digital imaging system, an example is shown in figure 2.1.

Table 2.4 Primer sequences for genotyping

Primer	Type	Sequence
AMPKα1$^{+/+}$	Forward	AGCCGACTTTGGTAAAGGATG
	Reverse	CCCACTTTCCATTTTCTCCA
AMPKα1$^{-/-}$	Forward	GGGCTGCAGGAATTCGATATCAAGC
	Reverse	CCTTCCTGAAATGACTTCTG
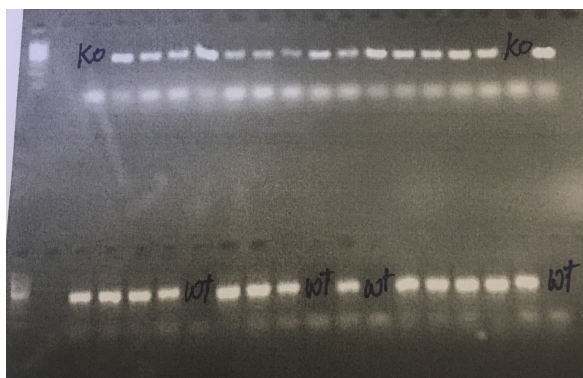
Figure 2.1 Genotyping of experimental animals.

With reference to a 100 bp ladder (left) the absence of a band on the upper (WT DNA primer) or lower (KO DNA primer) row indicates presence of knock out or wild type mice respectively. Presence of both bands indicates heterozygote.

2.6.2 High fat diet protocol

Male WT and KO mice were allocated in pairs to either normal chow or high fat diet (42% fat) between 8 and 10 weeks of age for 12 weeks. At this point they were individually housed and had weight measured weekly and food intake estimated by weighing their food at the beginning and end of a 24 h period. Constituents of high fat diet in Appendix 1.

2.6.3 Glucose tolerance tests

At the end of the 12 week diet intervention each mouse undertook a glucose tolerance test. Following a 16 h overnight fast mice were weighed and received an intraperitoneal injection of 1g/kg glucose. Tail vein blood sampling was performed at 0, 15, 30, 60, 90 and 120 min and glucose measured using a Freestyle glucose meter (Abbot Diabetes Care). Animals were then given free access to their allocated diet.

2.6.4 Serum measurements

Mice were fasted overnight then sacrificed by CO_2 narcosis prior to blood sampling by cardiac puncture using a 1 ml syringe and heparinised 23 gauge needle. Blood was transferred to a chilled centrifuge tube and kept on ice for at least 30 min. Samples were centrifuged for 10 min at 720 x g at 4°C then serum collected into 50 μl aliquots and stored at -80°C.

2.6.4.1 Insulin ELISA

Insulin concentration was determined using a Rat/Mouse insulin ELISA kit (Millipore) according to the manufacturer's instructions. In brief, using the microplate and strips provided, 10 μl of sample was added to 10 μl of assay buffer then 80 μl of detection antibody combined prior to incubating for 2 h at room temperature on a shaking platform at 500 rpm. The wells were emptied, washed and incubated with 100 μl of enzyme solution for 30 min, then emptied and washed again, incubated with substrate solution for 15 min then stop solution added and the absorbance at 485 nm determined using a FLUOstar OPTIMA microplate reader (BMG Labtech, Germany). Mean absorbance was determined from duplicate samples and concentration calculated by comparison to the standard curve.

2.6.4.2 RAAS analysis

Serum samples were sent to the Attoquant Diagnostics lab (Austria) for analysis of aldosterone, angiotensin I, angiotensin II, angiotensin 1-7 and angiotensin I formation rate by mass spectrometry.

2.6.5.1 Liver histology

Livers were isolated and weighed then collected into 10% zinc formalin for 24 hours then stored in ethanol until paraffin embedding. Using a Citadel 1000 tissue processor liver samples were passed through different ethanol concentrations (70% (v/v), 85% (v/v), 90% (v/v), 100% (v/v)), followed by histoclear then paraffin prior to embedding in paraffin wax blocks using a Shandon Histocentre 3 embedding centre. Blocks were cut into 5 μm slices using a Leica Finesse 325 microtome, slices placed onto glass plates prior yo haematoxylin and eosin staining. Paraffin was removed by immersion of plates into xylene then slides rehydrated through an ethanol gradient (100% (v/v), 90% (v/v), 70% (v/v) for 5 min each then washed in running water for 5 min. Sections were stained with Harris haematoxylin for 4 min then washed in running water prior to placement in 1% (v/v) HCl in ethanol for 30 sec. Slides were then washed in water for 1 min then placed in 1% (v/v) eosin for 2 min prior to further 5 min wash in deionised water. Sections were then dehydrated by ethanol immersions (70% (v/v), 90% (v/v), 100% (v/v)) followed by 10 min in Histoclear. The cover slips were fixed over the section using DPX mounting medium.

2.6.5.2 Liver triglyceride assay

Liver (25mg) was homogenised in 1 ml 5% (v/v) NP-40 in a Dounce homogeniser (15 passes), heated to 100°C for 5 min then cooled to room temperature. Homogenates were heated to 100°C again for 5 min, cooled to room temperature and centrifuged (21,910 x g, 3 min). Supernatants were diluted in 9 vol of H_2O and 25 μl assayed using an Abcam Triglyceride Quantification Assay Kit (ab65336), measuring absorbance at 570 nm.

2.6.6 Adipose measurements

Adipose tissue was isolated from subcutaneous (inguinal, excluding lymph node), epididymal, mesenteric, perinephric and interscapular (brown adipose tissue) regions and weighed. Samples were then snap frozen for protein or RNA analysis.

2.6.6.1 Adipose tissue protein extraction

Tissue samples were weighed then homogenised with 4 vol of lysis buffer by 10 passes with a Dounce homogeniser. Homogenates were transferred to a microcentrifuge tube, vortex mixed and placed on ice for 20 min. Homogenates were subsequently centrifuged (21,910 x g, 4°C, 10 min). Supernatants were stored at -80°C. Protein lysates were separated by SDS-PAGE and immunoblotting was used to analyse proteins of interest.

2.6.6.2 Adipose tissue RNA extraction

Tissue samples were homogenised with 750 µl Qiazol using a Precellys bead beating homogeniser. Homogenates were combined with 200 µl chloroform and incubated at room temperature for 2 min. Homogenates were subsequently centrifuged (12,000 x g at 4°C for 15 min). The upper aqueous phase (300 µl) was mixed with 500 µl of isopropanol and incubated at room temperature for 10 min. The mixture was then centrifuged (12,000 x g at 4°C for 10 min) and supernatant combined with 500 µl 75% (v/v) ethanol. Samples were further centrifuged (8,000 x g at 4°C for 5 min) then sample pellets were dried prior to the addition of 40 µl nuclease free water and kept on ice. After 1 h samples were incubated at 65°C for 5 min then returned to ice. The RNA concentration was measured using the NanoDrop then stored at -80°C. This protocol was performed by Carol Thomson, University of Glasgow.

2.7 Statistical Analysis

Results are expressed as mean ± standard error of the mean. Where multiple experimental conditions exist and experiments have been repeated, results

were compared to a designated control or maximally stimulated sample within each experiment. Data were analysed using GraphPad Prism software (California, U.S.A.). Normal distribution has been assumed throughout as sample numbers were insufficient to determine normal distribution. Statistical significance was determined by one-way or two-way ANOVA or t-test depending on number of treatments being compared, $p<0.05$ is regarded as significant. Given that normal distribution was assumed, selected data have been re-analysed using non-parametric analytic methods as indicated in the figure legend to allow further interpretation to readers.

3 Chapter 3 – The evaluation of SW872 cells as a human adipocyte model for the study of AMPK activation and the local adipocyte RAAS.

3.1 Introduction

3.1.1 Adipocyte models

Obesity and its associated cardiometabolic disorders including diabetes are a major threat to the health of current and future populations. Although prevention is the simplest way to address these problems (Schellenberg et al. 2013, Stevens et al. 2015), present measures have not been able to control this global epidemic estimated to affect over 650 million adults worldwide (WHO Obesity and overweight, 2017). Adipose tissue is a logical place for investigation and targeting therapeutics. Adipose tissue contains many constituent cell types, however the principal site of fat storage is the adipocyte. In addition to its metabolic functions reviewed in 1.2 it has a complex endocrine function and can secrete in excess of 600 adipocytokines (Lehr et al. 2012). Dysfunctional secretion of pro-inflammatory mediators is one of the proposed mechanisms leading to systemic metabolic dysfunction associated with obesity (Esser et al. 2014). In addition, demand for fat storage can exceed the capacity of adipose tissue and result in ectopic fat deposition in key metabolic organs such as the liver and pancreas impacting on insulin secretion and action (Sattar and Gill, 2014).

The adipocyte is therefore a complex cell with dynamic functions which are of great interest in the study of obesity and diabetes. The 3T3-L1 pre-adipocyte is the most widely studied cell line in adipose research with highly standardised culture and differentiation protocols (Ruiz-Ojeda et al. 2016). However, as the 3T3-L1 adipocyte is derived from a mouse it may therefore not necessarily mimic human adipocyte function. The SW872 cell line is derived from humans and is also able to be differentiated into a lipid storing cell. It is derived from a liposarcoma and therefore its behaviour as a mature human adipocyte may also differ from adipocytes in normal adipose depots. Both of these cells require differentiation using a cocktail of hormones to reach adipocyte status (as described in 2.2.2 and 2.2.6).

3.1.2 AMPK activity in adipocytes

AMP-activated protein kinase is a ubiquitously expressed heterotrimeric kinase activated in low energy states. In adipocytes AMPK activation inhibits insulin-stimulated glucose uptake, lipogenesis, adipogenesis and stimulates fatty acid oxidation (Bijland et al. 2013). AMPK is also known to have anti-inflammatory properties and can regulate the expression of adipocytokines (Bijland et al. 2013). It is activated by a wide range of substances including metformin, the first line medication for type 2 diabetes (Boyle et al. 2011). The experimental pharmacological AMPK activator AICAR has been widely used in the investigation of AMPK, it is metabolized to ZMP which acts as an AMP mimic which has given rise to some concerns regarding its specificity (Guigas et al. 2009). The small molecule A769662 was described as an AMPK activator in 2006, it binds directly to heterotrimers containing the β1 subunit of AMPK resulting in activation (Cool et al. 2006). ACC is a downstream AMPK signalling target and phosphorylation of ACC at Ser79 (rat ACC1 sequence) is an indicator of AMPK activation (Hardie, 1989).

3.1.3 The local adipocyte RAAS

The RAAS has been implicated in the pathogenesis of metabolic disorders associated with obesity (Underwood and Adler, 2013). The systemic upregulation of RAAS may be the predominant contributing factor however intriguingly there is now known to be a complete RAAS within adipocytes which must also be considered (Briones et al. 2012, Marcus et al. 2013). Indeed studies have linked the local adipose RAAS with systemic insulin resistance (Marcus et al. 2013).

3.1.4 Aims

This study set out to characterise insulin and AMPK signalling in the SW872 cell line with comparison to 3T3-L1 as a benchmark for *in vitro* investigation of adipocytes. In addition, the presence of RAAS components was examined in these two adipocyte models.

3.2 Results

3.2.1 Differentiation of 3T3-L1 and SW872 adipocytes

Lipid uptake and storage is the characteristic function of an adipocyte. To determine the effect of adipocyte differentiation in both 3T3-L1 and SW872 cells, oil red O staining was carried out on cells cultured for the same duration treated with or without adipocyte differentiation media. In 3T3-L1 cells there was no basal staining with oil red O (Fig. 3.1A) however a marked increase in staining was seen in cells which had been treated with the adipocyte differentiation protocol (Fig. 3.1B). In SW872 cells a small amount of oil red O uptake was observed in cells which had not been treated with adipocyte differentiation media (Fig. 3.1C). There was a definite increase in oil red O staining observed following treatment with differentiation media (Fig. 3.1D) yet not to the extent seen in 3T3-L1 adipocytes.

3.2.2.1 Insulin signalling in SW872 adipocytes

Insulin signalling in adipocytes leads to translocation of GLUT4 to the cell membrane and influx of glucose. Insulin responsiveness has been established in 3T3-L1 adipocytes, a classic tool for studying insulin stimulated glucose transport (Salt et al. 2000, Ewart et al. 2005, Sadler et al. 2015). Studies in our laboratory have demonstrated that 10 nM insulin will stimulate a robust signalling response in 3T3-L1 adipocytes (Boyle et al. 2011). To examine the insulin responsiveness of SW872 adipocytes, cells were incubated in insulin (10 nM) for various durations or at different concentrations for 10 min. Akt Ser473 phosphorylation was used as a marker of insulin signalling. Insulin increased Akt phosphorylation maximally at a concentration of 100 nM after 10 min (58% increase, p=0.0002). Lower concentrations of insulin tended to increase Akt Ser473 phosphorylation, yet this did not achieve statistical significance.

3.2.2.2 Insulin stimulated glucose transport in SW782 adipocytes

Given the muted insulin signalling response in SW872 adipocytes, a 2-deoxy-[^{3}H]-glucose uptake assay was performed. Insulin stimulation (10 nM) led to a 22% increase in glucose uptake (p=0.0036)(Fig 3.3A) which although significant was a smaller increase than expected. Therefore, stimulation with different insulin concentrations (10 nM, 100 nM and 1 µM) and after different durations of incubation with 2-deoxy-[H^3]-glucose (1, 3 and 6 min) was carried out (Fig 3.3B). This experiment demonstrated that basal 2-Deoxy-[^{3}H]-glucose increased with time in a linear fashion however increasing concentrations of insulin did not result in a robust increase in glucose uptake. In contrast to previous studies in our laboratory using 3T3-L1 adipocytes, there was only minimal stimulation of 2-deoxy-[^{3}H]-glucose uptake in response to insulin in SW872 adipocytes. Further investigation of glucose transport was therefore conducted in 3T3-L1 adipocytes (5.2.3.4).

3.2.2.3 Basal Akt phosphorylation in SW872 adipocytes compared to 3T3-L1 adipocytes

In light of the lack of insulin responsiveness, a comparison was performed to identify differences in basal Akt phosphorylation between 3T3-L1 adipocytes and SW872 adipocytes. Basal phosphorylation of Akt was significantly higher in SW872 adipocytes when compared to 3T3-L1 adipocytes (0.29 vs 2.28 a.u., p=0.0001) which, assuming similar species avidity of the antibody, may be one explanation for the reduced response to insulin even at concentrations up to 1 µM.
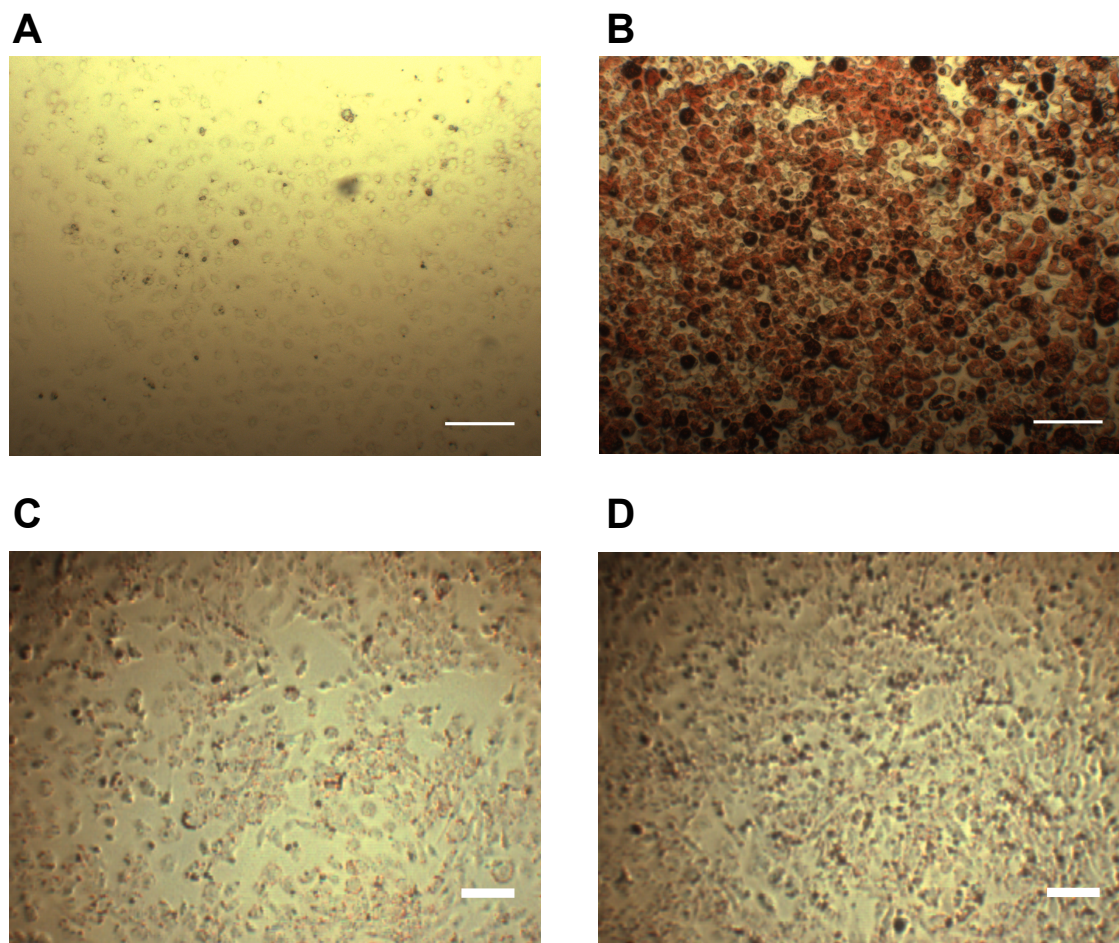
Figure 3.1 Oil red O staining of 3T3-L1 and SW872 adipocytes pre- and post-differentiation.

3T3-L1 and SW872 cells were cultured until confluence prior to differentiation (as described in 2.2.2). A. Undifferentiated 3T3-L1 fibroblasts, B. Differentiated 3T3-L1 adipocytes, C. SW872 cells without differentiation medium and D. SW872 cells with differentiation medium were stained with oil red O and images obtained. Representative images are shown from 2 independent experiments. Scale bars represent arbitrary distance to allow comparison within cell types.
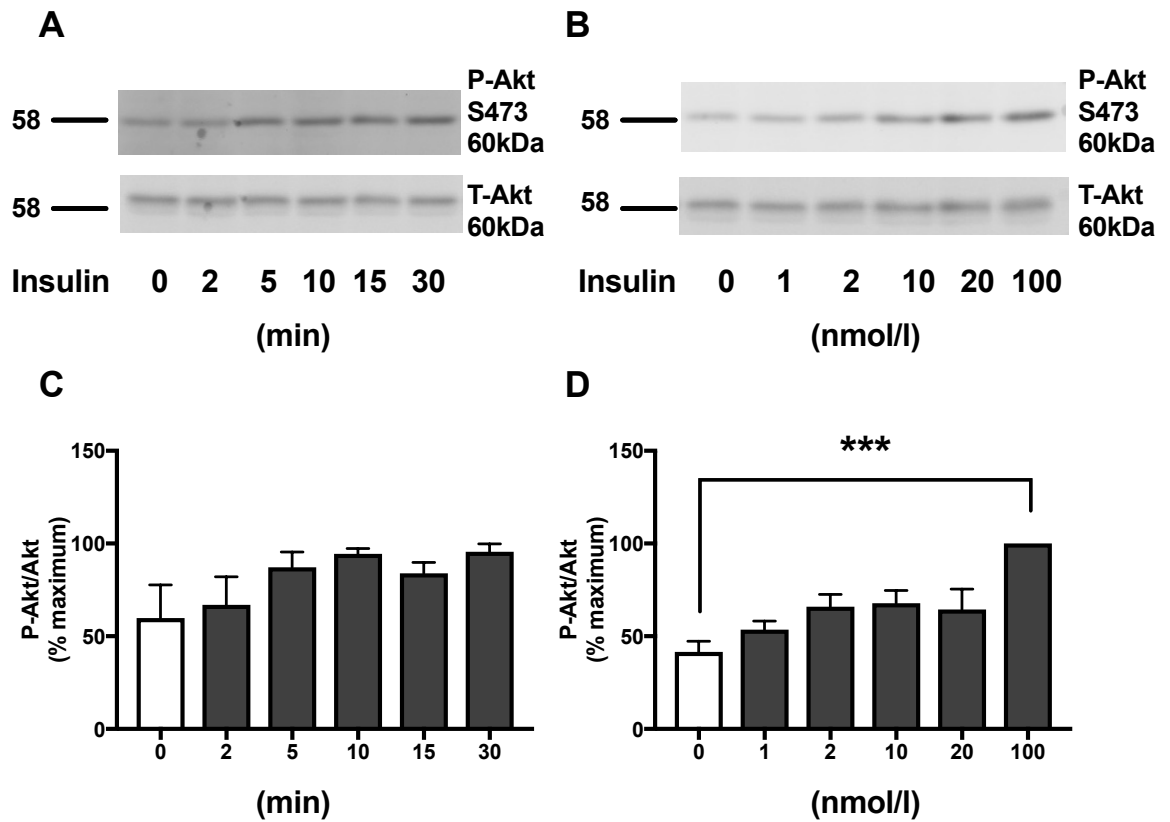
Figure 3.2 Insulin signalling in SW872 adipocytes

SW872 adipocytes were incubated in serum free media for 2 h then stimulated with insulin (10 nM) for the durations indicated or at the concentrations indicated for 10 min. Cell lysates were prepared, proteins resolved by SDS-PAGE and immunoblotted for the indicated proteins (P-Akt, phospho-Akt Ser473; T-Akt, total Akt). A. & B. Representative immunoblots with the molecular masses of marker proteins (in kDa) shown. C. & D. Quantification of P-Akt levels relative to Akt. n=3, ***P<0.001, one-way ANOVA.

A

B
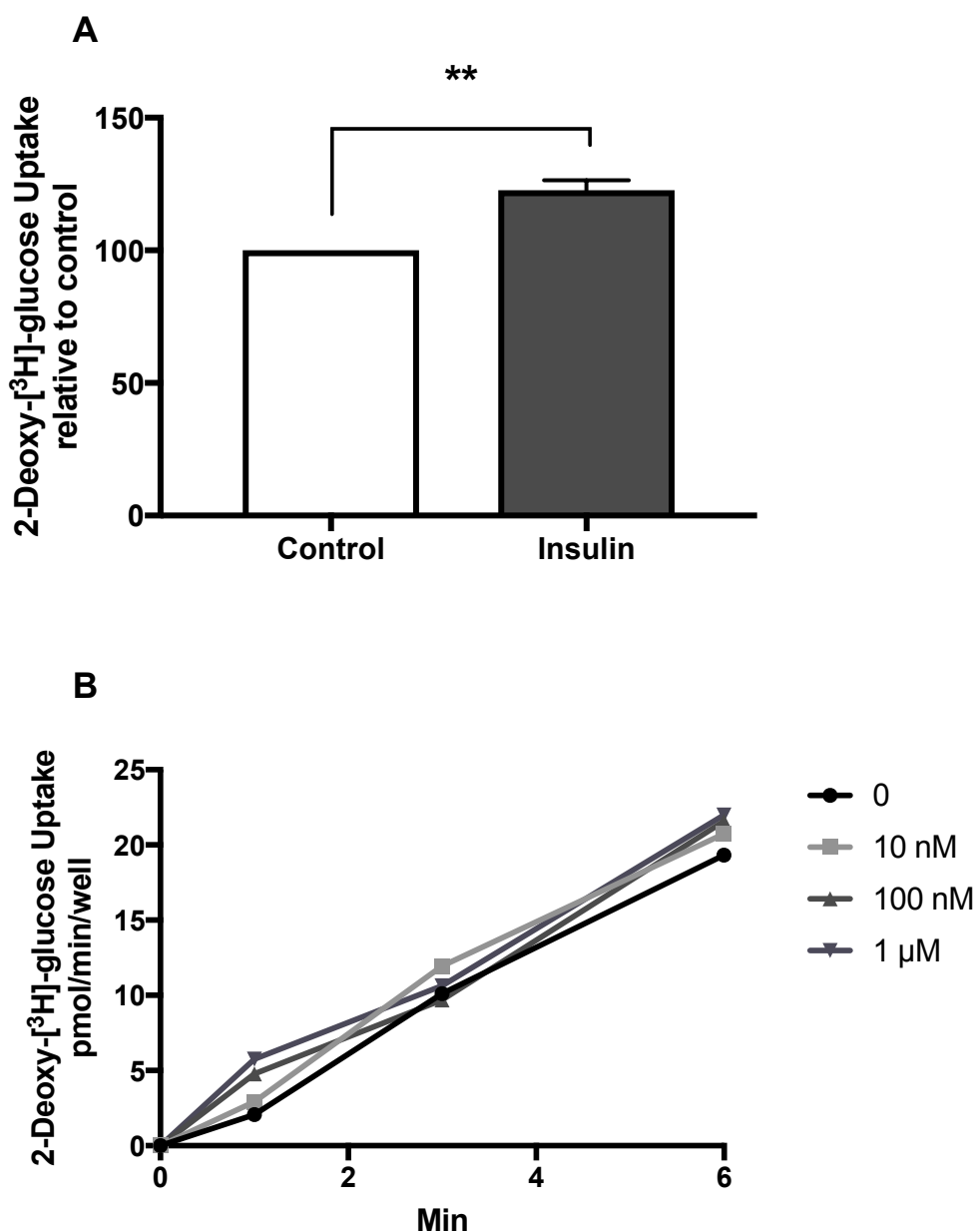
Figure 3.3 Glucose transport in SW872 adipocytes

SW872 adipocytes were incubated in serum free media for 2 h then media changed to KRP for 1 h prior to stimulation with A. 10 nM insulin for 10 min prior to incubation with 2-deoxy-[3H]-glucose for 3 min or B. various concentrations of insulin as indicated for 10 min, prior to incubation with 2-deoxy-[3H]-glucose for the times indicated. Cell-associated [3H] was measured using a scintillation counter, all experiments were performed in duplicate. A. n=3, t-test **p<0.01. B. n=1.
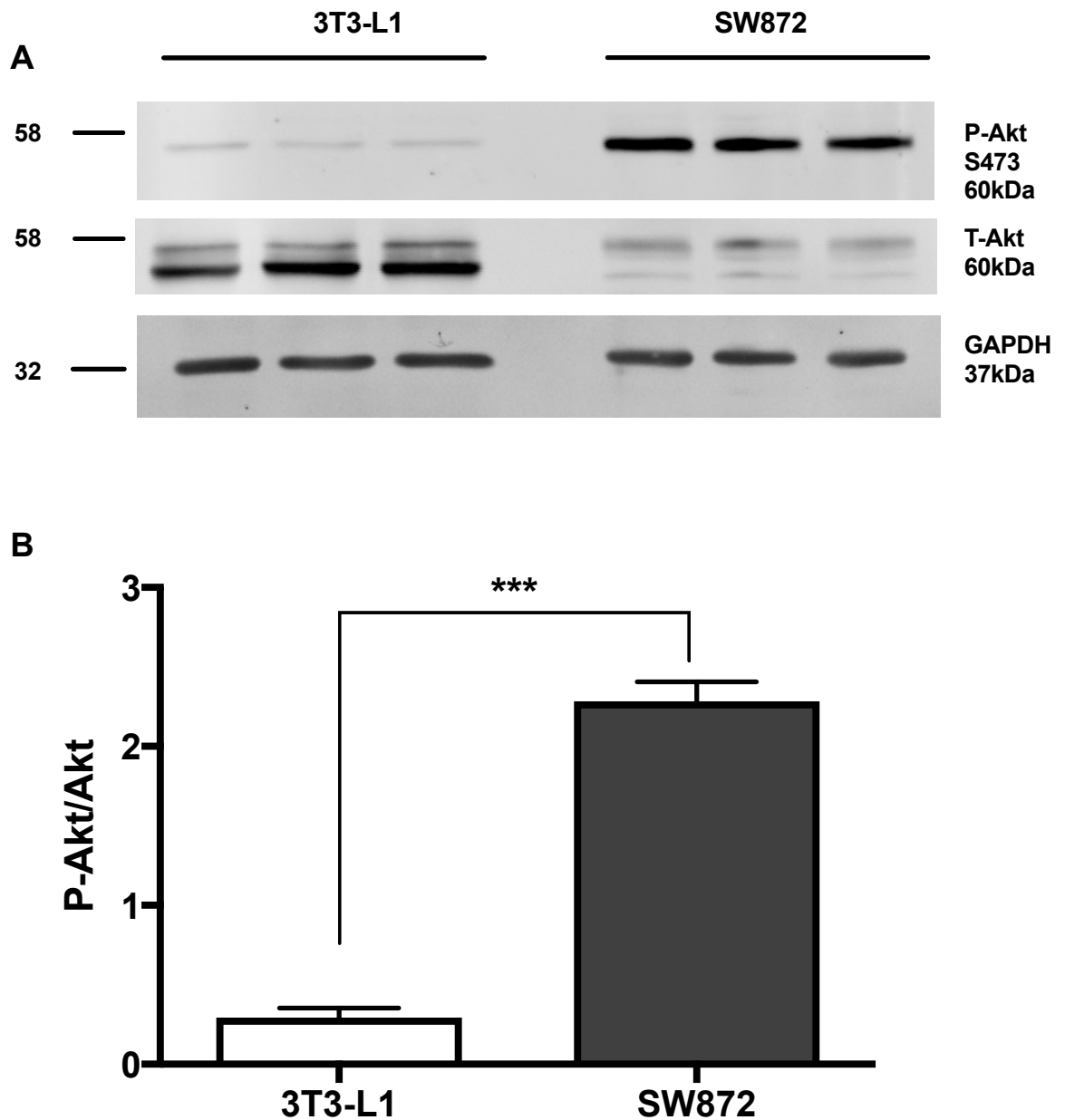
Figure 3.4 Immunoblot analysis of basal Akt signalling in 3T3-L1 and SW872 adipocytes

*3T3-L1 and SW872 adipocytes were incubated in serum free media for 2 h. Cell lysates were prepared, proteins resolved by SDS-PAGE and immunoblotted for the indicated proteins. A. Representative immunoblot. B. Quantification of P-Akt levels relative to Akt. n=3, t-test ***P<0.001. Mann Whitney test not significant.*

3.2.3.1 The effects of AICAR and A769662 on AMPK signalling in SW872 adipocytes

Our laboratory has previously demonstrated that both AICAR and A769662 stimulate AMPK activity in 3T3-L1 adipocytes (Boyle et al. 2011, Mancini et al. 2017), yet whether AICAR and A769662 activate AMPK in SW872 adipocytes remains uncharacterised. SW872 cells were therefore incubated with different concentrations of AICAR or A769662 for different durations to assess their effect on AMPK activity as measured by phosphorylation of ACC. Stimulation of SW872 adipocytes with 1 mM AICAR significantly stimulated ACC phosphorylation within 60 min, an effect sustained for at least a further 60 min (Figs 3.5A & 3.5B). Lower concentrations of AICAR tended to increase ACC phosphorylation, yet this did not achieve statistical significance (Fig 3.5D). ACC phosphorylation was significantly increased within 30 min of the addition of 300 μM A769662, a response sustained for a further 30 min (Fig 3.6). An incremental response to concentration was observed however a statistically significant increase in ACC phosphorylation was only achieved with 300 μM of A769662 (Figs 3.6C & 3.6D).
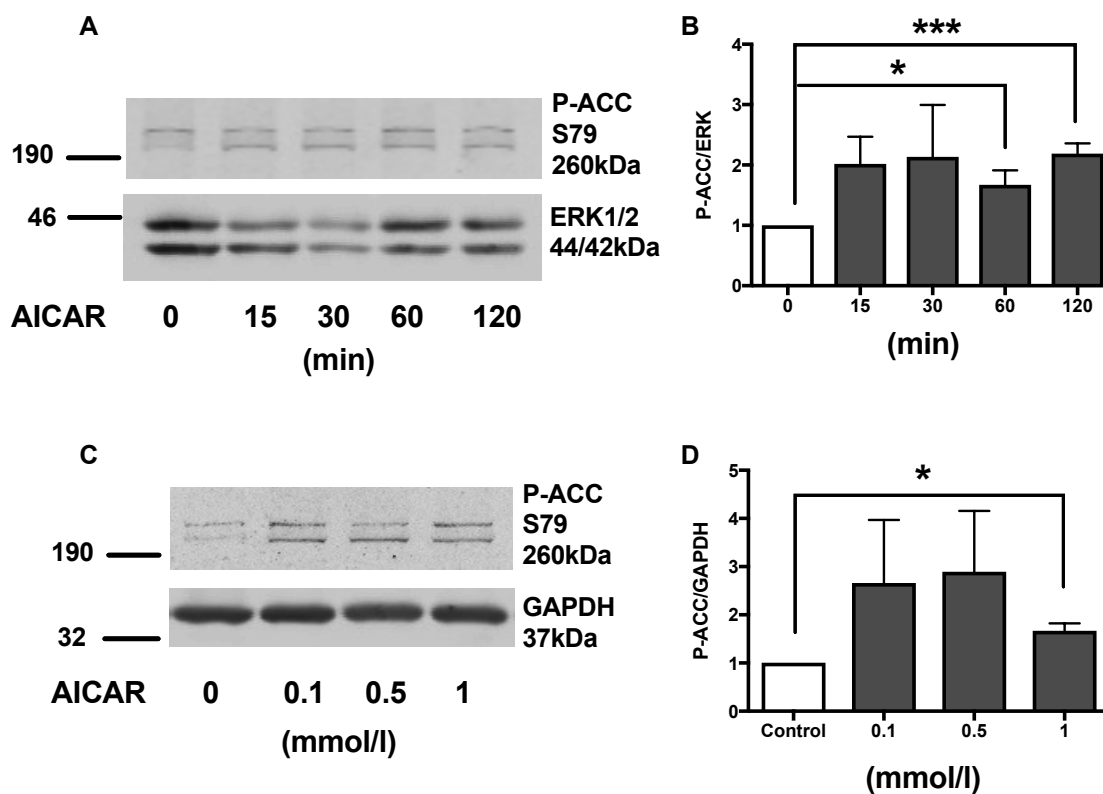
Figure 3.5 Effects of AICAR on AMPK signalling in SW872 adipocytes.

SW872 adipocytes were incubated in serum free medium for 2 h prior to stimulation with 1 mM AICAR for the times indicated in A. and B. (min) and at concentrations indicated in C. and D. for 1 h. Cell lysates were prepared, proteins resolved by SDS-PAGE and immunoblotted for the indicated proteins (P-ACC; phospho-ACC Ser79). A. and C. Representative immunoblots with the molecular masses of marker proteins (in kDa) shown. B. and D. Quantification of P-ACC levels relative to ERK or GAPDH. n=3, t-test *p<0.05, ***p<0.001.
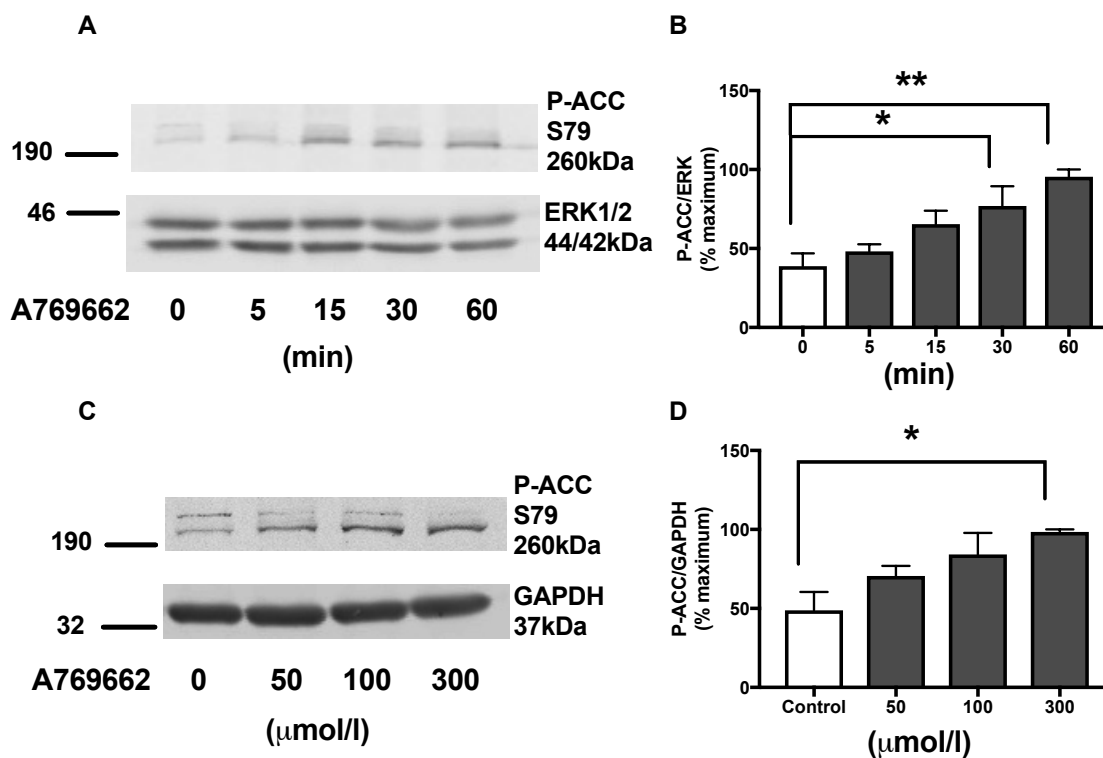
Figure 3.6 Effects of A769662 on AMPK signalling in SW872 adipocytes.

SW872 adipocytes were incubated in serum free medium for 2 h prior to stimulation with 300 µM A769662 for the times indicated in A. and B. (min) and at concentrations indicated in C. and D. for 30 min. Cell lysates were prepared, proteins resolved by SDS-PAGE and immunoblotted for the indicated proteins. A. and C. Representative immunoblots are shown. B. and D. Quantification of P-ACC levels relative to ERK or GAPDH as indicated. n=3, one-way ANOVA *p<0.05, **p<0.01.

3.2.4 The effect of adipocyte differentiation on expression of components of the renin angiotensin aldosterone system in SW872 adipocytes

Gene expression of components of the RAAS in SW872 cells before and after adipocyte differentiation was next examined. The change in expression was determined relative to differentiated cells.

Differentiation of SW872 cells resulted in a significant increase in mRNA expression of angiotensinogen (3.6-fold, p=0.012), type 2 angiotensin II receptor (7.1-fold, p=0.021) and the mineralocorticoid receptor (1.9-fold, p=0.01)(Fig. 3.7). In contrast, there was no change in the mRNA expression of the glucocorticoid receptor. Taqman® qPCR was also performed for the angiotensin II type 1 receptor however the result was undetectable after 40 amplification cycles. The same probe was used with duplicate samples of human adipose tissue cDNA yielding a result with a Ct value of 36.

3.2.5 Expression of components of the renin angiotensin aldosterone system in cultured SW872 and 3T3-L1 adipocytes

To determine the basal mRNA expression level of RAAS components in 3T3-L1 and SW872 adipocytes the mean Ct values of untreated samples were determined and are reported here with the standard error of the mean (Table 3.1). The mean Ct values were lowest, indicating higher gene expression, for angiotensinogen (mean Ct 21.58 in 3T3-L1 and 23.36 in SW872) and the glucocorticoid receptor (mean Ct 25.06 in 3T3-L1 and 21.78 in SW872) in both groups. The mineralocorticoid receptor (mean Ct 27.22 in 3T3-L1 and 30.83 in SW872) had the next highest expression level followed by angiotensin type 2 receptor (mean Ct 29.17 in 3T3-L1 and 34.77 in SW872). The AT1 receptor was not detectable in either cell type under these conditions. When the murine probe for AT1 receptor was used in mouse adipose tissue the Ct value was detected at 25 cycles.
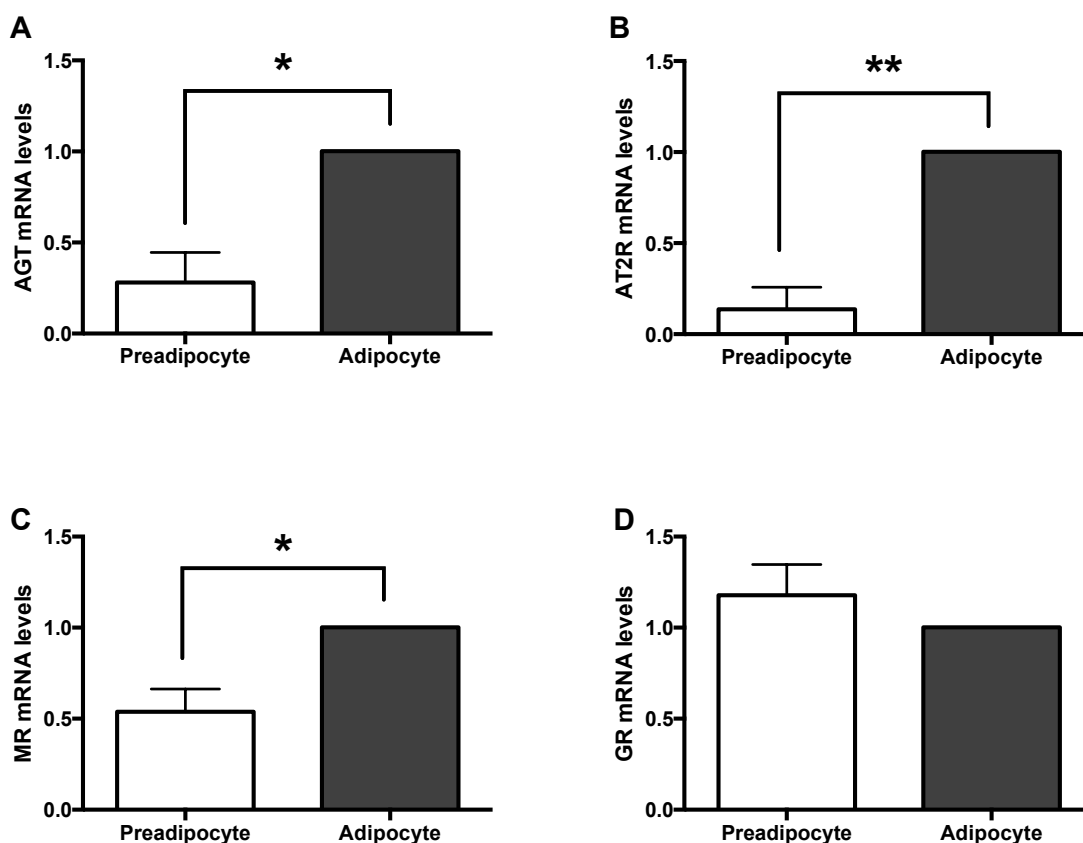
Figure 3.7 RAAS component gene expression pre- and post-differentiation in SW872 adipocytes.

RNA was extracted from SW872 cells pre- and post-differentiation into adipocytes. Reverse transcription was carried out prior to Taqman qPCR assays for A. angiotensinogen (AGT), B. angiotensin II type 2 receptor (AT2R), C. mineralocorticoid receptor (MR) and D. glucocorticoid receptor (GR). All mRNA levels were normalised to TATA-box binding protein expression. A. and B. n=3, C. and D. n=4, t-test *p<0.05, **p<0.01.

	3T3-L1 (Mean Ct)	S.E.M.	SW872 (Mean Ct)	S.E.M.
AGT	21.58	0.7729	23.36	0.4156
AT1R	>40		>40	
AT2R	29.17	1.085	34.77	0.4058
MR	27.22	0.9196	30.83	0.2945
GR	25.06	0.9784	21.78	0.2013

Table 3.1 Mean Ct value of RAAS genes in 3T3-L1 adipocytes and SW872 adipocytes.

RNA was extracted from 3T3-L1 adipocytes and SW872 adipocytes. Reverse transcription was carried out prior to Taqman qPCR assays for angiotensinogen (AGT), angiotensin II type 1 receptor (AT1R), angiotensin II type 2 receptor (AT2R), mineralocorticoid receptor (MR) and glucocorticoid receptor (GR), normalized to TATA-binding protein mRNA expression. n=11-12.

3.3 Discussion

In this study two adipocyte models have been used, the widely investigated 3T3-L1 adipocyte and the less commonly studied SW872 adipocyte. In many cases studies related to human disorders are carried out in adipocytes of mouse, rat or human descent and may be performed in whole adipose tissue, isolated adipocytes or cell lines. This results in a somewhat mixed and conflicted literature. In this work we aim to perform studies in the human white adipocyte model SW872 but reflect on 3T3-L1 as the standard, albeit murine, model.

Initial studies determined the effect of adipocyte differentiation on lipid storage. Here, a marked staining of oil red O was observed in 3T3-L1 adipocytes compared to undifferentiated fibroblasts, consistent with previous reports (Ruiz-Ojeda et al. 2016). In SW872 adipocytes, there was again an increase in lipid storage observed by increased oil red O staining of cells treated with differentiation media compared to untreated, however there was a small amount of oil red O visible on the untreated cells. Within the literature it is noted that this cell line will take up lipid without any specific adipogenic stimulus (Wassef et al. 2004). Another human adipocyte model, SGBS, was recently compared to SW872, in this regard SGBS was found to express some markers consistent with a brown adipocyte phenotype. Whereas SGBS cells stained positively for UCP-1, this was not the case for SW872 (Guennoun et al. 2015). The authors identified the SW872 cells took on a white adipocyte phenotype from day 7 of differentiation and this phenotype remained consistent over subsequent days of culture, suggesting they are a preferable human model for the study of white adipocytes (Guennoun et al. 2015). It must be noted that oil red o staining was poor in comparison to 3T3-L1 adipocytes. Another method to assess adipocyte status which would compliment this work would be to assess for the presence of differentiation markers including PPARɣ, adiponectin and leptin.

Insulin stimulated glucose transport in skeletal muscle and adipose tissue is crucial for maintaining normoglycaemia. Insulin signalling via PI3 kinase and Akt leads to GLUT4 translocation and glucose influx (Summers et al. 2000).

3T3-L1 adipocytes have been demonstrated to be insulin sensitive and are therefore useful tools for the study of adipose glucose metabolism. According to the published literature at the start of these studies, SW872 adipocytes had been used to study lipid transfer and production but not insulin signalling or glucose transport (Richardson et al. 1996, Vassiliou et al. 2001). In this study, insulin signalling was examined by time and concentration response in SW872 adipocytes. At 10 nM, a concentration stimulating a robust response in 3T3-L1 adipocytes, insulin was unable to significantly increase Akt phosphorylation at a range of time points up to 30 min. However, a significant increase in Akt phosphorylation was achieved with 100 nM insulin in SW872 adipocytes. One previous study has reported that insulin reduced apoC-1 and apoE secretion from SW872 adipocytes, although this was only at a very high insulin concentrations (1 µM) and no effect on insulin signalling pathways was evaluated (Wassef et al. 2004).

Given that Akt phosphorylation was increased with insulin at 100 nM, glucose transport was examined next. Glucose enters mature adipocytes via two glucose transporters: GLUT1 which is present basally and GLUT4 which is insulin dependent and restricted largely to adipose and skeletal muscle (Hoffman and Elmendorf, 2011). Initial findings here identified a statistically significant yet very small increase in 2-deoxy-[^{3}H]-glucose uptake with 10 nM insulin. Despite increasing concentrations of insulin up to 1 µM there remained a lack of robust increase in glucose uptake although a linear response to time exposed to 2-deoxy-[^{3}H]-glucose was demonstrated. It is possible that this model lacks the vesicular trafficking machinery required to translocate GLUT4 to the cell membrane efficiently, or may lack GLUT4 completely, though there are many plausible explanations. Indeed, a crude comparison between basal Akt phosphorylation in 3T3-L1 and SW872 adipocytes revealed increased basal signalling in SW872 adipocytes. Perhaps this is because the cells are derived from liposarcoma and therefore may have a high level of mitogenicity. Another possible cause for elevated basal Akt signalling could be SV40 transformation (Skoczylas et al. 2004), however this cell line was not SV40 tranformend (direct communication, ATCC, LGC, Middlesex, UK). From these data in SW872 adipocytes it can be concluded that SW872 adipocytes are not a useful model to study insulin stimulated glucose

transport nor insulin signalling. Therefore, later studies investigating glucose transport will be conducted in 3T3-L1 adipocytes.

Stimulation of SW872 adipocytes with both AICAR and A769662 led to significant increases in ACC phosphorylation in this study at concentrations that were also effective in 3T3-L1 adipocytes. Establishing the use of these AMPK activators in this human white adipocyte model will allow further studies exploring the role of AMPK in its regulation of inflammation and the RAAS in SW872 adipocytes.

In order to study the influence of AMPK on the adipocyte RAAS expression of components was first identified. This study found that expression of angiotensinogen, the AT2 receptor and the mineralocorticoid receptor were significantly increased following SW872 adipocyte differentiation. The increase in expression of angiotensinogen is consistent with studies in both 3T3-L1 (Saye et al. 1990) and human adipocytes (Janke et al. 2002; Wang et al. 2005). The increase in AT2 receptor expression following adipocyte differentiation has been reported in one study which found very low expression in pre-adipocytes which was slightly increased following differentiation (Janke et al. 2002). One recent study found that the AT2 receptor may be anti-adipogenic as deletion of the AT2 receptor accelerated adipocyte differentiation in murine mesenchymal stem cells and decreased Wnt10b expression (Matsushita et al. 2016), a finding which somewhat opposes the data presented here where AT2R is induced upon differentiation.

The MR is proposed to be a crucial player in obesity and cardiometabolic disorders. The data presented in this chapter found an increase in expression of the MR in differentiated SW872 adipocytes with no change in the expression of the GR. This is consistent with another report that the MR was induced with adipocyte differentiation in 3T3-L1 cells at both the level of mRNA and protein, with no change in GR (Caprio et al. 2007). The function of the MR in adipose is not fully understood but it does appear to have an important role in adipogenesis where it is likely to be activated by glucocorticoids (Caprio et al. 2007). Knockdown of the MR but not the GR inhibited adipogenesis therefore suggesting a critical role for MR over the GR in adipogenesis (Caprio et al.

2007). Similarly, preadipocytes from mice with genetic knockout of the MR did not accumulate lipid, however those from GR knockout mice did accumulate lipid following adipogenic stimuli (Hoppmann et al. 2010). Conversely, in cells derived from human subcutaneous adipose tissue, stable knockdown of the GR not the MR impaired adipogenic responses to cortisol (Lee and Fried, 2014). Glucocorticoids are undoubtedly important in adipogenesis where they appear to mediate effects via either MR or GR, with studies in mice favouring MR and humans favouring GR as the key receptor mediating adipogenic effects (Caprio et al. 2007; Hoppmann et al. 2010; Lee and Fried 2014).

In this study the AT1R was undetectable in both the SW872 and 3T3-L1 adipocytes. This was an unexpected finding as there is a literature describing effects of angiotensin II in 3T3-L1 adipocytes being mediated through the AT1R (Asamizu et al. 2009, Than et al. 2012). The same probes were able to identify the AT1R in murine adipose tissue and human adipose tissue. Both of these samples contained other cell types than adipocytes, which may indicate AT1R is largely expressed by stromal-vascular cells in adipose tissue. Alternatively, the lack of AT1R in either cell line may be due to the differentiation process used or the conditions in our laboratory although standard protocols were followed. Multiple passaging or freeze-thaw cycles may also have led to poor expression of the AT1R. It is possible that the lack of AT1R altered the dynamics of the RAAS in these cells systems and may impact the findings in later chapters.

In summary, the human-derived SW872 white adipocyte model was able to store lipid but not to the same degree as 3T3-L1. High concentrations of insulin were required to achieve Akt signalling in SW872 adipocytes which appear to be a poor model for the study of insulin-stimulated glucose uptake. However, AMPK signalling was evident with similar doses of AICAR and A769662 to 3T3-L1 adipocytes and the RAAS system was present and induced with adipocyte differentiation. In the coming chapters the cross-talk between AMPK and the RAAS is explored in these two adipocyte models.

4 Chapter 4 – The effect of AMPK activators on the renin angiotensin aldosterone system in cultured adipocytes

4.1 Introduction

4.1.1 Local adipose tissue RAAS and interactions with AMPK

The principal RAAS hormones angiotensin II and aldosterone have been implicated in the development of adipose tissue inflammation and subsequent obesity-related metabolic disorders including insulin resistance (Underwood and Adler, 2013). Expression of the MR is elevated in adipose tissue of obese rodent models and individuals with increased BMI (Hirata et al. 2012) and MR blockade is associated with adipokine release and improved insulin sensitivity in rodent models (Hirata et al. 2009). Complete local RAASs have been identified in several tissues including adipose tissue generating interest into their physiological role (Briones et al. 2012).

AMPK is an energy sensing kinase which is activated by cellular stressors such as low energy (AMP abundance) and hypoxia in order to liberate ATP by several methods including increased mitochondrial biogenesis (Hardie et al. 2012). Within adipose tissue AMPK has a role in glucose and lipid metabolism and an increasingly well-characterised anti-inflammatory function (Bijland et al. 2013).

As the RAAS appears to play a causative role in obesity-related metabolic complications and AMPK is known to have anti-obesogenic actions in adipose tissue, the interaction between these two components was of great interest. At the start of the studies described in this chapter, interactions between AMPK and the RAAS had been studied in renal and cardiovascular models but not adipose tissue or adipocyte models (Nagata et al. 2004, Stuck et al. 2008, Lee et al. 2013). One study had also provided evidence that adipose tissue AMPK and RAAS are associated, in which both decreased AMPK activity and increased angiotensinogen expression were observed in subcutaneous adipose tissue of insulin resistant, but not insulin sensitive, obese individuals (Xu et al. 2012).

4.1.2 Aims

As alterations in AMPK activity and RAAS have been reported in adipose tissue from insulin resistant, obese individuals, the current study set out to determine the expression of RAAS components in murine (3T3-L1) and human (SW782) adipocyte cultured cell models and subsequently assess the influence of pharmacological AMPK activators on their expression and function.

4.2 Results

4.2.1 The effect of AICAR on expression of components of the renin angiotensin aldosterone system in 3T3-L1 adipocytes

In previous studies, AICAR has been demonstrated to activate AMPK for up to 24 h in 3T3-L1 adipocytes (Boyle et al. 2011). To determine whether AMPK activation influenced mRNA expression of RAAS components, differentiated 3T3-L1 adipocytes were incubated with AICAR at a concentration of 1 mM for 5, 9 or 25 h. Incubation with AICAR downregulated gene expression of the angiotensin II type 2 receptor by 94% (p<0.0001) and the mineralocorticoid receptor by 39% (p=0.0439) after 25 h, but no significant effect was seen with shorter durations of incubation (Fig. 4.1). AICAR had no significant effect on mRNA expression of angiotensinogen or the glucocorticoid receptor at any time point examined.

4.2.2 The effect of AICAR on expression of components of the renin angiotensin aldosterone system in SW872 adipocytes

In chapter 3, AICAR and A769662 were demonstrated to activate AMPK for up to 120 and 60 min respectively in SW872 adipocytes. To determine whether AMPK activation influenced mRNA expression of RAAS components in SW872 adipocytes, cells were incubated with 1 mM AICAR for 9 or 25 h and RAAS gene expression analysed. Stimulation with AICAR resulted in significantly reduced mRNA expression of angiotensinogen by 44% after 9 h (p=0.0001) and 40% after 25 h (p<0.0001) and the mineralocorticoid receptor by 53% after 9 h (p=0.01) and 59% after 25 h (p=0.0068) (Fig. 4.2) without significantly altering the mRNA levels of either the type 2 angiotensin II receptor or the glucocorticoid receptor. AMPK activity was present up to 24 h (Fig. 4.4C).
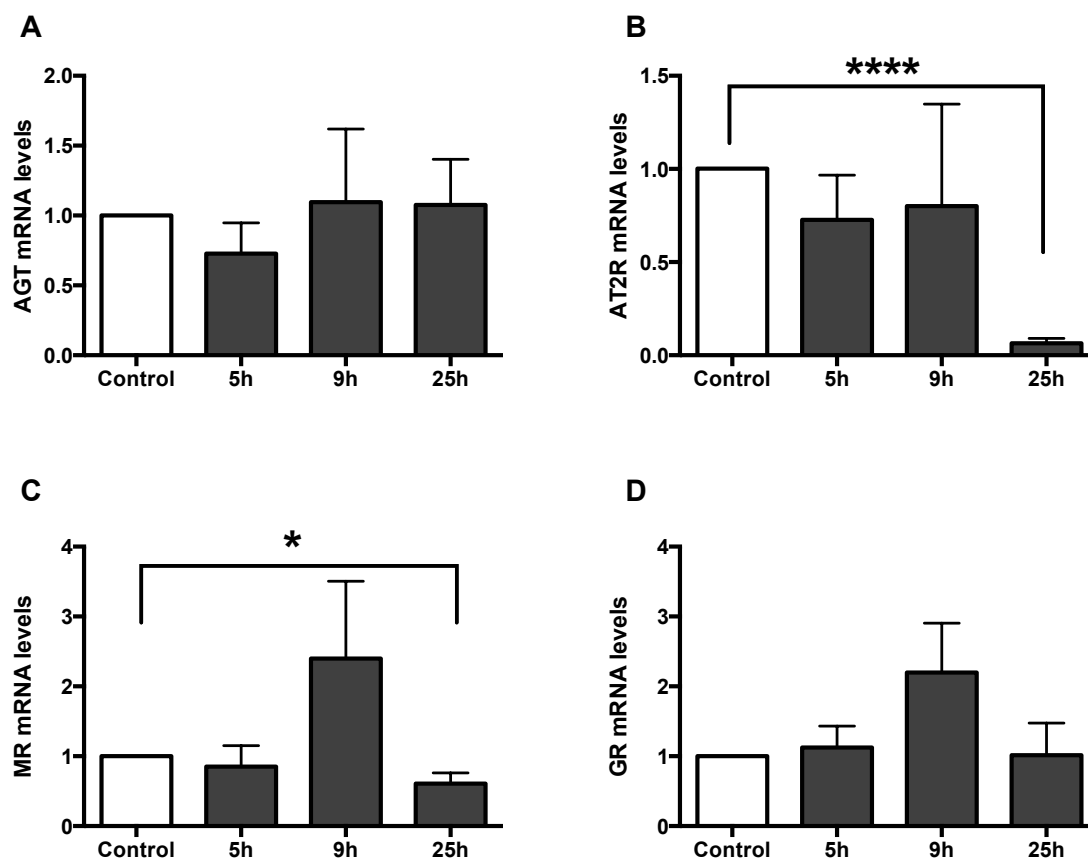
Figure 4.1 Effects of AICAR on gene expression of renin angiotensin aldosterone system components in 3T3-L1 adipocytes.

RNA was extracted from 3T3-L1 adipocytes incubated in the presence (filled bars) or absence (open bars) of AICAR (1 mM) for the indicated durations. Reverse transcription was carried out prior to Taqman qPCR assays for A. angiotensinogen (AGT), B. angiotensin II type 2 receptor (AT2R), C. mineralocorticoid receptor (MR) and D. glucocorticoid receptor (GR). Data are normalised to TATA-binding protein mRNA expression. n=4, unpaired t-test, *p<0.05, ****p<0.0001.
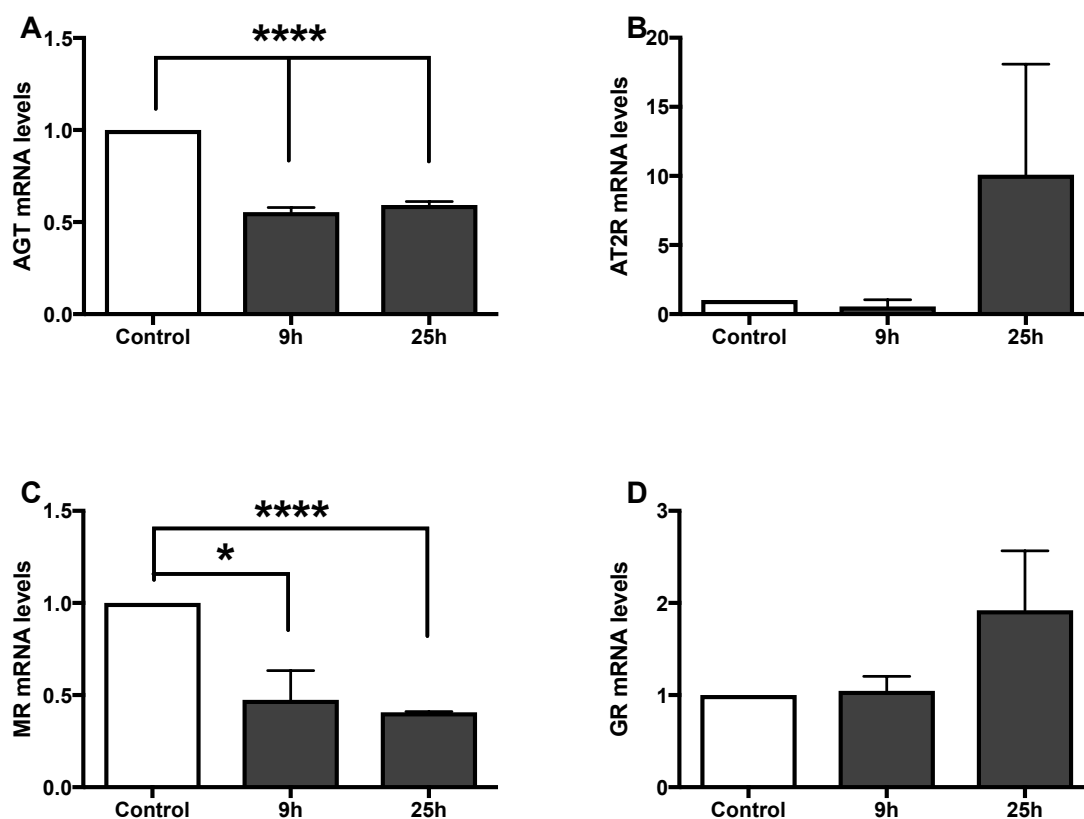
Figure 4.2 Effects of AICAR on gene expression of components of the renin angiotensin aldosterone system in SW872 adipocytes.

RNA was extracted from SW872 adipocytes incubated in the presence or absence of AICAR (1 mM) for the indicated durations. Reverse transcription was carried out prior to Taqman qPCR assays for A. angiotensinogen (AGT), B. angiotensin II type 2 receptor (AT2R), C. mineralocorticoid receptor (MR) and D. glucocorticoid receptor (GR). Data are normalised to TATA-binding protein mRNA expression. n=3 except for the 9 h time point in panels A. and B., where n=2. Unpaired t-test, *p<0.05, ****p<0.0001.

4.2.3 The effect of A769662 on expression of components of the renin angiotensin aldosterone system in SW872 adipocytes

Having determined the effects of AICAR on RAAS gene expression in SW872 adipocytes, the effect of the direct AMPK-activator A769662 was examined. Incubation with A769662 decreased expression of angiotensinogen and the mineralocorticoid receptor without any significant effect on the type 2 angiotensin II receptor or the glucocorticoid receptor (Fig. 4.3), similar to the effects of AICAR (Fig. 4.2). There was a 40% decrease in angiotensinogen at 24 h (p=0.004) but no significant change at 8 h. Furthermore, A769662 inhibited mineralocorticoid receptor mRNA expression with a consistent decrease at 8 (50% decrease, p=0.0008) and 24 h (49% decrease, p=0.0015).

4.2.4 The effect of A769662 on protein expression of the mineralocorticoid receptor in SW872 adipocytes

Given the common inhibitory effect of AICAR in both murine and human adipocyte models as well as A769662 in SW872 adipocytes on mineralocorticoid receptor gene expression, it was important to determine the effect on protein expression. In SW872 adipocytes A769662 significantly decreased protein expression of the mineralocorticoid receptor by 65% after 24 h (p=0.02)(Fig. 4.4). There was no significant decrease observed with AICAR (Fig. 4.4C).

4.2.5 The effect of AMPK activators on expression of alternative RAAS components in SW872 adipocytes

As both AICAR and A769662 decreased angiotensinogen and MR expression in SW872 adipocytes, the alternative arm of the RAAS was investigated. Expression of the Mas receptor was not significantly affected by either AMPK activator used (Fig 4.5A). However, AICAR decreased expression of ACE (42% decrease, p=0.0369) but A769662 had no effect. In contrast, ACE 2 expression was increased by A769662 (40% increase, p=0.0119), but was not influenced by AICAR. When ACE2 was normalised to ACE the ratio was significantly

increased by AICAR (35% increase, p=0.032, Fig 4.5 D) suggesting a shift towards the alternative from the classical RAAS.
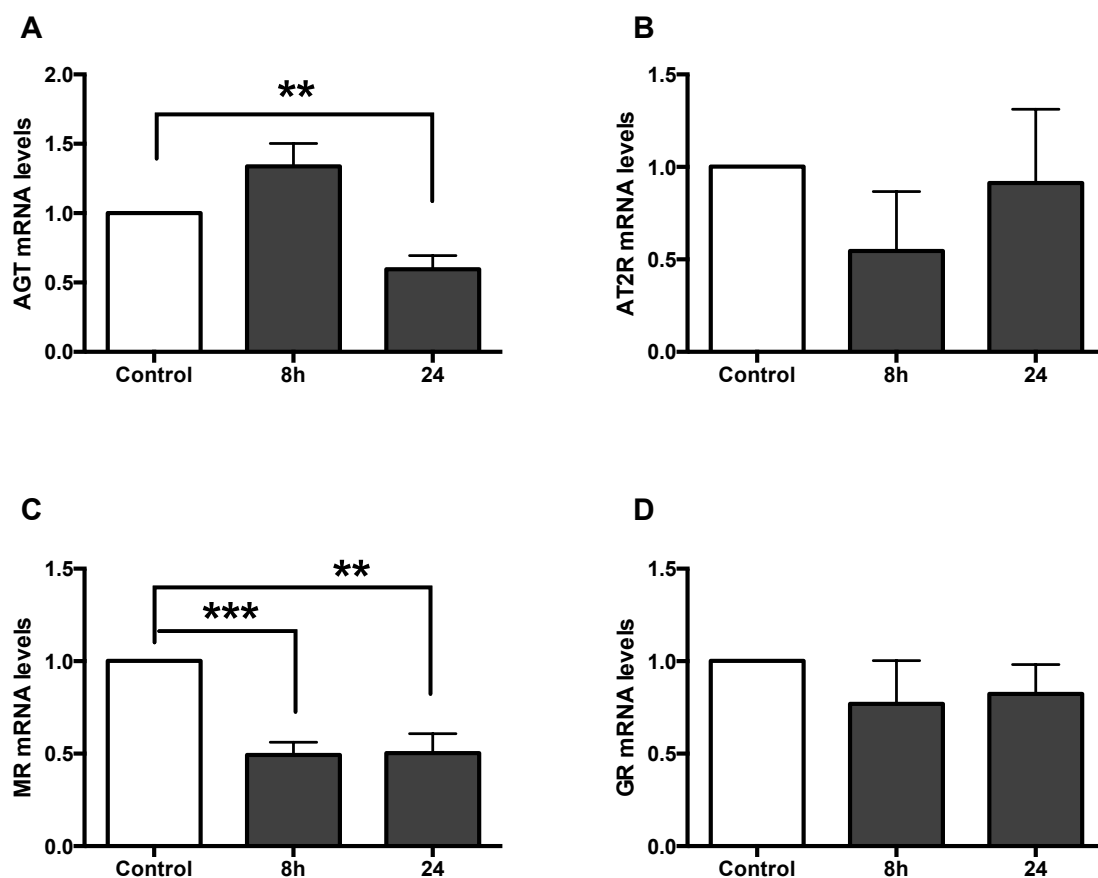
Figure 4.3 Effects of A769662 on gene expression of components of the renin angiotensin aldosterone system in SW872 adipocytes.

RNA was extracted from SW872 adipocytes incubated in the presence or absence of A769662 (300 μM) for the indicated durations. Reverse transcription was carried out prior to Taqman qPCR assays for A. angiotensinogen (AGT), B. angiotensin II type 2 receptor (AT2R), C. mineralocorticoid receptor (MR) and D. glucocorticoid receptor (GR). Data are normalised to TATA-binding protein mRNA expression. n=4 control and 8 h, n=3 24 h, unpaired t-test, **p<0.01, ***p<0.001.
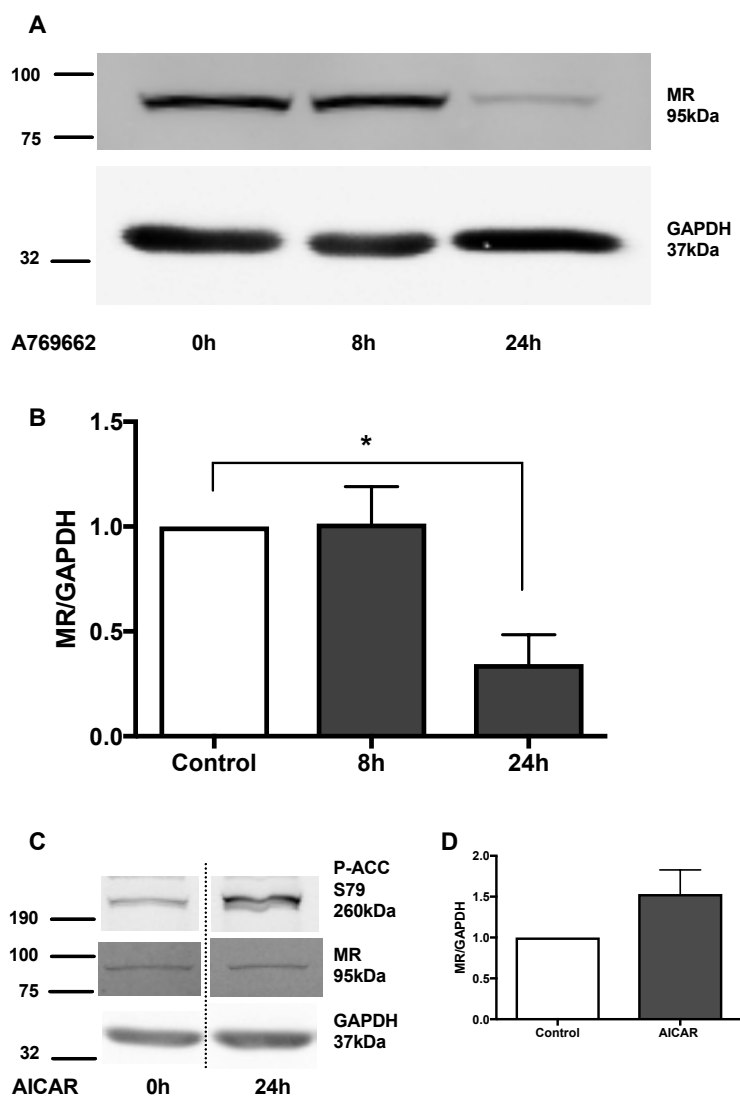
Figure 4.4 Effects of A769662 on protein levels of the mineralocorticoid receptor in SW872 adipocytes.

SW872 adipocytes were incubated in medium containing 1% (v/v) NCS overnight prior to stimulation with A., B. 300 µM A769662 for the times indicated or C., D. 1 mM AICAR for 24 h. Cell lysates were prepared, proteins resolved by SDS-PAGE and immunoblotted for the indicated proteins. A. and C. Representative immunoblots are shown, with the molecular masses of marker proteins (in kDa) indicated. In panel C. unrelated lanes have been removed for clarity. B. Quantification of MR levels relative to GAPDH for A769662 experiment, n=3. D. Quantification of MR levels relative to GAPDH for AICAR experiment, n=4. one-way ANOVA *p<0.05. P-ACC, phospho-ACC Ser79; MR, mineralocorticoid receptor.
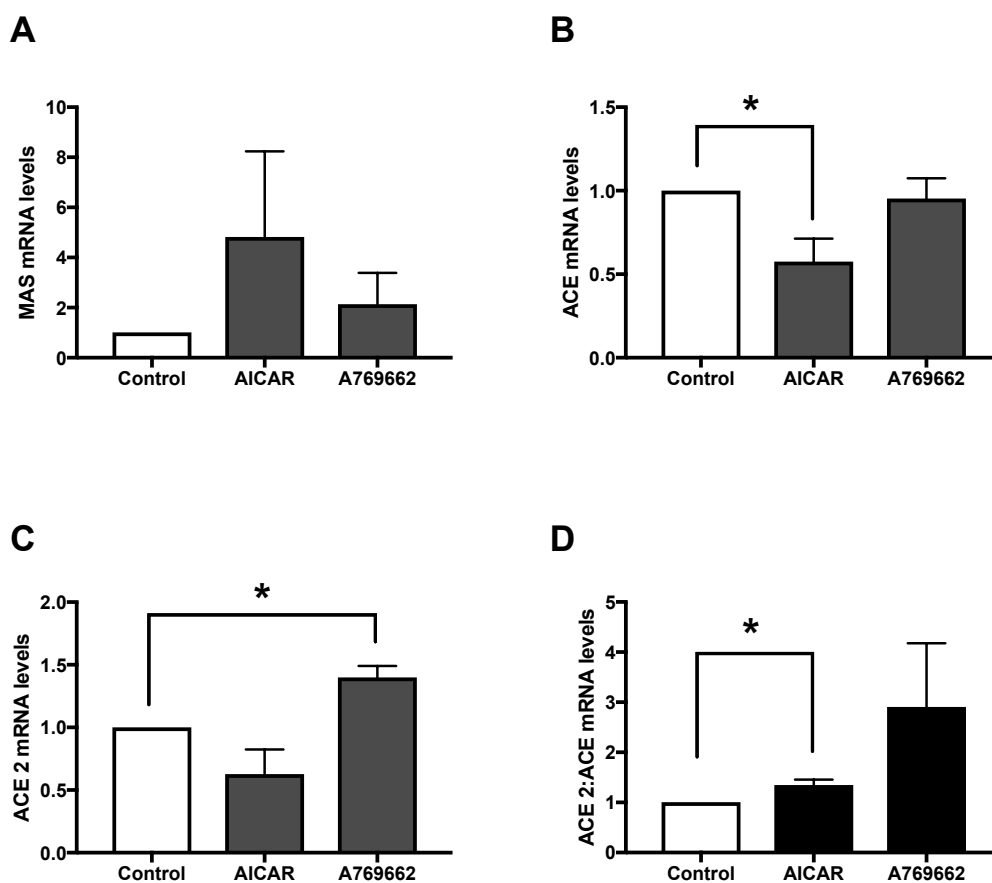
Figure 4.5 The effect of AMPK activators on the expression of Mas, ACE and ACE 2 in SW872 adipocytes

*RNA was extracted from SW872 adipocytes incubated in the presence of AICAR 1 mM or A769662 300 µM for 7 h. Reverse transcription was carried out prior to Taqman qPCR assays for A. Mas, B. ACE and C. ACE 2. For A. – C. data are normalised to TATA-binding protein mRNA expression. For D. ACE 2 is normalised to ACE. n=3, unpaired t-test *p<0.05.*

4.2.6 The effect of AMPK activators on release of aldosterone from cultured adipocytes

In view of the actions of AMPK activators on RAAS gene expression, aldosterone secretion in response to AMPK activators was also assessed. Figure 4.6 demonstrates that AICAR increased aldosterone secretion by 42.5% after 8 h stimulation (p=0.0165) in 3T3-L1 adipocytes. In SW872 adipocytes, AICAR tended to increase aldosterone secretion, yet this did not achieve statistical significance, whereas A769662 increased aldosterone secretion into culture medium of SW872 adipocytes by an additional 135% compared to vehicle (p=0.0002) (Fig. 4.6).

4.2.7 The effect of AMPK activators on StAR gene expression in cultured adipocytes.

Steroid acute regulatory protein (StAR) is a crucial early component of steroidogenesis, regulating mitochondrial cholesterol transfer, and is therefore required for the production of aldosterone (Hattangady et al. 2012). Given the marked effect of AMPK activators on aldosterone secretion in cultured adipocytes, the effect of AMPK activation on the expression of StAR was therefore assessed. Figure 4.7 demonstrates that AICAR in 3T3-L1 adipocytes tended to increase StAR mRNA by 99%, yet this did not achieve statistical significance (p=0.0528), whereas A769662 stimulated a significant 34.8% increase in StAR mRNA expression in SW872 adipocytes (p=0.0052).
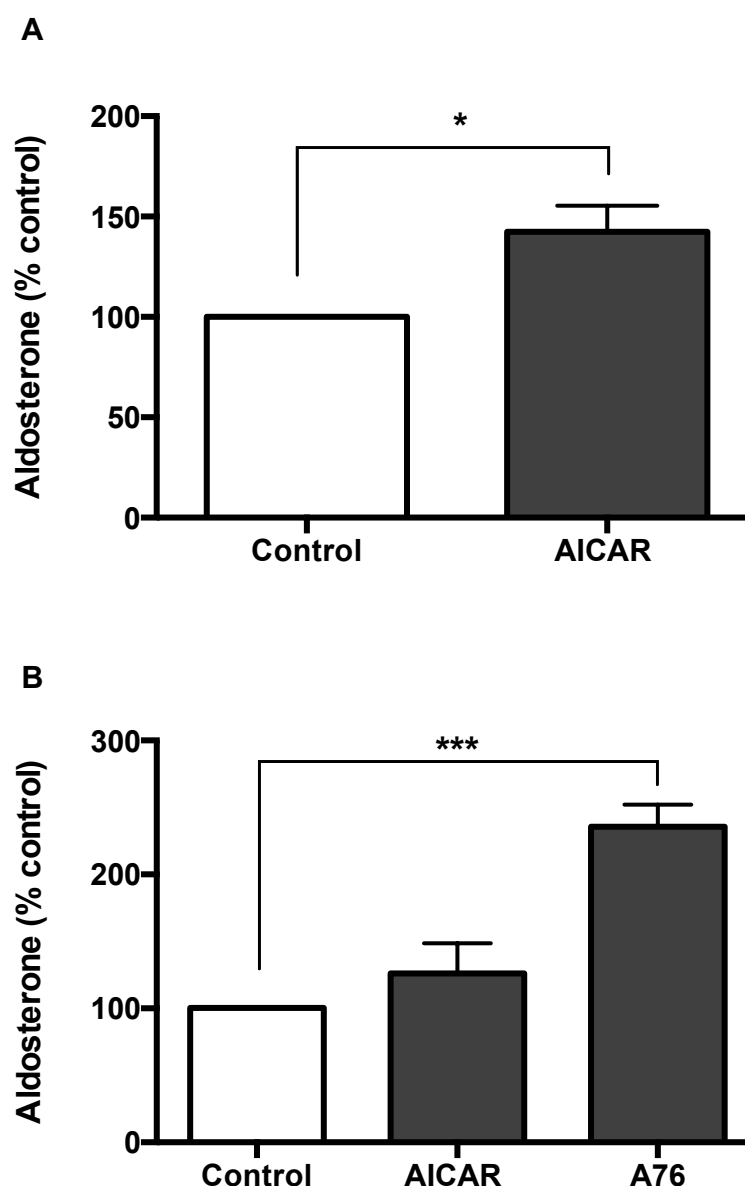
Figure 4.6 Effects of AMPK activators on aldosterone secretion from cultured adipocytes.

*A. 3T3-L1 adipocytes or B. SW872 adipocytes were incubated in medium containing 1% (v/v) NCS overnight then stimulated with 1 mM AICAR or 300 μM A769662 (A76, SW872 adipocytes only) for 8 h. Culture medium was collected and aldosterone quantified by ELISA. A. n=4, unpaired t-test, B. Control and A76 n=4, AICAR n=3, one-way ANOVA, *p<0.05, ***p<0.001.*
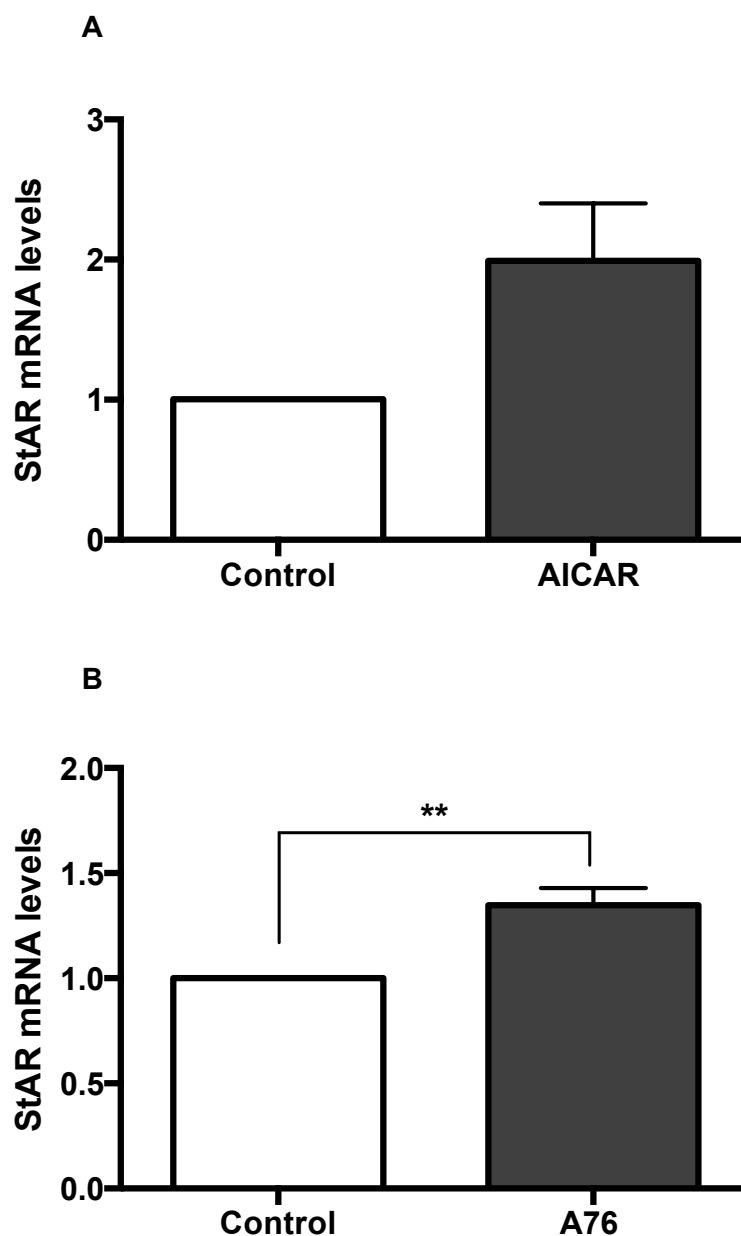
Figure 4.7 The effect of AMPK activators on StAR gene expression in cultured adipocytes.

RNA was extracted from A. 3T3-L1 and B. SW872 adipocytes incubated in the presence or absence of A. AICAR (1 mM) or B. A769662 (A76 300 µM) for 8 h. Reverse transcription was carried out prior to Taqman qPCR assays for StAR. Data are normalised to TATA-binding protein mRNA expression. n=4, unpaired t-test, **p<0.01.

4.2.8 The effect of A769662 on mineralocorticoid receptor signalling in SW872 adipocytes

4.2.8.1 The effect of A769662 on down-stream target of the mineralocorticoid receptor – SGK1 in SW872 adipocytes

Serum and glucocorticoid-regulated protein kinase (SGK1) is known to be a target of aldosterone induced mineralocorticoid receptor activation (Pearce, 2001). Given that A769662 increases aldosterone secretion yet decreases mineralocorticoid receptor expression, the effect on the target protein SGK1 was assessed. Stimulation of SW872 adipocytes with A769662 significantly increased SGK1 protein levels by 4.2 fold after 24 h (p=0.0099)(Fig. 4.8).

4.2.8.2 The effect of compound C and eplerenone on A769662 induced SGK1 in SW872 adipocytes

The AMPK inhibitor, compound C, was used to determine whether the induction of SGK-1 identified in response to A769662 in SW872 adipocytes was likely to be AMPK-dependent. In addition, the MR antagonist eplerenone was used to assess the MR-dependence of the SGK1 induction. Adipocytes were pre-incubated with compound C or eplerenone prior to stimulation with A769662 for 8 h or 24 h. After 8 h stimulation with A769662 ACC phosphorylation was increased 2.4 fold (p=0.0487) (Fig. 4.9A), an effect prevented by compound C. A769662 increased SGK1 6.3-fold (p=0.2270) whereas in the presence of compound C A769662 increased SGK1 ~60-fold compared to compound C alone (p=0.0007) and 3.1-fold compared to A769662 alone (p=0.0045) (Fig. 4.9B). After 24 h stimulation with A769662, SGK1 was significantly increased (4.2-fold, p=0.0192) but neither compound C nor eplerenone altered this response (5.2-fold increase with A769662 in the presence of compound C, p=0.013; 6-fold increase with A769662 in the presence of eplerenone, p=0.0361) (Fig. 4.10).
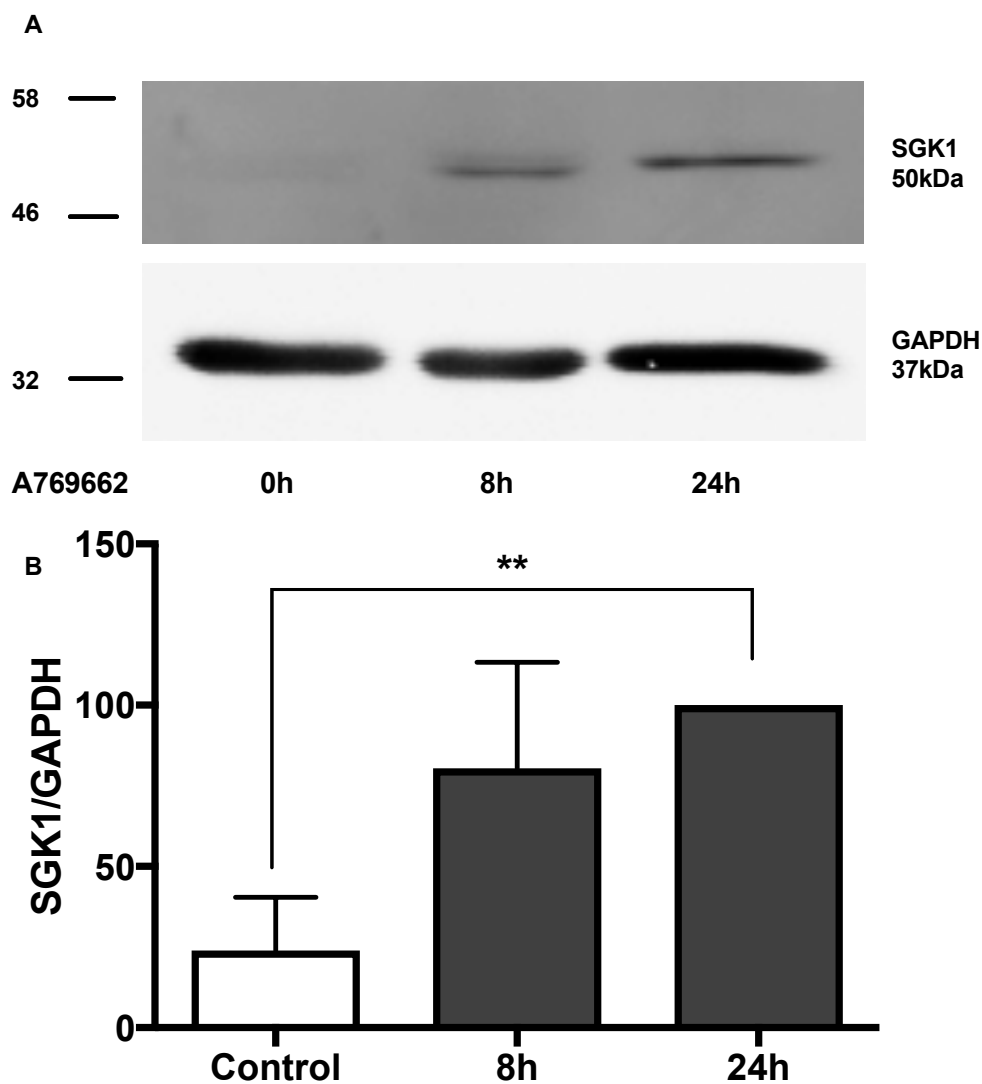
Figure 4.8 The effect of A769662 on SGK1 levels in SW872 adipocytes.

*SW872 adipocytes were incubated in medium containing 1% (v/v) NCS overnight prior to stimulation with 300 μM A769662 for the times indicated. Cell lysates were prepared, proteins resolved by SDS-PAGE and immunoblotted for the indicated proteins. A. Representative immunoblots are shown with the molecular masses of marker proteins (in kDa) indicated. B. Quantification of SGK-1 levels relative to GAPDH. n=3, unpaired t-test **p<0.01.*

A

B
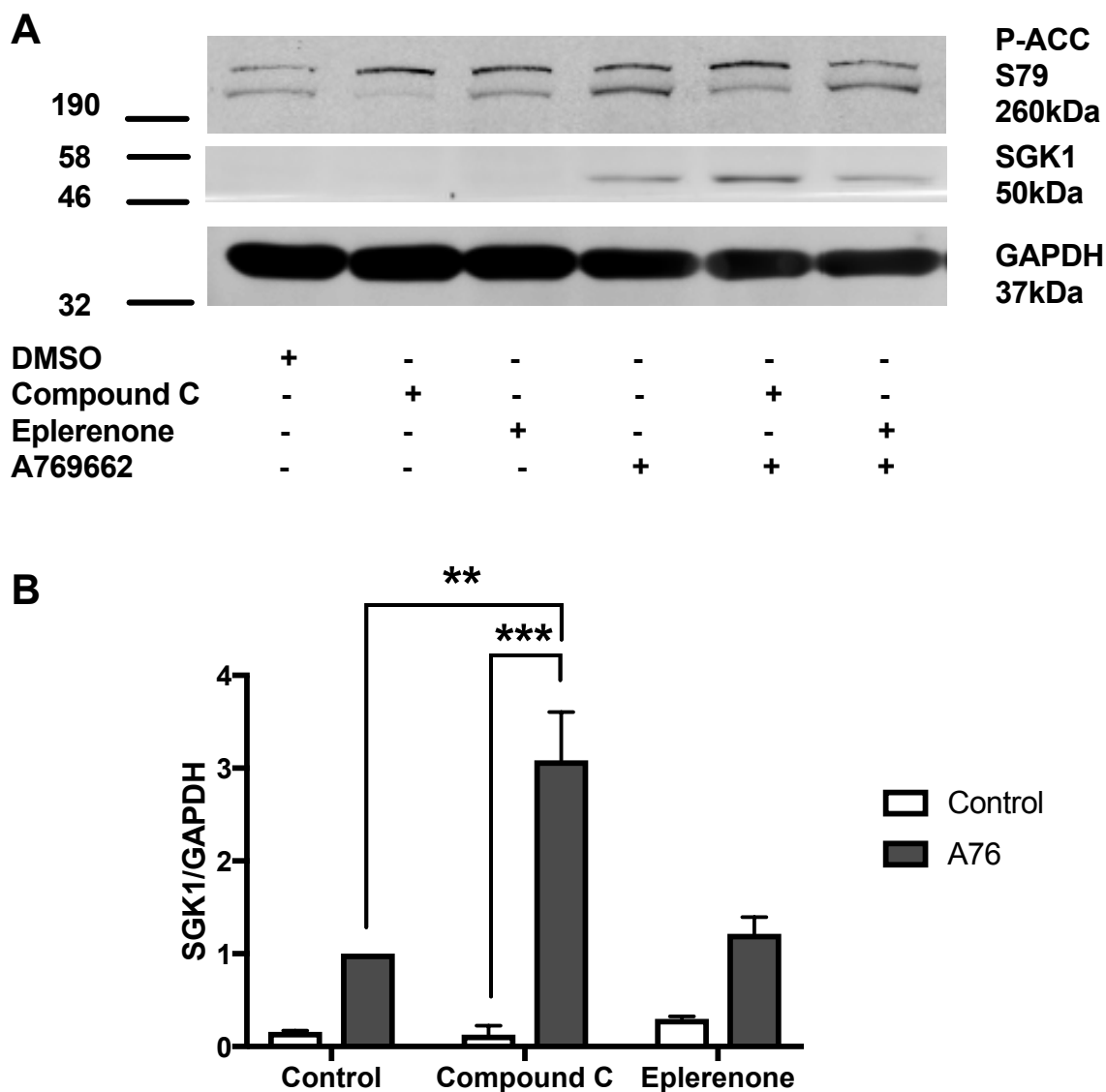
Figure 4.9 The effect of compound C on A769662 (8 h)-induced SGK1 levels in SW872 adipocytes.

SW872 adipocytes were incubated in medium containing 1% (v/v) NCS overnight then preincubated in the presence or absence of 30 μM compound C (Myers et al. 2017) or 1 μM eplerenone (Hirata et al. 2012) prior to stimulation with 300 μM A769662 for 8 h. Cell lysates were prepared and proteins resolved by SDS-PAGE and immunoblotted for P-ACC, SGK1 and GAPDH. A. Representative immunoblots are shown, with the molecular masses of marker proteins (in kDa) indicated. B. quantification of SGK1:GAPDH levels. n=2, two-way ANOVA, **p<0.01, ***p<0.001. P-ACC S79: Phospho-ACC Ser79.

A

DMSO	+	-	-	-	-	-
Compound C	-	+	-	-	+	-
Eplerenone	-	-	+	-	-	+
A769662	-	-	-	+	+	+

B
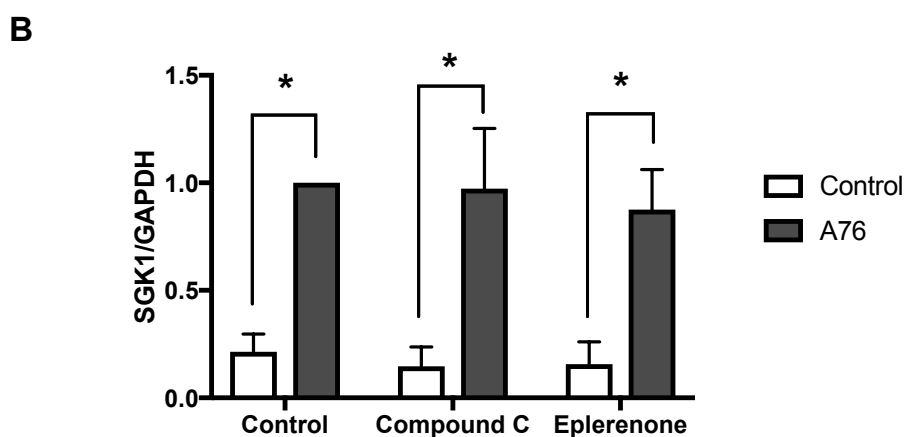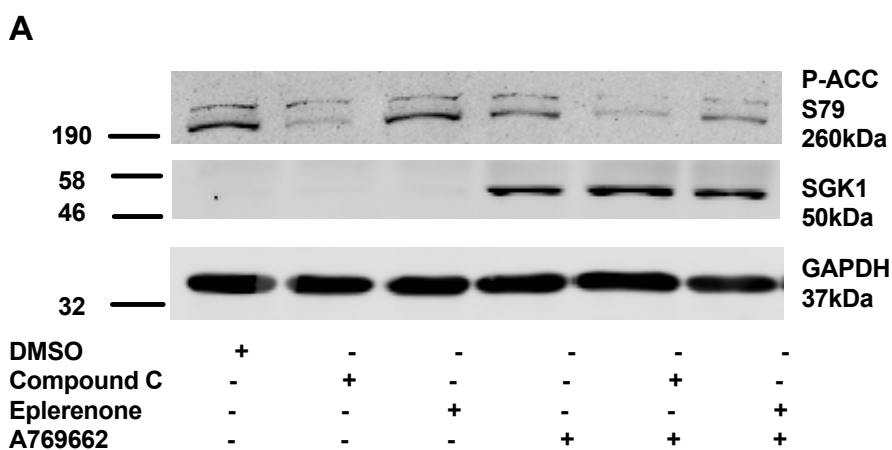
Figure 4.10 The effect of compound C on A769662 (24 h)-induced SGK1 levels in SW872 adipocytes.

SW872 adipocytes were incubated in medium containing 1% (v/v) NCS overnight then preincubated in the presence or absence of 30 µM compound C or 1 µM eplerenone prior to stimulation with 300 µM A769662 for 24 h. Cell lysates were prepared and proteins resolved by SDS-PAGE and immunoblotted for P-ACC, SGK1 and GAPDH. A. Representative immunoblots are shown, with the molecular masses of marker proteins (in kDa) indicated. B. Quantification of SGK1:GAPDH levels. n=4, *p<0.05, two-way ANOVA. P-ACC S79: Phospho-ACC Ser79.

4.2.8.3 The effect of AMPK activators on SGK1 in wild type and AMPK knock out mouse embryonic fibroblasts

Complete AMPK knockout is lethal in mice however mouse embryonic fibroblasts lacking either AMPKα catalytic subunit isoform have been generated (Laderoute et al. 2006). Therefore, these AMPK knock out mouse embryonic fibroblasts were used as a genetic tool lacking AMPK activity entirely, to further examine the AMPK-dependence of AICAR- and A769662-stimulated SGK1 expression. Stimulation of wild type mouse embryonic fibroblasts with AICAR or A769662 for 24 h markedly stimulated ACC phosphorylation, whereas ACC phosphorylation was entirely lacking in AMPK knock out mouse embryonic fibroblasts. Unlike SW872 adipocytes, A769662 had no effect on SGK1 levels. Furthermore, AICAR also had no effect on SGK1 levels in wild type mouse embryonic fibroblasts. Intriguingly, AICAR, but not A769662 stimulated a significant 181% increase in SGK1 in the knock out fibroblasts (p=0.008)(Fig. 4.11).

4.2.8.4 The effect of compound C and eplerenone on A769662 effects on mineralocorticoid receptor expression in SW872 adipocytes

The results described suggest that decreasing AMPK activity using pharmacological or genetic tools leads to an exacerbation of the observed effects of AMPK activators on SGK1. Given A769662 markedly reduced mineralocorticoid receptor levels in SW872 adipocytes (Fig. 4.4), the effect of pre-incubation with compound C or eplerenone was examined on the reduction of MR levels after 24 h. After 24 h A769662 did not increase ACC phosphorylation whilst compound C decreased AMPK activity. Prior addition of compound C led to a further decrease of mineralocorticoid receptor protein expression in response to A769662 in SW872 adipocytes (A769662 decreased MR by 36% whereas compound C with A769662 decreased MR by 82% compared to compound C alone p=0.0074). Similarly, eplerenone had no independent effect on expression of the MR and rather than inhibit the effects of A769662,

they were more pronounced (88% reduction in MR compared to eplerenone alone, p=0.0042) (Fig. 4.12).

4.2.9 The effect of A769662 on AMPK protein expression in SW872 adipocytes

In view of these data, the effect of prolonged stimulation with A769662 on AMPK levels was examined. AMPKα1 is the predominant catalytic isoform in adipocytes in terms of activity in whole cell extracts (Bijland et al. 2013). After 8 h incubation with A769662, ACC phosphorylation was increased 2.5 fold (p=0.0489) but after 24 h activity had returned to baseline. However, AMPK phosphorylation was unchanged from basal levels following 8 h incubation with A769662, yet after 24 h it had significantly reduced (P-AMPK:GAPDH 71% reduction, p=0.0001; P-AMPK:AMPK 22% reduction, p=0.0244). Indeed, following 24 h of stimulation with A769662, total levels of AMPKα1 protein decreased by 60% (p=0.0007) (Fig. 4.13).
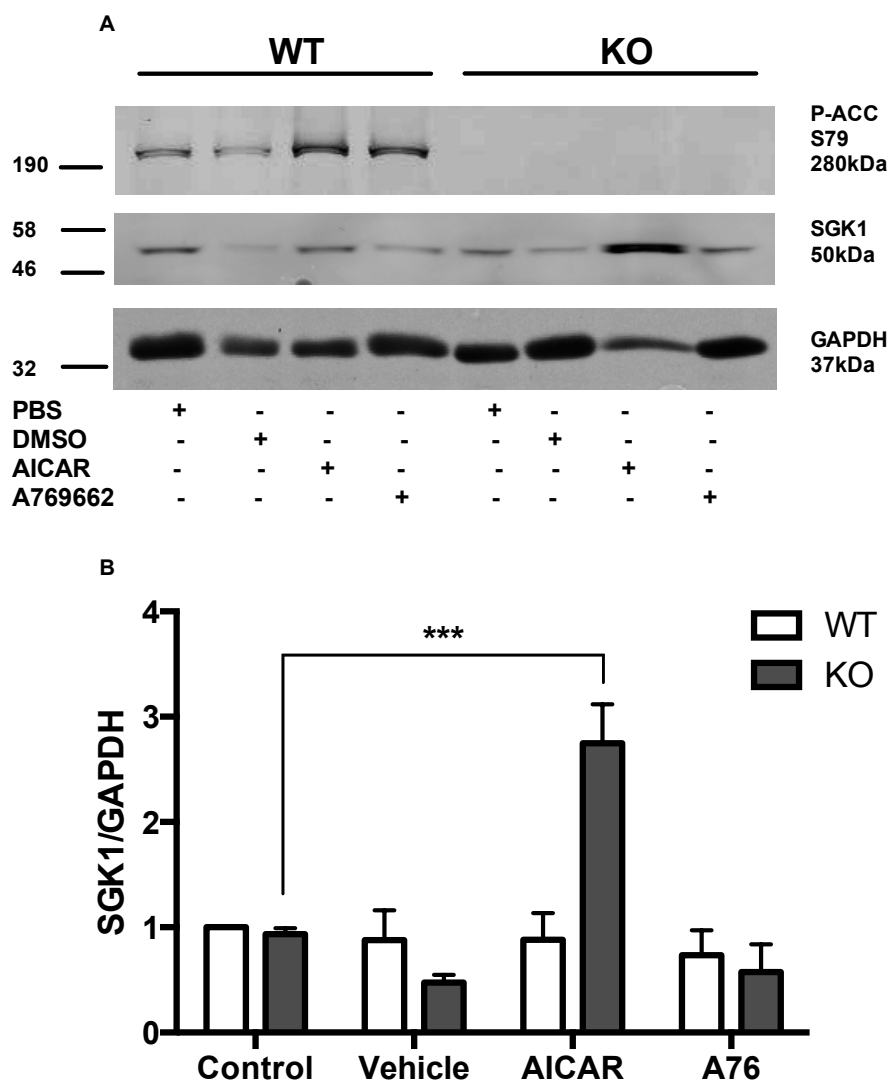
Figure 4.11 The effect of A769662 on SGK1 levels in mouse embryonic fibroblasts lacking AMPKα.

Mouse embryonic fibroblasts containing (WT) or lacking (KO) AMPKa were incubated overnight in medium containing 1% (v/v) NCS then stimulated with AICAR (500 μM) or A769662 (30 μM) for 24 h. Cell lysates were prepared and proteins resolved by SDS-PAGE and immunoblotted for the indicated proteins. A. Representative immunoblots are shown, with the molecular masses of marker proteins (in kDa) indicated. B. Quantification of SGK-1 levels relative to GAPDH. n=3, two-way ANOVA **p<0.01.P-ACC S79: Phospho-ACC Ser79.

A

DMSO	+	-	-	-	-	-
Compound C	-	+	-	-	+	-
Eplerenone	-	-	+	-	-	+
A769662	-	-	-	+	+	+

B
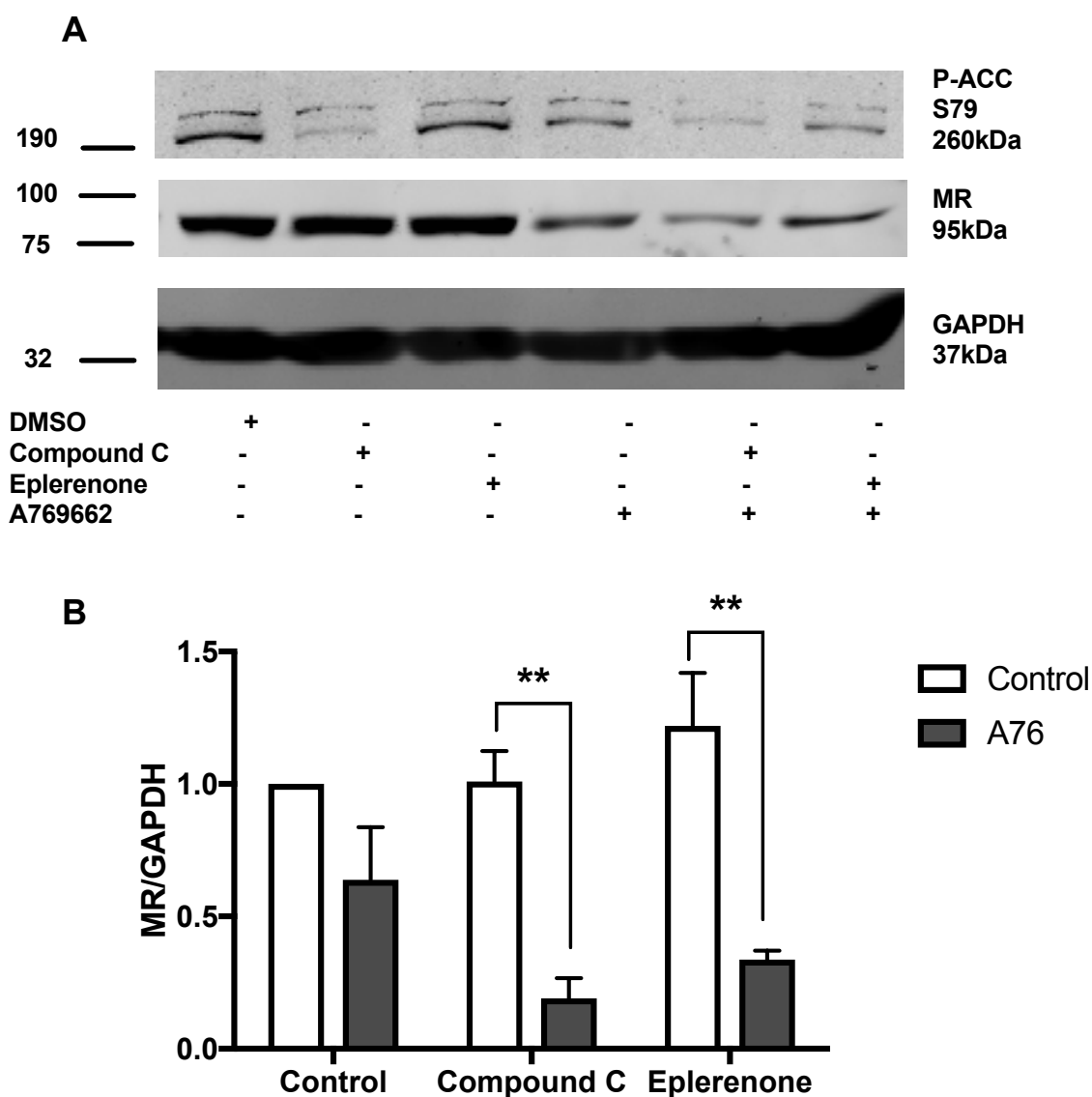
Figure 4.12 The effect of compound C on A769662 mediated mineralocorticoid receptor downregulation

SW872 adipocytes were incubated in medium containing 1% (v/v) NCS overnight then preincubated in the presence or absence of 30 µM compound C or 1 µM eplerenone prior to stimulation with 300 µM A769662 for 24 h. Cell lysates were prepared and proteins resolved by SDS-PAGE and immunoblotted for indicated proteins. A. Representative immunoblots are shown, with the molecular masses of marker proteins (in kDa) indicated. B. Quantification of MR levels relative to GAPDH n=3, two-way ANOVA **p<0.01. P-ACC S79: Phospho-ACC Ser79.
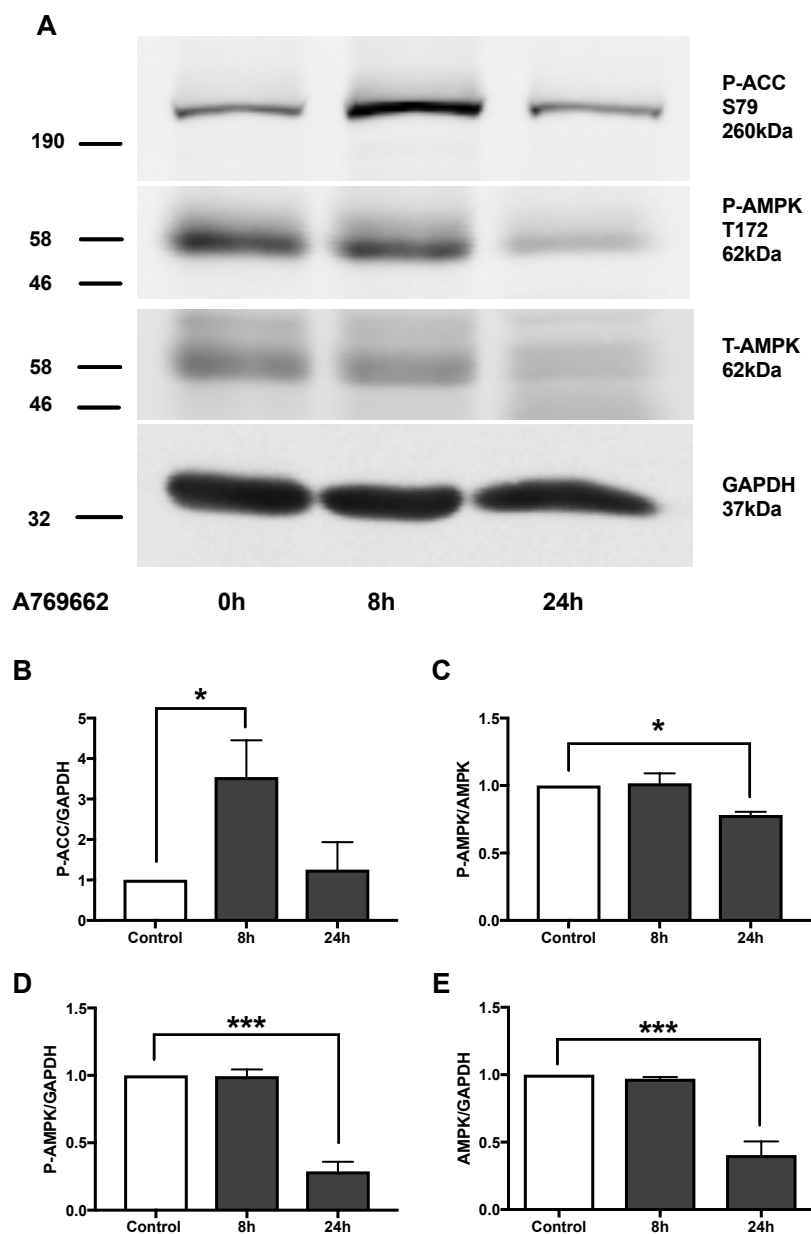
Figure 4.13 The effect of A769662 on AMPK protein expression in SW872 adipocytes.

*SW872 adipocytes were incubated in medium containing 1% (v/v) NCS overnight prior to stimulation with 300 µM A769662 for the times indicated. Cell lysates were prepared, proteins resolved by SDS-PAGE and immunoblotted for the indicated proteins. A. Representative immunoblots are shown, with the molecular masses of marker proteins (in kDa) indicated. B. Quantification of AMPK levels relative to GAPDH. n=3, one-way ANOVA ***p<0.001. P-ACC S79, Phospho-ACC Ser79; P-AMPK T172, Phospho-AMPKaThr172; T-AMPK, total AMPKa1.*

4.2.10 The effect of aldosterone on AMPK activity in murine adipose tissue

As shown in Figures 4.6 and 4.7, stimulation of adipocyte cell lines with AMPK activators stimulated aldosterone secretion, SGK protein levels and StAR mRNA expression. Whether aldosterone regulates AMPK in adipose tissue remains uncharacterised, however. To assess the effects of aldosterone on adipose tissue AMPK and inflammatory processes, phosphorylation of AMPKα and ACC was examined in whole epididymal adipose tissue lysates from mice treated with or without aldosterone infusion. Aldosterone infusion had no effect on ACC or AMPK phosphorylation in epididymal adipose tissue (Fig. 4.14). However, there was a significant increase in SGK1 protein levels in adipose tissue of mice infused with aldosterone (3.5-fold increase, p=0.0013)(Fig. 4.15A and B). In addition, protein levels of MR, NGAL and MCP-1 were not significantly affected by aldosterone infusion (Fig. 4.15A, C, D and E).
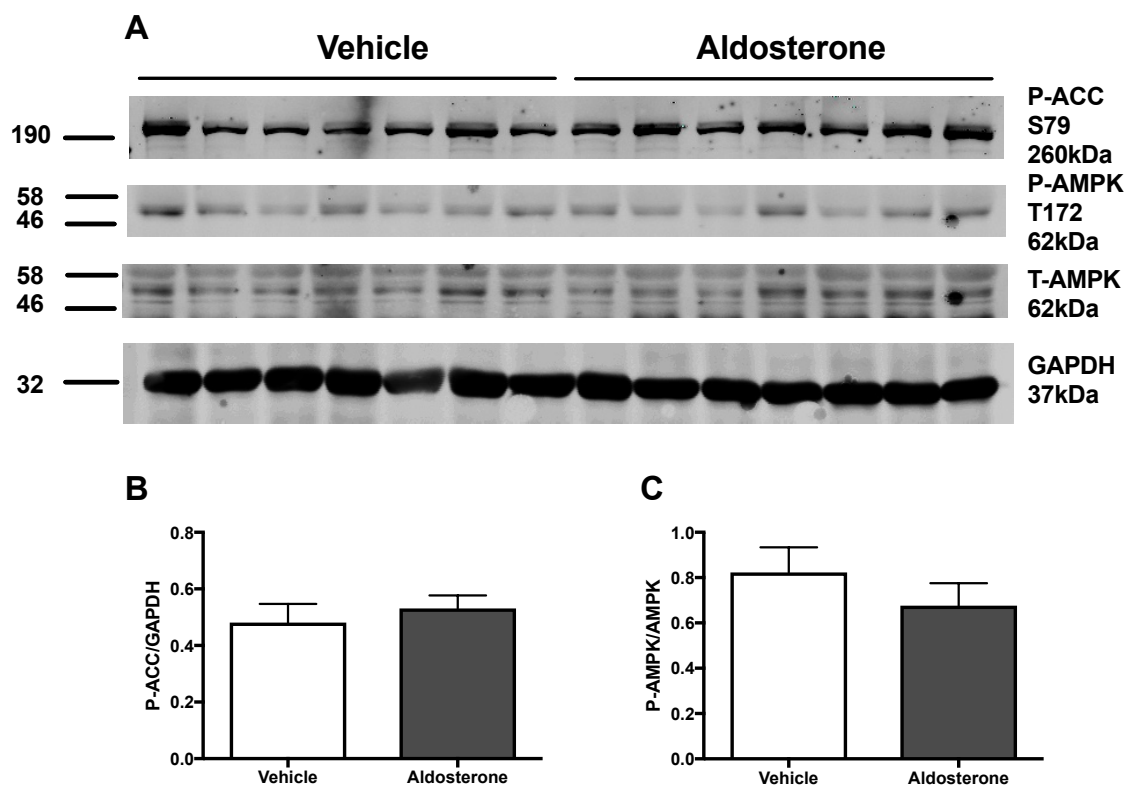
Figure 4.14 The effect of aldosterone on AMPK activity in murine adipose tissue

Epididymal adipose tissue lysates were prepared from 12-week old wild type mice (C57/Bl6J/FV129) treated with saline or aldosterone infusion (600 mcg/kg/d) for 28 days. Protein was resolved by SDS-PAGE and immunoblotted for the indicated proteins. A. Representative immunoblots with the molecular masses of marker proteins (in kDa) shown. Quantification of B. P-ACC levels relative to GAPDH and C. P-AMPK levels relative to AMPK, n=7 in each group.
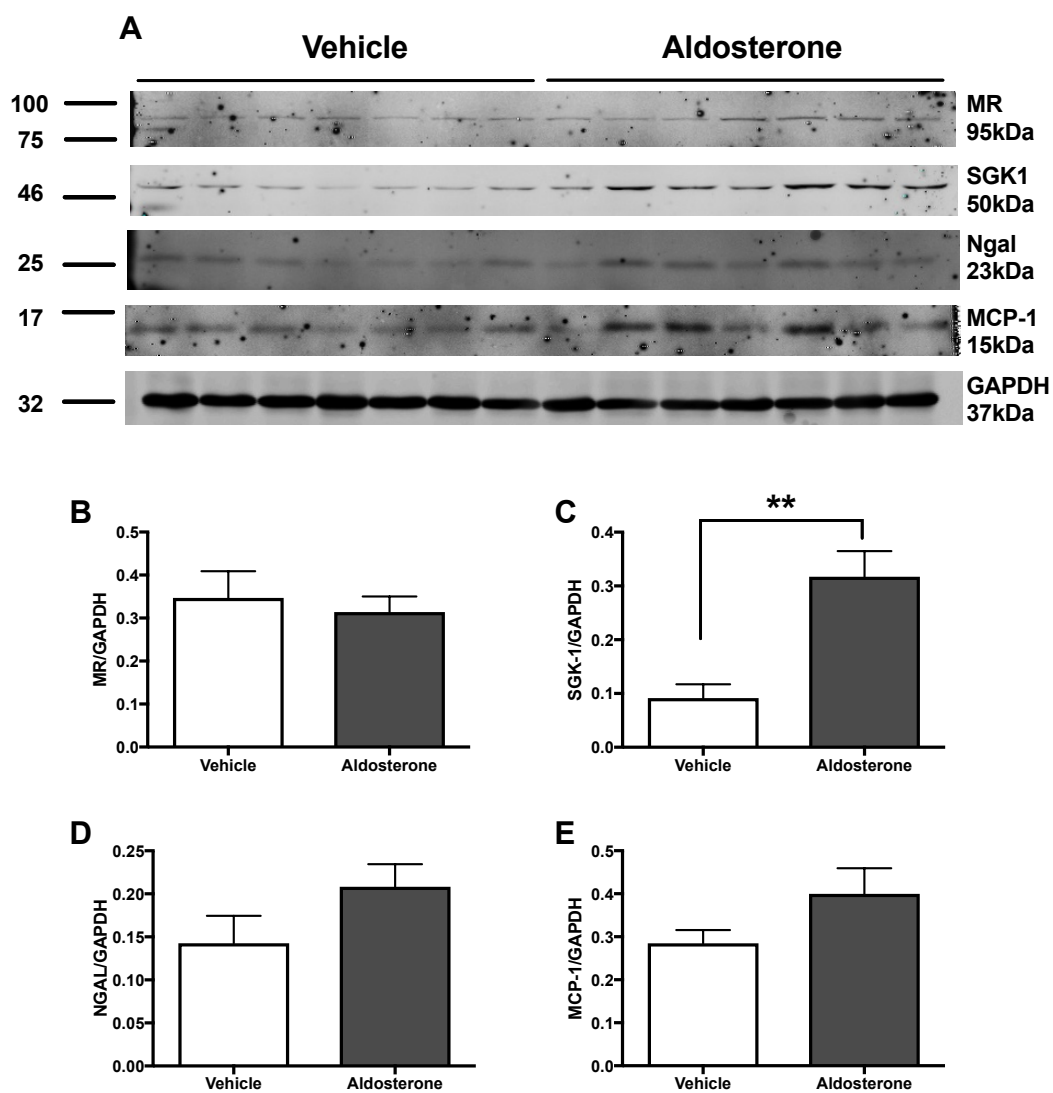
Figure 4.15 The effect of aldosterone on MR, SGK1 and pro-inflammatory protein levels in murine adipose tissue

Epididymal adipose tissue lysates were prepared from 12-week old wild type mice (C57/Bl6J/FV129) treated with saline or aldosterone infusion (600 mcg/kg/d) for 28 days. Protein was resolved by SDS-PAGE and immunoblotted for the indicated proteins. A. Representative immunoblots with the molecular masses of marker proteins (in kDa) shown. Quantification of B. MR levels, C. SGK1 levels, D. NGAL levels and E. MCP-1 levels relative to GAPDH. n=7 in each group, unpaired t-test **p<0.01. Mann Whitney test for C. p=0.0023.

4.3 Discussion

Adipose tissue dysfunction is implicated early in the pathogenesis of metabolic disorders such as type 2 diabetes (Esser et al. 2014). Upregulation of the renin-angiotensin-aldosterone system (RAAS) has been proposed as a contributing factor to the disordered lipid storage and adipokine secretion which can occur in such conditions (Jing et al. 2013). Altering the activity of the local adipose tissue RAAS may therefore be a strategy for preventing metabolic disease processes. The energy regulator AMPK has been demonstrated to have anti-inflammatory (Bijland et al. 2013, Mancini et al. 2017) and vasculo-protective properties (Salt and Hardie, 2017). At the beginning of this work a handful of studies, reviewed in 1.5, demonstrated that AMPK activation could inhibit RAAS effects, since then two recent studies have added to this literature. These studies showed that metformin, via AMPK, attenuates detrimental effects of angiotensin II in models of vascular endoplasmic reticulum stress (Duan et al. 2017) and cardiac fibrosis (Chen et al. 2018).

This chapter examined the effects of AMPK activation on expression and secretion of components of the RAAS within the cultured adipocyte models 3T3-L1 (murine) and SW872 (human). The key findings in this chapter were that activation of AMPK was associated with increased secretion of aldosterone and expression of the downstream MR target SGK1 in addition to decreased expression of the MR in SW872 adipocytes.

The initial hypothesis was that AMPK activation would downregulate the classical RAAS in adipocytes. In 3T3-L1 adipocytes, prolonged AICAR exposure downregulated gene expression of the AT2R and the MR. In SW872 adipocytes, incubation with AICAR decreased expression of angiotensinogen and the MR after 9 and 25 h. These effects on angiotensinogen and the MR were replicated by incubation with A769662 in SW872 adipocytes. Focus is drawn to the effects on the MR which is consistent between species and with both AMPK activators. A significant decrease in MR protein was confirmed with A769662 in SW872 adipocytes. Knowing that there is an increase in adipose tissue MR in obesity (Hirata et al. 2012) and that MR blockade can have

metabolic benefits (Sindelka et al. 2000, Wada et al. 2010), it would be of great interest to evaluate the effect of AMPK activation on MR expression in human adipose tissue.

Angiotensinogen is the initial precursor of the RAAS. In the human SW872 adipocyte model both AICAR and A769662 significantly decreased gene expression of angiotensinogen. Rodent studies with adipose tissue specific angiotensinogen knockout mice have found resistance to high fat diet-induced glucose intolerance and blood pressure elevation despite unchanged weight gain (Yiannikouris et al. 2012, LeMieux et al. 2016). Similarly, overexpression of angiotensinogen in adipose tissue was associated with increased adiposity, insulin resistance and adipose tissue inflammation (Kalupahana et al. 2012). Adipose tissue angiotensinogen also appears to be regulated by weight and insulin in humans. In obese individuals a 5% weight loss decreased both adipose tissue angiotensinogen and circulating angiotensinogen (Engeli et al. 2005). Subcutaneous adipocytes exposed to insulin *ex vivo* showed an incremental increase in angiotensinogen protein expression with increasing concentrations of insulin (Harte et al. 2003), which is consistent with hyperinsulinaemia having an important early role in metabolic syndrome. These studies highlight the potential impact of the local adipose tissue RAAS on systemic blood pressure and metabolic function. The finding that AMPK activators downregulate angiotensinogen in the human adipocyte model used here may be linked to the association between decreased AMPK and increased angiotensinogen identified in obese insulin resistant individuals by Xu et al (2012) highlighted in 4.1.1. However, in 3T3-L1 adipocytes gene expression of angiotensinogen was not affected by AICAR at a concentration which activated AMPK, such that this may alternatively therefore be a species-specific effect of AMPK.

The finding that angiotensinogen and the MR may be negatively regulated by AMPK activation is consistent with the beneficial known metabolic effects of AMPK. The alternative arm of the RAAS which has been identified as counteracting many of the traditional actions of angiotensin II was therefore of interest. This study has identified that AMPK may regulate the alternative RAAS as well as the classical RAAS in adipocytes. The expression of ACE was

decreased following AICAR exposure and ACE 2 was increased with A769662. Although the two AMPK activators have had different effects they both drive the system towards the alternative RAAS with AICAR significantly increasing the ACE 2:ACE ratio. Indeed the widely prescribed ACE inhibitors, discussed in detail in chapter 1, are known to prevent new onset diabetes and have been shown to activate AMPK (Scheen 2004, Tian et al. 2014). It would be of interest to study the effect of AMPK activators on ACE and ACE 2 activity in adipocytes in addition to expression.

The secretion of aldosterone from adipocytes was first identified in 2012 and may regulate local vascular tone in adipose tissue and in vessels within perivascular adipose tissue (Briones et al. 2012). Another key finding reported here is the increase in aldosterone secretion from adipocyte models in response to AMPK activators and a corresponding increase in StAR. This is an interesting finding considering the downregulation of the RAAS precursor angiotensinogen, however there are stimuli of aldosterone secretion other than angiotensin II. One possible explanation for this finding is that in response to cellular stress or low energy states, AMPK is activated and aldosterone is secreted in order to increase vascular tone and decrease blood (and nutrient) delivery to adipose tissue as storage is not required. It may also be worth considering that the mitochondria are the site of steroidogenesis, and mitochondrial biosynthesis is increased by AMPK (Hardie et al. 2012). It may purely be an increase in number of mitochondria leading to increased aldosterone production. The effects of AMPK activation on steroidogenesis have previously been studied in the adrenal gland and the gonads but not in adipose tissue. AMPK signalling was required for the adiponectin-mediated increase in cortisol production from the adrenocortical cell line H295R (Ramanjaneya et al. 2011). However, AICAR inhibited hCG- and forskolin-induced steroidogenesis in leydig cells and had no autonomous effect on hormone release (Abdou et al. 2014). These cell-based studies suggest a role for AMPK in steroidogenesis in adrenal but not testicular steroidogenesis. At a systemic level, it has been reported that the AMPK activating diabetes medications metformin and pioglitazone are associated with decreased circulating aldosterone levels (Eguchi et al. 2007), this discrepancy from the

current study could be due to direct effects on the adrenal gland or potentially more long term effects of AMPK activation.

Effects of AMPK activation on serum and glucocorticoid inducible protein kinase 1 (SGK1), a downstream target of the MR, were next examined (Terada et al. 2012). SGK1 has been identified in adipocytes where it is induced by aldosterone and dexamethasone and it is increased in adipose tissue from individuals with obesity and diabetes compared to healthy lean individuals (Li et al. 2013). In SW872 adipocytes, A769662 induced SGK1 protein expression. Prior addition of the AMPK inhibitor compound C did not inhibit this effect of A769662, rather unexpectedly it exacerbated the initial rise in SGK1 (at 8 h) although this effect was lost by 24 h. Similarly, eplerenone, the MR antagonist, did not alter this response. This suggests that the A769662-stimulated increase in SGK1 levels is neither AMPK- nor MR-dependent. Indeed, in wild type MEFs AICAR and A769662 did not induce SGK1, whereas it was induced by AICAR in AMPK knockout MEFs. However, following 24 h of A769662 exposure in SW872 adipocytes there was a significant downregulation of total AMPK protein and markedly reduced ACC phosphorylation, indicative of reduced AMPK activity. The impact of 24 h exposure may mimic extreme circumstances, such as hypoxia or hypoperfusion, which then become toxic to the cell resulting in altered processes including mitochondrial function. One article has examined the effect of AICAR on dexamethasone induced SGK1 and found no significant effect, however they did show that as SGK1 increased in response to dexamethasone, the tumour suppressor LKB1 was downregulated (Lützner et al. 2012). Knowing that LKB1 is one of two upstream AMPK kinases (Shaw et al. 2004) raises the question as to whether the observations in this report have identified a negative feedback process regulating AMPK activity involving aldosterone, the MR, SGK1, LKB1 and AMPK (Fig 4.16). However, it must be taken into consideration that in adipose tissue from mice infused with aldosterone, whilst SGK1 was increased, there was no significant effect on AMPK activity.

Despite the common effects on angiotensinogen, the MR, aldosterone secretion and SGK1 of the AMPK activators used in this study there are some discrepancies which should not be overlooked. The possibility of a species

specific effect is one potential explanation why AICAR induces effects in murine cells whereas A769662 does in human cells but AICAR does not. For example, A769662 but not AICAR increased aldosterone secretion in the human adipocyte model, whereas AICAR induced SGK1 in KO MEFs but A769662 did not. Indeed AICAR and A769662 have different modes of action leading to possible non-AMPK mediated effects. AICAR has been widely studied as an AMPK activator yet as an AMP mimetic it can affect other enzymes that are regulated by or require AMP (Guigas et al. 2009). In addition, although A769662 is a highly selective AMPK activator it also has off target effects and was shown to inhibit Na^+-K^+-ATPase in L6 myotubes (Benziane et al. 2009).
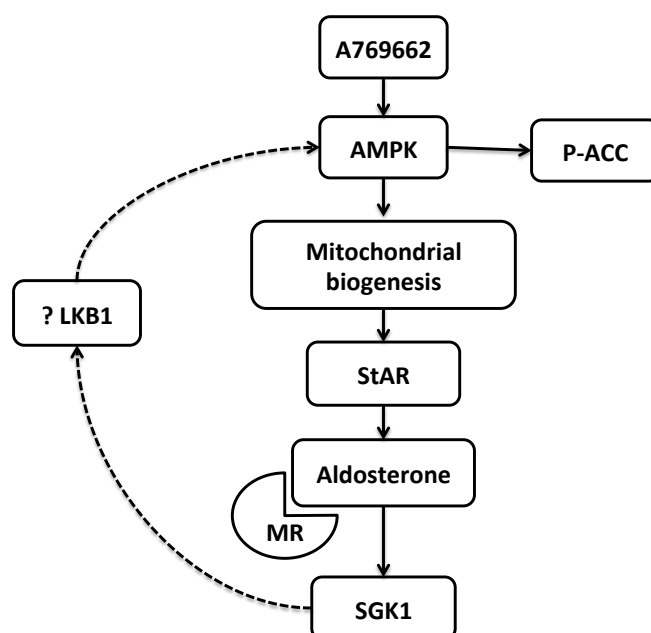
Figure 4.16 Proposed feedback mechanism regulating AMPK-induced aldosterone secretion.

A769662 activates AMPK which phosphorylates ACC. AMPK activation is known to increase number of mitochondria, the site of steroidogenesis. This may lead to increased StAR and aldosterone secretion which increases SGK1 via the MR. SGK1 may decrease LKB1 and subsequently negatively regulate AMPK. Full arrow = positive association, incomplete arrow = negative association.

In summary, this study has identified that two structurally-unrelated AMPK activators, AICAR and A769662, that activate AMPK by different mechanisms, negatively regulate classical RAAS components including the mineralocorticoid receptor whilst increasing aldosterone secretion in adipocyte models. These findings may represent a response to cellular stress where adipocytes play a crucial role in regulating nutrient delivery to adipose tissue by increasing vascular tone with aldosterone and preventing further (MR-dependent) adipogenesis.

5 Chapter 5 - The effect of angiotensin II and angiotensin 1-7 on AMPK activity in adipocytes

5.1 Introduction

5.1.1 The effects of RAAS components on adipose tissue

Angiotensin II has been reported to increase the production of pro-inflammatory adipocytokines from adipose tissue in both humans and rodents, suggesting an effect on adipocytes, as well as likely effects on other constituent cells of adipose tissue including stromal vascular cells (Kalupahana and Moustaid-Moussa, 2012). Mechanistically, angiotensin II-induced MCP-1 secretion from 3T3-L1 adipocytes was prevented by the NF-κB inhibitor BAY-11-7082 and NOX inhibitor apocynin suggesting that the pro-inflammatory effects of angiotensin II are mediated by NF-κB and NOXs (Kalupahana et al. 2012). Although angiotensin receptor blockers and ACE inhibitors have metabolic benefits and can reduce the incidence of type 2 diabetes, angiotensin II was reported to enhance insulin signalling and glucose uptake in rat adipocytes *ex vivo* (Juan et al. 2005).

Angiotensin II can be converted to ang 1-7 by ACE 2 (Patel et al. 2016). Ang 1-7 acts via the Mas receptor and has predominantly been studied in the cardiovascular system where it opposes angiotensin II effects and is therefore regarded as part of the 'alternative RAS' (Patel et al. 2016). In adipocytes, ang 1-7 also appears to have metabolic benefits. Ang1-7 enhanced basal and insulin stimulated glucose uptake in isolated C57 mouse epidydimal adipocytes and reduced ROS whilst increasing adiponectin expression in 3T3-L1 adipocytes (Liu et al. 2011). These actions were blocked by the Mas receptor antagonist A779 (Liu et al 2011). In transgenic rats secreting supraphysiological levels of ang 1-7, insulin sensitivity improved and body weight reduced compared to Sprague Dawley rats. Furthermore, there was an associated increase in circulating adiponectin suggesting an influence on adipose tissue (Santos et al. 2010). In addition, there was a decrease in angiotensinogen expression yet no change in expression of TNF-α or TGF-β was detected in adipose tissue of the transgenic rats (Santos et al. 2010).

There are therefore opposing potential metabolic actions of the classical and alternative RAS in adipose tissue which may become polarised towards the classical RAS in obesity. Rebalancing this system appears to have therapeutic potential in the context of obesity and diabetes and better understanding of the underlying mechanisms is therefore crucial in the search for preventative strategies.

5.1.2 The effect of RAAS components on AMPK activity

There is a small literature available regarding the cross-talk between AMPK and RAAS in cells relevant to cardiovascular and renal systems. In vascular smooth muscle cells (VSMCs) angiotensin II activated AMPK in an AT1 receptor-dependent manner (Nagata et al. 2004). However, in primary rat neonatal cardiomyocytes angiotensin II reduced AMPK activity (Stuck et al. 2008). Consistent with this AMPK activity was also reduced by angiotensin II in a renal model of fibrosis using HK2 tubular epithelial cells (Lee et al. 2013). The effect of angiotensin II on AMPK activity therefore varies in different cardiovascular cell types. The RAAS is now known to be an important factor in the pathogenesis of metabolic disorders yet the effect of angiotensin II on AMPK in metabolic cells and tissues such as adipocytes remains unknown.

5.1.3 Aims

Given the lack of published studies investigating the actions of the classical and alternative RAS in adipocytes, the effects of angiotensin II and ang 1-7 on AMPK, inflammatory and insulin signalling pathways were examined in human and murine adipocyte models.

5.2 Results

5.2.1 The effects of angiotensin II in SW872 adipocytes

5.2.1.1 Angiotensin II signalling in SW872 adipocytes

Angiotensin II has previously been reported to have pro-inflammatory effects in cultured adipocytes (Kalupahana et al. 2012). The effect of angiotensin II on proinflammatory and AMPK signalling in SW872 adipocytes was therefore examined. IL-1ß (10 ng/ml, 5 and 15 min) and AICAR (1 mM, 1 h) were used as positive controls. Angiotensin II (5 min) and AICAR both significantly increased ACC phosphorylation, however the level of phosphorylation was far greater with AICAR (Ang II 29% increase at 5 min, p=0.0084; AICAR 197% increase, p=0.0186)(Fig. 5.1B). IL-1ß had no significant effect on ACC phosphorylation. Given that the angiotensin II-induced ACC phosphorylation was small an AMPK activity assay was carried out. Angiotensin II did not significantly increase AMPK activity (p=0.089) (Fig. 5.5B).

The ERK signalling pathway is known to mediate effects of angiotensin II via the AT1R (Turner et al. 2001). In this study, activating ERK phosphorylation was not significantly affected by angiotensin II or IL-1ß (Fig. 5.1C). Phosphorylation of NF-κB was significantly increased by IL-1ß at both 5 and 15 min (2.27 fold increase at 5 min, 2.07 fold increase at 15 min, p=0.0001) whilst neither angiotensin II nor AICAR had any effect (Fig. 5.1D).

5.2.1.2 The mechanism of angiotensin II mediated AMPK signalling in SW872 adipocytes

As angiotensin II activated AMPK activity, as assessed by ACC phosphorylation in SW872 adipocytes, further experiments were performed to explore the mechanism. As these cells had low transcript levels for the AT1R, it was likely that the AMPK activation was mediated by the AT2R. Therefore cells were preincubated with the AT2R antagonist PD123319 prior to stimulation with different concentrations of angiotensin II for 5 min (Fig. 5.2A). Angiotensin II (100 nM) significantly increased ACC phosphorylation (p=0.012) yet at higher

concentrations no significant effect was observed. However, ACC phosphorylation tended to be increased in the presence of PD123319, whilst additional incubation with angiotensin II did not increase ACC phosphorylation at any concentration (Fig. 5.2B). Again, a small effect of angiotensin II was seen and the previously significant increase seen with 10 µM was no longer present.
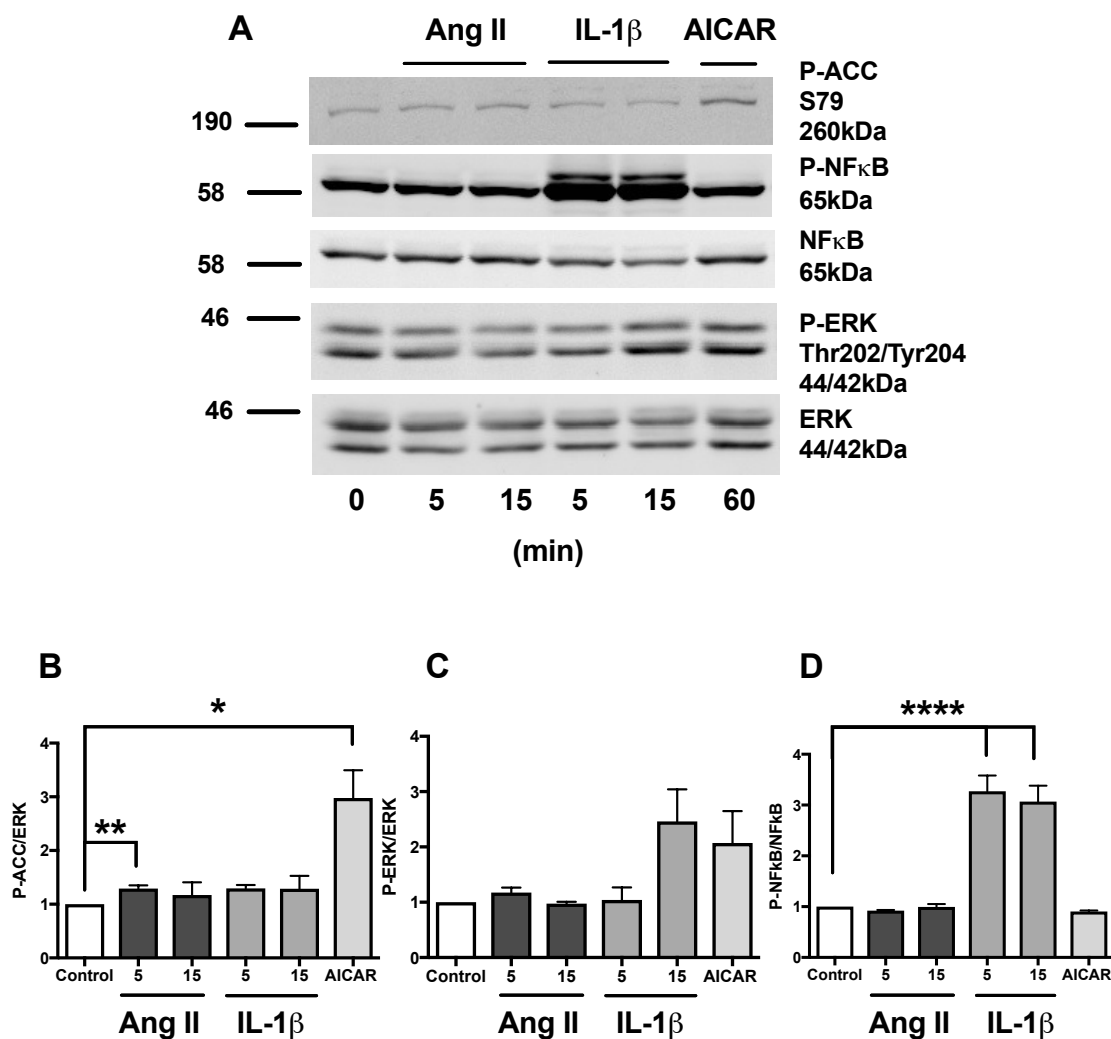
Figure 5.1 The effect of angiotensin II on AMPK and inflammatory signalling in SW872 adipocytes

SW872 adipocytes were incubated in serum free media for 2 h then stimulated with angiotensin II (10 μM) or IL-1β (10 ng/ml) for 5 or 15 min as indicated or AICAR (1 mM) for 1 h. Cell lysates were prepared, proteins resolved by SDS-PAGE and immunoblotted for the indicated proteins. A. Representative immunoblot with the molecular masses of marker proteins (in kDa) shown. Quantification of B. (P-, phospho-) P-ACC levels relative to ERK1, C. P-ERK1 levels relative to ERK1 and D. P-NFκB levels relative to NFκB. n=3, B. unpaired t-test, D. one-way ANOVA, *p<0.05, **p<0.01, ****p<0.0001.

A

B
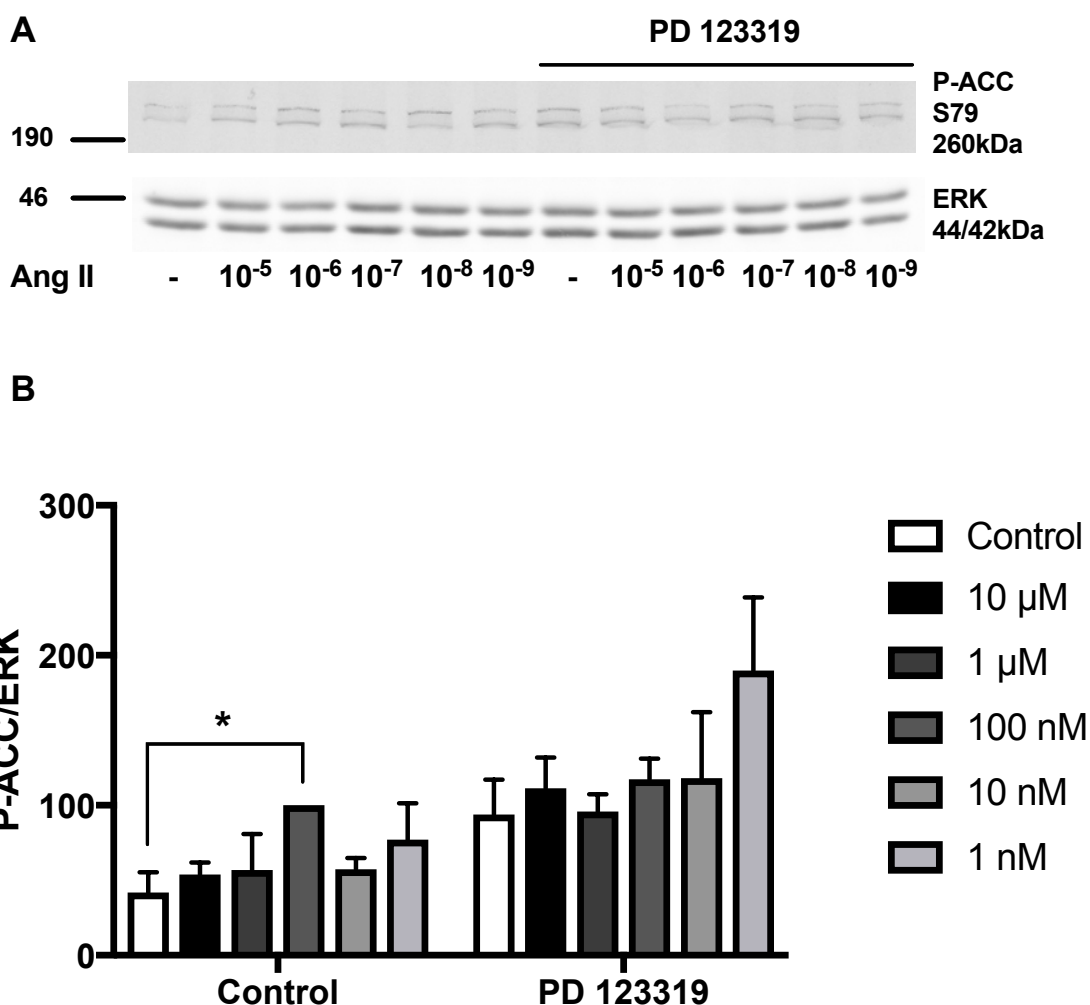
Figure 5.2 The effect of angiotensin II on AMPK signalling in SW872 adipocytes

SW872 adipocytes were incubated in 1% NCS (v/v) overnight then stimulated with angiotensin II at concentrations indicated for 5 min after preincubation for 1 h in the presence or absence of 10 µM PD123319 (Mabrouk et al. 2001). Cell lysates were prepared, proteins resolved by SDS-PAGE and immunoblotted for the indicated proteins. A. Representative immunoblot with the molecular masses of marker proteins (in kDa) shown. B. Quantification of phospho-ACC (P-ACC) levels relative to ERK1. n=3, unpaired t-test *p<0.05.

5.2.2 The effect of ang 1-7 in SW872 adipocytes

5.2.2.1 The effect of ang 1-7 on AMPK activity in SW872 adipocytes

Subsequent experiments focused on ang 1-7 to further explore the effect of the alternative RAS on AMPK activity. Ang 1-7 (1 µM) was applied to SW872 adipocytes for different durations or at different concentrations for 10 min. After 2 min, 1 µM ang 1-7 significantly increased phosphorylation of ACC (35% increase, p=0.0161) (Fig. 5.3B) whilst AMPK phosphorylation was significantly increased at 30 and 60 min (30 min 59% increase, p=0.004; 60 min 58% increase, p=0.0087) (Fig. 5.3C). After 10 min, AMPK phosphorylation was increased by ang 1-7 at concentrations of 30 nM (55% increase, p<0.0001), 100 nM (47% increase, p=0.0002), and 1 µM (42% increase, p=0.0276) (Fig 5.4C), whilst ACC phosphorylation was significantly increased by 30 nM ang 1-7 (89% increase, p=0.0087) but not higher concentrations (Fig. 5.4B). This increase in AMPK and ACC phosphorylation was associated with increased AMPK activity, assessed in AMPK immunoprecipitates. A 94% increase in AMPK activity was detected in SW872 adipocytes following exposure to ang 1-7 for 2 min (p=0.0167) (Fig. 5.5A).

5.2.2.2 The mechanism of ang 1-7 induced AMPK signalling in SW872 adipocytes

In order to determine the mechanism of AMPK activation by ang 1-7, SW872 adipocytes were pretreated with selective inhibitors of Mas (A779), AT2R (PD123319) and the AMPK Thr172 kinase, CaMKK (STO-609) prior to the application of ang 1-7 or AICAR. Compared to control ang 1-7 tended to modestly increase ACC phosphorylation (p=0.066) whilst AICAR led to a much greater increase in ACC phosphorylation (p=0.0002)(Fig. 5.6B). When compared to STO-609, A779 and PD123319 the tendency for angiotensin 1-7 to increase ACC phosphorylation was lost whilst AICAR still increased ACC phosphorylation (Fig 5.6A).

A
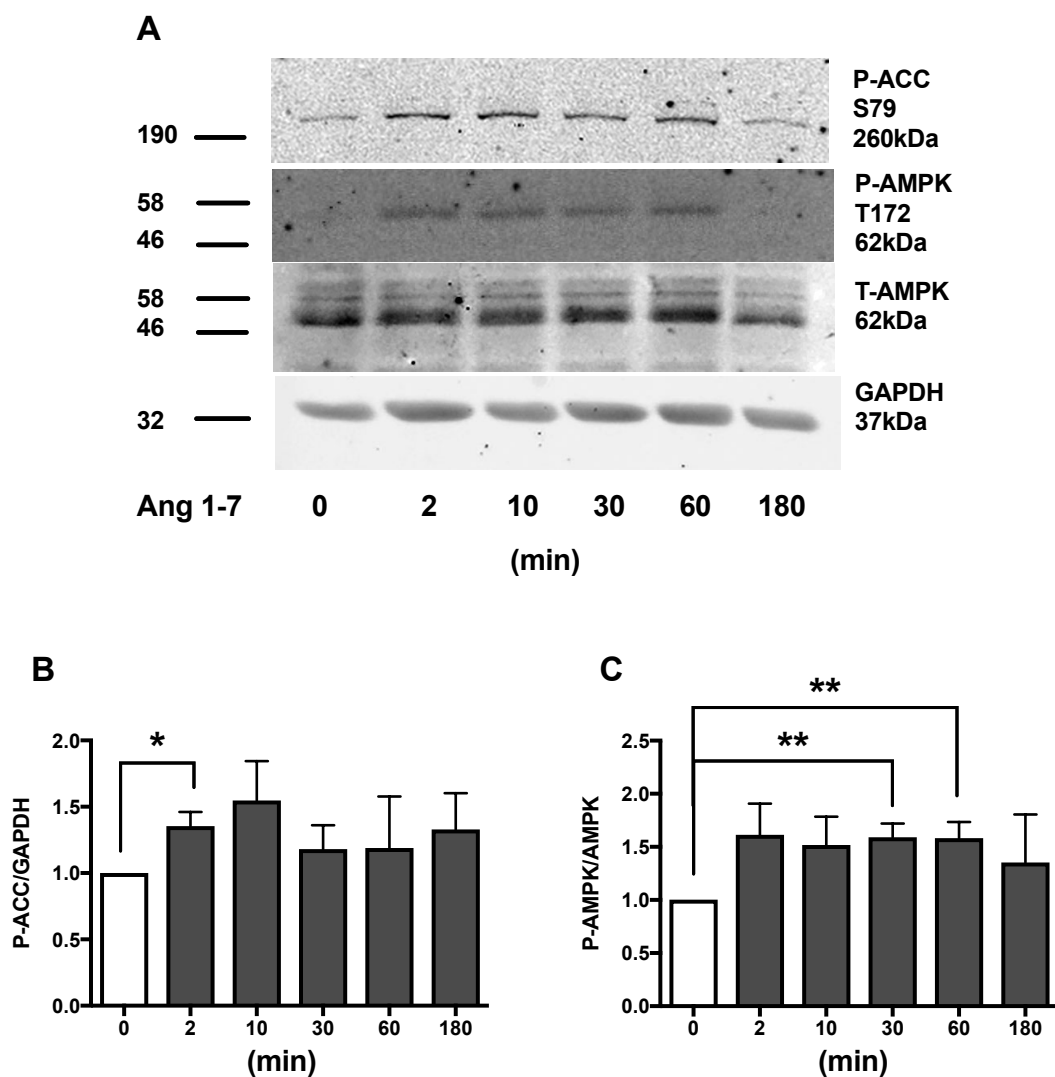
Figure 5.3 The effect of ang 1-7 on AMPK signalling in SW872 adipocytes

*SW872 adipocytes were incubated in 1% NCS (v/v) overnight then stimulated with ang 1-7 (1 µM) for durations indicated. Cell lysates were prepared, proteins resolved by SDS-PAGE and immunoblotted for the indicated proteins. A. Representative immunoblot with the molecular masses of marker proteins (in kDa) shown. B. Quantification of phospho-ACC (P-ACC) levels relative to GAPDH. C. Quantification of P-AMPK levels relative to AMPK. n=4, unpaired t-test *$p<0.05$, **$p<0.01$.*
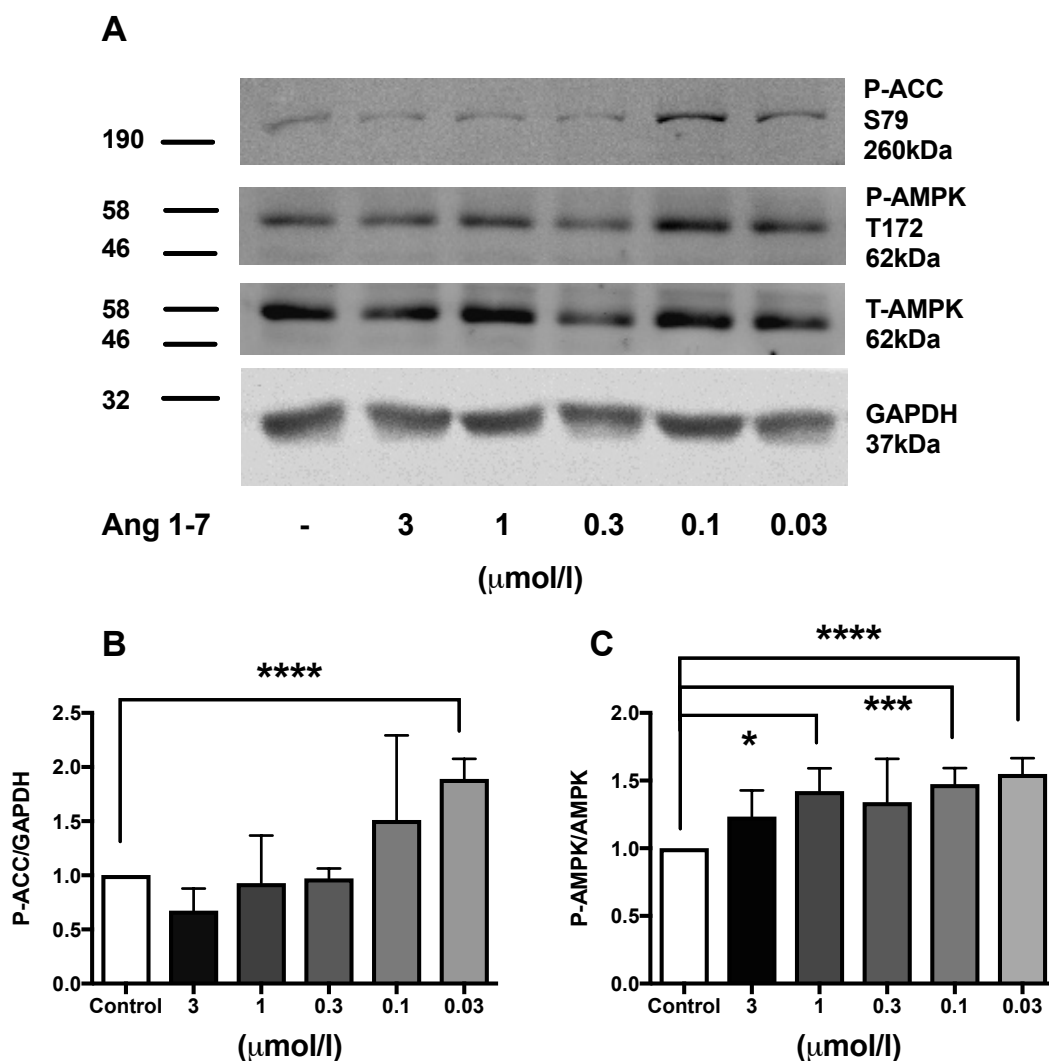
Figure 5.4 The effect of ang 1-7 on AMPK signalling in SW872 adipocytes

SW872 adipocytes were incubated in 1% NCS (v/v) overnight then stimulated with ang 1-7 at concentrations indicated for 10 min. Cell lysates were prepared, proteins resolved by SDS-PAGE and immunoblotted for the indicated proteins. A. Representative immunoblot with the molecular masses of marker proteins (in kDa) shown. B. Quantification of phospho-ACC (P-ACC) levels relative to GAPDH. C. Quantification of P-AMPK levels relative to AMPK. n=3, unpaired t-test *p<0.05, ***p<0.001, ****p<0.0001.
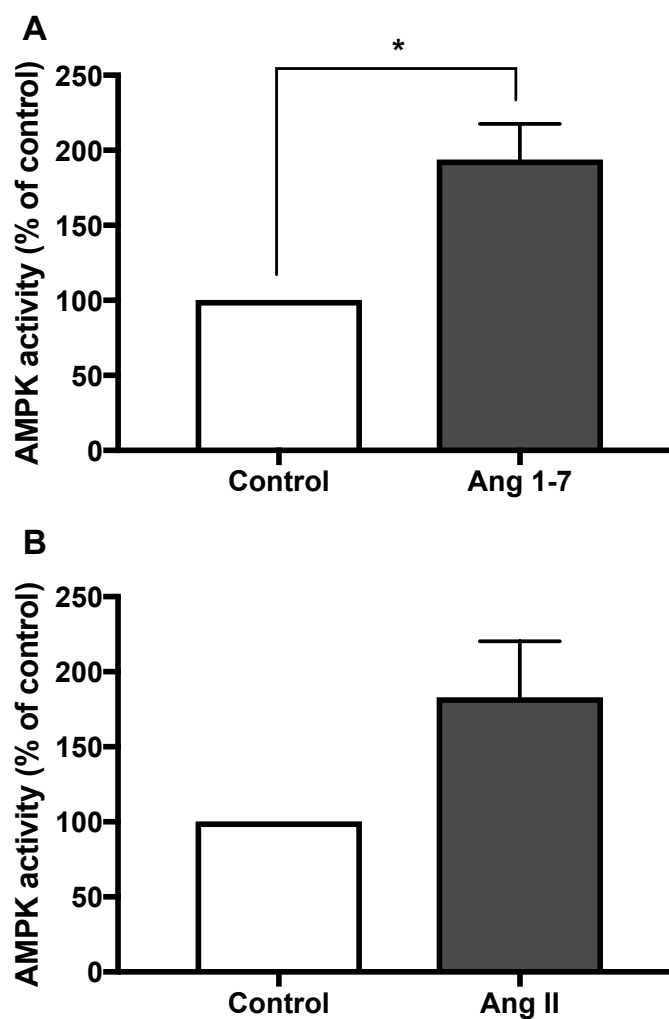
Figure 5.5 Effect of ang 1-7 and angiotensin II on AMPK kinase activity

SW872 adipocytes were incubated in 1% NCS (v/v) overnight then stimulated with A. ang 1-7 (1 μM) for 2 min or B. angiotensin II (10 μM) for 5 min. Cell lysates were prepared, AMPK immunoprecipitated and AMPK activity assayed in duplicate. n=3, unpaired t-test *p<0.05.
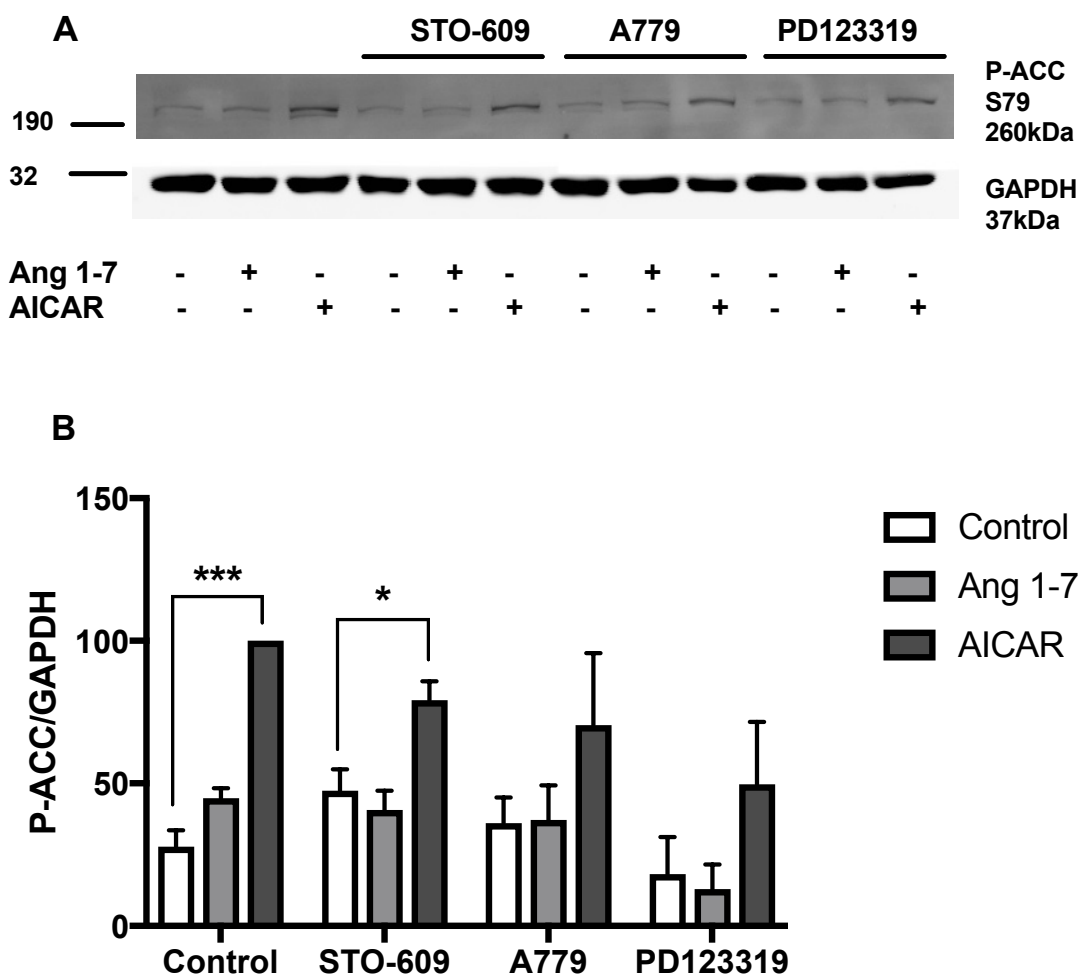
Figure 5.6 The mechanism of ang 1-7 induced AMPK signalling in SW872 adipocytes

SW872 adipocytes were incubated in 1% NCS (v/v) overnight then preincubated in the presence or absence of STO-609 (10 µM) (Nguyen et al. 2016), A779 (1 µM) (Liu et al. 2012) or PD123319 (10 µM) for 1 h prior to stimulation with ang 1-7 (100 nM) for 2 min or AICAR (1 mM) for 1 h. Cell lysates were prepared, proteins resolved by SDS-PAGE and immunoblotted for the indicated proteins. A. Representative immunoblot with the molecular masses of marker proteins (in kDa) shown. B. Quantification of phospho-ACC (P-ACC) levels relative to GAPDH. n=3, unpaired t-test, *p<0.05, ***p<0.001.

5.2.2.3 The effect of AMPK activators and ang 1-7 on CXCL-10 expression and secretion from SW872 adipocytes

During the course of this study, work in our laboratory demonstrated that AMPK has anti-inflammatory actions in cultured 3T3-L1 adipocytes, significantly inhibiting IL-1ß-stimulated secretion of the chemokine CXCL-10 (Mancini et al. 2017). The impact of AMPK activators AICAR and A769662 as well as ang 1-7 on IL-1ß-stimulated CXCL-10 mRNA expression was therefore assessed in SW872 adipocytes. Figure 5.7 demonstrates that IL-1ß (10 ng/ml for 6 h) significantly increased CXCL-10 mRNA levels in SW872 adipocytes (p=0.0004) and that this effect was attenuated by pre-incubation with AICAR (p=0.001) or A769662 (p=0.02).

To assess the functional impact of the ang 1-7-mediated AMPK activation on IL-1ß stimulated CXCL-10 mRNA levels and protein secretion, SW872 adipocytes were stimulated with ang 1-7 for 30 min prior to incubation with IL-1ß (10 ng/ml for 8 h) (Fig. 5.8). Again, IL-1ß significantly increased CXCL-10 mRNA levels and also increased CXCL-10 secretion into the culture medium. However, pre-incubation with ang 1-7 did not affect IL-1ß-stimulated CXCL-10 mRNA levels (Fig. 5.8A) or CXCL-10 secretion (Fig. 5.8B).

A
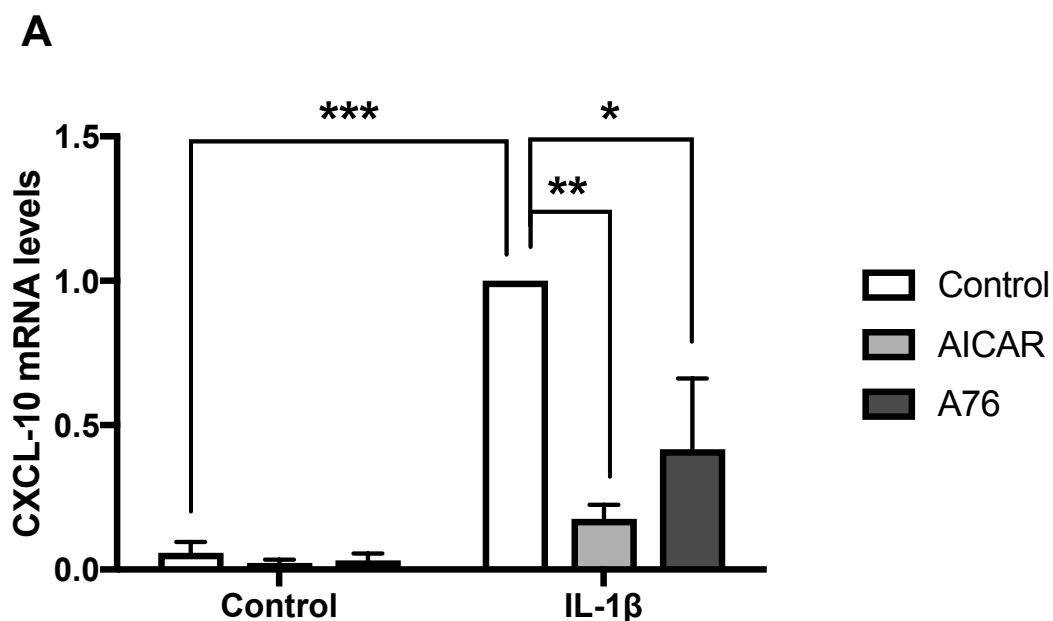
Figure 5.7 The effects of AMPK activators on CXCL-10 expression in SW872 adipocytes

RNA was extracted from SW872 adipocytes incubated in the presence or absence of IL-1β (10 ng/ml) for 6 h with or without the 1 h prior addition of AICAR (1 mM) or the 30 min prior addition of A769662 (300 μM). Reverse transcription was carried out prior to Taqman qPCR assays for CXCL-10. Data are normalised to TATA-binding protein mRNA expression. n=3, two-way ANOVA, *p<0.05, **p<0.01, ***p<0.001.

A

B
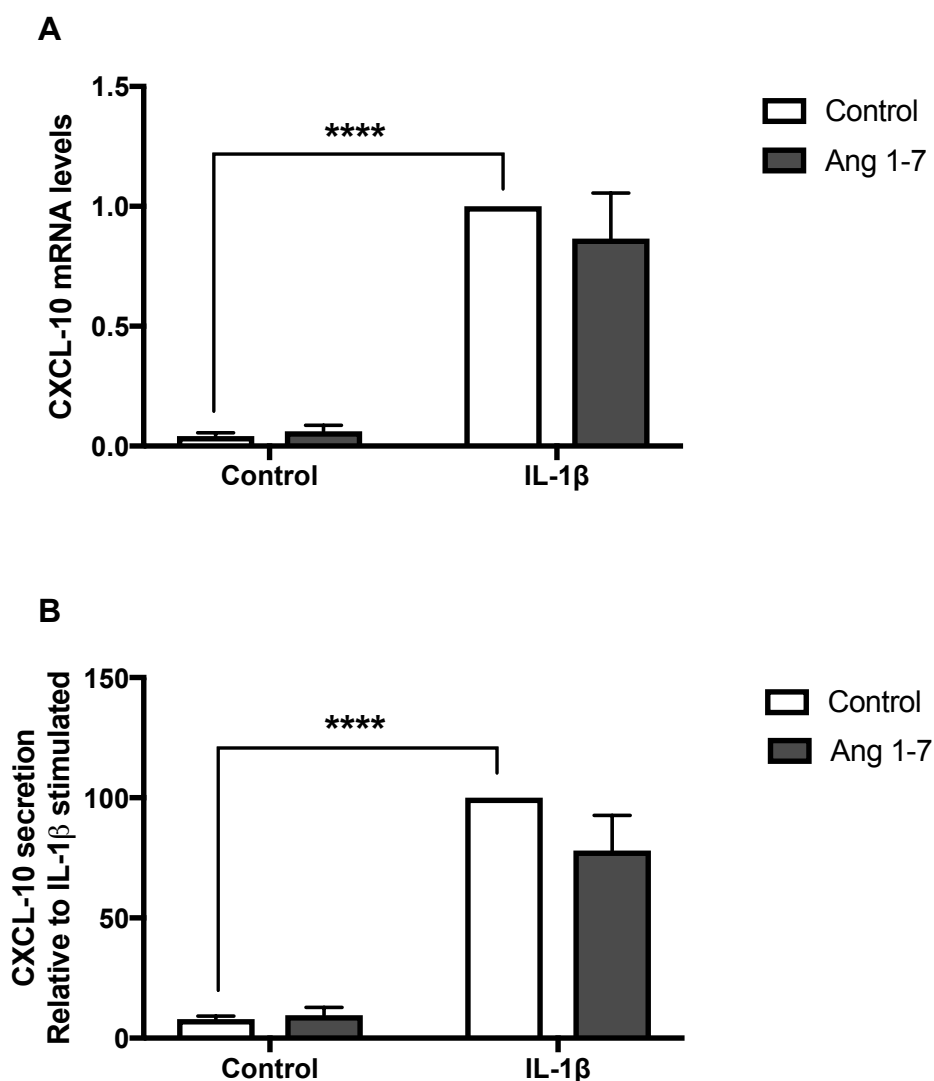
Figure 5.8 The effects of ang 1-7 on CXCL-10 expression and secretion in SW872 adipocytes

RNA was extracted and ELISA performed on culture medium from SW872 adipocytes incubated in the presence or absence of ang 1-7 (100 nM) for 30 min prior to stimulation in the presence or absence of IL-1β (10 ng/ml) for 8 h. A. Reverse transcription was carried out prior to Taqman qPCR assays for CXCL-10. Data are normalised to TATA-binding protein mRNA expression. B. CXCL-10 ELISA was performed and data quantified. n=4, two-way ANOVA, **p<0.01, ****p<0.0001.

5.2.3 The effect of ang 1-7 in 3T3-L1 adipocytes

5.2.3.1 The effect of ang 1-7 on AMPK signalling in 3T3-L1 adipocytes

Given the findings in SW872 adipocytes, the effect of ang 1-7 on AMPK in 3T3-L1 adipocytes was assessed, in addition to its impact on insulin signalling and glucose transport. Stimulation of 3T3-L1 adipocytes with ang 1-7 significantly increased ACC phosphorylation within 5 min, an effect that was sustained at 30 and 60 min (5 min 81% increase, p=0.0058; 30 min 134% increase, p=0.0018; 60 min 60% increase, p=0.0148)(Fig. 5.9B).

5.2.3.2 The mechanism of ang 1-7 signalling in 3T3-L1 adipocytes

Similar experiments to those described in 5.2.2.2 were performed in 3T3-L1 adipocytes to assess Mas-, AT2R- and CaMKK-dependence of ang 1-7-stimulated ACC phosphorylation. ACC phosphorylation tended to be increased by ang 1-7 whilst AICAR increased it robustly (p=0.002). The small tendency to increase phosphorylated ACC by ang 1-7 was lost in the presence of STO-609 and A779 yet maintained in the presence of PD123319 (Fig. 5.10B). However, as these effects were small and did not reach statistical significance the exact mechanism cannot be confirmed.

5.2.3.3 The effect of ang 1-7 on insulin signalling in 3T3-L1 adipocytes

As previously described, 3T3-L1 adipocytes are an excellent tool for the assessment of insulin signalling and insulin-stimulated glucose transport. To determine whether ang 1-7 influenced insulin signalling in 3T3-L1 adipocytes, cells were preincubated with ang 1-7 or AICAR prior to insulin stimulation and the phosphorylation of ERK, Akt and the Akt substrate, AS160 assessed. Insulin markedly increased phosphorylation of ERK1/2, Akt and AS160 (p<0.0001),

whereas ang 1-7 had no effect on basal or insulin-stimulated phosphorylation of any of these proteins. Intriguingly, AICAR increased basal Akt and AS160 phosphorylation without influencing insulin-stimulated phosphorylation of ERK1/2, Akt or AS160 (Fig 5.11).

5.2.3.4 The effects of ang 1-7 on glucose uptake in 3T3-L1 adipocytes

To determine the effects of ang 1-7 on insulin stimulated glucose transport, 3T3-L1 adipocytes were stimulated with insulin in the presence or absence of ang 1-7. Insulin stimulation increased glucose uptake 2.3-fold (p=0.0421) whilst ang 1-7 alone had no effect on basal or insulin stimulated glucose uptake (Fig. 5.12).

A

B
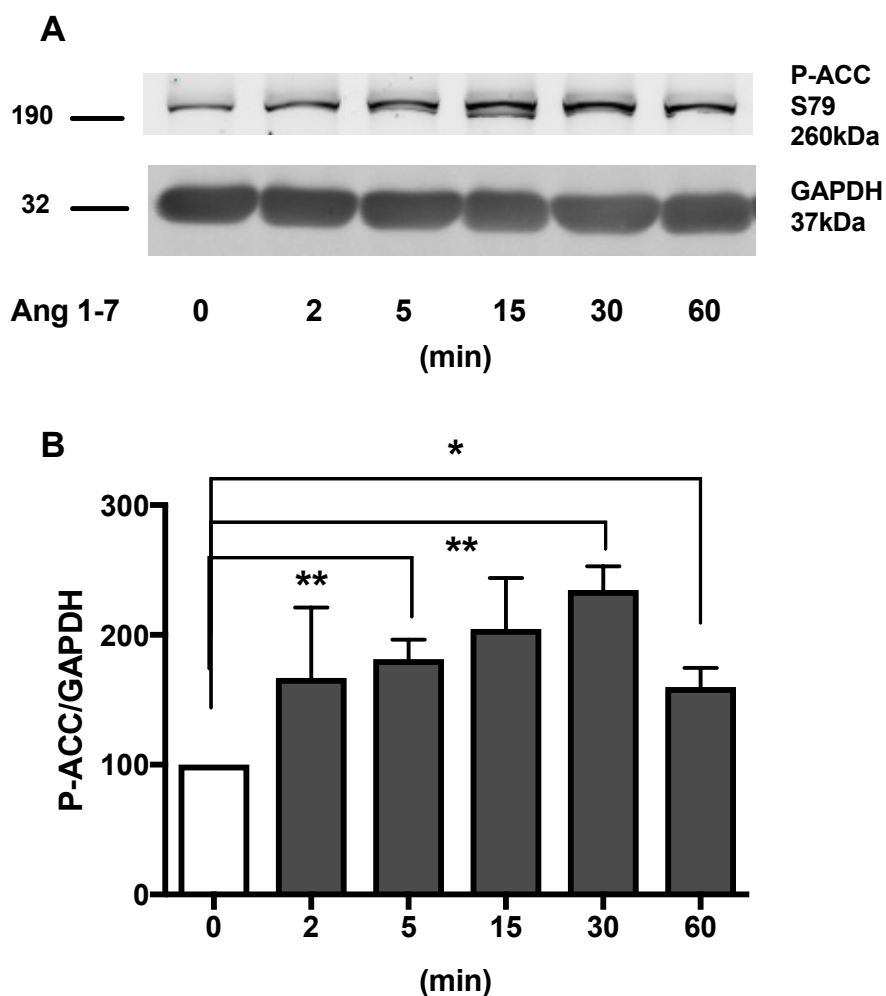
Figure 5.9 The effect of ang 1-7 on AMPK signalling in 3T3-L1 adipocytes

*3T3-L1 adipocytes were incubated in serum free media for 2 h then stimulated with ang 1-7 (1 µM) for durations indicated. Cell lysates were prepared, proteins resolved by SDS-PAGE and immunoblotted for the indicated proteins. A. Representative immunoblot with the molecular masses of marker proteins (in kDa) shown. B. Quantification of phospho-ACC (P-ACC) levels relative to GAPDH. n=3, unpaired t-test *p<0.05, **p<0.01. Repeat analysis using non-parametric test (Kruskal-Wallis) significant at 30 min, p=0.0366.*
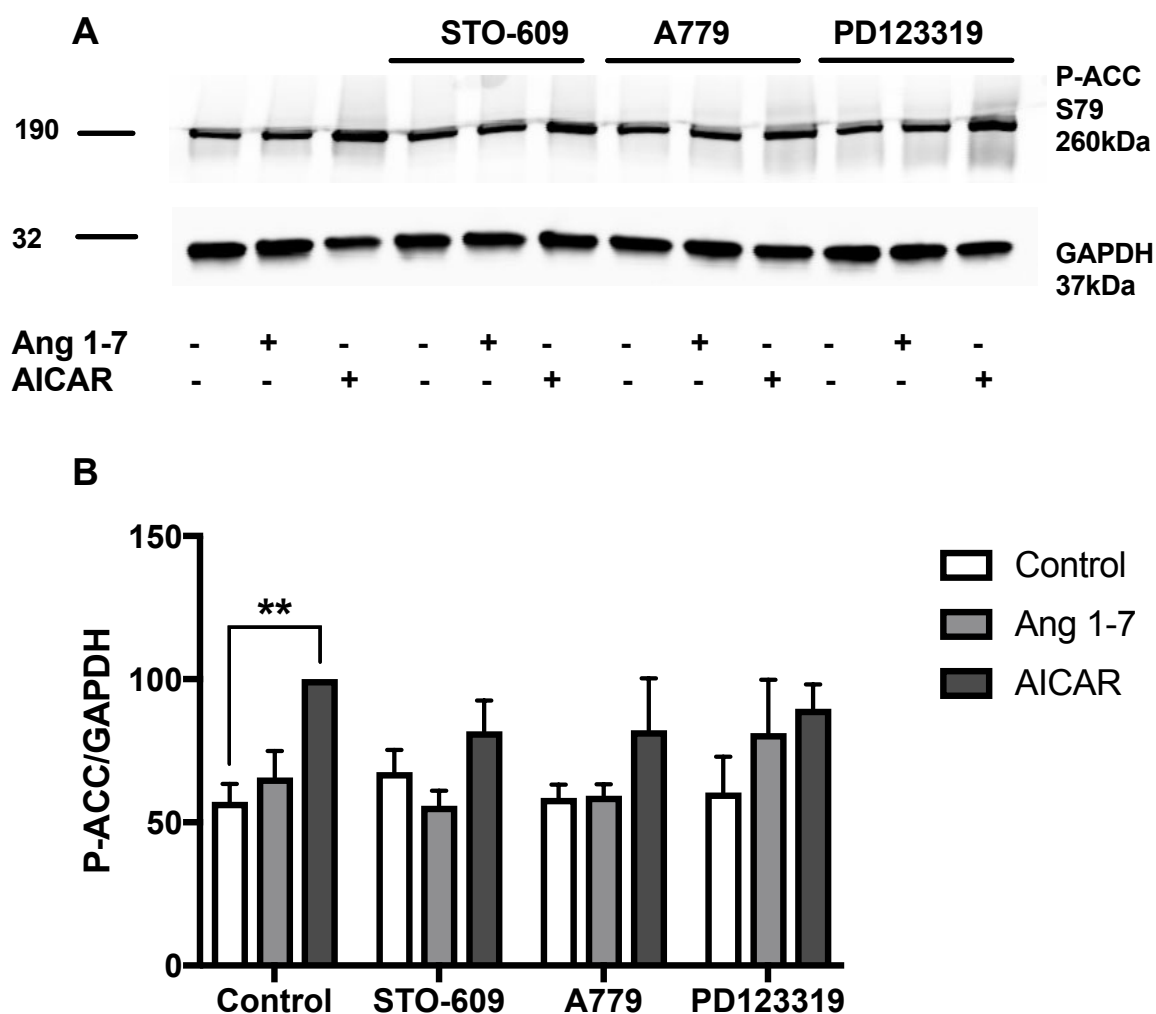
Figure 5.10 The mechanism of ang 1-7 signalling in 3T3-L1 adipocytes

3T3-L1 adipocytes were incubated in serum free media for 2 h then incubated in the presence or absence of STO-609 (10 µM), A779 (1 µM) or PD123319 (10 µM) for 1 h prior to stimulation with ang 1-7 (1 µM) for 30 min or AICAR (1 mM) for 1 h. Cell lysates were prepared, proteins resolved by SDS-PAGE and immunoblotted for the indicated proteins. A. Representative immunoblot with the molecular masses of marker proteins (in kDa) shown. B. Quantification of phospho-ACC (P-ACC) levels relative to GAPDH. n=3, unpaired t-test **p<0.01.
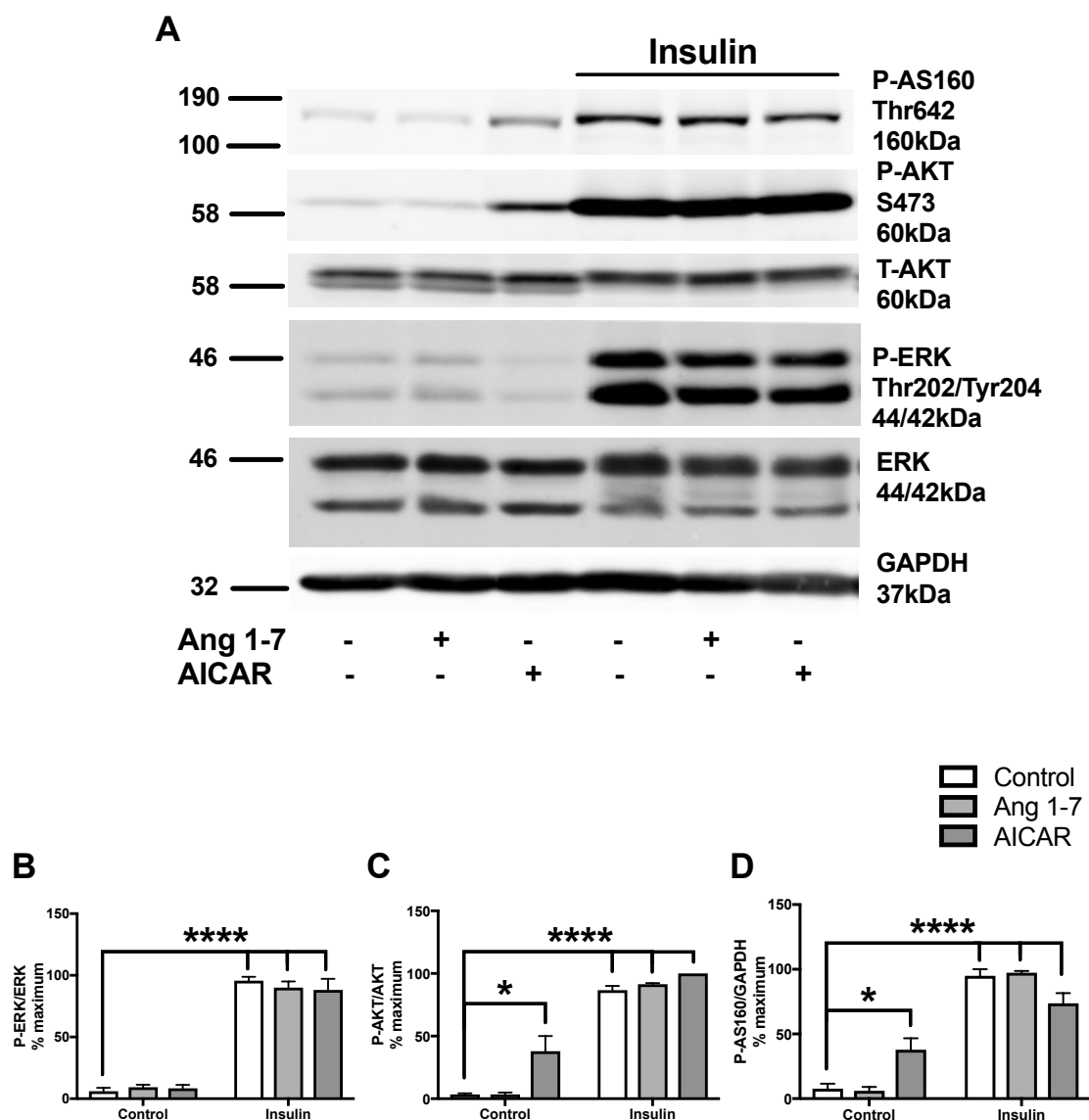
Figure 5.11 The effect of ang 1-7 and AICAR on insulin signalling in 3T3-L1 adipocytes

3T3-L1 adipocytes were incubated in serum free media for 2 h then stimulated with ang 1-7 (1 µM) for 30 min or AICAR (1 mM) for 1 h prior to insulin (100 nM) for 15 min. Cell lysates were prepared, proteins resolved by SDS-PAGE and immunoblotted for the indicated proteins. A. Representative immunoblot with the molecular masses of marker proteins (in kDa) shown. B. Quantification of phospho-ERK1 (P-ERK) levels relative to ERK1, C. phospho-Akt (P-Akt) levels relative to Akt and D. phospho-AS160 (P-AS160) levels relative to GAPDH. n=3, two-way ANOVA, *p<0.05, ****p<0.0001.
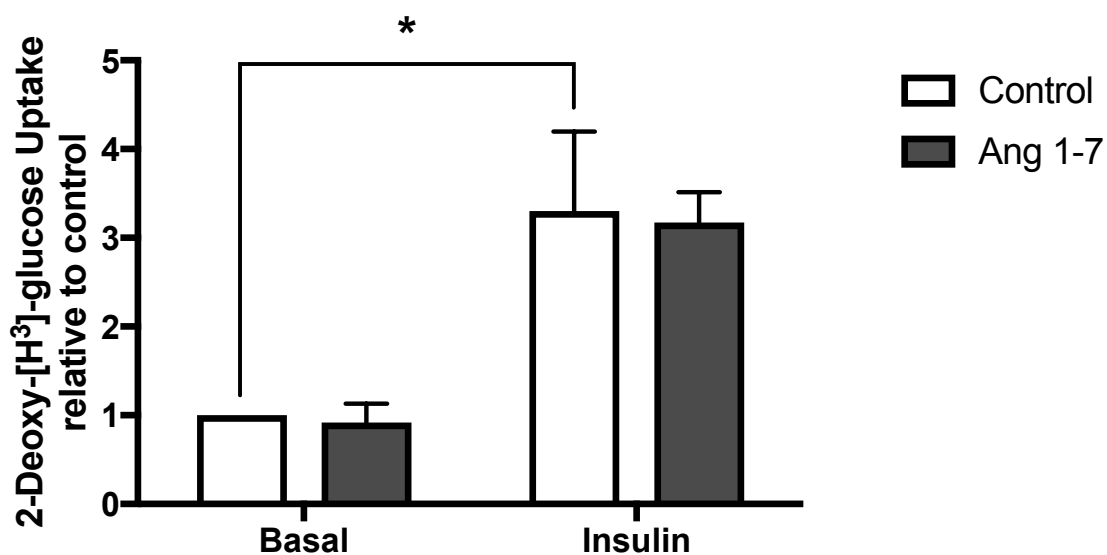
Figure 5.12 The effect of ang 1-7 on insulin-stimulated glucose transport in SW872 adipocytes

3T3-L1 adipocytes were incubated for 2 h in serum free DMEM then media changed to KRP + 0.1% (w/v) BSA for 1 h. Cells were subsequently stimulated with ang 1-7 (1 µM) for 30 min before addition of insulin (100 nM) for 10 min. 2-deoxy-^{3}H-glucose uptake was then assessed over 3 min, n=3, unpaired t-test *p<0.05.

5.3 Discussion

This chapter studied the effects of angiotensin hormones on AMPK signalling along with pro-inflammatory and insulin signalling pathways in cultured adipocytes. The initial finding that angiotensin II activated AMPK and this effect may be mediated by the AT2R led to investigation of the alternative RAAS focusing on angiotensin 1-7 which was also demonstrated to activate AMPK.

Aside from increasing aldosterone, angiotensin II has direct effects which are implicated in the development of metabolic syndrome. Plasma angiotensin II levels are elevated in obesity and ACE inhibitors and AT1R antagonists have been shown to prevent new onset type 2 diabetes (Goossens, 2012; Abuissa et al. 2005). The pro-diabetic effects of angiotensin II are therefore likely mediated by the AT1R. As previously discussed, the other angiotensin II receptor, AT2R, can mediate opposing effects to the AT1R. In this study, angiotensin II did not increase ERK 1/2 or NF-κB signalling in SW872 adipocytes. These pathways have previously been shown to mediate AT1R-mediated effects of angiotensin II (Than et al. 2012; Kalupahana et al. 2011) in adipocyte models. What was demonstrated was a rapid, yet modest, increase in the AMPK signalling which may, therefore, be mediated by the AT2R. In SW872 adipocytes angiotensin II initially activated AMPK at 10 μM yet when the concentration dependence was assessed, the increase in AMPK activity was only demonstrated at 100 nM. This inconsistency is likely a result of the modest activation observed at 10 μM and the variability in response. Indeed, increased AMPK activity was not confirmed by kinase assay. Differential effects of angiotensin II have been reported on AMPK activity in different cell types as outlined in 5.1.2. The other cell type in which AMPK has previously been reported to be activated by angiotensin II are VSMCs. In that case the stimulation of AMPK was reported to be via the AT1R at a concentration of 100 nM (Nagata et al. 2004). Interestingly, one study of AT2R knock out mice found smaller adipocytes and a protection from high fat diet induced obesity and insulin resistance thus implicating the AT2R in metabolic syndrome (Yvan-Charvet et al. 2005) which somewhat opposes the large clinical data on AT1R blockade. The absence of the AT1R in SW872 adipocytes

likely renders this model somewhat unique as actions may be swayed towards the alternative RAS. For this reason this study went on to explore the effects of ang 1-7.

This work demonstrated for the first time that ang 1-7 activates AMPK in human and murine derived adipocyte models. The mechanism of activation is likely to be Ca^{2+}- and MAS receptor- dependent. In keeping with this, the MAS receptor is a G-protein coupled receptor with Ca^{2+} considered a potential secondary messenger (Tirupula et al. 2014). One previous study identified AMPK activation in aortas from rats 10 min following an injection of ang 1-7 (Karpe and Tikoo, 2014). This occurred along with Akt and eNOS phosphorylation and activation (Karpe and Tikoo, 2014). In the present study, AMPK activation was rapid in SW872 adipocytes yet more sustained in 3T3-L1 adipocytes. Ang 1-7 did not increase Akt phosphorylation in 3T3-L1 adipocytes. It is worth noting that when compared to AICAR-stimulated ACC phosphorylation ang 1-7 was a far less potent stimulus and when the concentration-dependence was assessed the response of ACC phosphorylation to ang 1-7 was quite variable. This may be related to the length of exposure as ACC phosphorylation peaked rapidly in SW872 adipocytes whereas the AMPK phosphorylation appeared more sustained, as the concentration-dependence was determined after 10 min. As a consequence, it may be that the ACC phosphorylation had diminished in this time frame. However, contrary to the response to angiotensin II, when kinase assay was performed it confirmed increased activity in response to ang 1-7. The functional impact of this AMPK activation in adipocytes was explored by studying processes which are known to be influenced by AMPK and important in the pathogenesis of obesity and diabetes – inflammation and glucose transport (Bijland et al. 2013).

Ang 1-7 has previously been shown to increase production of the archetypal adipokines adiponectin and leptin (Santos et al. 2010, Uchiyama et al. 2017) and in 2013 it was reported to promote adipogenesis in cultured cells (Than et al. 2013). It has also been proposed to mediate the metabolic benefits of captopril as the decreased weight gain and adipose tissue mass associated with this ACE inhibitor were attenuated by A779, the mechanism was proposed to be related to phosphorylation of hormone sensitive lipase (Oh et

al. 2012). In this study, the AMPK activators AICAR and A769662 attenuated IL-1β-induced increases in CXCL-10 mRNA levels. In contrast, when ang 1-7 was applied prior to the addition of IL-1β there was no significant affect on the induction of CXCL-10 at the level of gene expression or protein secretion. This may be due to the modest degree of AMPK activation compared with that in response to AICAR or A769662. Similarly, no significant effect on either glucose transport or insulin signalling were identified in this study, suggesting that the role of ang 1-7 in adipocytes is not to acutely regulate insulin signalling. Within the literature there is a report of ang 1-7 enhancing basal and insulin-stimulated glucose transport in primary epididymal adipocytes (Liu et al. 2012). In the study of Liu et al. 1 nM ang 1-7 was used which is a major difference from this study (Liu et al. 2012). Additionally, the insulin concentration used is not reported and does not appear to have increased glucose uptake significantly (Liu et al. 2012).

When assessing the effects on insulin signalling it was demonstrated that AICAR increased both Akt Ser473 and AS160 Thr642 phosphorylation. AICAR was previously found by this lab to increase Akt Ser473 phosphorylation in human aortic endothelial cells (Morrow et al. 2003). Interestingly, the direct effect of AICAR on Akt activity was assessed by kinase assay in 3T3-L1 adipocytes and no change in Akt activity was seen (Salt et al. 2000). Whilst another group found that AICAR increased Akt Ser473 phosphorylation in muscle in a manner proposed to be AMPK-dependent, again suggesting cell specific effects of AMPK activation (Chen and Mackintosh, 2009). Yet another study found that AICAR had no effect on Akt phosphorylation but decreased AS160 phosphorylation in rat adipocytes (Gaidhu et al. 2010).

In summary, the major finding of this chapter was that AMPK is activated by the alternative RAS. Angiotensin II, likely via the AT2R, and ang 1-7, likely via the Mas receptor, both significantly increased AMPK activity. As AMPK is known to be a key energy regulator, this significantly contributes to our understanding of the metabolic benefits of ACE inhibitors and AT1R blockers previously identified. However, the underlying functional effects of this are yet to be identified and from this work do not appear to be related to inflammation or insulin signalling in adipocytes. Whilst this may be due to the

modest activation of AMPK observed, further studies of the metabolic effects of ang 1-7 would therefore be of great interest.

6 Chapter 6 – The impact of high fat diet on metabolism, adipose tissue inflammation and the RAAS in AMPKα1-/- mice

6.1 Introduction

6.1.1 Role of adipose tissue in obesity related problems

The consequences of high fat diet (HFD) on human populations are many and rodent models of this provide a useful tool in determining mechanisms of metabolic disease. Adipose tissue inflammation due to excess nutrition is associated with increased pro-inflammatory adipocytokine release which can decrease insulin signalling and reduce insulin sensitivity (Reilly and Saltiel, 2017). Despite this, when treatments targeting inflammation, such as neutralising antibodies targeting TNF and IL-1ß, have been trialled in humans to treat insulin resistance, results have been disappointing (Ofei et al. 1996; Sloan-Lancaster et al. 2013). It therefore remains crucial to identify key changes in obesity-induced adipose tissue inflammation which may be targets for diabetes therapies.

6.1.2 AMPK knockout mice

AMPKα1 is the predominant catalytic AMPK subunit in adipose tissue. Global AMPKα1-/- mice have reduced AMPK activity in adipose tissue yet no significant basal metabolic phenotype (Viollet et al. 2003). The AMPKα2-/- mouse however exhibits impaired glucose handling (Viollet. et al 2003). AMPKα2 is the predominant subunit in other key metabolic tissues including the liver and skeletal muscle. The AMPKα1-/- model therefore provides a useful tool to assess the importance of adipose AMPK in the sensitivity to metabolic stress and the development of metabolic disorders. Previous studies report small adipocyte size in AMPKα1-/- mice and an increase in both basal and stimulated lipolysis (Daval et al. 2005). In addition, AMPKα1 appears to be required for AICAR-induced aortic ring relaxation, which was absent in AMPKα1-/- mice but remained in AMPKα2-/- mice (Goirand et al. 2007). AMPKα1-/- mice also display a marked erythrocyte abnormality and anaemia with a marked compensatory splenomegaly (Foller et al. 2009).

6.1.3 Aims

This study aimed to identify the role that AMPKα1 plays in the development of adipose tissue dysfunction in obesity. Using wild type (WT) and AMPKα1-/- (KO) mice fed HFD or a normal chow diet, the impact of dietary excess on systemic metabolic physiology and adipose tissue was assessed.

6.2 Results

6.2.1 Weight gain during the 12-week dietary intervention

Littermate pairs of male WT and KO mice were allocated to receive either standard chow or high fat diet (HFD) for 12 weeks from 8-10 weeks old. Weight was charted weekly throughout the 12-week period (Fig. 6.1A). Mean baseline weight was similar between groups (25.64 g for WT chow, 26.23 g for KO chow, 23.66 g for WT HFD and 22.22 g for KO HFD). Both chow fed groups gained similar amounts of weight (14.4 WT, 7% KO). The WT mice fed HFD gained the most weight with a 35.5% rise from baseline, whilst the KO mice on HFD increased their weight by 28.7%. Although the WT mice on HFD gained the most weight, there was no significant difference compared to weight gain in KO mice (Fig 6.1B).

Food intake was also assessed weekly by measuring the mass change of hopper food in a 24 h period for each mouse. Both WT and KO mice on chow diet ate more food per day (WT 4.3g, KO 4.4g; mean over 12 weeks) than those eating the high fat diet (WT 3.2g, KO 3.1g; mean over 12 weeks)(Fig 6.2A&B). The mass of food consumed did not vary significantly over the course of the dietary intervention. The mean daily estimated KCal intake per day was similar between groups at 14.1 for WT chow, 14.5 for KO chow, 14.8 for WT HFD and 14.3 for KO HF.

A

B
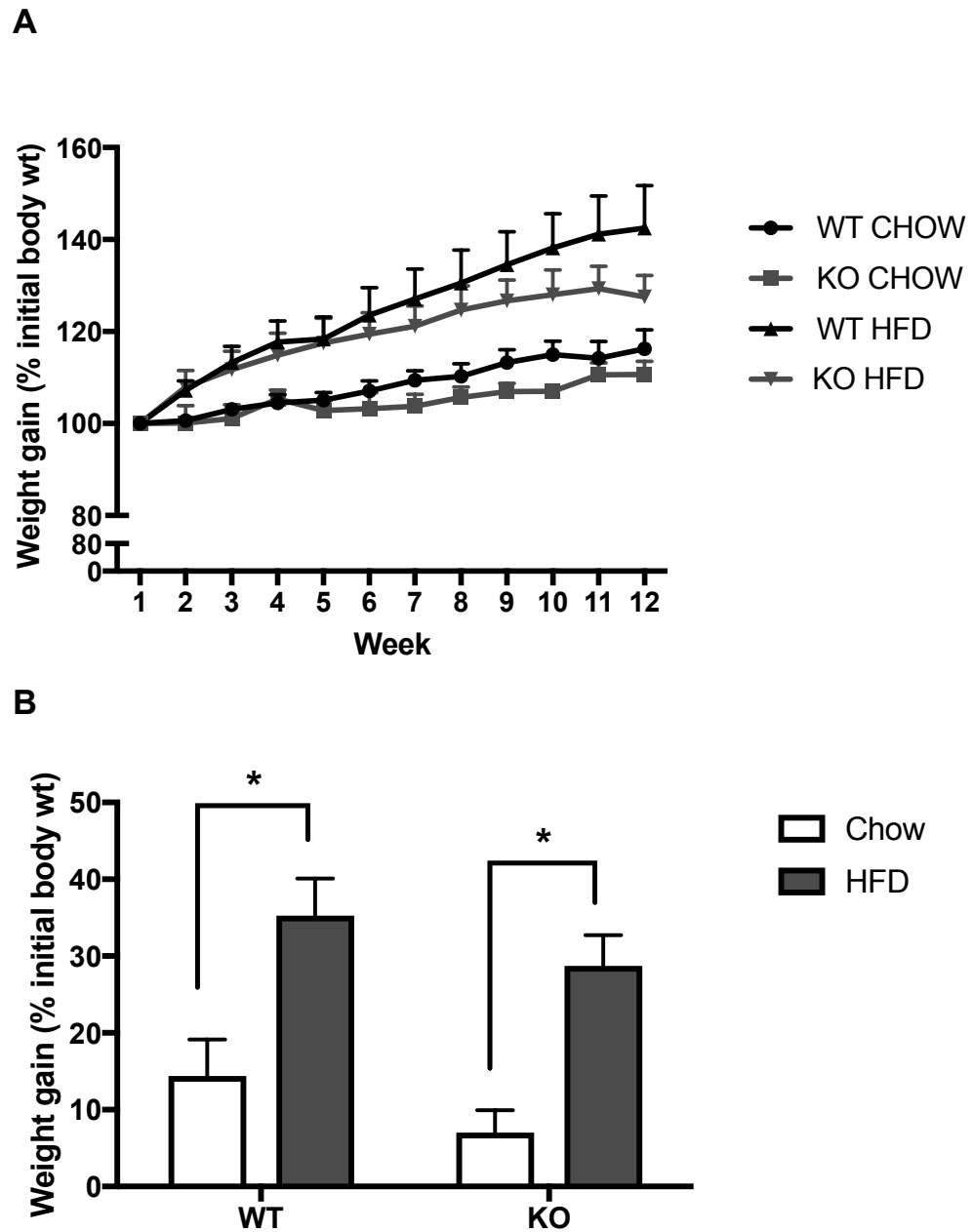
Figure 6.1 Weight gain during 12-week high fat diet intervention

Weight was measured weekly during the dietary intervention. A. Weekly weight gain as a percentage of initial body weight and B. Percent weight gain following the 12 week intervention. Two way ANOVA, *p<0.05. WT Chow n=5, WT HFD n=7, KO Chow n=3, KO HFD n=6.

A

B
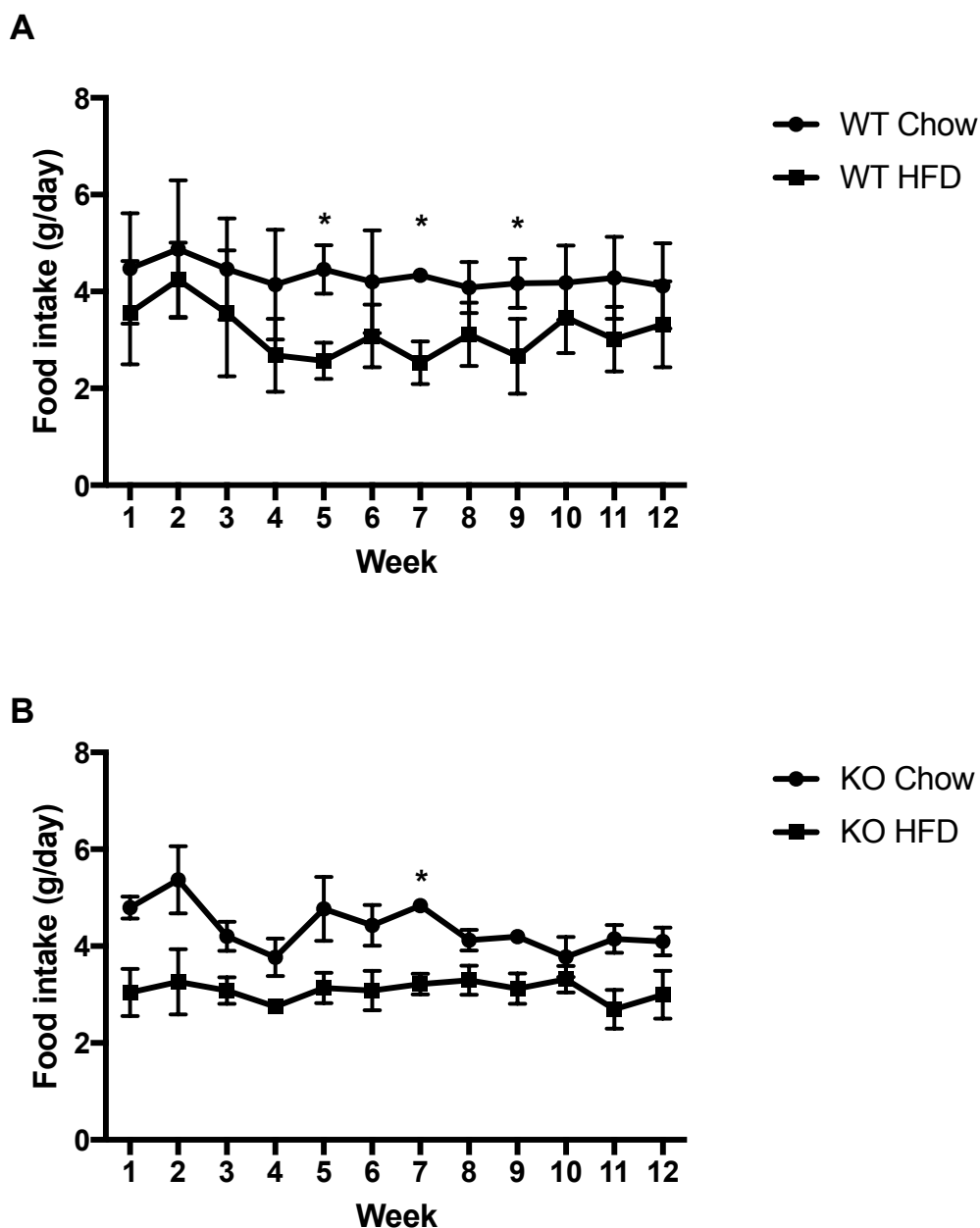
Figure 6.2 Food consumption during 12-week high fat diet intervention

Available food was measured before and after 24 h once per week throughout the 12-week dietary intervention. Values represented for A. WT and B. KO mice. Unpaired t-test, *p<0.05. WT Chow n=6, WT HFD n=7, KO Chow n=4, KO HFD n=6.

6.2.2 The effect of HFD on glucose tolerance and metabolic parameters in WT and KO mice

Fasting lipids, glucose and insulin were measured at the end of the dietary intervention as an index of metabolic health. There was a significant increase in total cholesterol in WT mice on high fat diet compared to chow (HFD 5.3 vs chow 3.9 mM, p=0.03)(Fig. 6.3A), whereas in KO mice the increase in cholesterol was close to significant (HFD 4.4 vs. chow 3.2 mM, p=0.053). There were no significant differences between groups for triglyceride concentration whereas HDL had a tendency to be higher in the KO HFD group compared to KO chow (p=0.056)(Fig. 6.3 A & B).

Fasting glucose was not significantly different between the groups however there was a tendency toward lower fasting glucose in the KO group on chow diet compared to HFD (Fasting glucose chow 4.3 mM vs. HFD 5.9 mM, p=0.076)(Fig. 6.4A). Fasting insulin levels were highest in the WT group on high fat diet however the difference was not statistically significant (HFD 0.91 vs. chow 0.57 ng/ml, p=0.064)(Fig. 6.4B).

Glucose tolerance testing was performed following a 16 h fast at the end of the intervention. Each group responded similarly to intraperitoneal glucose and there were no significant differences between the incremental area under the curve (Fig 6.5E). There was a significant difference between the 15 min glucose level in the KO HFD group compared to the KO chow group (KO HFD 215% increase vs KO chow 330% increase, p=0.008)(Fig 6.5D). It is not clear why the incremental glucose was higher at 15 min in the chow group compared to the HFD group however it may be related to the lower baseline glucose.
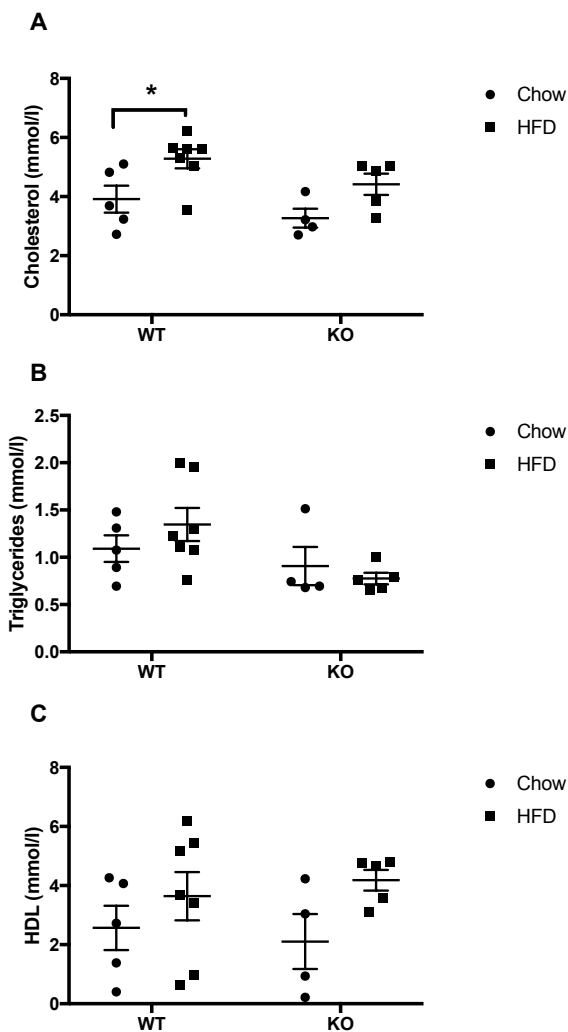
Figure 6.3 Serum lipids following 12-week dietary intervention

Whole blood was obtained at sacrifice by cardiac puncture. Serum lipids were analysed using a clinically validated automated platform (c311, Roche Diagnostics, Burgess Hill, UK). The analyser was calibrated and quality controlled using the manufacturers materials. Data for A. cholesterol, B. triglycerides and C. HDL are displayed as individual values with means with standard error. WT Chow n=5, WT HFD n=7, KO Chow n=4, KO HFD n=6.
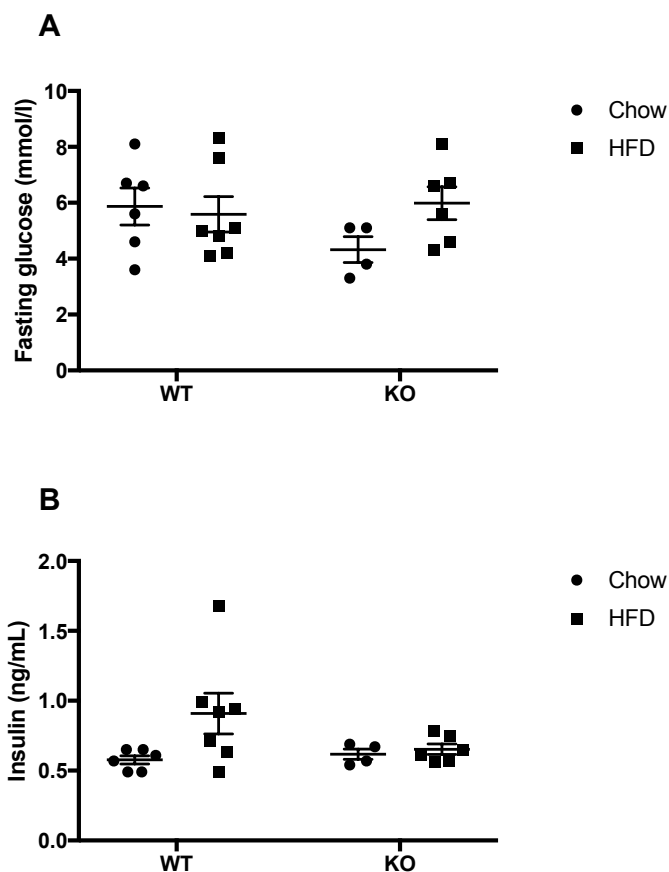
Figure 6.4 Fasting serum glucose and insulin following 12-week dietary intervention

A. Tail vein glucose was analysed following 16 h fast using a FreeStyle Optium glucometer. B. Whole blood was obtained at sacrifice by cardiac puncture. Serum insulin was analysed by ELISA. Data are displayed as individual values with means with standard error. WT Chow n=6, WT HFD n=7, KO Chow n=4, KO HFD n=6.
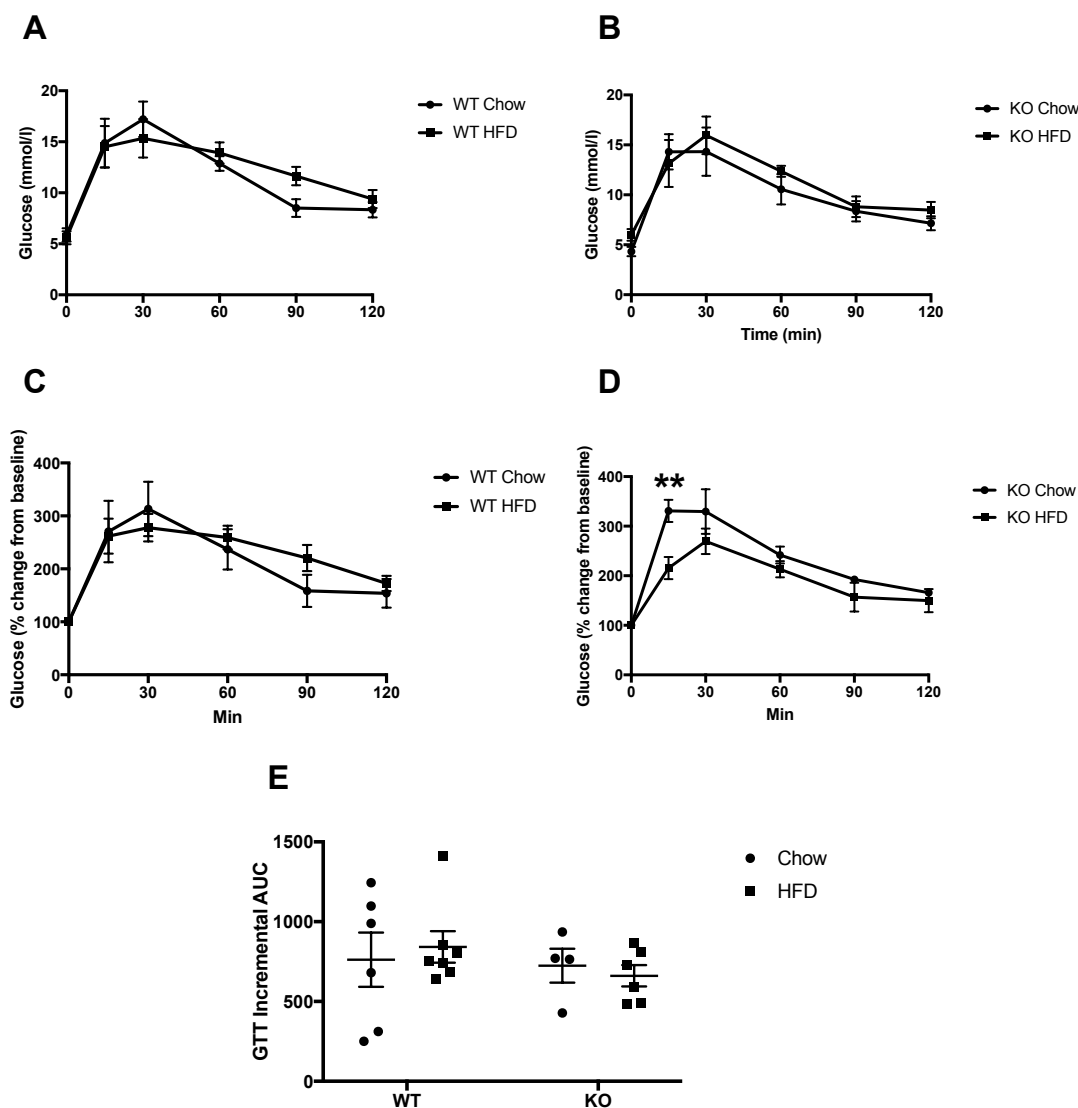
Figure 6.5 Glucose tolerance test

Glucose tolerance tests were performed 1-2 days prior to sacrifice following a 16 h fast. Tail vein blood glucose was measured before and after an intraperitoneal glucose injection. Free access to food was granted after the test. Changes from baseline glucose are represented by genotype A. WT and B. KO in mmol/l C. WT and D. KO as % change from baseline. E. Mean Incremental area under the curve for grouped mice. Unpaired t-test, **p<0.001. WT Chow n=6, WT HFD n=7, KO Chow n=4, KO HFD n=6.

6.2.3 The effect of HFD on serum RAAS and electrolytes in WT and KO mice

Serum aldosterone, angiotensin II, angiotensin I and renin concentration were measured following the intervention. Mean aldosterone concentration was similar between both WT chow (84.33 pg/ml) and HFD groups (90.13 pg/ml) and tended to be lower in the KO chow group (53.33 pg/ml) yet highest in the KO HFD group (250.46 pg/ml). Angiotensin II concentrations were again similar in the WT groups (chow 268.13 pg/ml, HFD 254.3 pg/ml) yet tended to be higher in the KO groups (chow 641.23 pg/ml, HFD 885 pg/ml). Angiotensin I levels were also highest in the KO HFD group although the difference was not statistically significant (WT chow 199.1 pg/ml, WT HFD 249.2 pg/ml, KO chow 267.5 pg/ml, KO HFD 469.64 pg/ml). In keeping with these findings, renin concentration (measured by ang I formation rate) was also highest in the KO HFD group (WT chow 21.2, WT HFD 43.36, KO chow 33.6, KO HFD 54) (Fig. 6.6). Serum sodium, potassium and chloride were not significantly different between the treatment groups (Fig. 6.7).
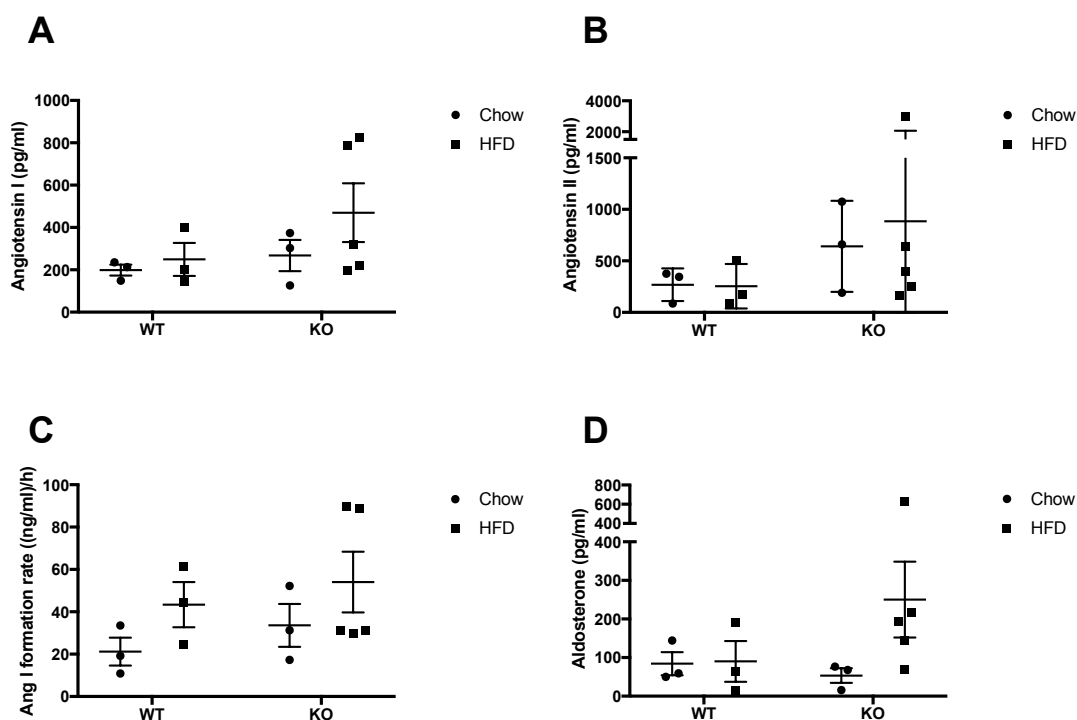
Figure 6.6 Serum RAAS measurements following 12-week dietary intervention

Whole blood was obtained at sacrifice by cardiac puncture. Serum RAAS components were analysed by liquid chromatography tandem mass spectrometry (LC-MS/MS) by Attoquant Diagnostics (Vienna, Austria). Data are displayed as individual values with means with standard error for A. angiotensin I, B. angiotensin II, C. angiotensin I formation rate and D. aldosterone. WT Chow n=3, WT HFD n=3, KO Chow n=3, KO HFD n=5.
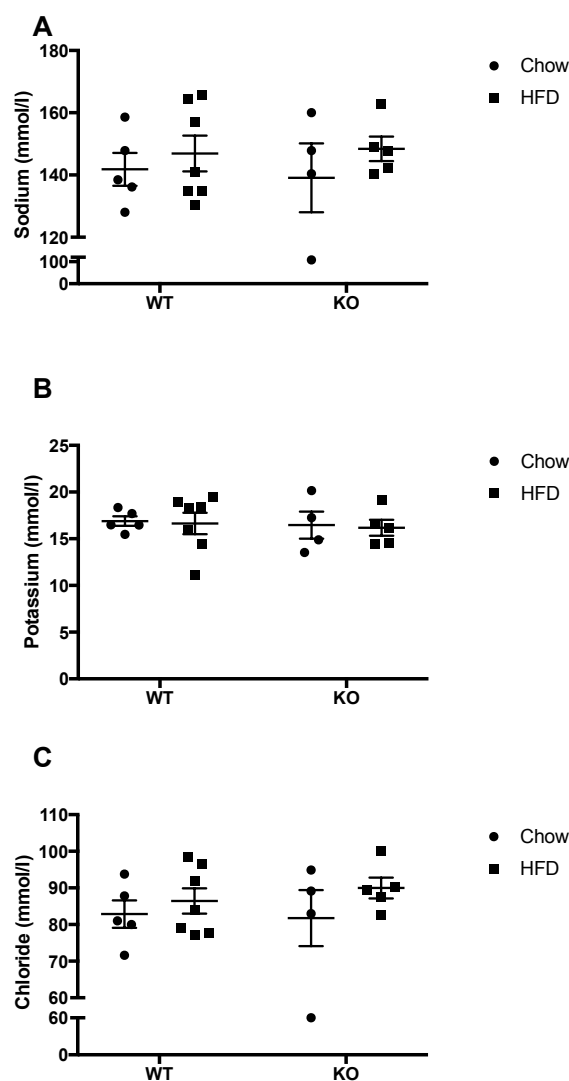
Figure 6.7 Serum electrolytes at the end of the 12-week dietary intervention

Whole blood was obtained at sacrifice by cardiac puncture. Serum electrolytes were analysed using a clinically validated automated platform (c311, Roche Diagnostics, Burgess Hill, UK). The analyser was calibrated and quality controlled using the manufacturers materials. Data for A. sodium, B. potassium and C. chloride are displayed as individual values with means with standard error. WT Chow n=5, WT HFD n=7, KO Chow n=4, KO HFD n=6.

6.2.4 The effect of HFD on organ weights in WT and KO mice

High fat diet increased liver weight in both WT and KO mice. WT liver weight increased following HFD from a mean weight of 838 mg to 1106 mg (p=0.008). A similar increase was observed in KO mice (mean chow liver weight 842 mg vs mean HFD liver weight 1120 mg) (p=0.048) (Fig 6.8A). Spleen weights were significantly increased in KO mice and spleen weight was not affected by dietary intake (mean spleen weight WT chow 58 mg, KO chow 230 mg, p<0.0001) (Fig. 6.8B). HFD had no significant effect on heart or kidney weight. When corrected for body weight, the significance of the increased liver mass was lost, but the spleen mass remained significantly increased in the KO mice on either diet. Both WT and KO mice on chow diet displayed normal liver architecture with evidence of normal sinusoids. Following high fat diet liver architecture was altered and fat droplets were evident in both WT and KO liver samples (Fig. 6.9). Mean liver triglyceride content was not significantly different between genotype at baseline. Following HFD liver triglyceride significantly increased in both genotypes (WT chow 11.44 vs WT HFD 30.51 nmol/mg, p=0.049) (KO chow 7.78 vs KO HFD 21.39 nmol/mg, p=0.038) (Fig 6.10). There was no significant difference in liver triglyceride content between genotype following HFD.
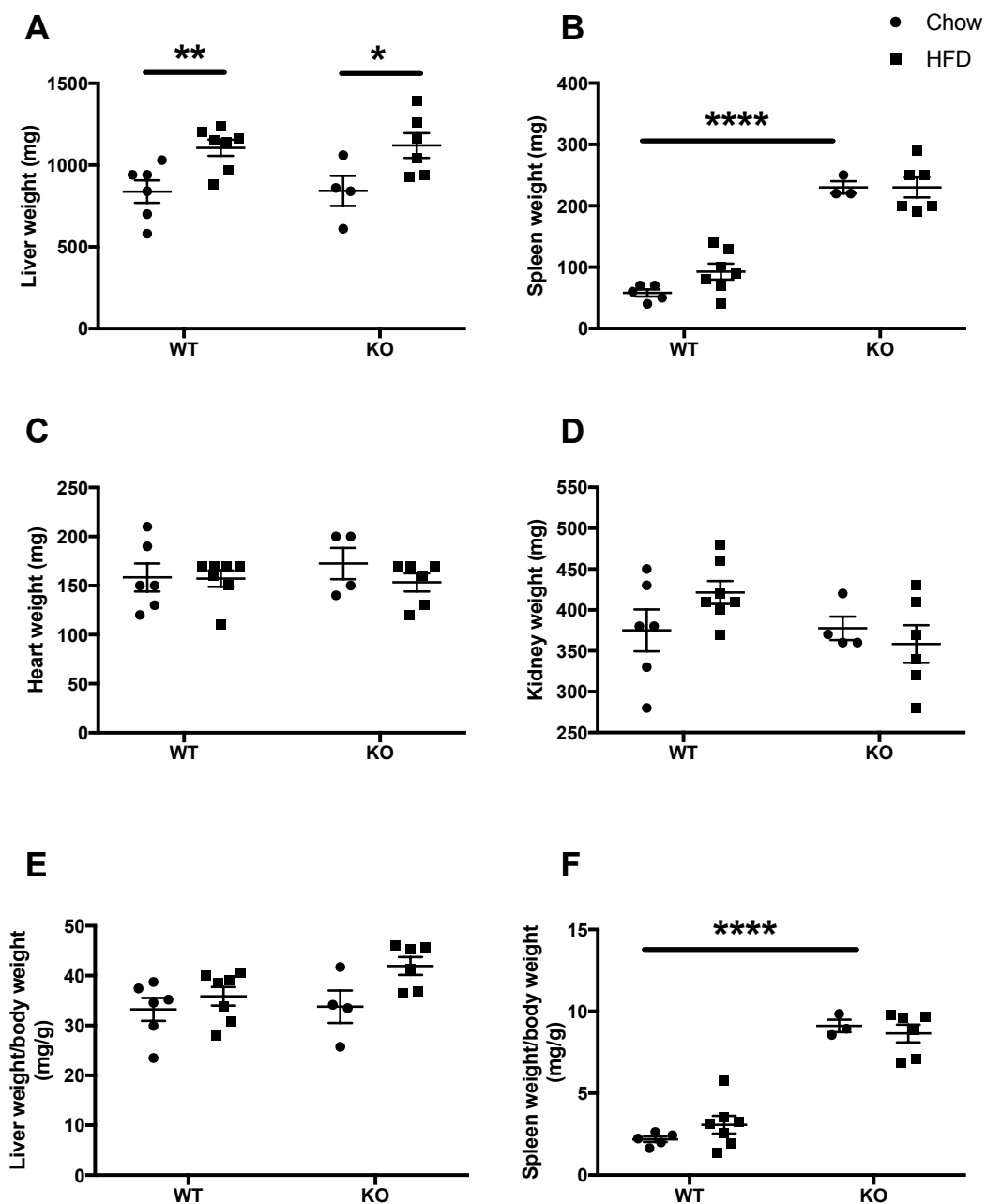
Figure 6.8 Organ weights

A. liver, B. spleen, C. heart and D. kidneys were collected and weighed at the time of sacrifice. E. liver and F. spleen weights have been corrected to body weight. T-test, *p<0.05, **p<0.01, ****p<0.0001. WT Chow n=6, WT HFD n=7, KO Chow n=4, KO HFD n=6.

WT CHOW

KO CHOW

WT HFD

KO HFD
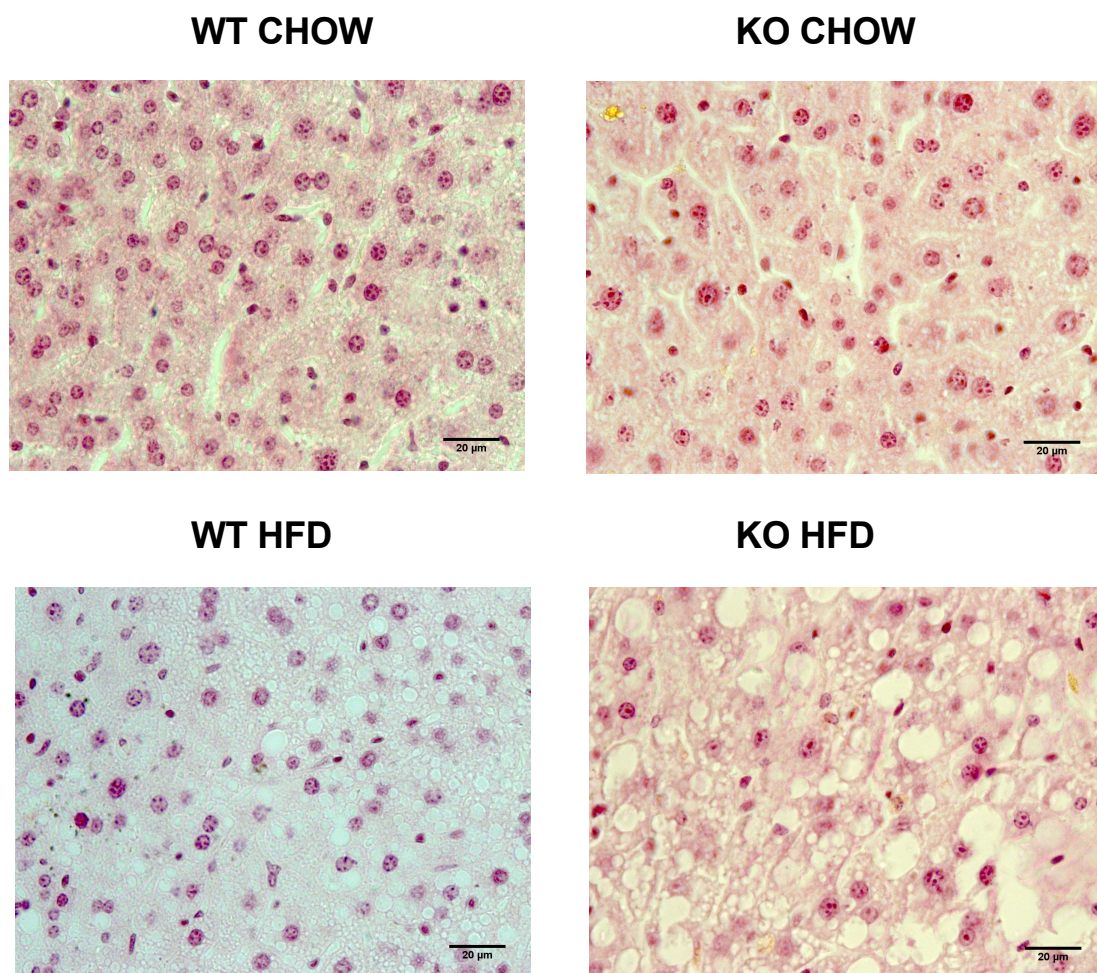
Figure 6.9 Liver histology

Representative micropictographs of liver sections stained with haemotoxylin and eosin from experimental mice. Images (40 x magnification) were generated by Omar Katwan (University of Glasgow).
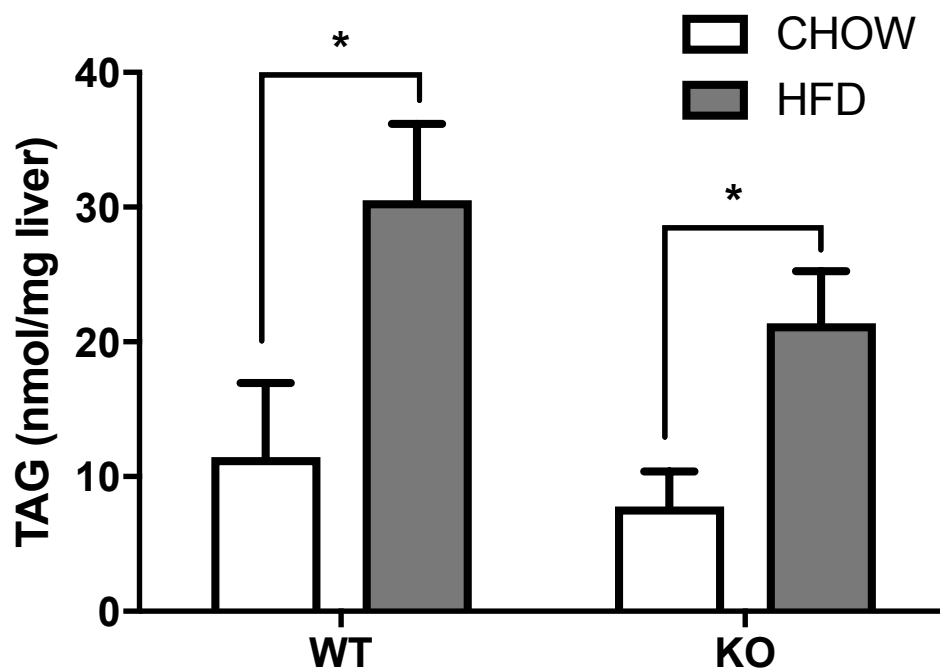
Figure 6.10 Liver triglyceride content

Triglyceride content of liver homogenates was assayed using an Abcam Triglyceride Quantification Assay Kit. T-test *p<0.05. Data shown is from four chow-fed animals of each genotype and five animals of each genotype fed high fat diet (HFD). Assay conducted by Dr Ian Salt (University of Glasgow).

6.2.5 The effect of HFD on adipose tissue in WT and KO mice

6.2.5.1 Adipose tissue mass

Subcutaneous (SCUT) and epididymal (EVAT) adipose tissue depot weights at the time of sacrifice were corrected to final body weight. High fat diet significantly increased EVAT weight in WT and KO mice (Fig 6.10B). However, SCUT weight increased significantly only in the WT group (Fig. 6.11).

6.2.5.2 AMPK phosphorylation in adipose tissue

AMPK Thr172 phosphorylation was significantly lower in SCUT and EVAT of KO mice compared to WT mice (Fig. 6.12). As the antibody used recognizes activating phosphorylation sites in both AMPKα1 and AMPKα2, the remaining immunoreactivity in KO mice reflects phospho-AMPKα2 levels.

6.2.5.3 STAT3 phosphorylation in adipose tissue

STAT3 is a transcription factor with a crucial role in IL-6 mediated JAK-STAT signalling and the induction of chemokines such as MCP-1 (Fasshauer et al. 2004) but also mediates anti-inflammatory effects of IL-10 (MacPherson et al. 2015). This group previously identified an increase in STAT3 phosphorylation in gonadal and SCUT adipose tissue from female KO mice compared to WT (Mancini et al. 2017). To determine the effect of HFD on adipose STAT3 phosphorylation western blotting was performed on adipose tissue lysates. In SCUT, STAT3 phosphorylation was significantly reduced in KO mice fed a HFD, compared to those fed chow diet (p=0.0004), a similar tendency was observed in WT mice although this difference was not statistically significant (Fig. 6.13A). In EVAT, STAT3 phosphorylation was significantly increased in KO mice compared to wild type mice fed chow diet. Interestingly, STAT3 phosphorylation in KO mice fed HFD was significantly reduced compared to chow-fed KO mice, yet diet had no effect on WT mice (Fig. 6.13B).

6.2.5.4 JNK phosphorylation in adipose tissue

Another pro-inflammatory signalling pathway which can be attenuated by AMPK is the JNK signalling pathway (Mancini et al. 2017). In SCUT from WT mice JNK phosphorylation increased in response to HFD (p=0.02)(Fig. 6.14A & B). In SCUT from KO mice, however, JNK phosphorylation was not changed by HFD. In EVAT from WT mice there was a tendency for HFD to increase JNK phosphorylation whilst in KO mice JNK phosphorylation was unchanged by diet (Fig 6.14C & D). Therefore, KO mice appear resistant to the effect of HFD on JNK phosphorylation.
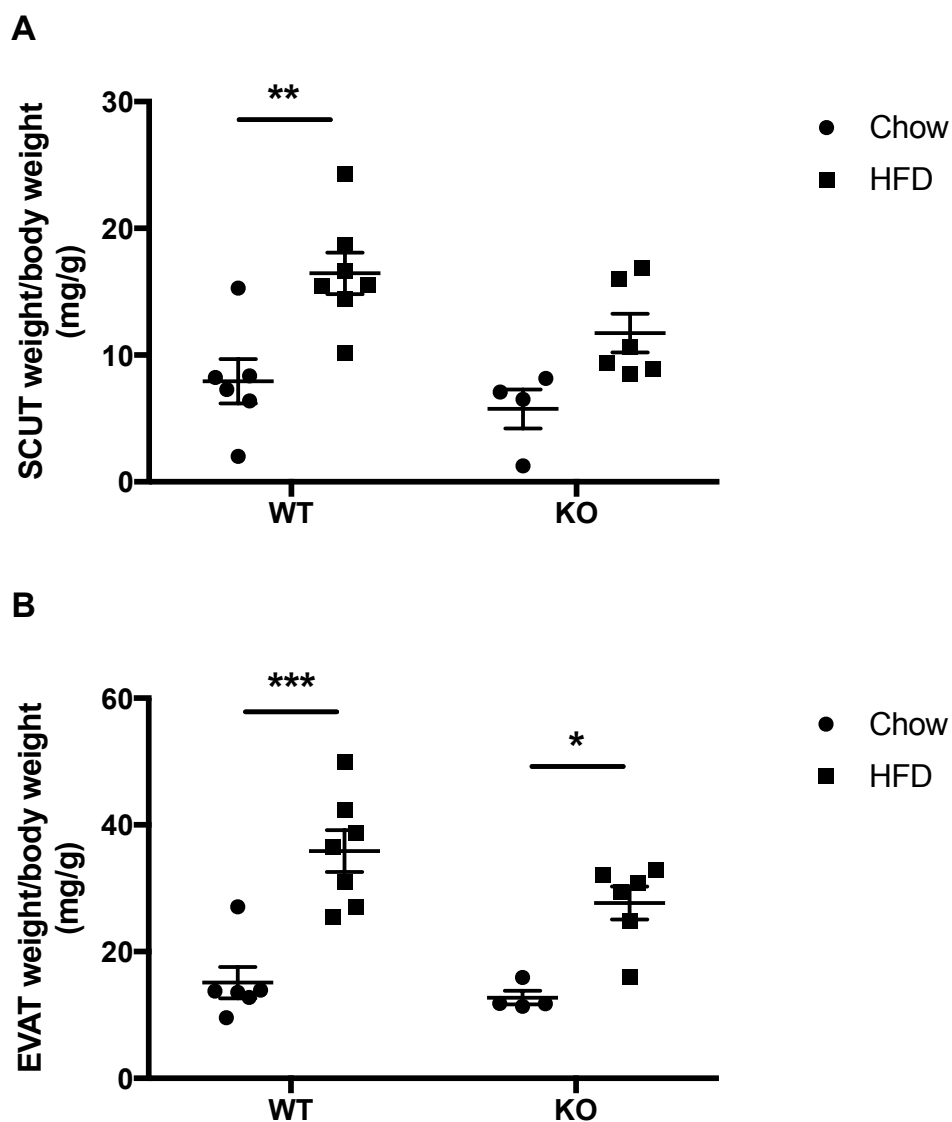
Figure 6.11 Adipose tissue weights

Inguinal subcutaneous (SCUT) and epididymal (EVAT) fat pads were collected and weighed following sacrifice. Weights corrected to body weight are presented for A. subcutaneous and B. epididymal adipose tissue depots. Two-way ANOVA, *p<0.05, **p<0.01, ***p<0.001. WT Chow n=6, WT HFD n=7, KO Chow n=4, KO HFD n=6.
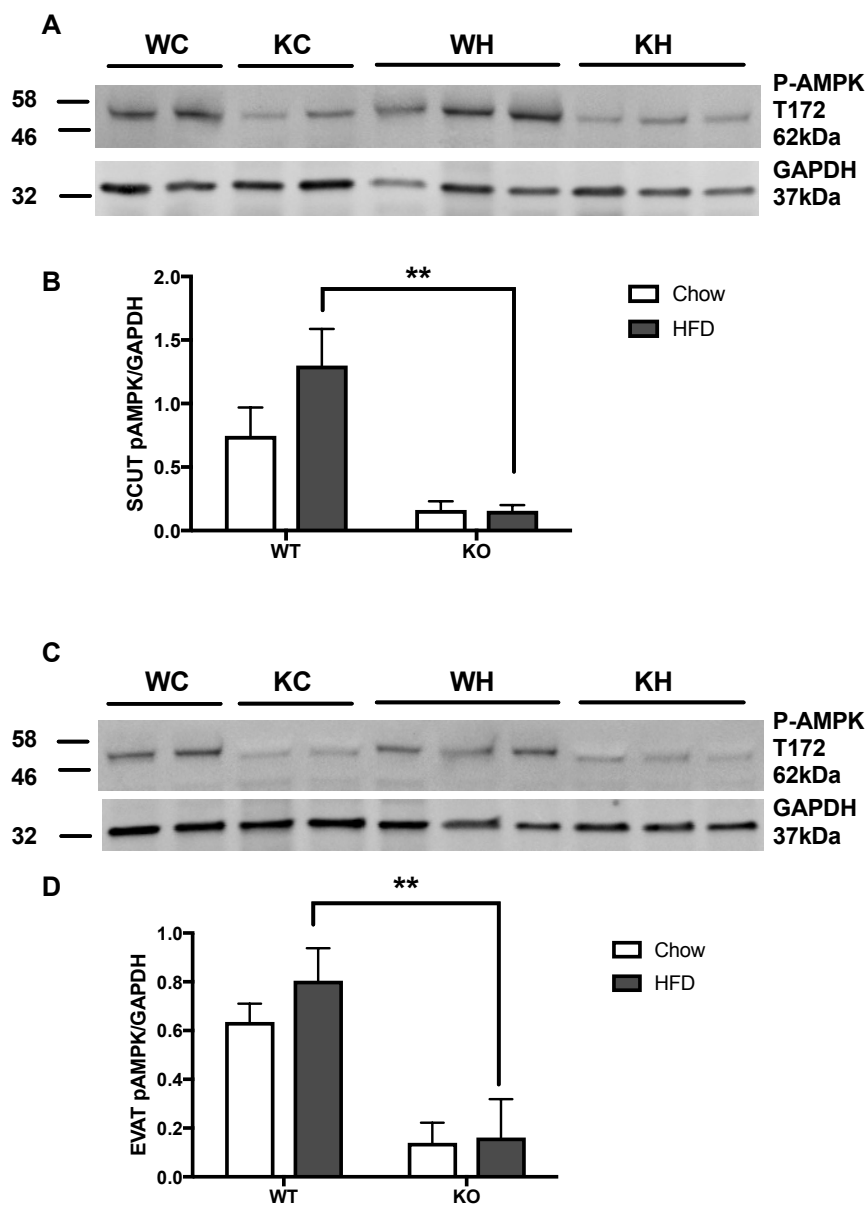
Figure 6.12 AMPK phosphorylation in adipose tissue following 12-week dietary intervention

SCUT (A. and B.) or EVAT (C. and D.) lysate proteins were resolved by SDS-PAGE and immunoblotted for the indicated proteins. A. and C. Representative immunoblots with the molecular masses of marker proteins (in kDa) shown. Quantification of P-AMPK relative to GAPDH for B. SCUT and D. EVAT. Two-way ANOVA, **p<0.01. WT Chow (WC) n=6, WT HFD (WH) n=6 (SCUT) or 7 (EVAT), KO Chow (KC) n=4, KO HFD (KH) n=6.
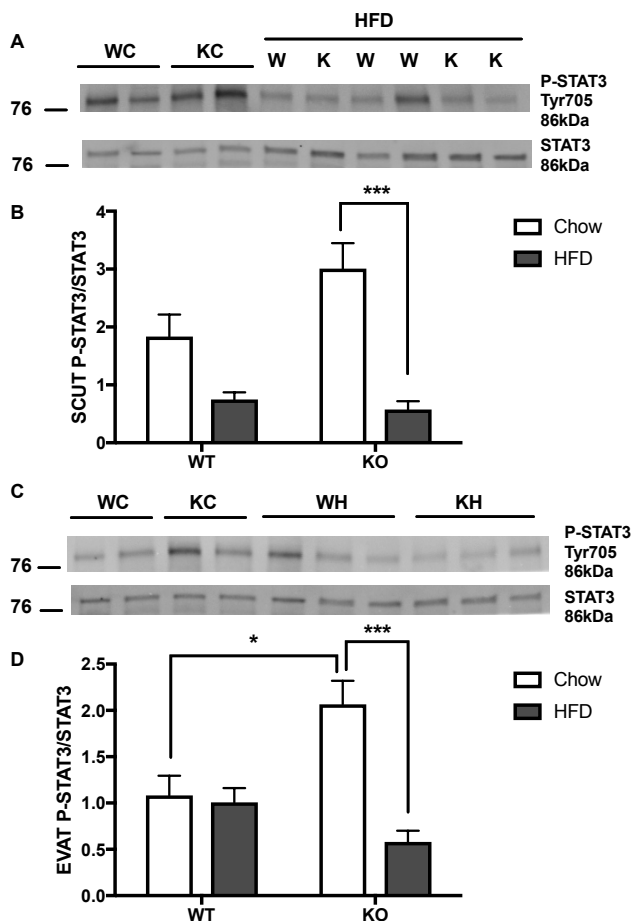
Figure 6.13 STAT3 phosphorylation in adipose tissue following 12-week dietary intervention

SCUT (A. and B.) or EVAT (C. and D.) lysate proteins were resolved by SDS-PAGE and immunoblotted for the indicated proteins. A. and C. Representative immunoblots with the molecular masses of marker proteins (in kDa) shown. Quantification of P-STAT3 relative to STAT3 for B. SCUT and D. EVAT. Two-way ANOVA, *p<0.05, ***p<0.001. WT Chow (WC) n=6, WT HFD (WH) n=3 (SCUT) or 7 (EVAT), KO Chow (KC) n=4, KO HFD (KH) n=6.
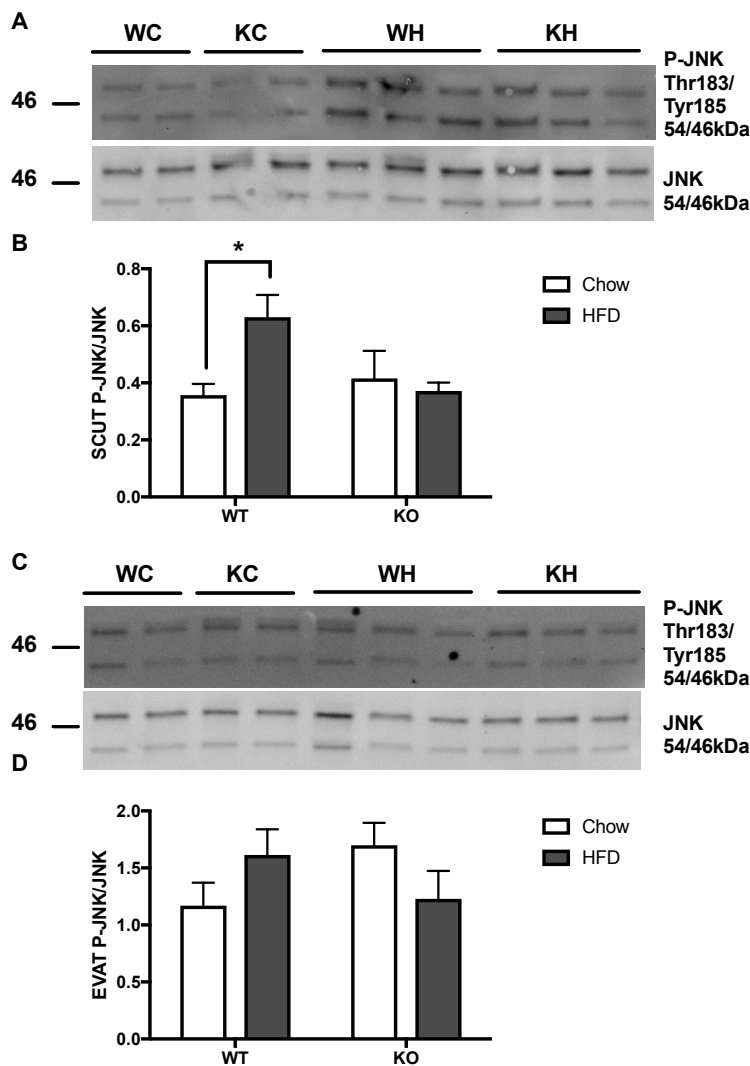
Figure 6.14 JNK phosphorylation in adipose tissue following 12-week dietary intervention

*SCUT (A. and B.) or EVAT (C. and D.) lysate proteins were resolved by SDS-PAGE and immunoblotted for the indicated proteins. A. and C. Representative immunoblots with the molecular masses of marker proteins (in kDa) shown. Quantification of P-JNK 54 relative to JNK 54 for B. SCUT and D. EVAT. Two-way ANOVA, *p<0.05. WT Chow (WC) n=6, WT HFD (WH) n=6 (SCUT) or 7 (EVAT), KO Chow (KC) n=4, KO HFD (KH) n=6.*

6.2.5.5 MR expression in adipose tissue

Previous reports have identified increased adipose tissue MR expression in obesity (Urbanet et al. 2015). MR protein levels were not significantly altered by genotype nor by dietary intake (Fig. 6.15) in this study however there was a trend towards increase with HFD.

6.2.5.6 Adiponectin expression in adipose tissue

Circulating levels of the insulin-sensitising adipokine adiponectin usually decrease with increased adiposity (Lara-Castro et al. 2007). As shown in figure 6.16, adipose tissue adiponectin protein levels tended to be higher in the HFD groups, particularly in SCUT of KO mice (p=0.055 vs chow).

6.2.5.7 MCP-1 expression in adipose tissue

Lastly, protein levels of the chemokine MCP-1 were determined in SCUT and EVAT. MCP-1 levels in SCUT were unchanged between the groups (Fig 6.17A). In EVAT however, MCP-1 levels were increased with HFD, a change which was more prominent in the WT mice (p=0.035) and did not reach statistical significance in KO mice (Fig. 6.17B).
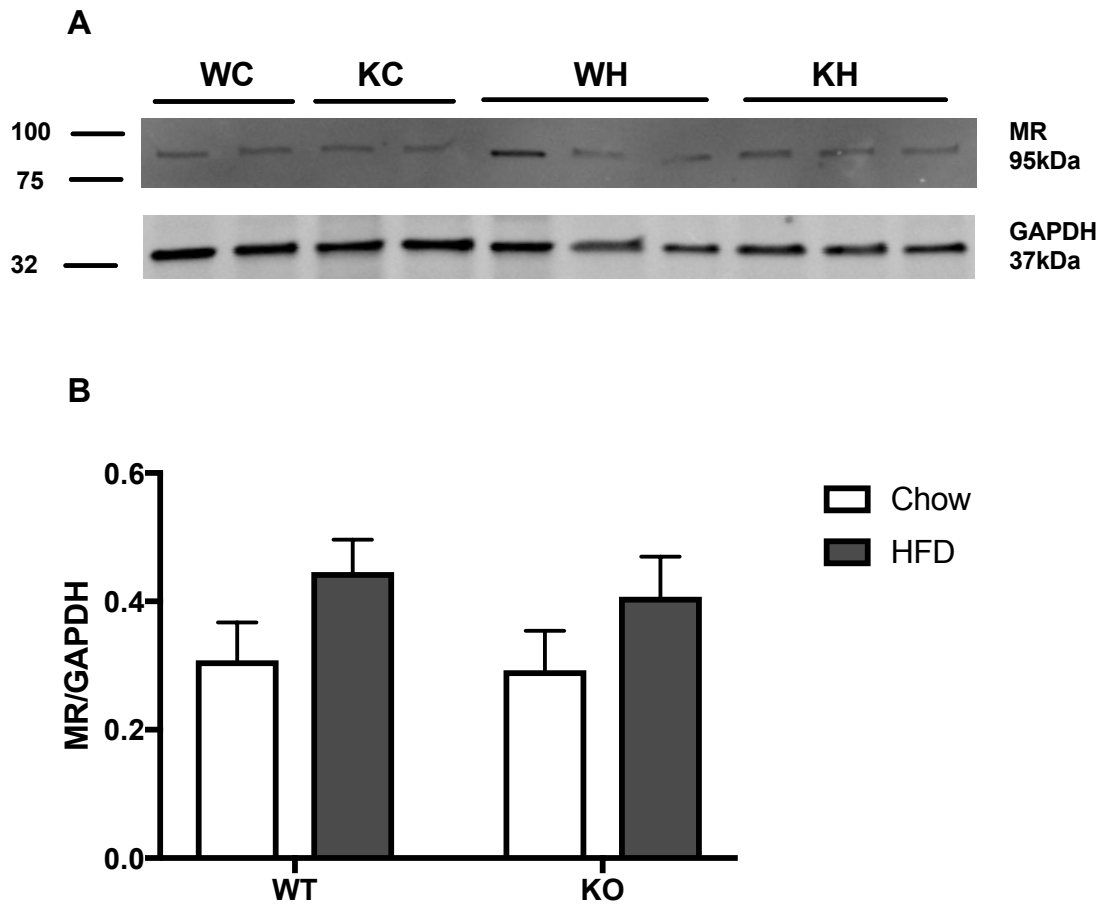
Figure 6.15 Expression of MR in adipose tissue following 12-week dietary intervention

EVAT lysate proteins were resolved by SDS-PAGE and immunoblotted for the indicated proteins. A. Representative immunoblots with the molecular masses of marker proteins (in kDa) shown. B. Quantification of MR relative to GAPDH. WT Chow (WC) n=6, WT HFD (WH) n= 7, KO Chow (KC) n=4, KO HFD (KH) n=6.
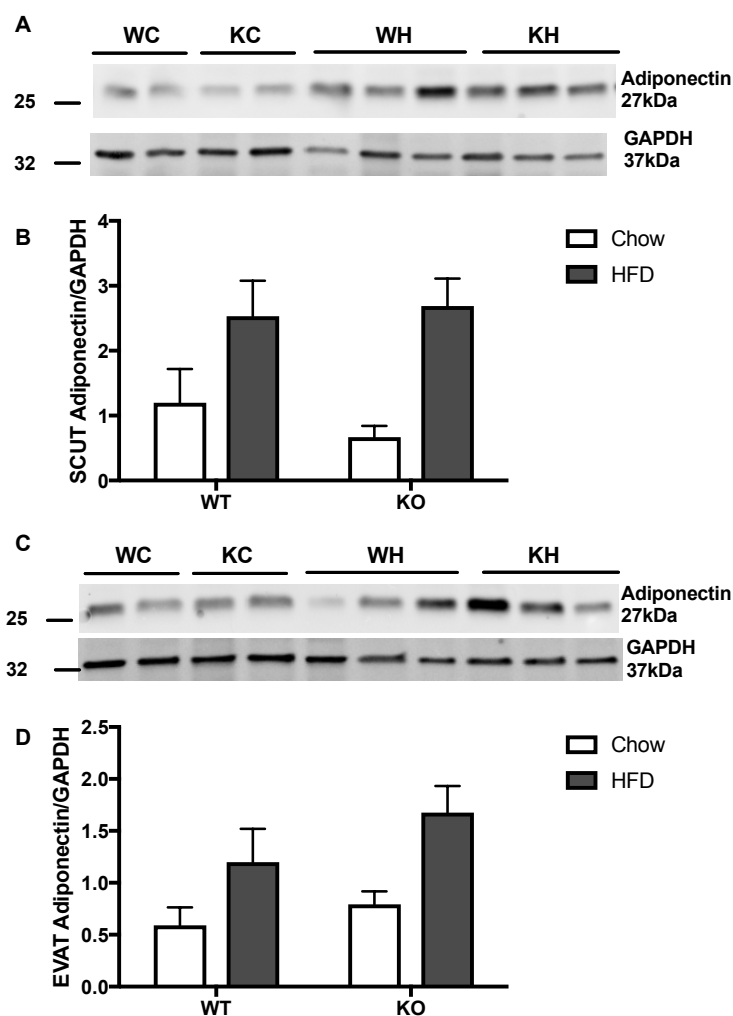
Figure 6.16 Expression of adiponectin in adipose tissue following 12-week dietary intervention

SCUT (A. and B.) or EVAT (C. and D.) lysate proteins were resolved by SDS-PAGE and immunoblotted for the indicated proteins. A. and C. Representative immunoblots with the molecular masses of marker proteins (in kDa) shown. Quantification of adiponectin relative to GAPDH for B. SCUT and D. EVAT. WT Chow (WC) n=6, WT HFD (WH) n=6 (SCUT) or 7 (EVAT), KO Chow (KC) n=4, KO HFD (KH) n=6.
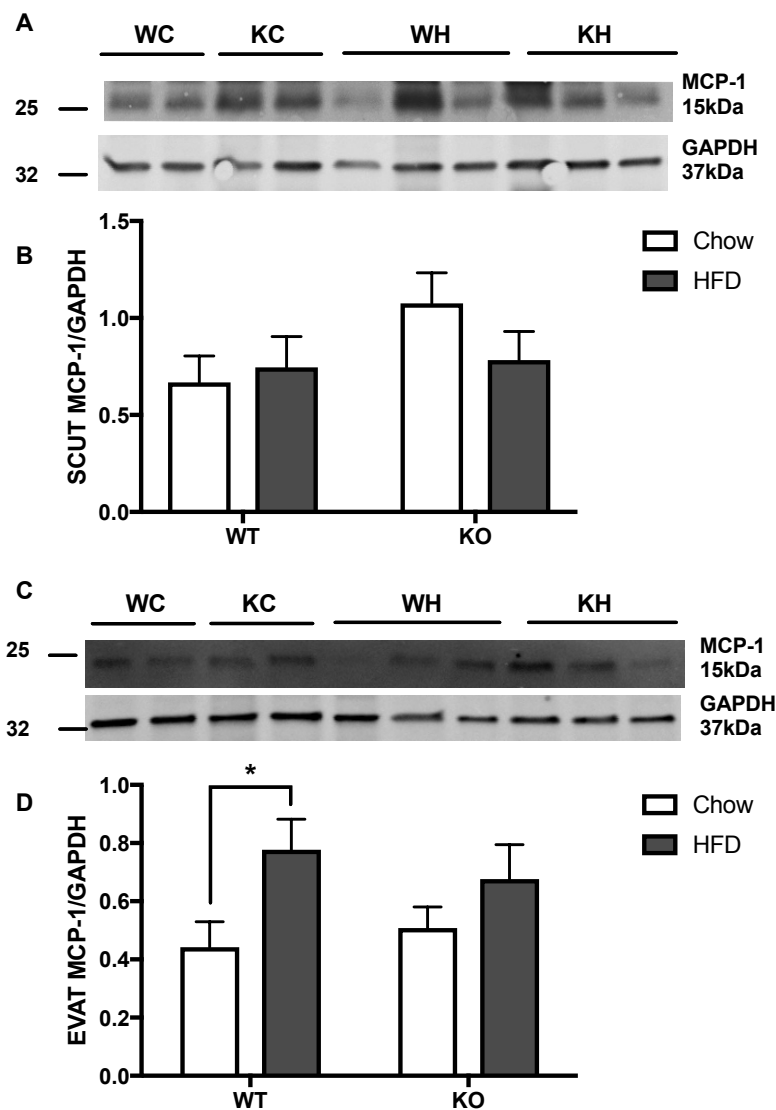
Figure 6.17 Expression of MCP-1 in adipose tissue following 12-week dietary intervention

*SCUT (A. and B.) or EVAT (C. and D.) lysate proteins were resolved by SDS-PAGE and immunoblotted for the indicated proteins. A. and C. Representative immunoblots with the molecular masses of marker proteins (in kDa) shown. Quantification of MCP-1 relative to GAPDH for B. SCUT and D. EVAT. T-test, *p<0.05. WT Chow (WC) n=6, WT HFD (WH) n=6 (SCUT) or 7 (EVAT), KO Chow (KC) n=4, KO HFD (KH) n=6. Repeat analysis with non-parametric test (Mann-Whitney) D. WC vs. WH p=0.0734.*

6.2.5.8 CXCL-10 gene expression in adipose tissue

As demonstrated in 5.2.2.3, CXCL-10 is secreted from adipocytes in response to pro-inflammatory stimuli such as IL-1ß. In this study, CXCL-10 mRNA levels in SCUT were not changed between genotype or dietary intervention (Fig. 6.18A). However, in EVAT it tended to increase with HFD in WT mice. There was also a trend for CXCL-10 mRNA levels to be higher in KO animals however when they were exposed to HFD the CXCL-10 mRNA levels decreased although RNA from only two KO mice fed HFD were analysed (Fig. 6.18B).

6.2.5.9 IL-1ß gene expression in adipose tissue

IL-1ß mRNA levels were determined in EVAT samples. Basal IL-1ß mRNA levels were increased in KO compared to WT mice (p=0.017) and there was a tendency for HFD to increase levels in WT EVAT (p=0.07) but not in KO mice where levels were unchanged (Fig 6.19).

6.2.5.10 Angiotensinogen gene expression in adipose tissue

The RAAS precursor angiotensinogen was increased in adipose tissue from insulin resistance obese individuals when compared to non-insulin resistant obese individuals (Xu et al. 2012). In this study however, there was a tendency for HFD to decrease SCUT angiotensinogen expression. This finding was most pronounced in KO mice yet the change did not reach statistical significance (p=0.08) (Fig 6.20).
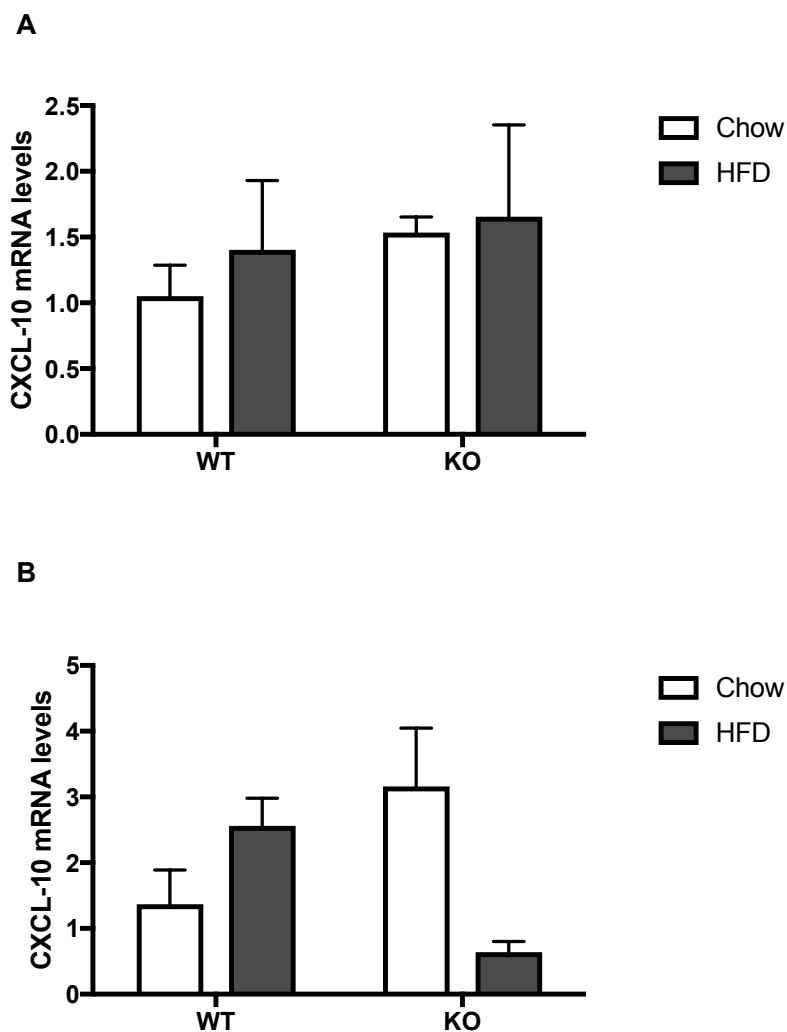
Figure 6.18 mRNA expression of CXCL-10 in adipose tissue following 12-week dietary intervention

RNA was extracted from A. SCUT or B. EVAT. Reverse transcription was carried out prior to Taqman qPCR assays for CXCL-10. Data are normalised to TATA-binding protein mRNA expression. A. SCUT: WT Chow n=6, WT HFD n=4 KO Chow n=4, KO HFD n=2. B. EVAT: WT Chow n=3, WT HFD n=6, KO Chow n=3, KO HFD n=6.
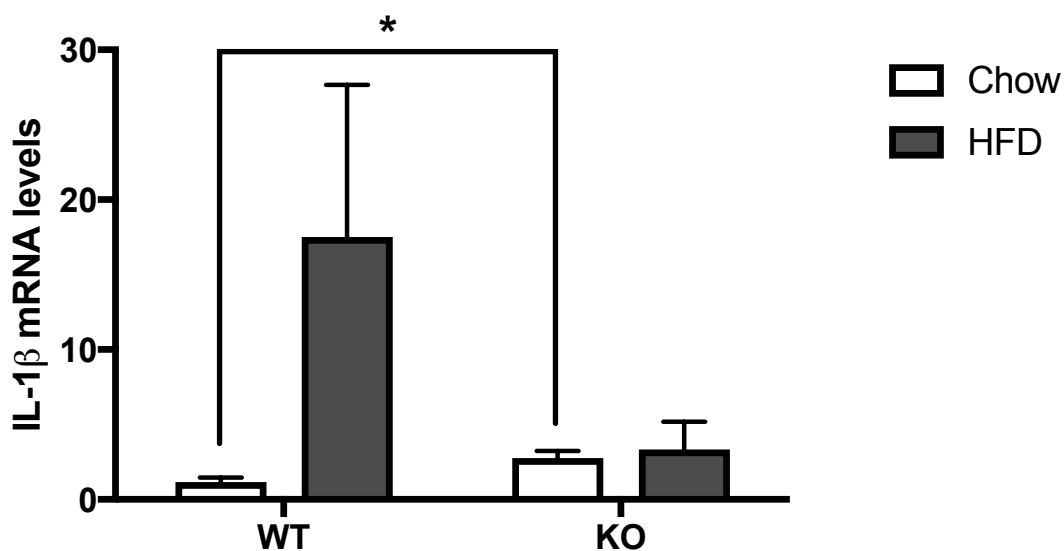
Figure 6.19 Expression of IL-1ß in adipose tissue following 12-week dietary intervention

RNA was extracted from EVAT samples. Reverse transcription was carried out prior to Taqman qPCR assays for IL-1ß. Data are normalised to TATA-binding protein mRNA expression. T-test *p<0.05. WT Chow n=6, WT HFD n=4 KO Chow n=4, KO HFD n=3.
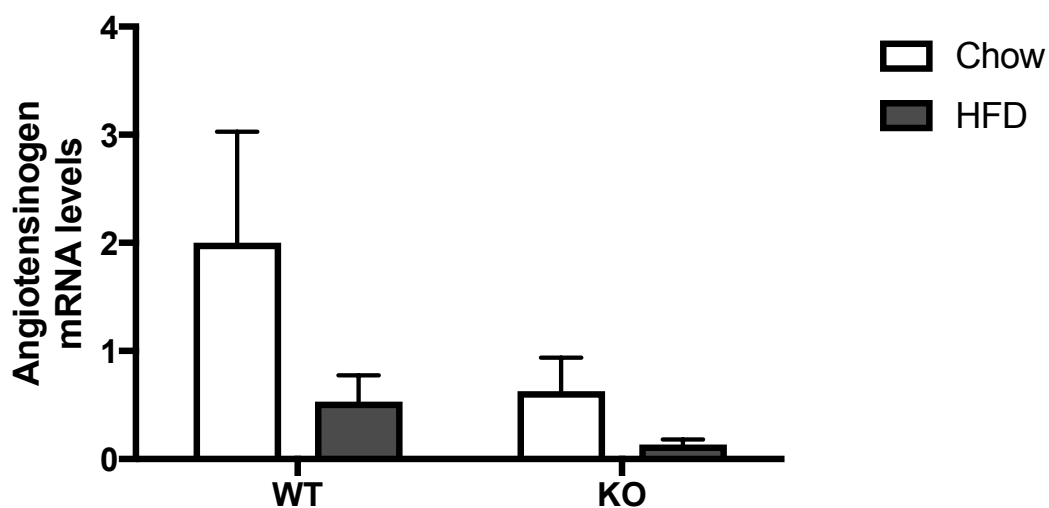
Figure 6.20 Expression of angiotensinogen in adipose tissue following 12-week dietary intervention

RNA was extracted from SCUT samples. Reverse transcription was carried out prior to Taqman qPCR assays for angiotensinogen. Data are normalised to TATA-binding protein mRNA expression. WT Chow n=6, WT HFD n=7, KO Chow n=4, KO HFD n=6.

6.3 Discussion

This chapter sought to identify the impact of HFD on mice with decreased AMPK activity in adipose tissue. The effects on systemic and adipose tissue specific parameters were examined in chow- and HFD-fed WT and AMPKα1 KO mice with a focus on inflammation and the RAAS.

In this study, WT and KO mice on HFD gained a similar percentage of body weight which was significantly more than those on chow diet. A tendency for the WT to gain more weight was observed and consistent with this the increased weight of EVAT and SCUT depots in WT reached higher degrees of significance than in KO mice where the SCUT depot did not significantly increase in weight.

Despite gaining weight and significantly expanding adipose tissue depots, no major glycaemic dysregulation was detected as a result of HFD. Intraperitoneal glucose tolerance testing showed similar glucose dynamics between the groups. At 15 minutes there was a significant decrease in the % glucose rise from baseline in the KO HFD group compared to the KO chow group. Suggesting a benefit of the high fat diet in the KO mice. Consistent with these findings, fasting blood glucose was lowest in the KO chow group and insulin was highest in the WT HFD group leading to a tendency for HOMA-IR to be highest in the WT HFD group. It certainly would have been anticipated that HFD would lead to impaired glucose tolerance however several factors can influence this response (Kleinert et al. 2018). It may be a consequence of the length of this study where longer exposure to the HFD would result in metabolic dysregulation. In addition, the Sv129 strain is known to be more resistant than others to diet-induced obesity and may explain the lack of response. (Xiao et al. 2017). It should be noted that it was not possible to integrate the C57/Bl6 background into the KO mice (Benoit Viollet, Institut Cochin, personal communication).

Fatty liver is an important metabolic consequence of obesity and can result in cirrhosis (Tilg & Hotamisligil, 2006). In this study, liver weight and triglyceride content increased in both HFD groups however there was no difference

between genotypes at baseline or following dietary intervention. Similarly, there was evidence of ectopic lipid deposition in both groups when liver section examined by H&E staining. The liver plays a key role in cholesterol synthesis. Here, the WT HFD group had a significantly higher serum cholesterol concentration than the chow-fed WT mice whilst the KO HFD mice did have a rise in cholesterol it did not reach statistical significance. Indeed it is very well described that in metabolic disorders when human adipose capacity becomes overwhelmed fatty liver can develop (Bertot et al. 2017). Given the known anti-steatotic effect of AMPK, it is interesting that there was not more steatosis evident in the KO mice, however as the liver would have normal functioning AMPKα2 this may well compensate for the lack of α1 (Smith et al. 2016, Woods et al. 2017).

This group and others have shown that activators of AMPK have anti-inflammatory properties in adipocytes (Shibata et al. 2013, Mancini et al. 2017). Here the effect of HFD on inflammatory mediators was examined in SCUT and EVAT depots which contain many cells types including adipocytes. Immunoblotting for phosphorylation of AMPK at Thr 172 found significantly less AMPK activity in KO mice, confirming the key role of AMPKα1 in adipose tissue where it is known to be the predominant catalytic isoform (Lihn et al. 2004, Daval et al. 2005). There was no difference in AMPK phosphorylation following HFD in SCUT or EVAT in WT mice, however we have shown that HFD decreased AMPK activity in perivascular adipose tissue from WT mice (Almabrouk et al. 2018). In WT mice HFD led to significant increases in adipose tissue JNK phosphorylation and MCP-1 protein whilst there was a tendency for increased IL-1β gene expression. These findings have previously been identified and are consistent with the pro-inflammatory effects of HFD and obesity (Cranford et al. 2016). Interestingly, STAT3 signalling was not increased with HFD in WT mice, but was increased in EVAT of KO chow mice compared to WT and most strikingly, this was decreased in response to HFD. In agreement with this, STAT3 signalling was increased in female gonadal and SCUT adipose tissue from KO mice compared to WT (Mancini et al. 2017). Similarly, JNK phosphorylation did not increase in response to HFD in KO mice. However, there was no difference between chow WT and KO adipose JNK phosphorylation, a difference which was observed in the gonadal adipose

of the female cohort (Mancini et al. 2017), this could be a gender difference. In a report of nicotine induced insulin resistance examining adipose specific AMPKα1 and AMPKα2 deletion, no difference was seen in basal JNK phosphorylation in white adipose tissue (Wu et al. 2015). In the present study there was a trend towards increased MCP-1 expression in KO chow compared to WT and again this tended to decrease with HFD. Considering the only difference in glucose tolerance observed was a decrease in 15 min incremental glucose in KO HFD compared to KO chow mice, the data suggest that KO mice fed a chow diet have a pro-inflammatory adipose tissue, when compared to WT mice, yet this is in some way improved in response to high fat diet. This finding is certainly intriguing if not confusing. This may explain the finding that adiponectin protein expression was highest in the KO mice on high fat diet, whereas others have reported lower adipose expression of adiponectin following this dietary intervention (Barnea et al. 2006). Adiponectin secretion from PVAT was decreased by HFD and decreased in KO mice despite no significant change in mRNA expression (Almabrouk et al. 2018). It may be that release of adiponectin, rather than production or storage, is the main alteration in response to HFD.

Upregulation of adipose RAAS in obesity is one potential mechanism underlying the pro-inflammatory changes in obesity giving rise to cardiometabolic disorders. In this study, the systemic RAAS was not significantly affected by HFD in WT mice. However, KO mice tended to have higher basal angiotensin II levels, and when exposed to HFD, KO mice had the highest levels of angiotensin I and II, aldosterone and renin activity. Although these findings were not statistically significant, likely due to low number of samples, there was a clear trend which suggests a relationship between decreased AMPK and increased RAAS. Certainly this would be consistent with findings in chapter 4 of this thesis. No significant changes in adipose tissue MR protein or angiotensinogen mRNA levels were identified between the groups studied here. Previous reports have shown that adipose MR is increased in obesity (Urbanet et al. 2015). Whilst angiotensinogen mRNA levels were increased in adipose tissue from insulin resistant obese individuals but not those who were insulin sensitive (Xu et al. 2012).

Whilst considering these findings it is important to note that rodent HFD studies can differ considerably in nature between constituent diet and duration of intervention. In this study a 42% calories from fat diet was used which may be considered as a modest % of fat, closer to the 30% fat intake of humans. Certainly studies commonly use 60% calories from fat or even higher (Kleinert et al. 2018). Additionally, some diets use a combination of fat and sugars to try and replicate diabetes more closely. Or employ an injection of streptozotocin to injure the pancreatic beta cells and make diabetes more likely (Kleinert et al. 2018). Longer duration of HFD is likely to induce a more marked metabolic injury and could be utilised to further study some of the changes identified in this cohort of mice. One must also be mindful of the global AMPKα1 knockout in these mice, there have been recent reports from mice with adipose specific knock down of different AMPK subunits including α1 which would be of interest to this work (Wu et al. 2015).

In conclusion, AMPKα1 deficient mice had no significant metabolic features basally, or when exposed to HFD. There was evidence of pro-inflammatory changes in the KO adipose tissue basally which intriguingly improved with HFD. However, the systemic RAAS appeared to be upregulated in the KO HFD group. Overall this draws more interest to the role of AMPK in adipose tissue and the development of metabolic disorders. Certainly, the paradoxical effect of improvements with HFD in the KO mice requires further exploration.

7 Chapter 7 - Discussion and summary

7.1 Discussion

Obesity is a major threat to the health of current and future generations with projected global rates of 18% in men and 21% in women by 2025 (NCD risk factor collaboration, 2016). Adipose tissue inflammation appears to be an important factor in the development of obesity-related insulin resistance which may lead to type 2 diabetes if not addressed. This work sought to identify a mechanism whereby a known metabolically active kinase, AMPK, could regulate the local RAAS in adipocytes/adipose tissue and determine the effects of RAAS on AMPK activity.

7.1.1 The effects of AMPK on adipocyte RAAS, inflammation and metabolism

One of the major findings in this study was downregulation of the adipocyte MR by AMPK activators. As the MR mediates metabolic effects of both mineralocorticoids and glucocorticoids in adipocytes and is reportedly increased in obese adipose tissue, the negative regulation by AMPK is an important and relevant new finding (Caprio et al. 2007, Hoppmann et al. 2010, Hirata et al. 2012, Lee and Fried 2014). It would be of interest to determine if similar effects were seen in other cell types including those relevant to renal and vascular tissues. Previous reports demonstrate that AMPK activation attenuates the pro-fibrotic effects of aldosterone however, do not assess the effect of AMPK on MR expression (Lee et al. 2013, Mummidi et al. 2016). Interestingly, the current work was not able to implicate aldosterone in metabolic dysfunction. Determining the effect of AMPK activation on MR expression in primary human adipocytes would strengthen this study. In keeping with the original hypothesis, this work also demonstrated that AICAR and A769662 affected expression of the angiotensin converting enzymes. AICAR decreased ACE gene expression and increased the ACE2:ACE ratio whilst A769662 increased ACE2 expression. However, it must also be considered that further investigation revealed that aldosterone secretion from adipocytes was increased by AICAR in 3T3-L1 adipocytes and A769662 in SW872 adipocytes. Adipose-derived aldosterone may have a role in the regulation of local vascular function which is of particular relevance for

nutrient delivery (Briones et al. 2012, Nguyen et al. 2018). However, when systemic RAAS was assessed *in vivo* there was a tendency for an increase in the AMPK KO mice, and in fact AMPK was downregulated in the context of prolonged AMPK activation in adipocytes which leads to the hypothesis that aldosterone secretion may be acting to negatively regulate AMPK levels within adipocytes, potentially via SGK1 and LKB1. Given the paucity of published data in relation to this area it is difficult to compare these findings to those previously reported. Indeed, the regulation of adipose MR is not well understood but it has been established that blockade of the MR improves metabolic function and cardiovascular outcomes for people with diabetes and therefore downregulation of the MR by AMPK activation is highly likely to be a beneficial thing.

There are now more specific AMPK activators available which have recently been used *in vivo* in primate and rodent models. PF-739 (non-selective) and PF-249 (ß1 activator) were compared to assess the impact on glycaemia in cynomolgus monkeys, with only the non-selective activator able to reduce glucose levels, through skeletal muscle dispersal, due to the predominance of ß2 in skeletal muscle compared to ß1 (Cokorinos et al. 2017). This study goes some way towards confirming the importance for skeletal muscle over the liver in glucose homeostasis. Another group assessed MK-8722, which activates all AMPK complexes, assessing its effect on diabetes in rhesus monkeys, it reduced HbA1c in 10 monkeys but increased it in 3 monkeys, these 3 monkeys exhibited the more severe glycaemic disturbance at baseline (Myers et al. 2017). In addition, they found that MK-8722 increased cardiac hypertrophy and glycogen storage in the heart which may have clinical implications if translated to humans (Myers et al. 2017). The most recent report, of PF-06409577 (ß1 activator), found benefits in rodents with hepatic steatosis and fibrosis and reported a decrease in cholesterol after 6 weeks treatment in monkeys. However, again as the ß1 expression is low in skeletal muscle in humans and primates this may explain the lack of glucose lowering effect (Esquejo et al. 2018). It would be of major interest to utilise these agents to assess the effect on adipose RAAS and inflammation in addition to glycaemic control in the context of obesity and diabetes. Ultimately, due to the ubiquitous expression of AMPK, tissue or cell targeted therapies would be the

optimal method of targeting adipose AMPK with the avoidance of potential adverse effects in the heart and hypothalamus. Certainly the use of adipose AMPK KO mice is beneficial for the characterisation of adipose-specific effects.

In this study, AMPKα1-/- mice did not exhibit any major metabolic phenotype, consistent with previous reports of AMPKα1-/- mice (Viollet et al. 2003). In the current work AMPKα1-/- mice exposed to HFD responded similarly to WT mice in terms of metabolic dysfunction and in fact were protected against some of the increases in markers of adipose inflammation seen in WT mice. However, there was a trend toward an increase in circulating RAAS in the AMPKα1-/- mice on HFD suggesting that despite a lack of metabolic disturbance, the RAAS was still upregulated. However, no change was seen in adipose tissue MR although isolated adipocytes were not examined and angiotensinogen expression tended to be reduced by HFD. It is possible that the background genotype of mouse or the length of dietary intervention may have influenced the outcomes of this work. Interestingly, data from adipose specific KO mice has recently revealed the role of adipose AMPK. Wu et al. demonstrated nicotine-induced insulin resistance and increased lipolysis in WT and adipose-specific α1 KO but not α2 KO mice. Suggesting that, although less abundant, the α2 subunit in adipose tissue is required for the pro-inflammatory effects of nicotine. This study also identified glucose intolerance in response to nicotine in WT and α1 KO but not α2 KO mice (Wu et al. 2015). In the current study the α1 deletion was global and therefore the systemic effects on metabolic processes must be considered relevant. This work would certainly be enhanced by the use of adipose specific AMPK KO mice with HFD to determine the effect on adipose RAAS, inflammation and systemic metabolism. In 2016, an inducible adipose specific AMPK KO of ß1 and ß2 deletion (adiponectin promoter) was found to have a major influence in brown adipose tissue function leading to cold intolerance in addition to steatosis and glucose intolerance in response to HFD. The mechanism was proposed to be due to impaired mitophagy leading to impaired mitochondrial function. Very interestingly, the authors did not find an effect of AMPK on lipolysis *in vivo* (Mottillo et al. 2016).

7.1.2 The effects of the RAAS on AMPK in adipocytes

This study set out to explore the pro-inflammatory effects of RAAS in adipocytes, however in the models used here, pro-inflammatory signalling with angiotensin II was not demonstrable despite previous reports of this available in the literature (Kalupahana et al. 2012). Alternately, there was a signal for AMPK activation by angiotensin II which may be AT2 receptor mediated. Angiotensin II was found to activate AMPK in skeletal muscle, yet decrease AMPK activity in cardiomyocytes and renal cells (Nagata et al. 2004, Stuck et al. 2008, Lee et al. 2013). In this report ang 1-7 also activated AMPK in adipocytes, yet had no effect on inflammatory processes or on insulin signalling. The AMPK activation, although relatively weak, appeared to be calcium and Mas receptor dependent. Given previous findings that AMPK decreased MR and increased aldosterone secretion from adipocytes, the effect of ang 1-7 on aldosterone secretion could be further explored and understanding if and how the alternative RAAS may regulate the classic RAAS through AMPK.

7.2 Limitations

This study focused on the actions of AMPK activators and components of the RAAS in cultured adipocytes. One significant limitation of adipocyte models is the lack of response to molecular biology techniques such as siRNA to manipulate protein function. Indeed, in our lab, attempts to up- or down-regulate AMPK genetically in terminally differentiated adipocytes have been unsuccessful. This project therefore utilised two different AMPK activators and the AMPK-/- MEFs to explore AMPKs actions as best as possible. Additional attempts were made to differentiate AMPK-/- MEFs into adipocytes however these also proved unsuccessful. Cultured adipocytes such as those used in this study have relatively uniform characteristics whereas adipocytes from different origin sites likely have unique behaviour depending on location as well as body weight and fitness of the individual they come from. It is therefore challenging to create a reliably translatable adipocyte cell model. As discussed above, this study employed a global AMPKα1-/- mouse model, an adipose tissue specific model would be preferable to elucidate the adipose

component of effects seen. Indeed as AMPK is expressed ubiquitously, and activation may have adverse effects in the hypothalamus and the heart, selective and tissue-targeted pharmacological therapies would be of great benefit. To date, targeting specific tissues in humans is not routine practice, in particular targeting cells so widespread as adipocytes may be of particular complexity.

7.3 Future work

This study has opened a number of lines for further investigation. One of the main points of interest would be to reproduce two of the principal findings, of AMPK activation on the MR and of ang 1-7 on AMPK activity, in isolated human adipocytes to determine the possible clinical relevance of this. Indeed the effect of A769662 on aldosterone secretion and SGK1 would be of great interest in isolated human adipocytes but also in an adrenal model to see if AMPK regulated adrenal aldosterone secretion. It would be prudent to assess the effect of AMPK activators on the secretion of a panel of steroids, not just focused on aldosterone. If there were an increase in glucocorticoid this may be relevant to the anti-inflammatory effects of AMPK activation. As mentioned above, the systemic use of AMPK activators in primate models and the adipose specific AMPK KO mice would certainly add weight to the current study. The systemic AMPK activators could be used in a primate study to determine the effect on adipose RAAS and inflammation in the context of diabetes and clarify the impact on systemic RAAS. Whilst the adipose specific models would be very useful to isolate effects on MR expression and inflammation in adipose tissue in addition to understanding the full metabolic impact of adipose AMPK. A possible clinical study may involve the use of metformin, which has been shown to activate AMPK in human adipose tissue, to determine whether MR is reduced in adipose tissue and assess the effects on adipose classic and alternative RAAS activity (Boyle et al. 2011).

It is not clear at this stage what the functional effects of ang 1-7-mediated AMPK activation are, however, whether it activates AMPK in other cell types, particularly those of the vasculature would be relevant. In addition, the

mechanism of activation has been tested using pharmacological inhibitors, genetic tools such as siRNA may be a way to confirm the observations here.

7.4 Summary

In summary, this study has demonstrated for the first time that the energy regulating kinase AMPK regulates the local adipose RAAS and that ang 1-7 is an AMPK activator in adipocytes. AMPKα1 may be involved in systemic RAAS regulation and does not protect against the effects of HFD. Future studies are required to improve our understanding of the therapeutic potential within this system given its relevance to the worldwide obesity crisis.

List of References

Abdou, H. S., Bergeron, F. & Tremblay, J. J. 2014. A cell-autonomous molecular cascade initiated by AMP-activated protein kinase represses steroidogenesis. Mol Cell Biol, 34(23), pp 4257-71.

Abuissa, H., Jones, P. G., Marso, S. P. & O'Keefe, J. H., Jr. 2005. Angiotensin-converting enzyme inhibitors or angiotensin receptor blockers for prevention of type 2 diabetes: a meta-analysis of randomized clinical trials. J Am Coll Cardiol, 46(5), pp 821-6.

Abuissa, H. & O'Keefe, J., Jr. 2008. The role of renin-angiotensin-aldosterone system-based therapy in diabetes prevention and cardiovascular and renal protection. Diabetes Obes Metab, 10(12), pp 1157-66.

Aguirre, V., Uchida, T., Yenush, L., Davis, R. & White, M. F. 2000. The c-Jun NH(2)-terminal kinase promotes insulin resistance during association with insulin receptor substrate-1 and phosphorylation of Ser(307). J Biol Chem, 275(12), pp 9047-54.

Almabrouk, T. A. M., White, A. D., Ugusman, A. B., Skiba, D. S., Katwan, O. J., Alganga, H., Guzik, T. J., Touyz, R. M., Salt, I. P. & Kennedy, S. 2018. High Fat Diet Attenuates the Anticontractile Activity of Aortic PVAT via a Mechanism Involving AMPK and Reduced Adiponectin Secretion. Front Physiol, 9(51.

Andreelli, F., Foretz, M., Knauf, C., Cani, P. D., Perrin, C., Iglesias, M. A., Pillot, B., Bado, A., Tronche, F., Mithieux, G., Vaulont, S., Burcelin, R. & Viollet, B. 2006. Liver adenosine monophosphate-activated kinase-alpha2 catalytic subunit is a key target for the control of hepatic glucose production by adiponectin and leptin but not insulin. Endocrinology, 147(5), pp 2432-41.

Asamizu, S., Urakaze, M., Kobashi, C., Ishiki, M., Norel Din, A. K., Fujisaka, S., Kanatani, Y., Bukahari, A., Senda, S., Suzuki, H., Yamazaki, Y., Iwata, M., Usui, I., Yamazaki, K., Ogawa, H., Kobayashi, M. & Tobe, K. 2009. Angiotensin

II enhances the increase in monocyte chemoattractant protein-1 production induced by tumor necrosis factor-{alpha} from 3T3-L1 preadipocytes. J Endocrinol, 202(2), pp 199-205.

Astapova, O. & Leff, T. 2012. Adiponectin and PPARgamma: cooperative and interdependent actions of two key regulators of metabolism. Vitam Horm, 90(143-62.

Banks, W. A. & Farrell, C. L. 2003. Impaired transport of leptin across the blood-brain barrier in obesity is acquired and reversible. Am J Physiol Endocrinol Metab, 285(1), pp E10-5.

Barnea, M., Shamay, A., Stark, A. H. & Madar, Z. 2006. A high-fat diet has a tissue-specific effect on adiponectin and related enzyme expression. Obesity (Silver Spring), 14(12), pp 2145-53.

Bashan, N., Kovsan, J., Kachko, I., Ovadia, H. & Rudich, A. 2009. Positive and negative regulation of insulin signaling by reactive oxygen and nitrogen species. Physiol Rev, 89(1), pp 27-71.

Bateman, A. 1997. The structure of a domain common to archaebacteria and the homocystinuria disease protein. Trends Biochem Sci, 22(1), pp 12-3.

Benziane, B., Bjornholm, M., Lantier, L., Viollet, B., Zierath, J. R. & Chibalin, A. V. 2009. AMP-activated protein kinase activator A-769662 is an inhibitor of the Na(+)-K(+)-ATPase. Am J Physiol Cell Physiol, 297(6), pp C1554-66.

Bijland, S., Mancini, S. J. & Salt, I. P. 2013. Role of AMP-activated protein kinase in adipose tissue metabolism and inflammation. Clin Sci (Lond), 124(8), pp 491-507.

Bindom, S. M., Hans, C. P., Xia, H., Boulares, A. H. & Lazartigues, E. 2010. Angiotensin I-converting enzyme type 2 (ACE2) gene therapy improves glycemic control in diabetic mice. Diabetes, 59(10), pp 2540-8.

Black, H. R., Davis, B., Barzilay, J., Nwachuku, C., Baimbridge, C., Marginean, H., Wright, J. T., Jr., Basile, J., Wong, N. D., Whelton, P., Dart, R. A., Thadani, U., Antihypertensive & Lipid-Lowering Treatment to Prevent Heart Attack, T. 2008. Metabolic and clinical outcomes in nondiabetic individuals with the metabolic syndrome assigned to chlorthalidone, amlodipine, or lisinopril as initial treatment for hypertension: a report from the Antihypertensive and Lipid-Lowering Treatment to Prevent Heart Attack Trial (ALLHAT). Diabetes Care, 31(2), pp 353-60.

Bluher, M. 2012. Clinical relevance of adipokines. Diabetes Metab J, 36(5), pp 317-27.

Boyle, J. G., Logan, P. J., Ewart, M. A., Reihill, J. A., Ritchie, S. A., Connell, J. M., Cleland, S. J. & Salt, I. P. 2008. Rosiglitazone stimulates nitric oxide synthesis in human aortic endothelial cells via AMP-activated protein kinase. J Biol Chem, 283(17), pp 11210-7.

Boyle, J. G., Logan, P. J., Jones, G. C., Small, M., Sattar, N., Connell, J. M., Cleland, S. J. & Salt, I. P. 2011. AMP-activated protein kinase is activated in adipose tissue of individuals with type 2 diabetes treated with metformin: a randomised glycaemia-controlled crossover study. Diabetologia, 54(7), pp 1799-809.

Boyle, J. G., Salt, I. P. & McKay, G. A. 2010. Metformin action on AMP-activated protein kinase: a translational research approach to understanding a potential new therapeutic target. Diabet Med, 27(10), pp 1097-106.

Breton, C. 2013. The hypothalamus-adipose axis is a key target of developmental programming by maternal nutritional manipulation. J Endocrinol, 216(2), pp R19-31.

Briones, A. M., Nguyen Dinh Cat, A., Callera, G. E., Yogi, A., Burger, D., He, Y., Correa, J. W., Gagnon, A. M., Gomez-Sanchez, C. E., Gomez-Sanchez, E. P., Sorisky, A., Ooi, T. C., Ruzicka, M., Burns, K. D. & Touyz, R. M. 2012.

Adipocytes produce aldosterone through calcineurin-dependent signaling pathways: implications in diabetes mellitus-associated obesity and vascular dysfunction. Hypertension, 59(5), pp 1069-78.

Brown, M. S. & Goldstein, J. L. 2008. Selective versus total insulin resistance: a pathogenic paradox. Cell Metab, 7(2), pp 95-6.

Campbell, D. J. & Habener, J. F. 1987. Cellular localization of angiotensinogen gene expression in brown adipose tissue and mesentery: quantification of messenger ribonucleic acid abundance using hybridization in situ. Endocrinology, 121(5), pp 1616-26.

Caprio, M., Feve, B., Claes, A., Viengchareun, S., Lombes, M. & Zennaro, M. C. 2007. Pivotal role of the mineralocorticoid receptor in corticosteroid-induced adipogenesis. FASEB J, 21(9), pp 2185-94.

Carey, R. M. 2007. Angiotensin receptors and aging. Hypertension, 50(1), pp 33-4.

Ceddia, R. B. 2013. The role of AMP-activated protein kinase in regulating white adipose tissue metabolism. Mol Cell Endocrinol, 366(2), pp 194-203.

Chabowski, A., Coort, S. L., Calles-Escandon, J., Tandon, N. N., Glatz, J. F., Luiken, J. J. & Bonen, A. 2005. The subcellular compartmentation of fatty acid transporters is regulated differently by insulin and by AICAR. FEBS Lett, 579(11), pp 2428-32.

Cheatham, B., Vlahos, C. J., Cheatham, L., Wang, L., Blenis, J. & Kahn, C. R. 1994. Phosphatidylinositol 3-kinase activation is required for insulin stimulation of pp70 S6 kinase, DNA synthesis, and glucose transporter translocation. Mol Cell Biol, 14(7), pp 4902-11.

Chen, R., Feng, Y., Wu, J., Song, Y., Li, H., Shen, Q., Li, D., Zhang, J., Lu, Z., Xiao, H. & Zhang, Y. 2018. Metformin attenuates angiotensin II-induced

TGFbeta1 expression by targeting hepatocyte nuclear factor-4-alpha. Br J Pharmacol, 175(8), pp 1217-1229.

Chen, S. & Mackintosh, C. 2009. Differential regulation of NHE1 phosphorylation and glucose uptake by inhibitors of the ERK pathway and p90RSK in 3T3-L1 adipocytes. Cell Signal, 21(12), pp 1984-93.

Chu, K. Y., Lau, T., Carlsson, P. O. & Leung, P. S. 2006. Angiotensin II type 1 receptor blockade improves beta-cell function and glucose tolerance in a mouse model of type 2 diabetes. Diabetes, 55(2), pp 367-74.

Cildir, G., Akincilar, S. C. & Tergaonkar, V. 2013. Chronic adipose tissue inflammation: all immune cells on the stage. Trends Mol Med, 19(8), pp 487-500.

Cinti, S., Mitchell, G., Barbatelli, G., Murano, I., Ceresi, E., Faloia, E., Wang, S., Fortier, M., Greenberg, A. S. & Obin, M. S. 2005. Adipocyte death defines macrophage localization and function in adipose tissue of obese mice and humans. J Lipid Res, 46(11), pp 2347-55.

Clarke, M., Ewart, M. A., Santy, L. C., Prekeris, R. & Gould, G. W. 2006. ACRP30 is secreted from 3T3-L1 adipocytes via a Rab11-dependent pathway. Biochem Biophys Res Commun, 342(4), pp 1361-7.

Cokorinos, E. C., Delmore, J., Reyes, A. R., Albuquerque, B., Kjobsted, R., Jorgensen, N. O., Tran, J. L., Jatkar, A., Cialdea, K., Esquejo, R. M., Meissen, J., Calabrese, M. F., Cordes, J., Moccia, R., Tess, D., Salatto, C. T., Coskran, T. M., Opsahl, A. C., Flynn, D., Blatnik, M., Li, W., Kindt, E., Foretz, M., Viollet, B., Ward, J., Kurumbail, R. G., Kalgutkar, A. S., Wojtaszewski, J. F. P., Cameron, K. O. & Miller, R. A. 2017. Activation of Skeletal Muscle AMPK Promotes Glucose Disposal and Glucose Lowering in Non-human Primates and Mice. Cell Metab, 25(5), pp 1147-1159 e10.

Coleman, R. A. & Lee, D. P. 2004. Enzymes of triacylglycerol synthesis and their regulation. Prog Lipid Res, 43(2), pp 134-76.

Collaboration, N. C. D. R. F. 2016. Worldwide trends in diabetes since 1980: a pooled analysis of 751 population-based studies with 4.4 million participants. Lancet, 387(10027), pp 1513-30.

Collins, S., Cao, W. & Robidoux, J. 2004. Learning new tricks from old dogs: beta-adrenergic receptors teach new lessons on firing up adipose tissue metabolism. Mol Endocrinol, 18(9), pp 2123-31.

Connell, J. M., MacKenzie, S. M., Freel, E. M., Fraser, R. & Davies, E. 2008. A lifetime of aldosterone excess: long-term consequences of altered regulation of aldosterone production for cardiovascular function. Endocr Rev, 29(2), pp 133-54.

Cool, B., Zinker, B., Chiou, W., Kifle, L., Cao, N., Perham, M., Dickinson, R., Adler, A., Gagne, G., Iyengar, R., Zhao, G., Marsh, K., Kym, P., Jung, P., Camp, H. S. & Frevert, E. 2006. Identification and characterization of a small molecule AMPK activator that treats key components of type 2 diabetes and the metabolic syndrome. Cell Metab, 3(6), pp 403-16.

Copps, K. D. & White, M. F. 2012. Regulation of insulin sensitivity by serine/threonine phosphorylation of insulin receptor substrate proteins IRS1 and IRS2. Diabetologia, 55(10), pp 2565-2582.

Cranford, T. L., Enos, R. T., Velazquez, K. T., McClellan, J. L., Davis, J. M., Singh, U. P., Nagarkatti, M., Nagarkatti, P. S., Robinson, C. M. & Murphy, E. A. 2016. Role of MCP-1 on inflammatory processes and metabolic dysfunction following high-fat feedings in the FVB/N strain. Int J Obes (Lond), 40(5), pp 844-51.

Czech, M. P., Tencerova, M., Pedersen, D. J. & Aouadi, M. 2013. Insulin signalling mechanisms for triacylglycerol storage. Diabetologia, 56(5), pp 949-64.

Danaei, G., Finucane, M. M., Lu, Y., Singh, G. M., Cowan, M. J., Paciorek, C. J., Lin, J. K., Farzadfar, F., Khang, Y. H., Stevens, G. A., Rao, M., Ali, M. K., Riley, L. M., Robinson, C. A., Ezzati, M. & Global Burden of Metabolic Risk Factors of Chronic Diseases Collaborating, G. 2011. National, regional, and global trends in fasting plasma glucose and diabetes prevalence since 1980: systematic analysis of health examination surveys and epidemiological studies with 370 country-years and 2.7 million participants. Lancet, 378(9785), pp 31-40.

Daval, M., Diot-Dupuy, F., Bazin, R., Hainault, I., Viollet, B., Vaulont, S., Hajduch, E., Ferre, P. & Foufelle, F. 2005. Anti-lipolytic action of AMP-activated protein kinase in rodent adipocytes. J Biol Chem, 280(26), pp 25250-7.

Denes, A., Drake, C., Stordy, J., Chamberlain, J., McColl, B. W., Gram, H., Crossman, D., Francis, S., Allan, S. M. & Rothwell, N. J. 2012. Interleukin-1 mediates neuroinflammatory changes associated with diet-induced atherosclerosis. J Am Heart Assoc, 1(3), pp e002006.

Denver, R. J., Bonett, R. M. & Boorse, G. C. 2011. Evolution of leptin structure and function. Neuroendocrinology, 94(1), pp 21-38.

Diamond-Stanic, M. K. & Henriksen, E. J. 2010. Direct inhibition by angiotensin II of insulin-dependent glucose transport activity in mammalian skeletal muscle involves a ROS-dependent mechanism. Arch Physiol Biochem, 116(2), pp 88-95.

Diez, J. J. & Iglesias, P. 2003. The role of the novel adipocyte-derived hormone adiponectin in human disease. Eur J Endocrinol, 148(3), pp 293-300.

Donoghue, M., Hsieh, F., Baronas, E., Godbout, K., Gosselin, M., Stagliano, N., Donovan, M., Woolf, B., Robison, K., Jeyaseelan, R., Breitbart, R. E. & Acton, S. 2000. A novel angiotensin-converting enzyme-related carboxypeptidase (ACE2) converts angiotensin I to angiotensin 1-9. Circ Res, 87(5), pp E1-9.

Duan, Q., Song, P., Ding, Y. & Zou, M. H. 2017. Activation of AMP-activated protein kinase by metformin ablates angiotensin II-induced endoplasmic reticulum stress and hypertension in mice in vivo. Br J Pharmacol, 174(13), pp 2140-2151.

Eguchi, K., Tomizawa, H., Ishikawa, J., Hoshide, S., Numao, T., Fukuda, T., Shimada, K. & Kario, K. 2007. Comparison of the effects of pioglitazone and metformin on insulin resistance and hormonal markers in patients with impaired glucose tolerance and early diabetes. Hypertens Res, 30(1), pp 23-30.

El Mabrouk, M., Touyz, R. M. & Schiffrin, E. L. 2001. Differential ANG II-induced growth activation pathways in mesenteric artery smooth muscle cells from SHR. Am J Physiol Heart Circ Physiol, 281(1), pp H30-9.

Engeli, S., Bohnke, J., Gorzelniak, K., Janke, J., Schling, P., Bader, M., Luft, F. C. & Sharma, A. M. 2005. Weight loss and the renin-angiotensin-aldosterone system. Hypertension, 45(3), pp 356-62.

Esquejo, R. M., Salatto, C. T., Delmore, J., Albuquerque, B., Reyes, A., Shi, Y., Moccia, R., Cokorinos, E., Peloquin, M., Monetti, M., Barricklow, J., Bollinger, E., Smith, B. K., Day, E. A., Nguyen, C., Geoghegan, K. F., Kreeger, J. M., Opsahl, A., Ward, J., Kalgutkar, A. S., Tess, D., Butler, L., Shirai, N., Osborne, T. F., Steinberg, G. R., Birnbaum, M. J., Cameron, K. O. & Miller, R. A. 2018. Activation of Liver AMPK with PF-06409577 Corrects NAFLD and Lowers Cholesterol in Rodent and Primate Preclinical Models. EBioMedicine, 31(122-132).

Esser, N., Legrand-Poels, S., Piette, J., Scheen, A. J. & Paquot, N. 2014. Inflammation as a link between obesity, metabolic syndrome and type 2 diabetes. Diabetes Res Clin Pract, 105(2), pp 141-50.

Ewart, M. A., Clarke, M., Kane, S., Chamberlain, L. H. & Gould, G. W. 2005. Evidence for a role of the exocyst in insulin-stimulated Glut4 trafficking in 3T3-L1 adipocytes. J Biol Chem, 280(5), pp 3812-6.

Farooqi, I. S. 2002. Leptin and the onset of puberty: insights from rodent and human genetics. Semin Reprod Med, 20(2), pp 139-44.

Farooqi, I. S., Matarese, G., Lord, G. M., Keogh, J. M., Lawrence, E., Agwu, C., Sanna, V., Jebb, S. A., Perna, F., Fontana, S., Lechler, R. I., DePaoli, A. M. & O'Rahilly, S. 2002. Beneficial effects of leptin on obesity, T cell hyporesponsiveness, and neuroendocrine/metabolic dysfunction of human congenital leptin deficiency. J Clin Invest, 110(8), pp 1093-103.

Fisher-Wellman, K. H. & Neufer, P. D. 2012. Linking mitochondrial bioenergetics to insulin resistance via redox biology. Trends Endocrinol Metab, 23(3), pp 142-53.

Fliers, E., Kreier, F., Voshol, P. J., Havekes, L. M., Sauerwein, H. P., Kalsbeek, A., Buijs, R. M. & Romijn, J. A. 2003. White adipose tissue: getting nervous. J Neuroendocrinol, 15(11), pp 1005-10.

Flores-Munoz, M., Work, L. M., Douglas, K., Denby, L., Dominiczak, A. F., Graham, D. & Nicklin, S. A. 2012. Angiotensin-(1-9) attenuates cardiac fibrosis in the stroke-prone spontaneously hypertensive rat via the angiotensin type 2 receptor. Hypertension, 59(2), pp 300-7.

Foller, M., Sopjani, M., Koka, S., Gu, S., Mahmud, H., Wang, K., Floride, E., Schleicher, E., Schulz, E., Munzel, T. & Lang, F. 2009. Regulation of erythrocyte survival by AMP-activated protein kinase. FASEB J, 23(4), pp 1072-80.

Fredrikson, G., Tornqvist, H. & Belfrage, P. 1986. Hormone-sensitive lipase and monoacylglycerol lipase are both required for complete degradation of adipocyte triacylglycerol. Biochim Biophys Acta, 876(2), pp 288-93.

Fried, S. K., Bunkin, D. A. & Greenberg, A. S. 1998. Omental and subcutaneous adipose tissues of obese subjects release interleukin-6: depot difference and regulation by glucocorticoid. J Clin Endocrinol Metab, 83(3), pp 847-50.

Gaidhu, M. P., Perry, R. L., Noor, F. & Ceddia, R. B. 2010. Disruption of AMPKalpha1 signaling prevents AICAR-induced inhibition of AS160/TBC1D4 phosphorylation and glucose uptake in primary rat adipocytes. Mol Endocrinol, 24(7), pp 1434-40.

Gao, Z., Hwang, D., Bataille, F., Lefevre, M., York, D., Quon, M. J. & Ye, J. 2002. Serine phosphorylation of insulin receptor substrate 1 by inhibitor kappa B kinase complex. J Biol Chem, 277(50), pp 48115-21.

Giani, J. F., Mayer, M. A., Munoz, M. C., Silberman, E. A., Hocht, C., Taira, C. A., Gironacci, M. M., Turyn, D. & Dominici, F. P. 2009. Chronic infusion of angiotensin-(1-7) improves insulin resistance and hypertension induced by a high-fructose diet in rats. Am J Physiol Endocrinol Metab, 296(2), pp E262-71.

Gibbs, E. M., Lienhard, G. E. & Gould, G. W. 1988. Insulin-induced translocation of glucose transporters to the plasma membrane precedes full stimulation of hexose transport. Biochemistry, 27(18), pp 6681-5.

Glass, C. K. & Olefsky, J. M. 2012. Inflammation and lipid signaling in the etiology of insulin resistance. Cell Metab, 15(5), pp 635-45.

Goirand, F., Solar, M., Athea, Y., Viollet, B., Mateo, P., Fortin, D., Leclerc, J., Hoerter, J., Ventura-Clapier, R. & Garnier, A. 2007. Activation of AMP kinase alpha1 subunit induces aortic vasorelaxation in mice. J Physiol, 581(Pt 3), pp 1163-71.

Goossens, G. H. 2012. The renin-angiotensin system in the pathophysiology of type 2 diabetes. Obes Facts, 5(4), pp 611-24.

Group, A. C. E. I. i. D. N. T. 2001. Should all patients with type 1 diabetes mellitus and microalbuminuria receive angiotensin-converting enzyme inhibitors? A meta-analysis of individual patient data. Ann Intern Med, 134(5), pp 370-9.

Guennoun, A., Kazantzis, M., Thomas, R., Wabitsch, M., Tews, D., Seetharama Sastry, K., Abdelkarim, M., Zilberfarb, V., Strosberg, A. D. & Chouchane, L. 2015. Comprehensive molecular characterization of human adipocytes reveals a transient brown phenotype. J Transl Med, 13(135.

Guigas, B., Sakamoto, K., Taleux, N., Reyna, S. M., Musi, N., Viollet, B. & Hue, L. 2009. Beyond AICA riboside: in search of new specific AMP-activated protein kinase activators. IUBMB Life, 61(1), pp 18-26.

Guilherme, A., Virbasius, J. V., Puri, V. & Czech, M. P. 2008. Adipocyte dysfunctions linking obesity to insulin resistance and type 2 diabetes. Nat Rev Mol Cell Biol, 9(5), pp 367-77.

Guo, C., Yuan, L., Liu, X., Du, A., Huang, Y. & Zhang, L. 2008. Effect of ARB on expression of CD68 and MCP-1 in adipose tissue of rats on long-term high fat diet. J Huazhong Univ Sci Technolog Med Sci, 28(3), pp 257-60.

Gustafson, B. 2010. Adipose tissue, inflammation and atherosclerosis. J Atheroscler Thromb, 17(4), pp 332-41.

Haider, S. & Knofler, M. 2009. Human tumour necrosis factor: physiological and pathological roles in placenta and endometrium. Placenta, 30(2), pp 111-23.

Handa, M., Vanegas, S., Maddux, B. A., Mendoza, N., Zhu, S., Goldfine, I. D. & Mirza, A. M. 2013. XOMA 052, an anti-IL-1beta monoclonal antibody, prevents IL-1beta-mediated insulin resistance in 3T3-L1 adipocytes. Obesity (Silver Spring), 21(2), pp 306-9.

Hardie, D. G. 1989. Regulation of fatty acid synthesis via phosphorylation of acetyl-CoA carboxylase. Prog Lipid Res, 28(2), pp 117-46.

Hardie, D. G. 2003. Minireview: the AMP-activated protein kinase cascade: the key sensor of cellular energy status. Endocrinology, 144(12), pp 5179-83.

Hardie, D. G. 2008. AMPK: a key regulator of energy balance in the single cell and the whole organism. Int J Obes (Lond), 32 Suppl 4(S7-12.

Hardie, D. G., Ross, F. A. & Hawley, S. A. 2012. AMPK: a nutrient and energy sensor that maintains energy homeostasis. Nat Rev Mol Cell Biol, 13(4), pp 251-62.

Harte, A. L., McTernan, P. G., McTernan, C. L., Crocker, J., Starcynski, J., Barnett, A. H., Matyka, K. & Kumar, S. 2003. Insulin increases angiotensinogen expression in human abdominal subcutaneous adipocytes. Diabetes Obes Metab, 5(6), pp 462-7.

Hattangady, N. G., Olala, L. O., Bollag, W. B. & Rainey, W. E. 2012. Acute and chronic regulation of aldosterone production. Mol Cell Endocrinol, 350(2), pp 151-62.

Hawley, S. A., Fullerton, M. D., Ross, F. A., Schertzer, J. D., Chevtzoff, C., Walker, K. J., Peggie, M. W., Zibrova, D., Green, K. A., Mustard, K. J., Kemp, B. E., Sakamoto, K., Steinberg, G. R. & Hardie, D. G. 2012. The ancient drug salicylate directly activates AMP-activated protein kinase. Science, 336(6083), pp 918-22.

Hawley, S. A., Pan, D. A., Mustard, K. J., Ross, L., Bain, J., Edelman, A. M., Frenguelli, B. G. & Hardie, D. G. 2005. Calmodulin-dependent protein kinase kinase-beta is an alternative upstream kinase for AMP-activated protein kinase. Cell Metab, 2(1), pp 9-19.

Hawley, S. A., Ross, F. A., Chevtzoff, C., Green, K. A., Evans, A., Fogarty, S., Towler, M. C., Brown, L. J., Ogunbayo, O. A., Evans, A. M. & Hardie, D. G.

2010. Use of cells expressing gamma subunit variants to identify diverse mechanisms of AMPK activation. Cell Metab, 11(6), pp 554-65.

Hirata, A., Maeda, N., Hiuge, A., Hibuse, T., Fujita, K., Okada, T., Kihara, S., Funahashi, T. & Shimomura, I. 2009. Blockade of mineralocorticoid receptor reverses adipocyte dysfunction and insulin resistance in obese mice. Cardiovasc Res, 84(1), pp 164-72.

Hirata, A., Maeda, N., Nakatsuji, H., Hiuge-Shimizu, A., Okada, T., Funahashi, T. & Shimomura, I. 2012. Contribution of glucocorticoid-mineralocorticoid receptor pathway on the obesity-related adipocyte dysfunction. Biochem Biophys Res Commun, 419(2), pp 182-7.

Hoffman, N. J. & Elmendorf, J. S. 2011. Signaling, cytoskeletal and membrane mechanisms regulating GLUT4 exocytosis. Trends Endocrinol Metab, 22(3), pp 110-6.

Holt, R. I. G. 2010. Textbook of diabetes, 4th, Chichester, West Sussex: Wiley-Blackwell.

Hoppmann, J., Perwitz, N., Meier, B., Fasshauer, M., Hadaschik, D., Lehnert, H. & Klein, J. 2010. The balance between gluco- and mineralo-corticoid action critically determines inflammatory adipocyte responses. J Endocrinol, 204(2), pp 153-64.

Hotamisligil, G. S., Shargill, N. S. & Spiegelman, B. M. 1993. Adipose expression of tumor necrosis factor-alpha: direct role in obesity-linked insulin resistance. Science, 259(5091), pp 87-91.

Huang, S. & Czech, M. P. 2007. The GLUT4 glucose transporter. Cell Metab, 5(4), pp 237-52.

Investigators, D. T., Dagenais, G. R., Gerstein, H. C., Holman, R., Budaj, A., Escalante, A., Hedner, T., Keltai, M., Lonn, E., McFarlane, S., McQueen, M., Teo, K., Sheridan, P., Bosch, J., Pogue, J. & Yusuf, S. 2008. Effects of

ramipril and rosiglitazone on cardiovascular and renal outcomes in people with impaired glucose tolerance or impaired fasting glucose: results of the Diabetes REduction Assessment with ramipril and rosiglitazone Medication (DREAM) trial. Diabetes Care, 31(5), pp 1007-14.

Jager, J., Gremeaux, T., Cormont, M., Le Marchand-Brustel, Y. & Tanti, J. F. 2007. Interleukin-1beta-induced insulin resistance in adipocytes through down-regulation of insulin receptor substrate-1 expression. Endocrinology, 148(1), pp 241-51.

Janke, J., Engeli, S., Gorzelniak, K., Luft, F. C. & Sharma, A. M. 2002. Mature adipocytes inhibit in vitro differentiation of human preadipocytes via angiotensin type 1 receptors. Diabetes, 51(6), pp 1699-707.

Jiang, F., Lim, H. K., Morris, M. J., Prior, L., Velkoska, E., Wu, X. & Dusting, G. J. 2011. Systemic upregulation of NADPH oxidase in diet-induced obesity in rats. Redox Rep, 16(6), pp 223-9.

Jing, F., Mogi, M. & Horiuchi, M. 2013. Role of renin-angiotensin-aldosterone system in adipose tissue dysfunction. Mol Cell Endocrinol, 378(1-2), pp 23-8.

Jorgensen, S. B., Viollet, B., Andreelli, F., Frosig, C., Birk, J. B., Schjerling, P., Vaulont, S., Richter, E. A. & Wojtaszewski, J. F. 2004. Knockout of the alpha2 but not alpha1 5'-AMP-activated protein kinase isoform abolishes 5-aminoimidazole-4-carboxamide-1-beta-4-ribofuranosidebut not contraction-induced glucose uptake in skeletal muscle. J Biol Chem, 279(2), pp 1070-9.

Juan, C. C., Chien, Y., Wu, L. Y., Yang, W. M., Chang, C. L., Lai, Y. H., Ho, P. H., Kwok, C. F. & Ho, L. T. 2005. Angiotensin II enhances insulin sensitivity in vitro and in vivo. Endocrinology, 146(5), pp 2246-54.

Kadowaki, T., Yamauchi, T., Kubota, N., Hara, K., Ueki, K. & Tobe, K. 2006. Adiponectin and adiponectin receptors in insulin resistance, diabetes, and the metabolic syndrome. J Clin Invest, 116(7), pp 1784-92.

Kalupahana, N. S., Massiera, F., Quignard-Boulange, A., Ailhaud, G., Voy, B. H., Wasserman, D. H. & Moustaid-Moussa, N. 2012. Overproduction of angiotensinogen from adipose tissue induces adipose inflammation, glucose intolerance, and insulin resistance. Obesity (Silver Spring), 20(1), pp 48-56.

Kalupahana, N. S. & Moustaid-Moussa, N. 2012. The adipose tissue renin-angiotensin system and metabolic disorders: a review of molecular mechanisms. Crit Rev Biochem Mol Biol, 47(4), pp 379-90.

Kalupahana, N. S. & Moustaid-Moussa, N. 2012. The renin-angiotensin system: a link between obesity, inflammation and insulin resistance. Obes Rev, 13(2), pp 136-49.

Kamei, N., Tobe, K., Suzuki, R., Ohsugi, M., Watanabe, T., Kubota, N., Ohtsuka-Kowatari, N., Kumagai, K., Sakamoto, K., Kobayashi, M., Yamauchi, T., Ueki, K., Oishi, Y., Nishimura, S., Manabe, I., Hashimoto, H., Ohnishi, Y., Ogata, H., Tokuyama, K., Tsunoda, M., Ide, T., Murakami, K., Nagai, R. & Kadowaki, T. 2006. Overexpression of monocyte chemoattractant protein-1 in adipose tissues causes macrophage recruitment and insulin resistance. J Biol Chem, 281(36), pp 26602-14.

Karpe, P. A. & Tikoo, K. 2014. Heat shock prevents insulin resistance-induced vascular complications by augmenting angiotensin-(1-7) signaling. Diabetes, 63(3), pp 1124-39.

Kershaw, E. E. & Flier, J. S. 2004. Adipose tissue as an endocrine organ. J Clin Endocrinol Metab, 89(6), pp 2548-56.

Kleinert, M., Clemmensen, C., Hofmann, S. M., Moore, M. C., Renner, S., Woods, S. C., Huypens, P., Beckers, J., de Angelis, M. H., Schurmann, A., Bakhti, M., Klingenspor, M., Heiman, M., Cherrington, A. D., Ristow, M., Lickert, H., Wolf, E., Havel, P. J., Muller, T. D. & Tschop, M. H. 2018. Animal models of obesity and diabetes mellitus. Nat Rev Endocrinol, 14(3), pp 140-162.

Krum, H., McMurray, J. J., Horton, E., Gerlock, T., Holzhauer, B., Zuurman, L., Haffner, S. M., Bethel, M. A., Holman, R. R. & Califf, R. M. 2010. Baseline characteristics of the Nateglinide and Valsartan Impaired Glucose Tolerance Outcomes Research (NAVIGATOR) trial population: comparison with other diabetes prevention trials. Cardiovasc Ther, 28(2), pp 124-32.

Kwon, H. & Pessin, J. E. 2013. Adipokines mediate inflammation and insulin resistance. Front Endocrinol (Lausanne), 4(71.

Laderoute, K. R., Amin, K., Calaoagan, J. M., Knapp, M., Le, T., Orduna, J., Foretz, M. & Viollet, B. 2006. 5'-AMP-activated protein kinase (AMPK) is induced by low-oxygen and glucose deprivation conditions found in solid-tumor microenvironments. Mol Cell Biol, 26(14), pp 5336-47.

Lagathu, C., Yvan-Charvet, L., Bastard, J. P., Maachi, M., Quignard-Boulange, A., Capeau, J. & Caron, M. 2006. Long-term treatment with interleukin-1beta induces insulin resistance in murine and human adipocytes. Diabetologia, 49(9), pp 2162-73.

Lara-Castro, C., Fu, Y., Chung, B. H. & Garvey, W. T. 2007. Adiponectin and the metabolic syndrome: mechanisms mediating risk for metabolic and cardiovascular disease. Curr Opin Lipidol, 18(3), pp 263-70.

Lee, J. & Pilch, P. F. 1994. The insulin receptor: structure, function, and signaling. Am J Physiol, 266(2 Pt 1), pp C319-34.

Lee, J. H., Kim, J. H., Kim, J. S., Chang, J. W., Kim, S. B., Park, J. S. & Lee, S. K. 2013. AMP-activated protein kinase inhibits TGF-beta-, angiotensin II-, aldosterone-, high glucose-, and albumin-induced epithelial-mesenchymal transition. Am J Physiol Renal Physiol, 304(6), pp F686-97.

Lee, M. J. & Fried, S. K. 2014. The glucocorticoid receptor, not the mineralocorticoid receptor, plays the dominant role in adipogenesis and adipokine production in human adipocytes. Int J Obes (Lond), 38(9), pp 1228-33.

Lehr, S., Hartwig, S. & Sell, H. 2012. Adipokines: a treasure trove for the discovery of biomarkers for metabolic disorders. Proteomics Clin Appl, 6(1-2), pp 91-101.

LeMieux, M. J., Ramalingam, L., Mynatt, R. L., Kalupahana, N. S., Kim, J. H. & Moustaid-Moussa, N. 2016. Inactivation of adipose angiotensinogen reduces adipose tissue macrophages and increases metabolic activity. Obesity (Silver Spring), 24(2), pp 359-67.

Li, P., Pan, F., Hao, Y., Feng, W., Song, H. & Zhu, D. 2013. SGK1 is regulated by metabolic-related factors in 3T3-L1 adipocytes and overexpressed in the adipose tissue of subjects with obesity and diabetes. Diabetes Res Clin Pract, 102(1), pp 35-42.

Lihn, A. S., Jessen, N., Pedersen, S. B., Lund, S. & Richelsen, B. 2004. AICAR stimulates adiponectin and inhibits cytokines in adipose tissue. Biochem Biophys Res Commun, 316(3), pp 853-8.

Lim, C. T., Kola, B. & Korbonits, M. 2010. AMPK as a mediator of hormonal signalling. J Mol Endocrinol, 44(2), pp 87-97.

Liu, C., Lv, X. H., Li, H. X., Cao, X., Zhang, F., Wang, L., Yu, M. & Yang, J. K. 2012. Angiotensin-(1-7) suppresses oxidative stress and improves glucose uptake via Mas receptor in adipocytes. Acta Diabetol, 49(4), pp 291-9.

Lopez, J. M., Santidrian, A. F., Campas, C. & Gil, J. 2003. 5-Aminoimidazole-4-carboxamide riboside induces apoptosis in Jurkat cells, but the AMP-activated protein kinase is not involved. Biochem J, 370(Pt 3), pp 1027-32.

Luo, P., Dematteo, A., Wang, Z., Zhu, L., Wang, A., Kim, H. S., Pozzi, A., Stafford, J. M. & Luther, J. M. 2013. Aldosterone deficiency prevents high-fat-feeding-induced hyperglycaemia and adipocyte dysfunction in mice. Diabetologia, 56(4), pp 901-10.

Lutz, T. A. & Woods, S. C. 2012. Overview of animal models of obesity. Curr Protoc Pharmacol, Chapter 5(Unit5 61.

Lutzner, N., Kalbacher, H., Krones-Herzig, A. & Rosl, F. 2012. FOXO3 is a glucocorticoid receptor target and regulates LKB1 and its own expression based on cellular AMP levels via a positive autoregulatory loop. PLoS One, 7(7), pp e42166.

Ma, T. K., Kam, K. K., Yan, B. P. & Lam, Y. Y. 2010. Renin-angiotensin-aldosterone system blockade for cardiovascular diseases: current status. Br J Pharmacol, 160(6), pp 1273-92.

Mancini, S. J., White, A. D., Bijland, S., Rutherford, C., Graham, D., Richter, E. A., Viollet, B., Touyz, R. M., Palmer, T. M. & Salt, I. P. 2017. Activation of AMP-activated protein kinase rapidly suppresses multiple pro-inflammatory pathways in adipocytes including IL-1 receptor-associated kinase-4 phosphorylation. Mol Cell Endocrinol, 440(44-56.

Mantzoros, C. S., Magkos, F., Brinkoetter, M., Sienkiewicz, E., Dardeno, T. A., Kim, S. Y., Hamnvik, O. P. & Koniaris, A. 2011. Leptin in human physiology and pathophysiology. Am J Physiol Endocrinol Metab, 301(4), pp E567-84.

Marcus, Y., Shefer, G. & Stern, N. 2013. Adipose tissue renin-angiotensin-aldosterone system (RAAS) and progression of insulin resistance. Mol Cell Endocrinol, 378(1-2), pp 1-14.

Mathers, C. D. & Loncar, D. 2006. Projections of global mortality and burden of disease from 2002 to 2030. PLoS Med, 3(11), pp e442.

Matsushita, K., Wu, Y., Pratt, R. E. & Dzau, V. J. 2016. Deletion of angiotensin II type 2 receptor accelerates adipogenesis in murine mesenchymal stem cells via Wnt10b/beta-catenin signaling. Lab Invest, 96(8), pp 909-17.

Miller, W. L. & Auchus, R. J. 2011. The molecular biology, biochemistry, and physiology of human steroidogenesis and its disorders. Endocr Rev, 32(1), pp 81-151.

Moon, H. S., Dalamaga, M., Kim, S. Y., Polyzos, S. A., Hamnvik, O. P., Magkos, F., Paruthi, J. & Mantzoros, C. S. 2013. Leptin's role in lipodystrophic and nonlipodystrophic insulin-resistant and diabetic individuals. Endocr Rev, 34(3), pp 377-412.

Morrow, V. A., Foufelle, F., Connell, J. M., Petrie, J. R., Gould, G. W. & Salt, I. P. 2003. Direct activation of AMP-activated protein kinase stimulates nitric-oxide synthesis in human aortic endothelial cells. J Biol Chem, 278(34), pp 31629-39.

Mottillo, E. P., Desjardins, E. M., Crane, J. D., Smith, B. K., Green, A. E., Ducommun, S., Henriksen, T. I., Rebalka, I. A., Razi, A., Sakamoto, K., Scheele, C., Kemp, B. E., Hawke, T. J., Ortega, J., Granneman, J. G. & Steinberg, G. R. 2016. Lack of Adipocyte AMPK Exacerbates Insulin Resistance and Hepatic Steatosis through Brown and Beige Adipose Tissue Function. Cell Metab, 24(1), pp 118-29.

Mummidi, S., Das, N. A., Carpenter, A. J., Kandikattu, H., Krenz, M., Siebenlist, U., Valente, A. J. & Chandrasekar, B. 2016. Metformin inhibits aldosterone-induced cardiac fibroblast activation, migration and proliferation in vitro, and reverses aldosterone+salt-induced cardiac fibrosis in vivo. J Mol Cell Cardiol, 98(95-102.

Muniyappa, R. & Sowers, J. R. 2013. Role of insulin resistance in endothelial dysfunction. Rev Endocr Metab Disord, 14(1), pp 5-12.

Munzenmaier, D. H. & Greene, A. S. 1996. Opposing actions of angiotensin II on microvascular growth and arterial blood pressure. Hypertension, 27(3 Pt 2), pp 760-5.

Murakami, M., Hibi, M., Nakagawa, N., Nakagawa, T., Yasukawa, K., Yamanishi, K., Taga, T. & Kishimoto, T. 1993. IL-6-induced homodimerization of gp130 and associated activation of a tyrosine kinase. Science, 260(5115), pp 1808-10.

Musi, N., Fujii, N., Hirshman, M. F., Ekberg, I., Froberg, S., Ljungqvist, O., Thorell, A. & Goodyear, L. J. 2001. AMP-activated protein kinase (AMPK) is activated in muscle of subjects with type 2 diabetes during exercise. Diabetes, 50(5), pp 921-7.

Myers, R. W., Guan, H. P., Ehrhart, J., Petrov, A., Prahalada, S., Tozzo, E., Yang, X., Kurtz, M. M., Trujillo, M., Gonzalez Trotter, D., Feng, D., Xu, S., Eiermann, G., Holahan, M. A., Rubins, D., Conarello, S., Niu, X., Souza, S. C., Miller, C., Liu, J., Lu, K., Feng, W., Li, Y., Painter, R. E., Milligan, J. A., He, H., Liu, F., Ogawa, A., Wisniewski, D., Rohm, R. J., Wang, L., Bunzel, M., Qian, Y., Zhu, W., Wang, H., Bennet, B., LaFranco Scheuch, L., Fernandez, G. E., Li, C., Klimas, M., Zhou, G., van Heek, M., Biftu, T., Weber, A., Kelley, D. E., Thornberry, N., Erion, M. D., Kemp, D. M. & Sebhat, I. K. 2017. Systemic pan-AMPK activator MK-8722 improves glucose homeostasis but induces cardiac hypertrophy. Science, 357(6350), pp 507-511.

Nagata, D., Takeda, R., Sata, M., Satonaka, H., Suzuki, E., Nagano, T. & Hirata, Y. 2004. AMP-activated protein kinase inhibits angiotensin II-stimulated vascular smooth muscle cell proliferation. Circulation, 110(4), pp 444-51.

Nguyen Dinh Cat, A., Callera, G. E., Friederich-Persson, M., Sanchez, A., Dulak-Lis, M. G., Tsiropoulou, S., Montezano, A. C., He, Y., Briones, A. M., Jaisser, F. & Touyz, R. M. 2018. Vascular dysfunction in obese diabetic db/db mice involves the interplay between aldosterone/mineralocorticoid receptor and Rho kinase signaling. Sci Rep, 8(1), pp 2952.

Nguyen Dinh Cat, A. & Jaisser, F. 2012. Extrarenal effects of aldosterone. Curr Opin Nephrol Hypertens, 21(2), pp 147-56.

Nguyen, T. M., Combarnous, Y., Praud, C., Duittoz, A. & Blesbois, E. 2016. Ca2+/Calmodulin-Dependent Protein Kinase Kinases (CaMKKs) Effects on AMP-Activated Protein Kinase (AMPK) Regulation of Chicken Sperm Functions. PLoS One, 11(1), pp e0147559.

Niemand, C., Nimmesgern, A., Haan, S., Fischer, P., Schaper, F., Rossaint, R., Heinrich, P. C. & Muller-Newen, G. 2003. Activation of STAT3 by IL-6 and IL-10 in primary human macrophages is differentially modulated by suppressor of cytokine signaling 3. J Immunol, 170(6), pp 3263-72.

Niklason, A., Hedner, T., Niskanen, L., Lanke, J. & Captopril Prevention Project Study, G. 2004. Development of diabetes is retarded by ACE inhibition in hypertensive patients--a subanalysis of the Captopril Prevention Project (CAPPP). J Hypertens, 22(3), pp 645-52.

Nonogaki, K. 2000. New insights into sympathetic regulation of glucose and fat metabolism. Diabetologia, 43(5), pp 533-49.

Nye, C., Kim, J., Kalhan, S. C. & Hanson, R. W. 2008. Reassessing triglyceride synthesis in adipose tissue. Trends Endocrinol Metab, 19(10), pp 356-61.

Ofei, F., Hurel, S., Newkirk, J., Sopwith, M. & Taylor, R. 1996. Effects of an engineered human anti-TNF-alpha antibody (CDP571) on insulin sensitivity and glycemic control in patients with NIDDM. Diabetes, 45(7), pp 881-5.

Oh, Y. B., Kim, J. H., Park, B. M., Park, B. H. & Kim, S. H. 2012. Captopril intake decreases body weight gain via angiotensin-(1-7). Peptides, 37(1), pp 79-85.

O'Keefe, J. H., Abuissa, H. & Pitt, B. 2008. Eplerenone improves prognosis in postmyocardial infarction diabetic patients with heart failure: results from EPHESUS. Diabetes Obes Metab, 10(6), pp 492-7.

Padmalayam, I. & Suto, M. 2013. Role of adiponectin in the metabolic syndrome: current perspectives on its modulation as a treatment strategy. Curr Pharm Des, 19(32), pp 5755-63.

Panee, J. 2012. Monocyte Chemoattractant Protein 1 (MCP-1) in obesity and diabetes. Cytokine, 60(1), pp 1-12.

Patel, P. S., Buras, E. D. & Balasubramanyam, A. 2013. The role of the immune system in obesity and insulin resistance. J Obes, 2013(616193.

Patel, V. B., Zhong, J. C., Grant, M. B. & Oudit, G. Y. 2016. Role of the ACE2/Angiotensin 1-7 Axis of the Renin-Angiotensin System in Heart Failure. Circ Res, 118(8), pp 1313-26.

Paz-Filho, G., Mastronardi, C., Franco, C. B., Wang, K. B., Wong, M. L. & Licinio, J. 2012. Leptin: molecular mechanisms, systemic pro-inflammatory effects, and clinical implications. Arq Bras Endocrinol Metabol, 56(9), pp 597-607.

Pearce, D. 2001. The role of SGK1 in hormone-regulated sodium transport. Trends Endocrinol Metab, 12(8), pp 341-7.

Pires, K. M., Ilkun, O., Valente, M. & Boudina, S. 2014. Treatment with a SOD mimetic reduces visceral adiposity, adipocyte death, and adipose tissue inflammation in high fat-fed mice. Obesity (Silver Spring), 22(1), pp 178-87.

Pscherer, S., Heemann, U. & Frank, H. 2010. Effect of Renin-Angiotensin system blockade on insulin resistance and inflammatory parameters in patients with impaired glucose tolerance. Diabetes Care, 33(4), pp 914-9.

Puig, O. & Tjian, R. 2005. Transcriptional feedback control of insulin receptor by dFOXO/FOXO1. Genes Dev, 19(20), pp 2435-46.

Qi, C. & Pekala, P. H. 2000. Tumor necrosis factor-alpha-induced insulin resistance in adipocytes. Proc Soc Exp Biol Med, 223(2), pp 128-35.

Quentin, T., Kitz, J., Steinmetz, M., Poppe, A., Bar, K. & Kratzner, R. 2011. Different expression of the catalytic alpha subunits of the AMP activated protein kinase--an immunohistochemical study in human tissue. Histol Histopathol, 26(5), pp 589-96.

Ramanjaneya, M., Conner, A. C., Brown, J. E., Chen, J., Digby, J. E., Barber, T. M., Lehnert, H. & Randeva, H. S. 2011. Adiponectin (15-36) stimulates steroidogenic acute regulatory (StAR) protein expression and cortisol production in human adrenocortical cells: role of AMPK and MAPK kinase pathways. Biochim Biophys Acta, 1813(5), pp 802-9.

Reilly, S. M. & Saltiel, A. R. 2017. Adapting to obesity with adipose tissue inflammation. Nat Rev Endocrinol, 13(11), pp 633-643.

Rena, G., Pearson, E. R. & Sakamoto, K. 2013. Molecular mechanism of action of metformin: old or new insights? Diabetologia, 56(9), pp 1898-906.

Richardson, M. A., Berg, D. T., Johnston, P. A., McClure, D. & Grinnell, B. W. 1996. Human liposarcoma cell line, SW872, secretes cholesteryl ester transfer protein in response to cholesterol. J Lipid Res, 37(5), pp 1162-6.

Rudich, A., Tirosh, A., Potashnik, R., Hemi, R., Kanety, H. & Bashan, N. 1998. Prolonged oxidative stress impairs insulin-induced GLUT4 translocation in 3T3-L1 adipocytes. Diabetes, 47(10), pp 1562-9.

Ruiz-Ojeda, F. J., Ruperez, A. I., Gomez-Llorente, C., Gil, A. & Aguilera, C. M. 2016. Cell Models and Their Application for Studying Adipogenic Differentiation in Relation to Obesity: A Review. Int J Mol Sci, 17(7), pp.

Sadler, J. B., Bryant, N. J. & Gould, G. W. 2015. Characterization of VAMP isoforms in 3T3-L1 adipocytes: implications for GLUT4 trafficking. Mol Biol Cell, 26(3), pp 530-6.

Sadur, C. N. & Eckel, R. H. 1982. Insulin stimulation of adipose tissue lipoprotein lipase. Use of the euglycemic clamp technique. J Clin Invest, 69(5), pp 1119-25.

Sakamoto, K., Goransson, O., Hardie, D. G. & Alessi, D. R. 2004. Activity of LKB1 and AMPK-related kinases in skeletal muscle: effects of contraction, phenformin, and AICAR. Am J Physiol Endocrinol Metab, 287(2), pp E310-7.

Salt, I. P., Connell, J. M. & Gould, G. W. 2000. 5-aminoimidazole-4-carboxamide ribonucleoside (AICAR) inhibits insulin-stimulated glucose transport in 3T3-L1 adipocytes. Diabetes, 49(10), pp 1649-56.

Salt, I. P. & Hardie, D. G. 2017. AMP-Activated Protein Kinase: An Ubiquitous Signaling Pathway With Key Roles in the Cardiovascular System. Circ Res, 120(11), pp 1825-1841.

Salt, I. P. & Palmer, T. M. 2012. Exploiting the anti-inflammatory effects of AMP-activated protein kinase activation. Expert Opin Investig Drugs, 21(8), pp 1155-67.

Santos, R. A., Ferreira, A. J. & Simoes, E. S. A. C. 2008. Recent advances in the angiotensin-converting enzyme 2-angiotensin(1-7)-Mas axis. Exp Physiol, 93(5), pp 519-27.

Santos, S. H., Andrade, J. M., Fernandes, L. R., Sinisterra, R. D., Sousa, F. B., Feltenberger, J. D., Alvarez-Leite, J. I. & Santos, R. A. 2013. Oral Angiotensin-(1-7) prevented obesity and hepatic inflammation by inhibition of resistin/TLR4/MAPK/NF-kappaB in rats fed with high-fat diet. Peptides, 46(47-52.

Santos, S. H., Braga, J. F., Mario, E. G., Porto, L. C., Rodrigues-Machado Mda, G., Murari, A., Botion, L. M., Alenina, N., Bader, M. & Santos, R. A. 2010. Improved lipid and glucose metabolism in transgenic rats with increased circulating angiotensin-(1-7). Arterioscler Thromb Vasc Biol, 30(5), pp 953-61.

Santos, S. H., Fernandes, L. R., Mario, E. G., Ferreira, A. V., Porto, L. C., Alvarez-Leite, J. I., Botion, L. M., Bader, M., Alenina, N. & Santos, R. A. 2008. Mas deficiency in FVB/N mice produces marked changes in lipid and glycemic metabolism. Diabetes, 57(2), pp 340-7.

Santos, S. H., Fernandes, L. R., Pereira, C. S., Guimaraes, A. L., de Paula, A. M., Campagnole-Santos, M. J., Alvarez-Leite, J. I., Bader, M. & Santos, R. A. 2012. Increased circulating angiotensin-(1-7) protects white adipose tissue against development of a proinflammatory state stimulated by a high-fat diet. Regul Pept, 178(1-3), pp 64-70.

Saponaro, C., Gaggini, M., Carli, F. & Gastaldelli, A. 2015. The Subtle Balance between Lipolysis and Lipogenesis: A Critical Point in Metabolic Homeostasis. Nutrients, 7(11), pp 9453-74.

Sattar, N. & Gill, J. M. 2014. Type 2 diabetes as a disease of ectopic fat? BMC Med, 12(123.

Saye, J., Lynch, K. R. & Peach, M. J. 1990. Changes in angiotensinogen messenger RNA in differentiating 3T3-F442A adipocytes. Hypertension, 15(6 Pt 2), pp 867-71.

Scheen, A. J. 2004. Renin-angiotensin system inhibition prevents type 2 diabetes mellitus. Part 1. A meta-analysis of randomised clinical trials. Diabetes Metab, 30(6), pp 487-96.

Schmitz, J., Weissenbach, M., Haan, S., Heinrich, P. C. & Schaper, F. 2000. SOCS3 exerts its inhibitory function on interleukin-6 signal transduction through the SHP2 recruitment site of gp130. J Biol Chem, 275(17), pp 12848-56.

Schuhmacher, S., Foretz, M., Knorr, M., Jansen, T., Hortmann, M., Wenzel, P., Oelze, M., Kleschyov, A. L., Daiber, A., Keaney, J. F., Jr., Wegener, G., Lackner, K., Munzel, T., Viollet, B. & Schulz, E. 2011. alpha1AMP-activated protein kinase preserves endothelial function during chronic angiotensin II

treatment by limiting Nox2 upregulation. Arterioscler Thromb Vasc Biol, 31(3), pp 560-6.

Scott, J. W., van Denderen, B. J., Jorgensen, S. B., Honeyman, J. E., Steinberg, G. R., Oakhill, J. S., Iseli, T. J., Koay, A., Gooley, P. R., Stapleton, D. & Kemp, B. E. 2008. Thienopyridone drugs are selective activators of AMP-activated protein kinase beta1-containing complexes. Chem Biol, 15(11), pp 1220-30.

Sedeek, M., Montezano, A. C., Hebert, R. L., Gray, S. P., Di Marco, E., Jha, J. C., Cooper, M. E., Jandeleit-Dahm, K., Schiffrin, E. L., Wilkinson-Berka, J. L. & Touyz, R. M. 2012. Oxidative stress, Nox isoforms and complications of diabetes--potential targets for novel therapies. J Cardiovasc Transl Res, 5(4), pp 509-18.

Semple, R. K., Savage, D. B., Cochran, E. K., Gorden, P. & O'Rahilly, S. 2011. Genetic syndromes of severe insulin resistance. Endocr Rev, 32(4), pp 498-514.

Senn, J. J., Klover, P. J., Nowak, I. A., Zimmers, T. A., Koniaris, L. G., Furlanetto, R. W. & Mooney, R. A. 2003. Suppressor of cytokine signaling-3 (SOCS-3), a potential mediator of interleukin-6-dependent insulin resistance in hepatocytes. J Biol Chem, 278(16), pp 13740-6.

Shaw, R. J., Kosmatka, M., Bardeesy, N., Hurley, R. L., Witters, L. A., DePinho, R. A. & Cantley, L. C. 2004. The tumor suppressor LKB1 kinase directly activates AMP-activated kinase and regulates apoptosis in response to energy stress. Proc Natl Acad Sci U S A, 101(10), pp 3329-35.

Shibata, T., Takaguri, A., Ichihara, K. & Satoh, K. 2013. Inhibition of the TNF-alpha-induced serine phosphorylation of IRS-1 at 636/639 by AICAR. J Pharmacol Sci, 122(2), pp 93-102.

Shimobayashi, M., Albert, V., Woelnerhanssen, B., Frei, I. C., Weissenberger, D., Meyer-Gerspach, A. C., Clement, N., Moes, S., Colombi, M., Meier, J. A.,

Swierczynska, M. M., Jeno, P., Beglinger, C., Peterli, R. & Hall, M. N. 2018. Insulin resistance causes inflammation in adipose tissue. J Clin Invest, 128(4), pp 1538-1550.

Shimomura, I., Matsuda, M., Hammer, R. E., Bashmakov, Y., Brown, M. S. & Goldstein, J. L. 2000. Decreased IRS-2 and increased SREBP-1c lead to mixed insulin resistance and sensitivity in livers of lipodystrophic and ob/ob mice. Mol Cell, 6(1), pp 77-86.

Sindelka, G., Widimsky, J., Haas, T., Prazny, M., Hilgertova, J. & Skrha, J. 2000. Insulin action in primary hyperaldosteronism before and after surgical or pharmacological treatment. Exp Clin Endocrinol Diabetes, 108(1), pp 21-5.

Skoczylas, C., Fahrbach, K. M. & Rundell, K. 2004. Cellular targets of the SV40 small-t antigen in human cell transformation. Cell Cycle, 3(5), pp 606-10.

Sloan-Lancaster, J., Abu-Raddad, E., Polzer, J., Miller, J. W., Scherer, J. C., De Gaetano, A., Berg, J. K. & Landschulz, W. H. 2013. Double-blind, randomized study evaluating the glycemic and anti-inflammatory effects of subcutaneous LY2189102, a neutralizing IL-1beta antibody, in patients with type 2 diabetes. Diabetes Care, 36(8), pp 2239-46.

Smith, B. K., Marcinko, K., Desjardins, E. M., Lally, J. S., Ford, R. J. & Steinberg, G. R. 2016. Treatment of nonalcoholic fatty liver disease: role of AMPK. Am J Physiol Endocrinol Metab, 311(4), pp E730-E740.

Smith, J. D., Borel, A. L., Nazare, J. A., Haffner, S. M., Balkau, B., Ross, R., Massien, C., Almeras, N. & Despres, J. P. 2012. Visceral adipose tissue indicates the severity of cardiometabolic risk in patients with and without type 2 diabetes: results from the INSPIRE ME IAA study. J Clin Endocrinol Metab, 97(5), pp 1517-25.

Stanley, T. L., Zanni, M. V., Johnsen, S., Rasheed, S., Makimura, H., Lee, H., Khor, V. K., Ahima, R. S. & Grinspoon, S. K. 2011. TNF-alpha antagonism with

etanercept decreases glucose and increases the proportion of high molecular weight adiponectin in obese subjects with features of the metabolic syndrome. J Clin Endocrinol Metab, 96(1), pp E146-50.

Steinberg, G. R., Dandapani, M. & Hardie, D. G. 2013. AMPK: mediating the metabolic effects of salicylate-based drugs? Trends Endocrinol Metab, 24(10), pp 481-7.

Steinberg, G. R., Michell, B. J., van Denderen, B. J., Watt, M. J., Carey, A. L., Fam, B. C., Andrikopoulos, S., Proietto, J., Gorgun, C. Z., Carling, D., Hotamisligil, G. S., Febbraio, M. A., Kay, T. W. & Kemp, B. E. 2006. Tumor necrosis factor alpha-induced skeletal muscle insulin resistance involves suppression of AMP-kinase signaling. Cell Metab, 4(6), pp 465-74.

Steinberg, G. R., Parolin, M. L., Heigenhauser, G. J. & Dyck, D. J. 2002. Leptin increases FA oxidation in lean but not obese human skeletal muscle: evidence of peripheral leptin resistance. Am J Physiol Endocrinol Metab, 283(1), pp E187-92.

Steinberg, G. R., Rush, J. W. & Dyck, D. J. 2003. AMPK expression and phosphorylation are increased in rodent muscle after chronic leptin treatment. Am J Physiol Endocrinol Metab, 284(3), pp E648-54.

Stuck, B. J., Lenski, M., Bohm, M. & Laufs, U. 2008. Metabolic switch and hypertrophy of cardiomyocytes following treatment with angiotensin II are prevented by AMP-activated protein kinase. J Biol Chem, 283(47), pp 32562-9.

Summers, S. A., Whiteman, E. L. & Birnbaum, M. J. 2000. Insulin signaling in the adipocyte. Int J Obes Relat Metab Disord, 24 Suppl 4(S67-70.

Tabony, A. M., Yoshida, T., Galvez, S., Higashi, Y., Sukhanov, S., Chandrasekar, B., Mitch, W. E. & Delafontaine, P. 2011. Angiotensin II upregulates protein phosphatase 2Calpha and inhibits AMP-activated protein kinase signaling and energy balance leading to skeletal muscle wasting. Hypertension, 58(4), pp 643-9.

Takeda, M., Yamamoto, K., Takemura, Y., Takeshita, H., Hongyo, K., Kawai, T., Hanasaki-Yamamoto, H., Oguro, R., Takami, Y., Tatara, Y., Takeya, Y., Sugimoto, K., Kamide, K., Ohishi, M. & Rakugi, H. 2013. Loss of ACE2 exaggerates high-calorie diet-induced insulin resistance by reduction of GLUT4 in mice. Diabetes, 62(1), pp 223-33.

Tarantino, G. & Caputi, A. 2011. JNKs, insulin resistance and inflammation: A possible link between NAFLD and coronary artery disease. World J Gastroenterol, 17(33), pp 3785-94.

Tateya, S., Kim, F. & Tamori, Y. 2013. Recent advances in obesity-induced inflammation and insulin resistance. Front Endocrinol (Lausanne), 4(93.

Terada, Y., Ueda, S., Hamada, K., Shimamura, Y., Ogata, K., Inoue, K., Taniguchi, Y., Kagawa, T., Horino, T. & Takao, T. 2012. Aldosterone stimulates nuclear factor-kappa B activity and transcription of intercellular adhesion molecule-1 and connective tissue growth factor in rat mesangial cells via serum- and glucocorticoid-inducible protein kinase-1. Clin Exp Nephrol, 16(1), pp 81-8.

Thalhamer, T., McGrath, M. A. & Harnett, M. M. 2008. MAPKs and their relevance to arthritis and inflammation. Rheumatology (Oxford), 47(4), pp 409-14.

Than, A., Tee, W. T. & Chen, P. 2012. Apelin secretion and expression of apelin receptors in 3T3-L1 adipocytes are differentially regulated by angiotensin type 1 and type 2 receptors. Mol Cell Endocrinol, 351(2), pp 296-305.

Tian, S., Ge, X., Wu, K., Yang, H. & Liu, Y. 2014. Ramipril protects the endothelium from high glucose-induced dysfunction through CaMKKbeta/AMPK and heme oxygenase-1 activation. J Pharmacol Exp Ther, 350(1), pp 5-13.

Tilg, H. & Hotamisligil, G. S. 2006. Nonalcoholic fatty liver disease: Cytokine-adipokine interplay and regulation of insulin resistance. Gastroenterology, 131(3), pp 934-45.

Tirosh, A., Garg, R. & Adler, G. K. 2010. Mineralocorticoid receptor antagonists and the metabolic syndrome. Curr Hypertens Rep, 12(4), pp 252-7.

Tirupula, K. C., Desnoyer, R., Speth, R. C. & Karnik, S. S. 2014. Atypical signaling and functional desensitization response of MAS receptor to peptide ligands. PLoS One, 9(7), pp e103520.

Tong, L. 2005. Acetyl-coenzyme A carboxylase: crucial metabolic enzyme and attractive target for drug discovery. Cell Mol Life Sci, 62(16), pp 1784-803.

Todaro, G. J. & Green, H. 1963. Quantitative studies of the growth of mouse embryo cells in culture and their development into established lines. J Cell Biol, 17(299-313.

Towler, M. C. & Hardie, D. G. 2007. AMP-activated protein kinase in metabolic control and insulin signaling. Circ Res, 100(3), pp 328-41.

Turner, N. A., Ball, S. G. & Balmforth, A. J. 2001. The mechanism of angiotensin II-induced extracellular signal-regulated kinase-1/2 activation is independent of angiotensin AT(1A) receptor internalisation. Cell Signal, 13(4), pp 269-77.

Uchiyama, T., Okajima, F., Mogi, C., Tobo, A., Tomono, S. & Sato, K. 2017. Alamandine reduces leptin expression through the c-Src/p38 MAP kinase pathway in adipose tissue. PLoS One, 12(6), pp e0178769.

Underwood, P. C. & Adler, G. K. 2013. The renin angiotensin aldosterone system and insulin resistance in humans. Curr Hypertens Rep, 15(1), pp 59-70.

Urbanet, R., Nguyen Dinh Cat, A., Feraco, A., Venteclef, N., El Mogrhabi, S., Sierra-Ramos, C., Alvarez de la Rosa, D., Adler, G. K., Quilliot, D., Rossignol, P., Fallo, F., Touyz, R. M. & Jaisser, F. 2015. Adipocyte Mineralocorticoid Receptor Activation Leads to Metabolic Syndrome and Induction of Prostaglandin D2 Synthase. Hypertension, 66(1), pp 149-57.

van Greevenbroek, M. M., Schalkwijk, C. G. & Stehouwer, C. D. 2013. Obesity-associated low-grade inflammation in type 2 diabetes mellitus: causes and consequences. Neth J Med, 71(4), pp 174-87.

Vassiliou, G., Benoist, F., Lau, P., Kavaslar, G. N. & McPherson, R. 2001. The low density lipoprotein receptor-related protein contributes to selective uptake of high density lipoprotein cholesteryl esters by SW872 liposarcoma cells and primary human adipocytes. J Biol Chem, 276(52), pp 48823-30.

Vehik, K., Ajami, N. J., Hadley, D., Petrosino, J. F. & Burkhardt, B. R. 2013. The changing landscape of type 1 diabetes: recent developments and future frontiers. Curr Diab Rep, 13(5), pp 642-50.

Vermes, E., Ducharme, A., Bourassa, M. G., Lessard, M., White, M., Tardif, J. C. & Studies Of Left Ventricular, D. 2003. Enalapril reduces the incidence of diabetes in patients with chronic heart failure: insight from the Studies Of Left Ventricular Dysfunction (SOLVD). Circulation, 107(9), pp 1291-6.

Villena, J. A., Viollet, B., Andreelli, F., Kahn, A., Vaulont, S. & Sul, H. S. 2004. Induced adiposity and adipocyte hypertrophy in mice lacking the AMP-activated protein kinase-alpha2 subunit. Diabetes, 53(9), pp 2242-9.

Viollet, B. & Andreelli, F. 2011. AMP-activated protein kinase and metabolic control. Handb Exp Pharmacol, 203), pp 303-30.

Viollet, B., Andreelli, F., Jorgensen, S. B., Perrin, C., Flamez, D., Mu, J., Wojtaszewski, J. F., Schuit, F. C., Birnbaum, M., Richter, E., Burcelin, R. & Vaulont, S. 2003. Physiological role of AMP-activated protein kinase (AMPK): insights from knockout mouse models. Biochem Soc Trans, 31(Pt 1), pp 216-9.

Viollet, B., Andreelli, F., Jorgensen, S. B., Perrin, C., Geloen, A., Flamez, D., Mu, J., Lenzner, C., Baud, O., Bennoun, M., Gomas, E., Nicolas, G., Wojtaszewski, J. F., Kahn, A., Carling, D., Schuit, F. C., Birnbaum, M. J., Richter, E. A., Burcelin, R. & Vaulont, S. 2003. The AMP-activated protein kinase alpha2 catalytic subunit controls whole-body insulin sensitivity. J Clin Invest, 111(1), pp 91-8.

Viollet, B., Athea, Y., Mounier, R., Guigas, B., Zarrinpashneh, E., Horman, S., Lantier, L., Hebrard, S., Devin-Leclerc, J., Beauloye, C., Foretz, M., Andreelli, F., Ventura-Clapier, R. & Bertrand, L. 2009. AMPK: Lessons from transgenic and knockout animals. Front Biosci (Landmark Ed), 14(19-44.

Viollet, B., Guigas, B., Leclerc, J., Hebrard, S., Lantier, L., Mounier, R., Andreelli, F. & Foretz, M. 2009. AMP-activated protein kinase in the regulation of hepatic energy metabolism: from physiology to therapeutic perspectives. Acta Physiol (Oxf), 196(1), pp 81-98.

Wada, T., Kenmochi, H., Miyashita, Y., Sasaki, M., Ojima, M., Sasahara, M., Koya, D., Tsuneki, H. & Sasaoka, T. 2010. Spironolactone improves glucose and lipid metabolism by ameliorating hepatic steatosis and inflammation and suppressing enhanced gluconeogenesis induced by high-fat and high-fructose diet. Endocrinology, 151(5), pp 2040-9.

Wada, T., Ohshima, S., Fujisawa, E., Koya, D., Tsuneki, H. & Sasaoka, T. 2009. Aldosterone inhibits insulin-induced glucose uptake by degradation of insulin receptor substrate (IRS) 1 and IRS2 via a reactive oxygen species-mediated pathway in 3T3-L1 adipocytes. Endocrinology, 150(4), pp 1662-9.

Wajant, H., Pfizenmaier, K. & Scheurich, P. 2003. Tumor necrosis factor signaling. Cell Death Differ, 10(1), pp 45-65.

Wallenius, K., Jansson, J. O. & Wallenius, V. 2003. The therapeutic potential of interleukin-6 in treating obesity. Expert Opin Biol Ther, 3(7), pp 1061-70.

Wang, B., Jenkins, J. R. & Trayhurn, P. 2005. Expression and secretion of inflammation-related adipokines by human adipocytes differentiated in culture: integrated response to TNF-alpha. Am J Physiol Endocrinol Metab, 288(4), pp E731-40.

Wang, C., Li, L., Zhang, Z. G., Fan, D., Zhu, Y. & Wu, L. L. 2010. Globular adiponectin inhibits angiotensin II-induced nuclear factor kappaB activation through AMP-activated protein kinase in cardiac hypertrophy. J Cell Physiol, 222(1), pp 149-55.

Wassef, H., Bernier, L., Davignon, J. & Cohn, J. S. 2004. Synthesis and secretion of apoC-I and apoE during maturation of human SW872 liposarcoma cells. J Nutr, 134(11), pp 2935-41.

Watkins, P. A. 1997. Fatty acid activation. Prog Lipid Res, 36(1), pp 55-83.

Weisberg, S. P., Hunter, D., Huber, R., Lemieux, J., Slaymaker, S., Vaddi, K., Charo, I., Leibel, R. L. & Ferrante, A. W., Jr. 2006. CCR2 modulates inflammatory and metabolic effects of high-fat feeding. J Clin Invest, 116(1), pp 115-24.

Whaley-Connell, A., Johnson, M. S. & Sowers, J. R. 2010. Aldosterone: role in the cardiometabolic syndrome and resistant hypertension. Prog Cardiovasc Dis, 52(5), pp 401-9.

Woods, A., Salt, I., Scott, J., Hardie, D. G. & Carling, D. 1996. The alpha1 and alpha2 isoforms of the AMP-activated protein kinase have similar activities in rat liver but exhibit differences in substrate specificity in vitro. FEBS Lett, 397(2-3), pp 347-51.

Woods, A., Williams, J. R., Muckett, P. J., Mayer, F. V., Liljevald, M., Bohlooly, Y. M. & Carling, D. 2017. Liver-Specific Activation of AMPK Prevents Steatosis on a High-Fructose Diet. Cell Rep, 18(13), pp 3043-3051.

World Health Organisation. 2017. Obesity and overweight. http://www.who.int/en/news-room/fact-sheets/detail/obesity-and-overweight.

Wu, J., Cohen, P. & Spiegelman, B. M. 2013. Adaptive thermogenesis in adipocytes: is beige the new brown? Genes Dev, 27(3), pp 234-50.

Wu, Y., Song, P., Zhang, W., Liu, J., Dai, X., Liu, Z., Lu, Q., Ouyang, C., Xie, Z., Zhao, Z., Zhuo, X., Viollet, B., Foretz, M., Wu, J., Yuan, Z. & Zou, M. H. 2015. Activation of AMPKalpha2 in adipocytes is essential for nicotine-induced insulin resistance in vivo. Nat Med, 21(4), pp 373-82.

Xiao, L., Sonne, S. B., Feng, Q., Chen, N., Xia, Z., Li, X., Fang, Z., Zhang, D., Fjaere, E., Midtbo, L. K., Derrien, M., Hugenholtz, F., Tang, L., Li, J., Zhang, J., Liu, C., Hao, Q., Vogel, U. B., Mortensen, A., Kleerebezem, M., Licht, T. R., Yang, H., Wang, J., Li, Y., Arumugam, M., Wang, J., Madsen, L. & Kristiansen, K. 2017. High-fat feeding rather than obesity drives taxonomical and functional changes in the gut microbiota in mice. Microbiome, 5(1), pp 43.

Xu, H., Barnes, G. T., Yang, Q., Tan, G., Yang, D., Chou, C. J., Sole, J., Nichols, A., Ross, J. S., Tartaglia, L. A. & Chen, H. 2003. Chronic inflammation in fat plays a crucial role in the development of obesity-related insulin resistance. J Clin Invest, 112(12), pp 1821-30.

Xu, X. J., Pories, W. J., Dohm, L. G. & Ruderman, N. B. 2013. What distinguishes adipose tissue of severely obese humans who are insulin sensitive and resistant? Curr Opin Lipidol, 24(1), pp 49-56.

Yamauchi, T., Kamon, J., Minokoshi, Y., Ito, Y., Waki, H., Uchida, S., Yamashita, S., Noda, M., Kita, S., Ueki, K., Eto, K., Akanuma, Y., Froguel, P., Foufelle, F., Ferre, P., Carling, D., Kimura, S., Nagai, R., Kahn, B. B. & Kadowaki, T. 2002. Adiponectin stimulates glucose utilization and fatty-acid oxidation by activating AMP-activated protein kinase. Nat Med, 8(11), pp 1288-95.

Yang, Z., Wang, X., He, Y., Qi, L., Yu, L., Xue, B. & Shi, H. 2012. The full capacity of AICAR to reduce obesity-induced inflammation and insulin resistance requires myeloid SIRT1. PLoS One, 7(11), pp e49935.

Yiannikouris, F., Gupte, M., Putnam, K., Thatcher, S., Charnigo, R., Rateri, D. L., Daugherty, A. & Cassis, L. A. 2012. Adipocyte deficiency of angiotensinogen prevents obesity-induced hypertension in male mice. Hypertension, 60(6), pp 1524-30.

Yusuf, S. 2000. [After the HOPE Study. ACE inhibitor now for every diabetic patient?. Interview by Dr. Dirk Einecke]. MMW Fortschr Med, 142(44), pp 10.

Yvan-Charvet, L., Even, P., Bloch-Faure, M., Guerre-Millo, M., Moustaid-Moussa, N., Ferre, P. & Quignard-Boulange, A. 2005. Deletion of the angiotensin type 2 receptor (AT2R) reduces adipose cell size and protects from diet-induced obesity and insulin resistance. Diabetes, 54(4), pp 991-9.

Zhang, W., Li, C., Liu, B., Wu, R., Zou, N., Xu, Y. Z., Yang, Y. Y., Zhang, F., Zhou, H. M., Wan, K. Q., Xiao, X. Q. & Zhang, X. 2013. Pioglitazone upregulates hepatic angiotensin converting enzyme 2 expression in rats with steatohepatitis. Ann Hepatol, 12(6), pp 892-900.

Appendix 1: Details of High fat diet

SDS Diet – 829100 – Western RD (P)

Specification as % kcal Crude Fat 42%, Crude Protein 15%, Carbohydrate 43%.

Kcal/g = 4.63 total AFE.

Ingredient	g% (w/w)
Sucrose	33.94
Milk Fat Anhydrous	20
Casein	19.5
Maltodextrin	10
Corn Strach	5
Cellulose	5
Corn Oil	1
Calcium carbonate	0.4
L-Cystine	0.3
Choline Bitartrate	0.2
Cholesterol	0.15
Antioxidant	0.01
AIN-76A-MX	3.5
AIN-76A-VX	1